Spring 1-1-2011

Improvement of the Immunoisolation Capacity of PEG Hydrogels through Bioactive Modifications

Patrick Scott Hume
University of Colorado at Boulde, pat.hume@gmail.com

Improvement of the Immunoisolation Capacity of PEG Hydrogels through Bioactive Modifications

By

Patrick Scott Hume

B.S., University of Colorado, 2005

A thesis submitted to the

Faculty of the Graduate School of the

University of Colorado in partial fulfillment

of the requirement for the degree of

Doctor of Philosophy

Department of Chemical and Biological Engineering

2011

This thesis entitled

Improvement of the immunoisolation capacity of PEG hydrogels through bioactive modifications

written by Patrick Scott Hume

has been approved for the Department of Chemical and Biological Engineering

_____

Kristi S. Anseth

_____

Christopher N. Bowman

Date _____

The final copy of this thesis has been examined by

the signatories, and we find that both the content and the form

meet acceptable presentation standards of scholarly work

in the above mentioned discipline

Abstract

Hume, Patrick S. (Ph.D., Chemical Engineering)
Department of Chemical and Biological Engineering, University of Colorado

Improvement of the immunoisolation capacity of PEG hydrogels through bioactive modifications

Thesis directed by Professor Kristi S. Anseth

Cell-based therapies are a promising approach for the treatment of diseases such as Type I diabetes mellitus (TIDM), where endogenous insulin production is restored via delivery of insulin-producing β-cells or islet of Langerhans clusters. Tissue rejection by the host's immune system, however, is a major hurdle limiting the broad use of transplanted tissues, so β-cell-based therapies require systemic immunosuppression. To reduce this requirement, tissues have been encapsulated within natural and synthetic barrier materials in a process known as immunoisolation. Immunoisolation materials, including poly(ethylene glycol) (PEG) hydrogels, create physical barriers between host immune cells and donor tissue while enabling the diffusion of small molecules like nutrients and oxygen. Unmodified immunoisolation barriers, however, are unable to prevent the diffusion of small cytotoxic molecules, including reactive oxygen species (ROS) (e.g., superoxide) and cytokines.

This research investigated strategies to introduce immunoactive modifications to PEG hydrogels for the purpose of improving their immunoisolation capacity. Towards this, a polymerizable superoxide dismutase mimetic (SODm) was covalently tethered within β-cell-laden hydrogels to significantly increase cell survival following challenges with superoxide, a major inflammatory mediator of the immune response. Next,

photoiniferter chemistry was employed to polymerize PEG chains co-functionalized with an apoptosis inducing factor (anti-fas) and a T cell adhesion ligand (ICAM-1) to locally reduce, through apoptosis, the population of T cells, the adaptive immune responder cells implicated in islet transplant rejection. Further, conformal, immunoactive coatings were formed directly on the surfaces of cell-laden PEG hydrogels using a versatile, reactive dip-coating strategy to present a high density of immunoactive signal while maintaining encapsulated cell cytocompatibility. Finally, towards preventing the development of deleterious adaptive immunity altogether, immunosuppressive hydrogels modified with TGF-β1 and IL-10 were introduced, and their capacity to reduce dendritic cell maturation was highlighted. The immunoactive materials developed within this thesis suggest innovative strategies for the engineering of future immunoisolation barriers to provide localized and targeted protection of transplanted cells.

This thesis is dedicated to my family

ACKNOWLEDGEMENTS

I would like to begin by acknowledging the funding sources that made this work possible. During my first rotation in the lab, I was funded by the University of Colorado's Medical Scientist Training program. Later, funding was provided by the National Institute of Health (R01DK076084) and the Howard Hughes medical institute. Additionally, I was the recipient of funding from the Department of Education's Graduate Assistance in Areas of National Need (GAANN) fellowship. Finally, I would like to thank the University of Colorado's Undergraduate Research Opportunities Program (UROP) for providing funding for Kristina Fuerst, an undergraduate who assisted me throughout several of these studies.

Next, I would like to thank my thesis committee. Professors Raul Torres and Stephanie Bryant each offered unique perspectives which enriched several areas of my dissertation work. Prof. Christopher Bowman provided valuable polymerization advice and he and his laboratory were very helpful throughout our collaboration utilizing glucose oxidase-mediated coatings. Finally, Prof. Kathryn Haskins and her lab provided vital input regarding islet biology and immunology. Dr. Haskins opened her laboratory to me, enabling several studies which would not have otherwise been possible. Further, thank you to Brenda Bradley and Jing He, members of the Haskins group. Breda conducted several *in vivo* studies with encapsulated islets. Jing offered vital advice regarding the primary murine dendritic cell studies. Jing additionally performed all BMDC flow cytometery experiments, graciously cultured cells for me and taught me how to harvest primary dendritic cells.

I would like to thank each member of the Anseth group whom I've had the pleasure of working with for the last several years. Each of you have offered valuable advice and technical assistance and made my time in graduate school as fun as it was rewarding. More specifically, I'd like to thank each member of the islet group within the Anseth lab: Chuck Cheung, Chien-Chi Lin, Alex Aimetti, Abby Bernard, and Kelly Trowbridge. When I began my thesis, I was very fortunate to work with Chuck Cheung, a former post-doctoral researcher who introduced work with active immunoisolation barriers to the Anseth lab. Chuck's research laid the groundwork for many aspects of my project, but beyond that, Chuck took the time to teach me a majority of the lab techniques that I used throughout my studies. Chien-Chi Lin is also a former post-doctoral researcher who provided numerous helpful discussions and was a particularly great resource for encapsulated β-cell culture. Alex Aimetti was instrumental throughout two collaborations involving the SODm project and studies with an anti-Fas peptide mimic. Abby Bernard provided much helpful advice, particularly with regard to the mask alignment system and β-cell cultures. Kelly Trowbridge offered helpful advice and provided nuetrophil cells. Finally, Laney Weber and Jay Blanchette, former islet group members, performed studies and established collaborations which paved the way for my work.

I'm also grateful to several other past and present Anseth group members. McKinley Lawson taught me surface grafting techniques. April Kloxin, Ben Fairbanks, Cole DeForest and Mark Tibbitt were always willing to listen and facilitated many helpful discussions. Josh McCall provided much advice, particularly in the area of my TGF-β work. Outside of the lab, I'm thankful for the strong friendships I've formed with many

Anseth group members which enabled numerous intramural championships, epic ski trips, and limitless fond memories. Finally, I wish like to thank Kristina Fuerst, a CU undergraduate who has provided helpful assistance throughout several research projects within my thesis over the last couple years. Thank for your positive attitude, diligent work ethic, and inquisitiveness.

Most importantly, thank you to my thesis advisor. I feel so fortunate to have had the opportunity to work with Kristi Anseth. The energy, curiosity, excitement, and passion which Kristi has for scientific investigation was a constant source of motivation throughout my studies. Kristi gave me the freedom to explore scientific questions in which I was interested, while remaining a constant source of helpful advice and encouragement. Ultimately, the vital guidance Kristi provided me with throughout my studies enabled this thesis.

Finally, I would like to thank my family for their constant support throughout my many, many years of education. My entire life, my parents have raised a Ph.D. researcher. They had infinite patience to answer the limitless questions I asked as a child. Further, they provided a strong emphasis on the importance of education and provided me with every opportunity I could have ever asked for. Last, but not least, I would like to thank my wife, Stephanie LaNasa Hume. Since we first met in the CU Chemical Engineering Department's summer REU program, Steph has been my constant source of encouragement, guidance, companionship, thesis editing and vital scientific discussions. Steph, you have enriched my life in ways I didn't know were possible. Thank you.

TABLE OF CONTENTS

CHAPTER 4

INDUCING LOCAL T CELL APOPTOSIS WITH ANTI-FAS-FUNCTIONALIZED POLYMERIC COATINGS FABRICATED VIA SURFACE-INITIATED PHOTOPOLYMERIZATIONS 78

CHAPTER 5

FUNCTIONALIZED PEG HYDROGELS THROUGH REACTIVE DIP-COATING FOR THE FORMATION OF IMMUNOACTIVE BARRIERS 108

CHAPTER 6

STRATEGIES TO REDUCE DENDRITIC CELL MATURATION AND PROMOTE TOLERANCE THROUGH FUNCTIONAL BIOMATERIAL DESIGN 139

List of Tables

List of Figures

Chapter 1

Introduction

1.1 OVERVIEW

Cell delivery systems, often consisting of donor tissue embedded within material scaffolds, have the potential to cure numerous diseases of the endocrine, cardiovascular, neurological and musculoskeletal systems. The goal of such strategies range from the regeneration of functional tissue equivalents to the controlled delivery of cell-secreted trophic factors. One widely investigated cell therapy is the transplantation of islets for the treatment of type I diabetes mellitus. Numerous advancements towards improved islet survival and function within biomaterials, as well as *in vivo* successes, continue to highlight the potential of this growing field. Despite many successes, however, several obstacles must be overcome before tissue engineered implants will become widely implemented in the clinical setting. Presently, a major hurdle to tissue transplantation is the threat of graft rejection by the host immune system. As such, harsh immunosuppressive medications are a hallmark of islet transplantation. In this introduction, type I diabetes mellitus and the treatment thereof with transplanted tissue, is reviewed. Further, strategies to decrease the necessity of systemic immunosuppression following islet transplantation, such as those explored in this thesis, are highlighted.

1.2 TYPE I DIABETES MELLITUS

1.2.1 Disease Overview

Type I diabeties mellitus (TIDM) is a chronic disease affecting over 3 million patients in the US alone [1]. TIDM results from the autoimmune-mediated destruction of insulin-producing β-cells, located within the pancreatic islet of Langerhans cell clusters, Fig. 1.1. Under normal circumstances, pancreatic β-cells secrete insulin in response to the increased blood glucose that follows a meal. Once secreted, insulin circulates throughout the body, binds to cells, and triggers the uptake of glucose [2]. Thus, if the insulin-producing β-cells are destroyed, as is the case in TIDM, insufficient insulin is secreted, so glucose gradually builds up in the bloodstream. The build-up of glucose

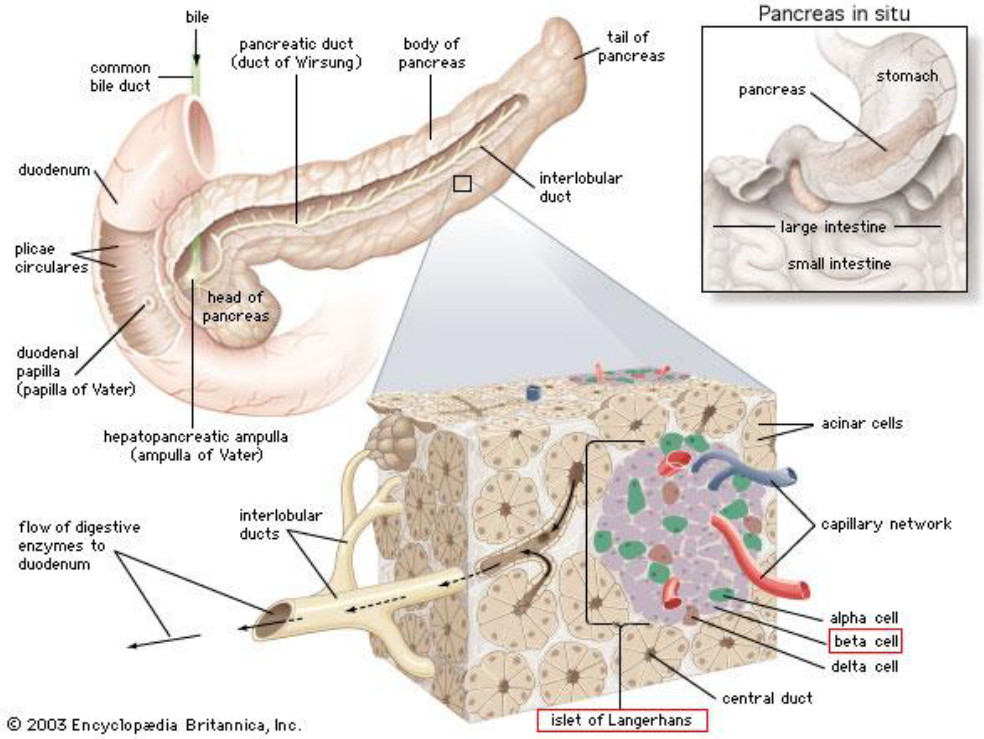

Fig. 1.1. Anatomy of the human pancreas. The pancreas contains exocrine and endocrine tissue. The endocrine tissue, located within Islets of Langerhans, contain the insulin-producing β-cells which are destroyed during the development of TIDM. Adapted from the Encyclopedia of Britannica.

results in a condition known as hyperglycemia. Unable to take up glucose, cells turn to other energy sources for fuel, particularly fatty acids. Increased fatty acid metabolism, however, results in the formation of acidic ketone bodies, which accumulate in the bloodstream [3]. Diabetic ketoacidosis (DKA), occurring from the build-up of glucose and ketoacids in the blood, is a life threatening emergency. Ketone acids reduce the blood pH, and the kidneys begin dumping fluid in an effort to excrete glucose and ketones, potentially resulting in severe dehydration. In 1 to 3% of DKA cases, death may occur from severe cerebral edema [4, 5]. In the US, It has been calculated that more children die each year from DKA than all cancers [3].

1.2.2 Treatment and complications

To maintain proper blood glucose levels, TIDM patients manage their blood sugar via daily insulin injections. TIDM most commonly presents in young patients, under the age of 20, so once afflicted, patients can anticipate a lifetime of insulin management. Even with diligent insulin management, though, numerous complications are likely when living a lifetime with diabetes [6]. Because it is difficult to maintain constant control over serum insulin concentration [7], it is common for TIDM patients to maintain higher-than-normal blood glucose levels. After many years with hyperglycemia, excess sugar builds up in blood vessels and other tissues in a process known as glycation [8]. When glycation occurs, many organ systems may be damaged, including the eyes, kidneys, nerves, and vessels, leading to blindness, kidney failure, neuropathies, and coronary artery disease [7, 8]. Fortunately, diligent blood sugar

monitoring and diabetes control decreases the occurrence of these severe complications [9].

While preventing chronic high blood glucose is important, particular care must also be taken to avoid reducing blood glucose levels below the healthy range, by properly timing insulin injections and carefully estimating insulin dosages for upcoming meals. If excess insulin is administered, blood glucose may fall below healthy levels, resulting in hypoglycemia. Severe hypoglycemia is an acute emergency because an insufficient amount of glucose is present in the blood to supply the brain. This can result in sudden, severe neurologic complications such as dizziness, seizure, coma and death [10]. Unfortunately, when patients tightly control blood sugar to minimize long-term complications from diabetes, they are at a 3-fold increased risk of experiencing a dangerous hypoglycemic episode [11]. Initially, patients are able to feel when his or her blood sugar is low and can ingest sugars to correct this. After living many years with TIDM, though, it is common for patients to begin to lose the sensation of low blood glucose, in a condition known as hypoglycemic unawareness [12]. When TIDM patients begin experiencing hypoglycemic unawareness, they are at greatly increased risk of experiencing dangerous hypoglycemic episodes [12].

1.3 ISLET & PANCREAS TRANSPLANTATION

Due to the long-term complications associated with TIDM, the tediousness of daily blood sugar management and the dangers of hypoglycemic unawareness, researchers have long searched for a means to reduce or eliminate the need for daily blood glucose

monitoring and insulin injections for TIDM patients. Many recent efforts towards this goal have focused on gene therapy [13, 14], electronic closed-loop glucose monitor / insulin pump systems [15, 16], and pancreas and islet transplantation. Herein, organ and cell transplants are considered. The rationale for transplantation is simple: replacing lost β-cells should re-enable the body to generate insulin.

1.3.1 Early Efforts

Two years after Minkowski discovered that the removal of the pancreas caused diabetes in dogs [17], the first pancreatic transplant was performed in 1894, when Williams implanted pieces of sheep pancreas into a boy in a futile effort to cure end-stage diabetes [18]. Despite relatively constant investigation, it was almost 80 years later, 1972, when Lacy *et al.* successfully reversed diabetes in rodents by islet transplantation [19]. While the rodents eventually succumbed to diabetes, this study demonstrated the efficacy of islet transplantation.

1.3.2 Success in humans and the Edmonton Protocol

Progress continued, and in 1988, Ricordi *et al.* developed a novel, automated method for human islet isolation which greatly increased donor cell yields [20]. Using this isolation strategy to obtain sufficient islet numbers, in 1989 Sharp *et al.* demonstrated that short-term insulin independence could be achieved in humans following allograft islet transplantation [21]. These transplanted islets eventually failed, likely due to long-term immune rejection, but researchers successfully demonstrated

that TIDM could be reversed in humans. While steady progress towards successful human islet transplantation proceeded throughout the 20th century, large leaps came with the introduction of steroid-free immunosuppression regimens to protect islet transplants. Chronic steroid use is associated with numerous negative side effects including immunosuppression, osteoporosis [22], and hyperglycemia due to increased insulin resistance [23]. In 1990, Ricordi *et al.* reported that the steroid-free agent tacrolimus (FK-506) was able to protect human islet transplants up to 5 years. Even more encouraging, in 2000 Shapiro*, et al.* at the University of Edmonton introduced the non-steroid rapamycin as an immunosuppressant to prevent islet graft rejection [24]. One year following transplantation, all seven patients who received islet transplants and chronic rapamycin treatment remained insulin independent [24].

1.3.3 Post-Edmonton Protocol

The Shapiro *et al.* approach, now known as the Edmonton protocol, invigorated the field of islet transplantation and was initially adopted at multiple sites, yielding encouraging results [25-27]. Over time, however, the promise of the Edmonton protocol has faded. In 2005, the Edmonton group published a follow-up to their initial report in which they documented that 90% of their original islet transplant recipients had become insulin-dependent. Further, in 2006, the Edmonton group conducted a multinational, nine-site clinical trial to evaluate the efficacy of the Edmonton protocol when conducted offsite [28]. In this study, 36 patients received islet transplants; of those, only 58% achieved insulin independence at some point in the study, while 76% of patients were

back on daily insulin injections within two years [28, 29]. Though insulin-independence seems to be unsustainable with present islet transplantation protocols, an important finding from these studies was that all patients were protected from dangerous hypoglycemic events [28]. This indicates that a significant number of islets are routinely lost in the years following a transplant, but enough survive to protect patients from hypoglycemia. Therefore, while not yet a cure for diabetes, islet transplantation is able to reduce the risk of life-threatening hypoglycemia and improve patient quality of life [30].

1.3.4 Pancreas transplantation

While the progress of islet transplantation has slowed in recent years, over 30,000 clinical trials with whole pancreas transplants have been conducted worldwide [31]. Pancreas transplantation requires a more invasive surgery than islet transplantation, but in the US, >75% of transplants survive one year [6, 32]. Further, pancreatic transplant recipients have been shown to have a reduced risk of developing several diabetic complications, including retinopathy, cardiovascular disease, and neuropathy, compared to patients managed with insulin therapy alone [6]. Likewise, the transplantation of islets only, though performed in limited numbers, has also been shown to improve cardiovascular function [33], retinopathy [34], and renal function [35] in TIDM patients. The benefits of receiving a pancreas or islet transplant, however, must constantly be measured against the side effects [36]. For example, transplant surgery is associated with a risk of bleeding and thrombosis in the portal vein [24, 28, 37]. Further,

chronic systemic immunosuppression, while preventing transplant rejection, is associated with increased risk of infection, toxicity to numerous organ systems, and malignancy [38]. Presently, pancreatic tissue transplants are only indicated for patients suffering from severe diabetes, including those with severe hypoglycemic unawareness or those undergoing immunosuppression for a second solid organ transplant (typically kidney) [39]. Thus, significant hurdles remain before pancreas and islet transplantations become viable options for many TIDM patients. Fortunately, there is promising evidence that if a tissue transplant can be properly implanted and protected, replacing lost pancreatic tissue will cure TIDM.

1.4 IMMUNOLOGICAL CHALLENGES TO ISLET TRANSPLANTATION

1.4.1 Innate immune responses

One of the major requirements for successful islet transplantation is the prevention of transplant rejection by the host immune system. When islets are implanted into the body, the innate and adaptive immune systems play critical roles in tissue rejection. Following surgery, innate immune cells, including neutrophils and macrophages, migrate to the surgical site and secrete cytokines to promote normal wound healing [40]. As Robitaille *et al.* observed, even minimally-invasive saline injections can elicit a large neutrophil infiltrate [41]. In addition to the insult from surgery, transplanted islets are known to secrete numerous inflammatory factors including TNF-α [42, 43], IL-1β [42, 43], monocyte chemotactic protein-1 (MCP-1) [44, 45], and nitric oxide (NO) [46], which further aggravate local inflammatory cells [47]. Activated innate

inflammatory cells accumulate over approximately the first 18 hours following a transplant [41, 48], and secrete inflammatory cytokines including IL-1β, IL-6, and TNF-α [41], as well as reactive oxygen species (ROS) like superoxide [49]. In addition to inducing direct toxicity against transplanted islets [46, 50-53], the presence of these inflammatory mediators can initiate the foreign body response, resulting in transplanted cells becoming walled off by macrophages [40]. Further, antigen presenting cells (APCs), including macrophages and dendritic cells (DCs), proceed to activate the adaptive immune response [54].

1.4.2 Adaptive immune responses

While the innate immune response poses a considerable threat to the initial survival of transplanted islets, the response of the adaptive immune system is a primary determinant of long-term graft survival. Following the transplantation of naked islets, T cells of the host adaptive immune system are exposed to immunogenic antigens from the donor tissue via *direct* and *indirect* antigen presentation, Fig. 1.2 [54, 55]. *Direct* antigen presentation is the predominant means by which T cells gain immunity to naked cell transplants, and occurs when host $CD8^+$ or $CD4^+$ T cells come into direct contact with donor APCs expressing major histocompatibility complex class I (MHC I) or MHC II proteins, respectively [54]. Once primed against donor tissue, these cytotoxic T cells become activated, migrate to foreign cells, and bind them to deliver signals resulting in

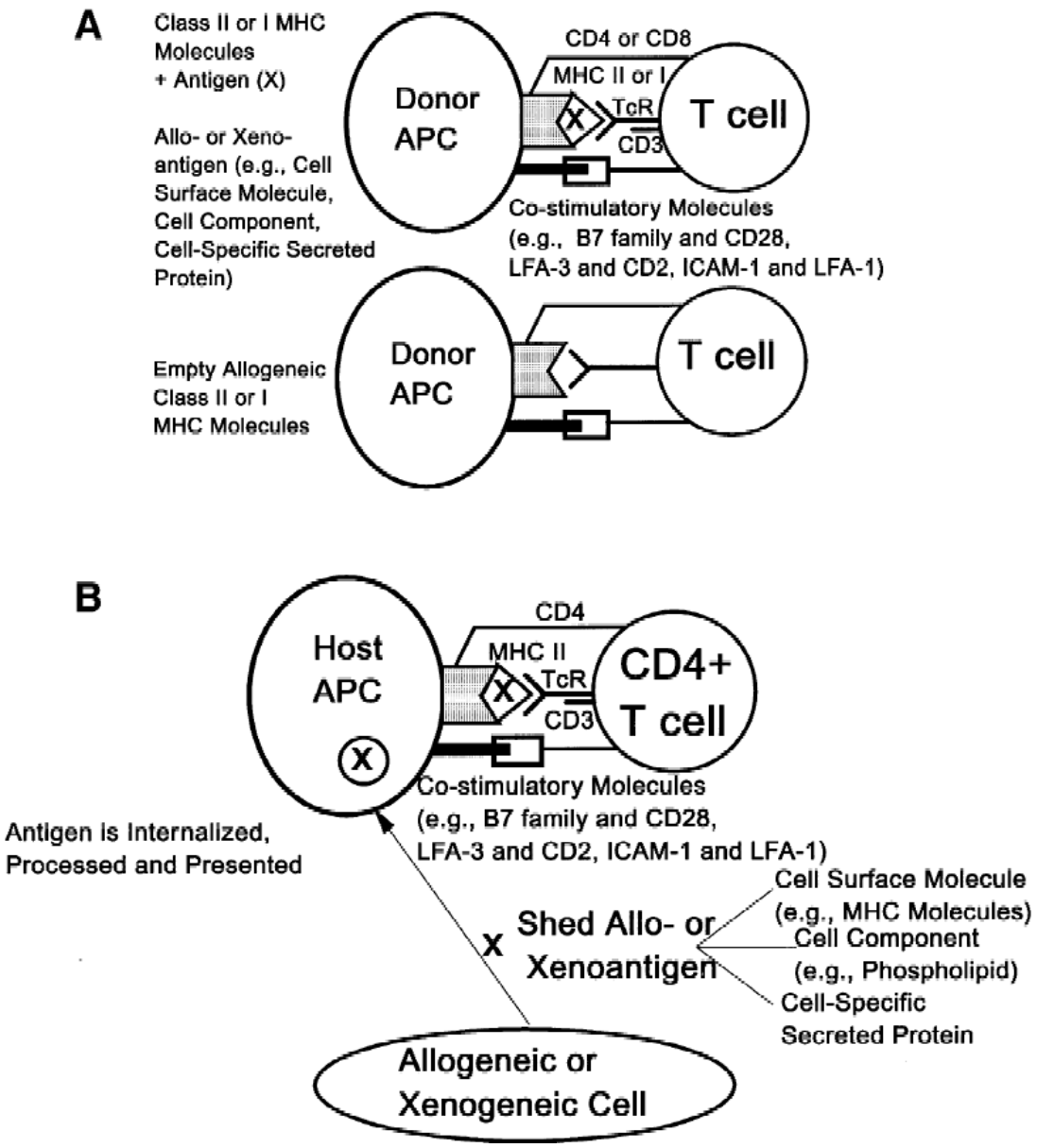

Fig. 1.2. Antigen presentation via the (A) direct pathway, (B) indirect pathway. In the direct pathway of antigen presentation (A), the T cell receptor (TcR) recognizes antigens presented by donor antigen presenting cells (APCs) in association with their Class I or II MHC molecules (top). Alternatively, host T cells can recognize empty allogeneic MHC molecules (bottom). Ligation of the appropriate co-stimulatory molecules is required for T cell activation that will result in T cells specific for the graft antigens presented by the APCs. These peptide antigens, of allogeneic (or xenogeneic) sources, could be derived from cell surface molecules (e.g., MHC molecules), cell components (e.g., phospholipids, DNA), cell-specific secreted proteins. In the indirect pathway of antigen presentation (B), allo- or xenoantigens shed from allogeneic or xenogeneic cells are internalized, processed into peptide fragments by host antigen presenting cells before binding to host Class II MHC molecules and being presented to host CD4 T helper cells. The CD4 molecule of the T cell interacts with the MHC class II molecule and ligation of co-stimulatory molecules are necessary for efficient T cell stimulation. Modified from Babensee *et al.* Adv Drug Deliv Rev, 1998 [40].

donor cell apoptosis (programmed cell death) [54]. T cells may also become activated via *indirect* antigen presentation, whereby immunogenic proteins and peptides are shed from transplanted islets and phagocytosed by host APCs [54]. These host APCs process this material and express it within surface MHC II. $CD4^+$ helper T cells bind these host APCs and, in turn, become activated against specific islet antigens [54]. While unable to induce transplanted cell death directly, $CD4^+$ T cells are involved with activating B cells to secrete anti-antigen antibodies. These antibodies bind to transplanted cells, targeting them for elimination. While direct and indirect antigen presentation are important considerations, Wang *et al.* demonstrated that $CD4^+$ T cell-mediated indirect antigen presentation is implicated in the recurrence of diabetes in non-obese diabetic (NOD) mice following a transplant [56].

1.4.3 Modern immunosuppression strategies

To overcome immune-mediated rejection, systemic immunosuppression remains a hallmark of whole-organ pancreas transplantation into TIDM patients. Many medications have been used to provide chronic immunosuppression, but a particularly effective combination includes mycophenolate mofetil (blocks lymphocyte activation & proliferation [57]) with either tacrolimus [58] or cyclosporin [59], which are thought to reduce T cell IL-2 production, preventing further T cell activation [32, 60, 61]. Unlike other organ transplants, one course of T cell depletion therapy prior to pancreas transplantation (thymoglobulin) is also used to improve outcome (i.e., 92% graft survival after 3 years) [32, 61]. Each of these medications target systemic T cells and the associated clinical success highlights the importance of controlling the T cell response

to transplanted pancreatic material in TIDM patients. While suppressing the host immune system has been shown to allow long-term insulin independence, immunosuppression has numerous side effects including infection, malignancy, and organ toxicity [38]. Thus, islet transplantation would likely become a desirable option for many more TIDM patients if the requirement of systemic immunosuppression was reduced or eliminated.

1.5 IMMUNOISOLATION VIA CELL ENCAPSULATION

Towards the goal of promoting transplant survival in the absence of systemic immunosuppression, researchers have long searched for methods to block direct antigen presentation by graft tissue. More than 60 years ago, Algire *et al.* proposed isolating cells within diffusion chambers to separate them from the host immune system [62]. Since then, researchers have extensively investigated strategies for cell encapsulation, or immunoisolation, prior to implantation. In 1975, Chick *et al.* created synthetic capillaries containing immunoisolated islets that were perfused with tissue culture media [63]. Five years later, Lim & Sun introduced islets encapsulated in semipermeable alginate/poly-L-lysine membranes for the treatment of diabetes in mice [64]. Immunoisolation occurs due to the size-exclusion membrane that is characteristic of encapsulation materials. Nutrients like glucose and oxygen readily diffuse into the capsule, and small, secreted proteins, like insulin, diffuse out. Large molecules and cells, however, including immune cells and antibodies, are prevented from diffusing through the capsule due to size exclusion [65].

1.5.1 Intravascular macroencapsulation

Three platforms are generally employed for islet encapsulation: intravascular macrocapsules (ie. diffusion chamber devices), extravascular microcapsules and

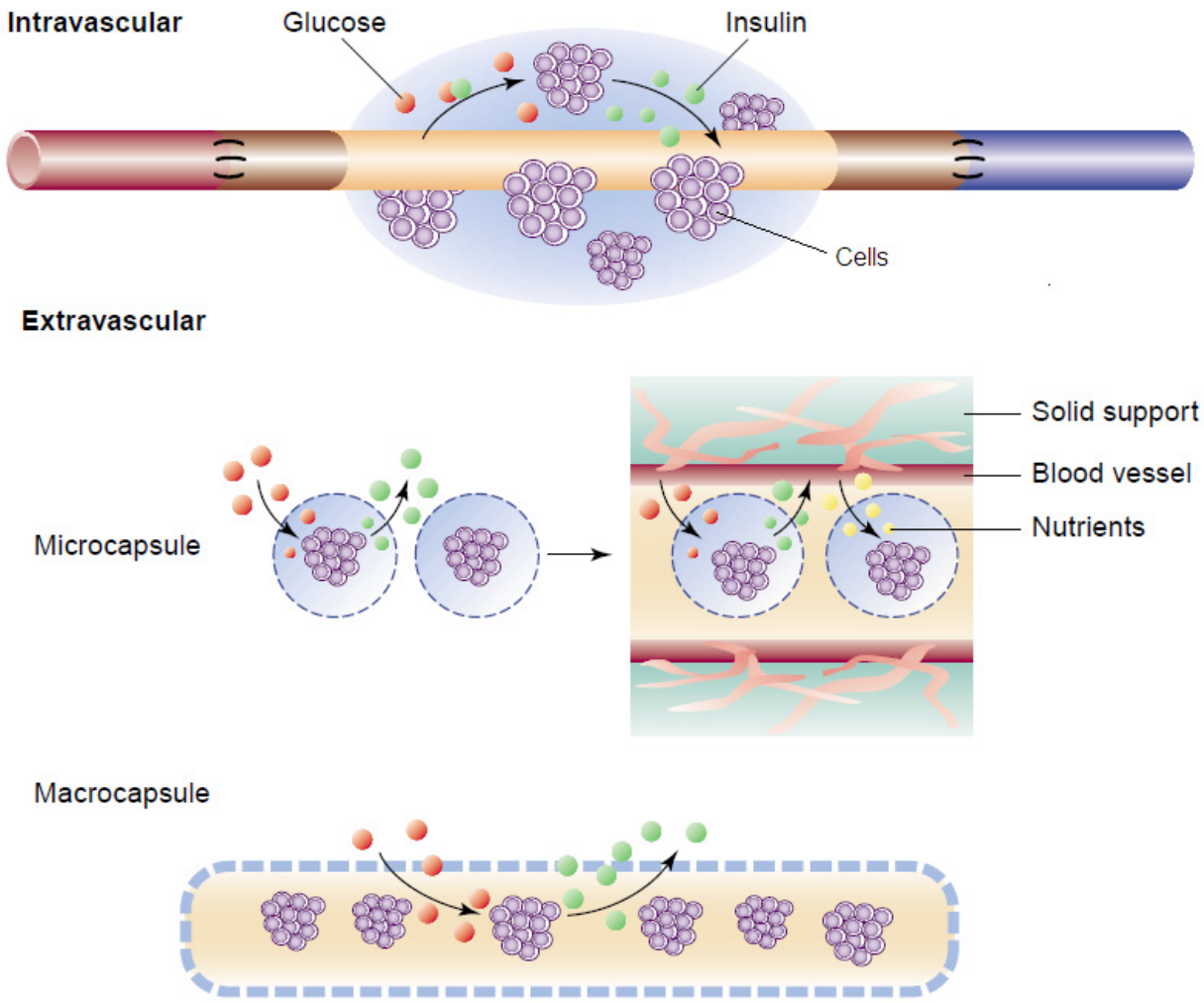

Fig. 1.3. Types of immunoisolation devices. (Top) Intravascular perfusion device with cells surrounding a central lumen with blood flow. (Middle) Extravascular microcapsules are fabricated around individual islets or cell clusters and placed near blood flow. (Bottom) Macrocapsules consist of many islets encapsulated within each a single membrane. Modified from de Vos *et al.* Trends in Mol Med. 2002 [66].

extravascular macrocapsules, Fig. 1.3 [66]. Intravascular devices consist of cells encapsulated in a material structure with a central lumen that may be surgically connected to a blood vessel. This architecture allows blood to flow through the capsule,

providing close contact between blood and cells and enabling rapid nutrient transport [63].

The modified diffusion chamber introduced by Chick *et al*., fabricated from polyacrylonitrile and polyvinylchloride copolymer (PAN-PVC), has been studied in several animal systems and was shown to provide some degree of islet function [63, 67, 68]. Unfortunately, these devices were prone to thrombosis, so systemic anticoagulation was required for success, ultimately limiting the feasibility of this approach [66].

1.5.2 Extravascular microencapsulation

During extravascular microencapsulation, materials are formed directly at the surface of individual cells or islet clusters to fabricate semi-permeable membranes. Islets are then implanted into the peritoneal cavity. While numerous materials have been investigated for islet microencapsulation [65, 69-71], the most extensively investigated platform utilizes alginate - poly-L-lysine – alginate (APA) microcapsules. As pioneered by Lim & Sun, single islets are suspended in alginate droplets and gelation is induced by the addition of a divalent cation solution containing Ca^{2+} [64]. Particles are further coated with a polycation, the most commonly utilized one being poly-L-lysine (PLL), to stabilize the alginate gel and create the semi-permeable immunoisolation membrane. These particles may be modified further with additional alginate to bind free, positively-charged PLL to reduce protein adhesion *in vivo* [72]. Extensive investigations with variations of this material have been performed over the last 30 years, including numerous *in vivo* trials [73-78]. Ultimately, however, overwhelming success is yet to be

achieved [65]. While some concerns about the biocompatibility of APA microcapsules remain, particularly when including PLL [41, 79], recent studies have evaluated specific material alternations, including alginate purification, to reduce protein interactions with capsules [80, 81].

Alternatively, another material platform that has been more recently investigated for pancreatic microencapsulation utilizes poly(ethylene glycol) hydrogels. PEG hydrogels are widely applied for cell encapsulations, as they are hydrophilic materials possessing a high internal water content, which often mimics native tissue properties, and resists protein adsorption. Further, PEG is easily modified chemically to introduce a wide variety of functionalities into capsules. Cruise *et al.* utilized interfacial photopolymerization to coat individual porcine and human islets with thin (<50 μm) layers of PEG hydrogel [82-85]. In this approach, the photoinitiator eosin Y was adsorbed directly to the surface of islets. In the presence of triethanolamine and light, radical polymerization was initiated at the islet surface, resulting in surface mediated gel formation and microencapsulation. Using this approach, greater than 90% islet viability was achieved [84]. This coating strategy has shown promise in preclinical animal studies as well as human trials conducted by Novocell (now known as ViaCyte).

1.5.3 Extravascular macroencapsulation

While some of the advantages of microencapsulation include a high capsule surface area to volume ratio to maximize nutrient transport and the ease of implantation via syringe injection, one major limitation to microencapsulation is that the small device

size makes transplant retrieval difficult [66]. Macrocapsules, conversely, consist of a bulk material with cells suspended throughout. They are larger in size, enabling transplant retrieval. While nutrient transport is a concern within macrocapsules, mathematical models [86] and experiments [87, 88] indicate that sufficient nutrient exchange occurs within macrocapsules as long as proper geometries are selected and islet volume does not exceed 5-10 % of device volume [66]. To date, many material platforms have been investigated for islet macroencapsulation. For example, Dufrane *et al.* recently encapsulated pig islets within alginate macrocapsules, implanted them into primates, and demonstrated 6 month transplant survival in the absence of systemic immunosuppression [87]. Likewise, Grundfest-Broniatowski *et al.* developed a synthetic, ampiphilic membrane and demonstrated *in vivo* survival of macroencapsulated islets [88]. Further, Qi *et al.* used a freeze / thawing technique to encapsulate islets within polymer sheets consisting of poly(vinyl alcohol) (PVA) and Euro-Collins (EC) solution [89]. These devices were able to provide normal glycemic control in diabetic mice for up to 30 days.

1.5.4 Encapsulation within PEG macrocapsules

Anseth *et al.* have previously explored the macroencapsulation of islets and β-cells within PEG hydrogels [90-96]. While many types of PEG hydrogels exist, researchers in the Anseth lab have focused on gels formed from PEG diacrylate (PEGDA) and PEG dimethacrylate (PEGDMA) monomers (2,000 – 10,000 Da), which may be photopolymerized in the presence of long-wave ultraviolet (UV) light and initiator

A

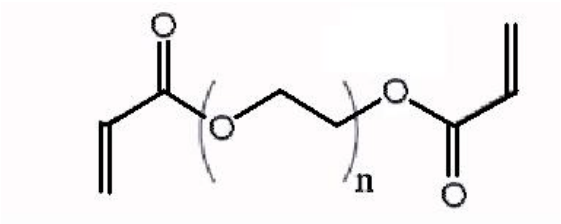

B

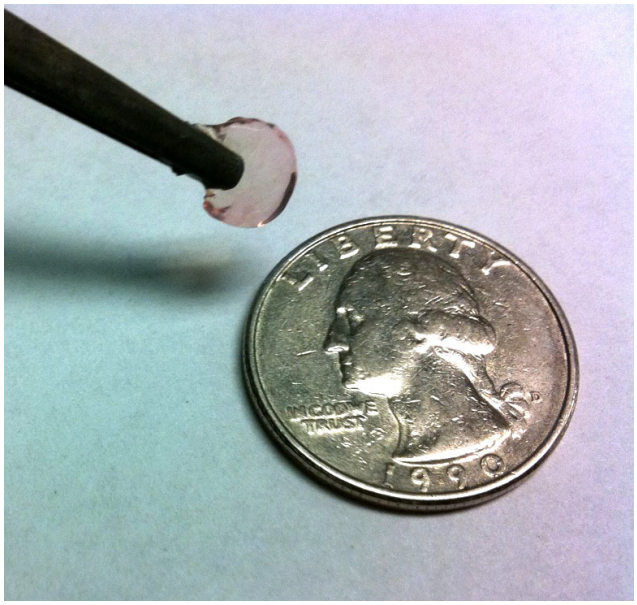

Fig. 1.4. (A) Chemical structure of poly(ethylene glycol) diacrylate (PEGDA). In the presence of initiator and ultraviolet light, PEGDA may be photopolymerized into solid hydrogels (B). Hydrogel shown in (B) appears red in color because rhodamine was included for visualization.

to form a covalently crosslinked polymer network, Fig. 1.4. β-cells and islets are suspended within the PEGDA prepolymer solution, and then immobilized upon photopolymerization. The photoencapsulation of cells [97] and islets [82] has been demonstrated to be highly cytocompatible and efficient, and Weber *et al.* showed that encapsulated β-cell and islet viability and function could be enhanced by the inclusion of extracellular membrane (ECM) proteins and peptide mimics in the hydrogel formulation [90-92]. Further, Lin *et al.* showed that the incorporation of glucagon-like peptide 1 (GLP-1) into hydrogel networks improved β-cell viability and function [94], and illustrated the importance of cell-cell contact within hydrogels for β-cell survival [95, 96]. Thus, PEG hydrogels provide a versatile platform for the incorporation of functional groups to promote healthy β-cell function. While PEG macrocapsules have been the focus of these recent studies, virtually all findings are relevant to PEG microcapsules and other encapsulation systems, and are therefore broadly applicable across multiple encapsulation platforms.

1.6 HOST REJECTION OF ENCAPSULATED TISSUE

1.6.1 Small molecule diffusion

Conceptually, immunoisolation seems to be a logical choice for protecting encapsulated tissue from the host immune system. In practice, however, simple encapsulation has been generally inadequate for the long-term protection of transplanted tissue. The permeability of barriers may be precisely controlled to limit antibodies and immune cells from diffusing within the capsule [65], but it is also crucial that small molecules like glucose and insulin remain able to diffuse freely through the network to allow donor cell survival and function. Unfortunately, nutrients and cellular products are not the only small molecules that pass through the capsule *in vivo*. Rather, low molecular weight cytokines like TNF-α, IL-1β and IL-6, as well as reactive oxygen species (ROS), have been demonstrated to pass through the membrane and injure encapsulated cells [51, 66]. Therefore, limiting the presence of these inflammatory molecules in proximity to a transplant has become a major focus of study.

1.6.2 Indirect antigen presentation

As discussed above (see 1.4 Immunological challenges to islet transplantation), the host's innate immune system likely becomes activated simply from the insult of minor implantation surgery. This activation can result in the production of inflammatory cytokines and ROS which are damaging to donor tissue. Further, the adaptive immune system of the host may become activated against tissue transplants via *indirect* antigen presentation. Encapsulation has been shown to do an adequate job preventing *direct*

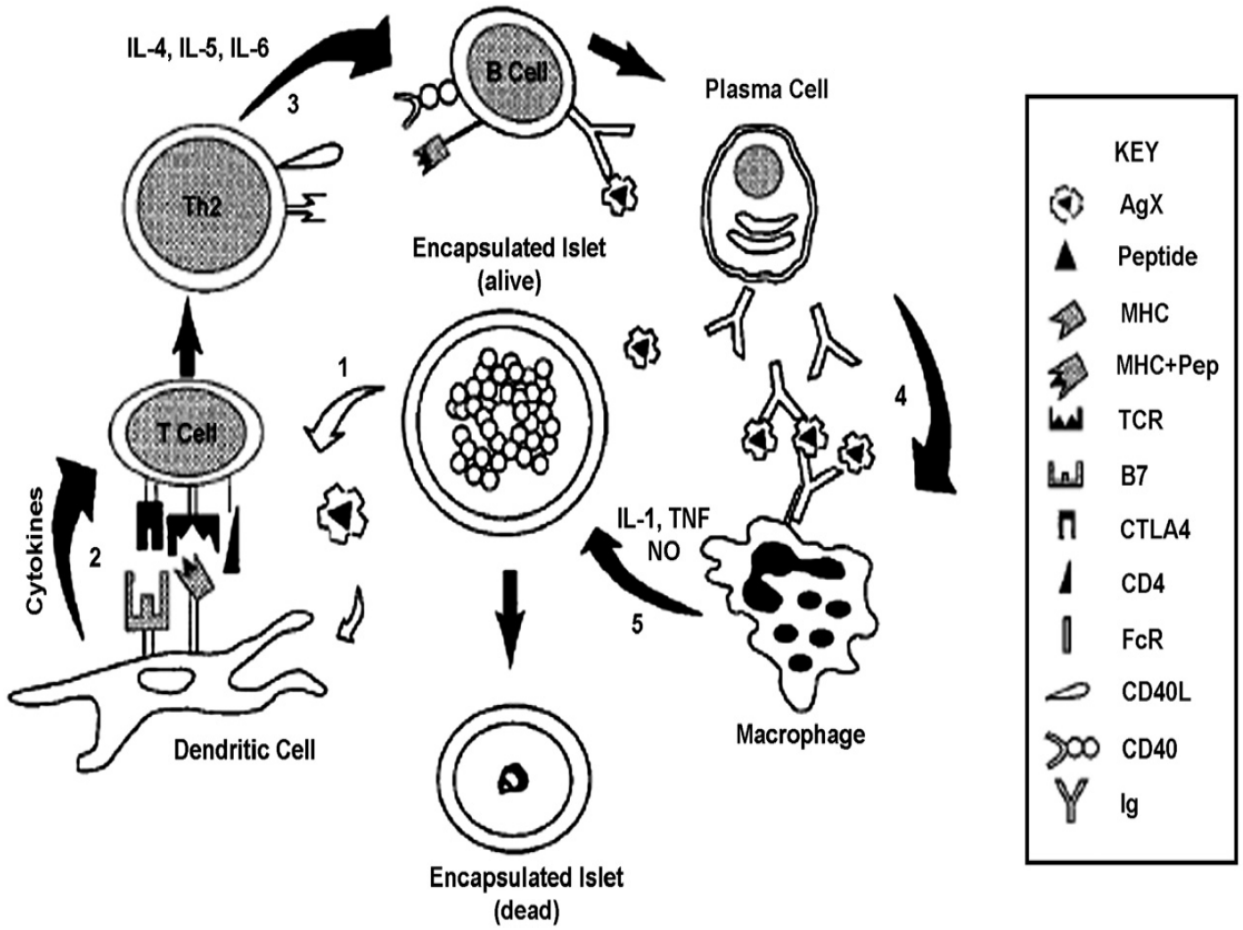

Fig. 1.5. Immune-mediated destruction of encapsulated islets. Foreign antigens are shed from encapsulated islets (1), taken up by host dendritic cells and presented to T cells via indirect antigen presentation (2). Activated $CD4^+$ T cells (Th2) activate host B cells (3) which mature into plasma cells and secrete anti-islet antibodies (Ig). These antibodies bind shed islet proteins outside of the capsule and bind the macrophage Fc receptor (FcR) (4) triggering the production of inflammatory cytokines. These molecules diffuse within the capsule and kill encapsulated islets (5). Adapted from Weber, *et al.* Cell Encapsulation Technology and Therapeutics, 1999.

antigen presentation, by limiting direct contact between host tissue and immune cells. *Indirect* antigen presentation, however, still occurs, Fig. 1.5. Even when encapsulated, antigens from donor cells continue to be shed into the surroundings. This process can occur as cells die and shed protein fragments [70]. Likewise, it is also possible for the immune system to become sensitized against cell products, like insulin [70]. These antigens are phagocytosed by host dendritic cells (DCs) and presented to $CD4^+$ helper T cells. Activated T cells begin secreting inflammatory cytokines and further elicit an immune response by activating B cells to secrete anti-islet antibodies. When local

antibodies bind antigen shed from islet-laden capsules, they can bind and activate macrophages to secrete additional inflammatory cytokines. Therefore, simple encapsulation regimens are likely inadequate for complete islet protection.

1.7 ACTIVE IMMUNOISOLATION BARRIERS

Given that encapsulation within unmodified immunoisolation barriers is unable to provide long-term protection of encapsulated cells, several researchers have recently investigated strategies to activate immunoisolation barriers. Active immunoisolation barriers are typically formed via the introduction of bioactive molecules within immunoisolation barriers. To date, many active immunoisolation barriers have been investigated and most fall into the general categories of materials which release anti-inflammatory molecules or scavenge free radicals and cytokines, Fig. 1.6. In this thesis, an immobilized enzyme is investigated to breakdown reactive oxygen species and two unique immune cell signaling pathways are mimicked to signal adaptive immune cells.

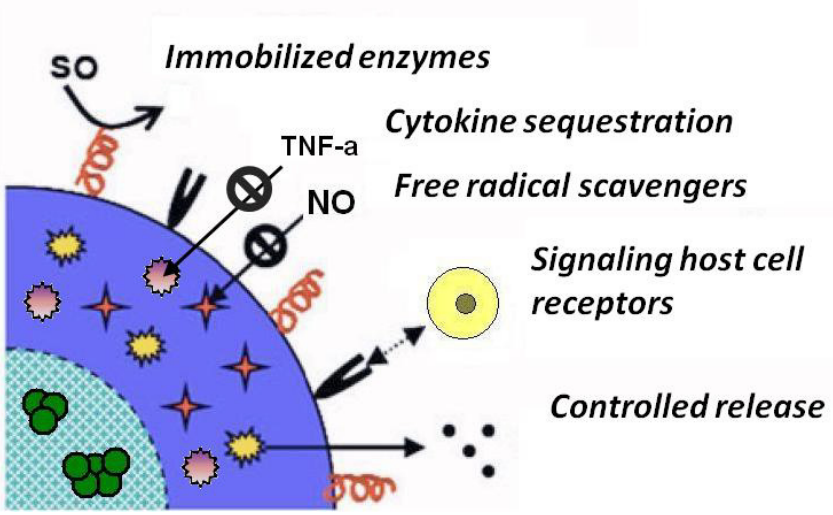

Fig. 1.6. Strategies to control local inflammatory and immune responses. Islets are encapsulated within materials functionalized with various strategies to reduce local inflammation. Modified from Wilson, *et al.* Adv Drug Del Revs. 2008 [70].

1.7.1 Limiting the effects of small cytotoxic molecules

As discussed above, encapsulated cells are thought to be injured by small, cytotoxic molecules able to diffuse within the network. To protect cells, researchers have investigated methods to sequester cytokines within materials, limiting their diffusion. For example, Lin *et al.* tethered anti-TNF-α affinity peptides within cell-laden PEG hydrogels and demonstrated improved cell survival when challenged with TNF-α [98]. To influence the cytokine profile around an encapsulation device, Washburn *et al.* conjugated antibodies against IL-1β and TNF-α to hyaluronic acid for cytokine sequestration and demonstrated fewer activated macrophages responding to adjacent wound sites *in vivo* [99]. To reduce immune cell activation by encapsulated cells, Lin *et al.* also incorporated an affinity peptide for monocyte chemotactic protein 1 (MCP-1) into cell-laden PEG hydrogels and demonstrated decreased antigen release [100]. Reactive oxygen species (ROS) also pose a considerable threat to encapsulated tissue. Towards protecting cells from ROS damage, erthyrocytes (red blood cells) and hemoglobin have been co-transplanted with islets because hemoglobin possesses the capacity to convert nitric oxide (NO) to less-reactive nitrate. These systems prolonged normoglycemia following islet transplants in mice [53, 101]. Further, Cheung *et al*. recently introduced a covalently crosslink-able superoxide dismutase mimetic (SODm) to catalyze the breakdown of superoxide and other ROS within polymeric biomaterials [102]. In this thesis, the capacity of this SODm to protect encapsulated cells from ROS damage is specifically explored.

1.7.2 Anti-inflammatory drug release

Tailoring implantable biomaterials for drug release has been widely explored, and several investigators have recently investigated drug release for the purpose of reducing inflammation. Because standard alginate/poly-lysine microcapsules are known to produce an inflammatory response [41], most anti-inflammatory release has been investigated in the presence of alginate/poly-lysine. For example, Bunger *et al.* co-encapsulated the immunosuppressive steroid dexamethasone within alginate capsules, to provide drug release over a period of 14 days. After 30 days *in vivo*, decreased fibrous capsule formation and improved islet survival was observed [103]. Giovagnoli, *et al.* incorporated the nonsteroidal anti-inflammatory drug (NSAID) ketoprofen and superoxide dismutase (SOD) into degradable poly(D, L-lactide-co-glycolide) (PLGA) and poly(D, L-lactide) (PLA) microspheres for controlled release. Upon incorporation within cell-laden alginate microcapsules and implantation into the mouse peritoneum, they observed a decrease in the number of macrophages and T cells in proximity to the transplantation site [104]. Similarly, Baruch *et al.* released an alternate NSAID, ibuprofen, from PLGA microspheres within alginate and observed increased *in vivo* transplant survival over the period of drug release [105]. Other release platforms have recently been explored, as Yu *et al.* incorporated the NSAIDs ketoprofen [106] and acetaminophen [107] into poly(vinyl pyrrolidone) (PVP) nanofibers for controlled release. Likewise, Aimetti *et al.* reported a degradable peptide-based drug release platform to deliver payload in response to human neutrophil elastase (HNE), an enzyme secreted by activated neutrophils [108].

1.7.3 Co-transplantation of immunosuppressive cell types

While the efficacy of controlled drug release by immunoisolation barriers has been demonstrated, these sorts of approaches are only able to function for a finite length of time; until all therapeutic has been released. In an effort to provide more long-term protection, immunosuppressive cells may be co-encapsulated along with donor cells. For example, Sertoli cells have been co-transplanted with islet allo- [109, 110] and xenografts [111] and significantly improved transplant survival in humans [112]. Sertoli cells are normally found within the testes and provide resistance from the autoimmune-mediated destruction of the developing germ cells [113]. Thus, the co-transplantation of Sertoli cells with islet grafts likely mimics the local immunosuppressive environment of the testes. This effect is thought to be mediated by the release of the immunomodulatory growth factor transforming growth factor beta (TGF-β) [114], the expression of Fas ligand (FasL) to deplete local T cells, and the release of clusterin [113]. Additionally, human mesenchymal stem cells (MSC) have been co-transplanted to promote graft survival [115]. Like Sertoli cells, MSC are thought to provide immunomodulatory signals to prevent rejection. For example, MSC have been shown to block T cell proliferation [116], likely via the secretion of immunomodulatory factors including TGF-β, hepatic growth factors, prostaglandin E2, and IL-10 [117]

1.7.4 Signaling immune cells from material surfaces

Throughout the field of tissue engineering, many investigators have researched interactions between material surfaces and cells. For example, proteins and adhesion

ligands are commonly incorporated on the surfaces of biomaterials, including PEG hydrogels, to promote cell attachment [118]. Growth factors and other bioactive molecules have been patterned on material surfaces to promote cell survival and guide development [119]. Conversely, numerous investigations have been made into understanding interactions between surfaces and innate immune cells, particularly in the settings of reducing macrophage attachment and fibrous capsule formation [40, 120], as well as characterizing dendritic cell activation by various material surfaces [121-123]. Presently, however, few strategies have been investigated whereby functionalized surfaces are employed to signal immune-cells [124, 125]. Two material platforms to reduce the local concentration of T cells, via surface receptor signaling, are considered in this thesis. Additionally, anti-inflammatory molecules are tethered to the surfaces of PEG hydrogels to signal dendritic cells and decrease their activation in response to immune stimuli in an effort to reduce indirect antigen presentation.

1.8 THESIS APPROACH

The overall objective of this thesis is to utilize PEG-based materials as modifiable platforms to investigate bioactive modifications to reduce immune-mediated inflammation toward cell-laden biomaterials. Tissue rejection is a major hurdle to the success of implanted cell-delivery devices so strategies to ameliorate or modify the host immune response have the potential to significantly improve transplant outcomes. The Specific Aims of this thesis, as well as their rationale, are outlined in Chapter 2. In Chapter 3, results from studies with a polymerizable superoxide dismutase mimetic (SODm) are presented. SODm is covalently incorporated within β-cell-laden hydrogels

to demonstrate and evaluate this molecule's capacity to protect encapsulated cells from reactive oxygen species (ROS)-mediated cell death. As described above, ROS are known to damage encapsulated tissue and, herein, it is demonstrated that the polymerizable SODm provides significant protection from chemically generated superoxide.

In Chapters 4 and 5, methods to signal T cells to undergo apoptosis via functionalized biomaterial surfaces are investigated. T cells are a primary mediator of the adaptive immune response so methods to reduce the local concentration of T cells in proximity to cell delivery devices have the capacity to improve transplant survival. In Chapter 4, surface-initiated, photoiniferter-based photopolymerizations are employed to fabricate PEG chains with pendant anti-fas antibody on hard plastic substrates. Surfaces are shown to induce T cell apoptosis, and this effect is increased by the addition of a T cell adhesion ligand, ICAM-1. In Chapter 5, immune cell signaling is provided by conformal, PEG-based coatings fabricated directly on the surfaces of PEG hydrogels via reactive dip coatings initiated by the glucose oxidase enzyme. This coating strategy is demonstrated to create highly-functionalized conformal polymer layers of precise thicknesses and with the capacity to induce significant T cell apoptosis.

In Chapter 6, biologically-functionalized PEG hydrogels are employed to signal dendritic cells (DCs). DCs present antigens to the adaptive immune system and play a critical role in determining whether or not to initiate an immune response. Herein, PEG hydrogels are functionalized with the anti-inflammatory molecules TGF-β1 and IL-10 to reduce the maturation state of bone marrow-derived dendritic cells when challenged with immune stimuli. This work furthers understanding of the interactions possible

between functionalized PEG materials and the immune system and lays a foundation for potential modifications to implantable biomaterials to provide greater immunoisolation. Finally, in Chapter 7, general conclusions are drawn from this work and future directions are discussed.

1.9 REFERENCES

1. Incidence and trends of childhood Type 1 diabetes worldwide 1990-1999. Diabet Med 2006 Aug;23(8):857-866.

2. Prentki M, Tornheim K, Corkey BE. Signal transduction mechanisms in nutrient-induced insulin secretion. Diabetologia 1997 Jul;40 Suppl 2:S32-41.

3. Vanelli M, Chiarelli F. Treatment of diabetic ketoacidosis in children and adolescents. Acta Biomed 2003 Aug;74(2):59-68.

4. Lawrence SE, Cummings EA, Gaboury I, Daneman D. Population-based study of incidence and risk factors for cerebral edema in pediatric diabetic ketoacidosis. The Journal of pediatrics 2005 May;146(5):688-692.

5. Siafarikas A, O'Connell S. Type 1 diabetes in children - emergency management. Australian family physician May;39(5):290-293.

6. Gremizzi C, Vergani A, Paloschi V, Secchi A. Impact of pancreas transplantation on type 1 diabetes-related complications. Current opinion in organ transplantation 2010 Feb;15(1):119-123.

7. Sheetz MJ, King GL. Molecular understanding of hyperglycemia's adverse effects for diabetic complications. Jama 2002 Nov 27;288(20):2579-2588.

8. Goh SY, Cooper ME. Clinical review: The role of advanced glycation end products in progression and complications of diabetes. The Journal of clinical endocrinology and metabolism 2008 Apr;93(4):1143-1152.

9. The effect of intensive treatment of diabetes on the development and progression of long-term complications in insulin-dependent diabetes mellitus. The Diabetes Control and Complications Trial Research Group. The New England journal of medicine 1993 Sep 30;329(14):977-986.

10. Cryer PE, Davis SN, Shamoon H. Hypoglycemia in diabetes. Diabetes care 2003 Jun;26(6):1902-1912.

11. Hypoglycemia in the Diabetes Control and Complications Trial. The Diabetes Control and Complications Trial Research Group. Diabetes 1997 Feb;46(2):271-286.

12. Boyle PJ, Kempers SF, O'Connor AM, Nagy RJ. Brain glucose uptake and unawareness of hypoglycemia in patients with insulin-dependent diabetes mellitus. The New England journal of medicine 1995 Dec 28;333(26):1726-1731.

13. Jun HS, Yoon JW. Approaches for the cure of type 1 diabetes by cellular and gene therapy. Current gene therapy 2005 Apr;5(2):249-262.

14. Yechoor V, Chan L. Gene therapy progress and prospects: gene therapy for diabetes mellitus. Gene therapy 2005 Jan;12(2):101-107.

15. Aye T, Block J, Buckingham B. Toward closing the loop: an update on insulin pumps and continuous glucose monitoring systems. Endocrinology and metabolism clinics of North America 2010 Sep;39(3):609-624.

16. Kumareswaran K, Evans ML, Hovorka R. Artificial pancreas: an emerging approach to treat Type 1 diabetes. Expert review of medical devices 2009 Jul;6(4):401-410.

17. Minkowski O. Untersuchungen über den Diabetes mellitus nach Extirpation des Pankreas. Berl Klin Wchnschr 1892;29:90.

18. Watson-Williams P. Notes on Diabetes treated with extract and by grafts of sheep's pancreas. British Medical Journal 1894;2:1303-1304.

19. Ballinger WF, Lacy PE. Transplantation of intact pancreatic islets in rats. Surgery 1972 Aug;72(2):175-186.

20. Ricordi C, Lacy PE, Finke EH, Olack BJ, Scharp DW. Automated method for isolation of human pancreatic islets. Diabetes 1988 Apr;37(4):413-420.

21. Scharp DW, Lacy PE, Santiago JV, McCullough CS, Weide LG, Falqui L, et al. Insulin independence after islet transplantation into type I diabetic patient. Diabetes 1990 Apr;39(4):515-518.

22. Alesci S, De Martino MU, Ilias I, Gold PW, Chrousos GP. Glucocorticoid-induced osteoporosis: from basic mechanisms to clinical aspects. Neuroimmunomodulation 2005;12(1):1-19.

23. Qi D, Rodrigues B. Glucocorticoids produce whole body insulin resistance with changes in cardiac metabolism. American journal of physiology 2007 Mar;292(3):E654-667.

24. Shapiro AM, Lakey JR, Ryan EA, Korbutt GS, Toth E, Warnock GL, et al. Islet transplantation in seven patients with type 1 diabetes mellitus using a glucocorticoid-free immunosuppressive regimen. The New England journal of medicine 2000 Jul 27;343(4):230-238.

25. Ryan EA, Lakey JR, Paty BW, Imes S, Korbutt GS, Kneteman NM, et al. Successful islet transplantation: continued insulin reserve provides long-term glycemic control. Diabetes 2002 Jul;51(7):2148-2157.

26. Goss JA, Schock AP, Brunicardi FC, Goodpastor SE, Garber AJ, Soltes G, et al. Achievement of insulin independence in three consecutive type-1 diabetic patients via pancreatic islet transplantation using islets isolated at a remote islet isolation center. Transplantation 2002 Dec 27;74(12):1761-1766.

27. Ricordi C. Islet transplantation: a brave new world. Diabetes 2003 Jul;52(7):1595-1603.

28. Shapiro AM, Ricordi C, Hering BJ, Auchincloss H, Lindblad R, Robertson RP, et al. International trial of the Edmonton protocol for islet transplantation. The New England journal of medicine 2006 Sep 28;355(13):1318-1330.

29. Bromberg JS, LeRoith D. Diabetes cure--is the glass half full? The New England journal of medicine 2006 Sep 28;355(13):1372-1374.

30. Poggioli R, Faradji RN, Ponte G, Betancourt A, Messinger S, Baidal DA, et al. Quality of life after islet transplantation. Am J Transplant 2006 Feb;6(2):371-378.

31. Gruessner AC, Sutherland DE. Pancreas transplant outcomes for United States (US) cases as reported to the United Network for Organ Sharing (UNOS) and the International Pancreas Transplant Registry (IPTR). Clinical transplants 2008:45-56.

32. White SA, Shaw JA, Sutherland DE. Pancreas transplantation. Lancet 2009 May 23;373(9677):1808-1817.

33. Fiorina P, Venturini M, Folli F, Losio C, Maffi P, Placidi C, et al. Natural history of kidney graft survival, hypertrophy, and vascular function in end-stage renal disease type 1 diabetic kidney-transplanted patients: beneficial impact of pancreas and successful islet cotransplantation. Diabetes care 2005 Jun;28(6):1303-1310.

34. Lee TC, Barshes NR, O'Mahony CA, Nguyen L, Brunicardi FC, Ricordi C, et al. The effect of pancreatic islet transplantation on progression of diabetic retinopathy and neuropathy. Transplantation proceedings 2005 Jun;37(5):2263-2265.

35. Fiorina P, Folli F, Zerbini G, Maffi P, Gremizzi C, Di Carlo V, et al. Islet transplantation is associated with improvement of renal function among uremic patients with type I diabetes mellitus and kidney transplants. J Am Soc Nephrol 2003 Aug;14(8):2150-2158.

36. Wiseman AC. Simultaneous pancreas kidney transplantation: a critical appraisal of the risks and benefits compared with other treatment alternatives. Advances in chronic kidney disease 2009 Jul;16(4):278-287.

37. Ryan EA, Paty BW, Senior PA, Bigam D, Alfadhli E, Kneteman NM, et al. Five-year follow-up after clinical islet transplantation. Diabetes 2005 Jul;54(7):2060-2069.

38. Leitao CB, Cure P, Tharavanij T, Baidal DA, Alejandro R. Current challenges in islet transplantation. Current diabetes reports 2008 Aug;8(4):324-331.

39. Ryan EA, Bigam D, Shapiro AM. Current indications for pancreas or islet transplant. Diabetes, obesity & metabolism 2006 Jan;8(1):1-7.

40. Babensee JE, McIntire LV, Anderson JM, Mikos AG. Host response to tissue engineered devices. Advanced drug delivery reviews 1998 Aug 3;33(1-2):111-139.

41. Robitaille R, Dusseault J, Henley N, Desbiens K, Labrecque N, Halle JP. Inflammatory response to peritoneal implantation of alginate-poly-L-lysine microcapsules. Biomaterials 2005 Jul;26(19):4119-4127.

42. Berney T, Molano RD, Cattan P, Pileggi A, Vizzardelli C, Oliver R, et al. Endotoxin-mediated delayed islet graft function is associated with increased intra-islet cytokine production and islet cell apoptosis. Transplantation 2001 Jan 15;71(1):125-132.

43. Matsuda T, Omori K, Vuong T, Pascual M, Valiente L, Ferreri K, et al. Inhibition of p38 pathway suppresses human islet production of pro-inflammatory cytokines and improves islet graft function. Am J Transplant 2005 Mar;5(3):484-493.

44. Ehrnfelt C, Kumagai-Braesch M, Uzunel M, Holgersson J. Adult porcine islets produce MCP-1 and recruit human monocytes in vitro. Xenotransplantation 2004 Mar;11(2):184-194.

45. Chen MC, Proost P, Gysemans C, Mathieu C, Eizirik DL. Monocyte chemoattractant protein-1 is expressed in pancreatic islets from prediabetic NOD mice and in interleukin-1 beta-exposed human and rat islet cells. Diabetologia 2001 Mar;44(3):325-332.

46. Thomas HE, Darwiche R, Corbett JA, Kay TW. Interleukin-1 plus gamma-interferon-induced pancreatic beta-cell dysfunction is mediated by beta-cell nitric oxide production. Diabetes 2002 Feb;51(2):311-316.

47. Johansson U, Olsson A, Gabrielsson S, Nilsson B, Korsgren O. Inflammatory mediators expressed in human islets of Langerhans: implications for islet transplantation. Biochemical and biophysical research communications 2003 Aug 29;308(3):474-479.

48. Anderson JM. Inflammatory response to implants. ASAIO transactions / American Society for Artificial Internal Organs 1988 Apr-Jun;34(2):101-107.

49. Di Matteo MA, Loweth AC, Thomas S, Mabley JG, Morgan NG, Thorpe JR, et al. Superoxide, nitric oxide, peroxynitrite and cytokine combinations all cause functional

impairment and morphological changes in rat islets of Langerhans and insulin secreting cell lines, but dictate cell death by different mechanisms. Apoptosis 1997;2(2):164-177.

50. Rabinovitch A, Suarez-Pinzon WL. Cytokines and their roles in pancreatic islet beta-cell destruction and insulin-dependent diabetes mellitus. Biochemical pharmacology 1998 Apr 15;55(8):1139-1149.

51. Jang JY, Lee DY, Park SJ, Byun Y. Immune reactions of lymphocytes and macrophages against PEG-grafted pancreatic islets. Biomaterials 2004 Aug;25(17):3663-3669.

52. Yoon JW, Jun HS, Santamaria P. Cellular and molecular mechanisms for the initiation and progression of beta cell destruction resulting from the collaboration between macrophages and T cells. Autoimmunity 1998;27(2):109-122.

53. Wiegand F, Kroncke KD, Kolb-Bachofen V. Macrophage-generated nitric oxide as cytotoxic factor in destruction of alginate-encapsulated islets. Protection by arginine analogs and/or coencapsulated erythrocytes. Transplantation 1993 Nov;56(5):1206-1212.

54. Gill RG. Antigen presentation pathways for immunity to islet transplants. Relevance to immunoisolation. Annals of the New York Academy of Sciences 1999 Jun 18;875:255-260.

55. Gray DW. Encapsulated islet cells: the role of direct and indirect presentation and the relevance to xenotransplantation and autoimmune recurrence. British medical bulletin 1997;53(4):777-788.

56. Wang Y, Pontesilli O, Gill RG, La Rosa FG, Lafferty KJ. The role of CD4+ and CD8+ T cells in the destruction of islet grafts by spontaneously diabetic mice. Proceedings of the National Academy of Sciences of the United States of America 1991 Jan 15;88(2):527-531.

57. Fulton B, Markham A. Mycophenolate mofetil. A review of its pharmacodynamic and pharmacokinetic properties and clinical efficacy in renal transplantation. Drugs 1996 Feb;51(2):278-298.

58. Klintmalm GB, Goldstein R, Gonwa T, Wiesner RH, Krom RA, Shaw BW, Jr., et al. Prognostic factors for successful conversion from cyclosporine to FK 506-based immunosuppressive therapy for refractory rejection after liver transplantation. US Multicenter FK 506 Liver Study Group. Transplantation proceedings 1993 Feb;25(1 Pt 1):641-643.

59. Faulds D, Goa KL, Benfield P. Cyclosporin. A review of its pharmacodynamic and pharmacokinetic properties, and therapeutic use in immunoregulatory disorders. Drugs 1993 Jun;45(6):953-1040.

60. Stegall MD, Simon M, Wachs ME, Chan L, Nolan C, Kam I. Mycophenolate mofetil decreases rejection in simultaneous pancreas-kidney transplantation when combined with tacrolimus or cyclosporine. Transplantation 1997 Dec 27;64(12):1695-1700.

61. Cantarovich D, Vistoli F. Minimization protocols in pancreas transplantation. Transpl Int 2009 Jan;22(1):61-68.

62. Algire GH. An adaption of the transparant chamber technique to the mouse. Journal of the National Cancer Institute 1943;4:1-11.

63. Chick WL, Like AA, Lauris V. Beta cell culture on synthetic capillaries: an artificial endocrine pancreas. Science (New York, NY 1975 Mar 7;187(4179):847-849.

64. Lim F, Sun AM. Microencapsulated islets as bioartificial endocrine pancreas. Science (New York, NY 1980 Nov 21;210(4472):908-910.

65. de Vos P, Spasojevic M, Faas MM. Treatment of diabetes with encapsulated islets. Advances in experimental medicine and biology 2010;670:38-53.

66. de Vos P, Marchetti P. Encapsulation of pancreatic islets for transplantation in diabetes: the untouchable islets. Trends Mol Med 2002 Aug;8(8):363-366.

67. Sun AM, Parisius W, Healy GM, Vacek I, Macmorine HG. The use, in diabetic rats and monkeys, of artificial capillary units containing cultured islets of Langerhans (artificial endocrine pancreas). Diabetes 1977 Dec;26(12):1136-1139.

68. Maki T, Lodge JP, Carretta M, Ohzato H, Borland KM, Sullivan SJ, et al. Treatment of severe diabetes mellitus for more than one year using a vascularized hybrid artificial pancreas. Transplantation 1993 Apr;55(4):713-717; discussion 717-718.

69. Beck J, Angus R, Madsen B, Britt D, Vernon B, Nguyen KT. Islet encapsulation: strategies to enhance islet cell functions. Tissue Eng 2007 Mar;13(3):589-599.

70. Wilson JT, Chaikof EL. Challenges and emerging technologies in the immunoisolation of cells and tissues. Advanced drug delivery reviews 2008 Jan 14;60(2):124-145.

71. de Vos P, Hamel AF, Tatarkiewicz K. Considerations for successful transplantation of encapsulated pancreatic islets. Diabetologia 2002 Feb;45(2):159-173.

72. Vandenbossche GM, Bracke ME, Cuvelier CA, Bortier HE, Mareel MM, Remon JP. Host reaction against empty alginate-polylysine microcapsules. Influence of preparation procedure. The Journal of pharmacy and pharmacology 1993 Feb;45(2):115-120.

73. Weber C, Ayres-Price J, Costanzo M, Becker A, Stall A. NOD mouse peritoneal cellular response to poly-L-lysine-alginate microencapsulated rat islets. Transplantation proceedings 1994 Jun;26(3):1116-1119.

74. Trivedi N, Keegan M, Steil GM, Hollister-Lock J, Hasenkamp WM, Colton CK, et al. Islets in alginate macrobeads reverse diabetes despite minimal acute insulin secretory responses. Transplantation 2001 Jan 27;71(2):203-211.

75. Soon-Shiong P, Feldman E, Nelson R, Heintz R, Yao Q, Yao Z, et al. Long-term reversal of diabetes by the injection of immunoprotected islets. Proceedings of the National Academy of Sciences of the United States of America 1993 Jun 15;90(12):5843-5847.

76. Sun Y, Ma X, Zhou D, Vacek I, Sun AM. Normalization of diabetes in spontaneously diabetic cynomologus monkeys by xenografts of microencapsulated porcine islets without immunosuppression. The Journal of clinical investigation 1996 Sep 15;98(6):1417-1422.

77. Leu FJ, Chen CF, Chiang WE, Chern HT, Shian LR, Chung TM, et al. Microencapsulated pancreatic islets: a pathologic study. Journal of the Formosan Medical Association = Taiwan yi zhi 1992 Sep;91(9):849-858.

78. O'Shea GM, Goosen MF, Sun AM. Prolonged survival of transplanted islets of Langerhans encapsulated in a biocompatible membrane. Biochimica et biophysica acta 1984 May 22;804(1):133-136.

79. Strand BL, Ryan TL, In't Veld P, Kulseng B, Rokstad AM, Skjak-Brek G, et al. Poly-L-Lysine induces fibrosis on alginate microcapsules via the induction of cytokines. Cell transplantation 2001;10(3):263-275.

80. Mallett AG, Korbutt GS. Alginate modification improves long-term survival and function of transplanted encapsulated islets. Tissue engineering 2009 Jun;15(6):1301-1309.

81. Langlois G, Dusseault J, Bilodeau S, Tam SK, Magassouba D, Halle JP. Direct effect of alginate purification on the survival of islets immobilized in alginate-based microcapsules. Acta biomaterialia 2009 Nov;5(9):3433-3440.

82. Hill RS, Cruise GM, Hager SR, Lamberti FV, Yu X, Garufis CL, et al. Immunoisolation of adult porcine islets for the treatment of diabetes mellitus. The use of photopolymerizable polyethylene glycol in the conformal coating of mass-isolated porcine islets. Annals of the New York Academy of Sciences 1997 Dec 31;831:332-343.

83. Cruise GM, Hegre OD, Lamberti FV, Hager SR, Hill R, Scharp DS, et al. In vitro and in vivo performance of porcine islets encapsulated in interfacially photopolymerized

poly(ethylene glycol) diacrylate membranes. Cell transplantation 1999 May-Jun;8(3):293-306.

84. Cruise GM, Hegre OD, Scharp DS, Hubbell JA. A sensitivity study of the key parameters in the interfacial photopolymerization of poly(ethylene glycol) diacrylate upon porcine islets. Biotechnology and bioengineering 1998 Mar 20;57(6):655-665.

85. Cruise GM, Scharp DS, Hubbell JA. Characterization of permeability and network structure of interfacially photopolymerized poly(ethylene glycol) diacrylate hydrogels. Biomaterials 1998 Jul;19(14):1287-1294.

86. Thrash M. Modeling oxygen transport in a cylindrical bioartificial pancreas. Asaio J 2010 Jul-Aug;56(4):338-343.

87. Dufrane D, Goebbels RM, Gianello P. Alginate Macroencapsulation of Pig Islets Allows Correction of Streptozotocin-Induced Diabetes in Primates up to 6 Months Without Immunosuppression. Transplantation Oct 22.

88. Grundfest-Broniatowski SF, Tellioglu G, Rosenthal KS, Kang J, Erdodi G, Yalcin B, et al. A new bioartificial pancreas utilizing amphiphilic membranes for the immunoisolation of porcine islets: a pilot study in the canine. ASAIO J 2009 Jul-Aug;55(4):400-405.

89. Qi M, Gu Y, Sakata N, Kim D, Shirouzu Y, Yamamoto C, et al. PVA hydrogel sheet macroencapsulation for the bioartificial pancreas. Biomaterials 2004 Dec;25(27):5885-5892.

90. Weber LM, Anseth KS. Hydrogel encapsulation environments functionalized with extracellular matrix interactions increase islet insulin secretion. Matrix Biol 2008 Oct;27(8):667-673.

91. Weber LM, Hayda KN, Haskins K, Anseth KS. The effects of cell-matrix interactions on encapsulated beta-cell function within hydrogels functionalized with matrix-derived adhesive peptides. Biomaterials 2007 Jul;28(19):3004-3011.

92. Weber LM, Hayda KN, Anseth KS. Cell-matrix interactions improve beta-cell survival and insulin secretion in three-dimensional culture. Tissue engineering 2008 Dec;14(12):1959-1968.

93. Weber LM, Cheung CY, Anseth KS. Multifunctional pancreatic islet encapsulation barriers achieved via multilayer PEG hydrogels. Cell transplantation 2008;16(10):1049-1057.

94. Lin CC, Anseth KS. Glucagon-Like Peptide-1 Functionalized PEG Hydrogels Promote Survival and Function of Encapsulated Pancreatic beta-Cells. Biomacromolecules 2009 Sep;10(9):2460-2467.

95. Hume PS. Polymerizable superoxide dismutase mimetic protects β-cells encapsulated in PEG hydrogels from reactive oxygen species-mediated damage. Tissue engineering 2011.

96. Lin CC. Cell-cell communication mimicry with PEG hydrogels for enhancing Beta-cell function. Proc Natl Acad Sci USA 2010 2010.

97. Bryant SJ, Nuttelman CR, Anseth KS. Cytocompatibility of UV and visible light photoinitiating systems on cultured NIH/3T3 fibroblasts in vitro. J Biomater Sci Polym Ed 2000;11(5):439-457.

98. Lin CC, Metters AT, Anseth KS. Functional PEG-peptide hydrogels to modulate local inflammation induced by the pro-inflammatory cytokine TNFalpha. Biomaterials 2009 Oct;30(28):4907-4914.

99. Sun LT, Bencherif SA, Gilbert TW, Farkas AM, Lotze MT, Washburn NR. Biological activities of cytokine-neutralizing hyaluronic acid-antibody conjugates. Wound Repair Regen May-Jun;18(3):302-310.

100. Lin CC, Boyer PD, Aimetti AA, Anseth KS. Regulating MCP-1 diffusion in affinity hydrogels for enhancing immuno-isolation. J Control Release 2010 Mar 19;142(3):384-391.

101. Chae SY, Lee M, Kim SW, Bae YH. Protection of insulin secreting cells from nitric oxide induced cellular damage by crosslinked hemoglobin. Biomaterials 2004 Feb;25(5):843-850.

102. Cheung CY, McCartney SJ, Anseth K. Synthesis of Polymerizable Superoxide Dismutase Mimetics to Reduce Reactive Oxygen Species Damage in Transplanted Biomedical Devices. Advanced Functional Materials 2008;18:3119-3126.

103. Bunger CM, Tiefenbach B, Jahnke A, Gerlach C, Freier T, Schmitz KP, et al. Deletion of the tissue response against alginate-pll capsules by temporary release of co-encapsulated steroids. Biomaterials 2005 May;26(15):2353-2360.

104. Giovagnoli S, Blasi P, Luca G, Fallarino F, Calvitti M, Mancuso F, et al. Bioactive long-term release from biodegradable microspheres preserves implanted ALG-PLO-ALG microcapsules from in vivo response to purified alginate. Pharmaceutical research 2010 Feb;27(2):285-295.

105. Baruch L, Benny O, Gilert A, Ukobnik M, Ben Itzhak O, Machluf M. Alginate-PLL cell encapsulation system Co-entrapping PLGA-microspheres for the continuous release of anti-inflammatory drugs. Biomedical microdevices 2009 Jun 11.

106. Yu DG, Branford-White C, Shen XX, Zhang XF, Zhu LM. Solid Dispersions of Ketoprofen in Drug-Loaded Electrospun Nanofibers. J Dispersion Sci Technol 2010;31(7):902-908.

107. Yu DG, Branford-White C, White K, Li XL, Zhu LM. Dissolution Improvement of Electrospun Nanofiber-Based Solid Dispersions for Acetaminophen. AAPS PharmSciTech Jun;11(2):809-817.

108. Aimetti AA, Tibbitt MW, Anseth KS. Human neutrophil elastase responsive delivery from poly(ethylene glycol) hydrogels. Biomacromolecules 2009 Jun 8;10(6):1484-1489.

109. Takeda Y, Gotoh M, Dono K, Nishihara M, Grochowiecki T, Kimura F, et al. Protection of islet allografts transplanted together with Fas ligand expressing testicular allografts. Diabetologia 1998 Mar;41(3):315-321.

110. Korbutt GS, Elliott JF, Rajotte RV. Cotransplantation of allogeneic islets with allogeneic testicular cell aggregates allows long-term graft survival without systemic immunosuppression. Diabetes 1997 Feb;46(2):317-322.

111. Dufour JM, Rajotte RV, Kin T, Korbutt GS. Immunoprotection of rat islet xenografts by cotransplantation with sertoli cells and a single injection of antilymphocyte serum. Transplantation 2003 May 15;75(9):1594-1596.

112. Valdes-Gonzalez RA, Dorantes LM, Garibay GN, Bracho-Blanchet E, Mendez AJ, Davila-Perez R, et al. Xenotransplantation of porcine neonatal islets of Langerhans and Sertoli cells: a 4-year study. Eur J Endocrinol 2005 Sep;153(3):419-427.

113. Dufour JM, Rajotte RV, Korbutt GS, Emerich DF. Harnessing the immunomodulatory properties of Sertoli cells to enable xenotransplantation in type I diabetes. Immunol Invest 2003 Nov;32(4):275-297.

114. Suarez-Pinzon W, Korbutt GS, Power R, Hooton J, Rajotte RV, Rabinovitch A. Testicular sertoli cells protect islet beta-cells from autoimmune destruction in NOD mice by a transforming growth factor-beta1-dependent mechanism. Diabetes 2000 Nov;49(11):1810-1818.

115. Abdi R, Fiorina P, Adra CN, Atkinson M, Sayegh MH. Immunomodulation by mesenchymal stem cells: a potential therapeutic strategy for type 1 diabetes. Diabetes 2008 Jul;57(7):1759-1767.

116. Le Blanc K, Tammik L, Sundberg B, Haynesworth SE, Ringden O. Mesenchymal stem cells inhibit and stimulate mixed lymphocyte cultures and mitogenic responses independently of the major histocompatibility complex. Scand J Immunol 2003 Jan;57(1):11-20.

117. Tyndall A, Walker UA, Cope A, Dazzi F, De Bari C, Fibbe W, et al. Immunomodulatory properties of mesenchymal stem cells: a review based on an interdisciplinary meeting held at the Kennedy Institute of Rheumatology Division, London, UK, 31 October 2005. Arthritis Res Ther 2007;9(1):301.

118. Tibbitt MW, Anseth KS. Hydrogels as extracellular matrix mimics for 3D cell culture. Biotechnology and bioengineering 2009 Jul 1;103(4):655-663.

119. Ito Y. Surface micropatterning to regulate cell functions. Biomaterials 1999 Dec;20(23-24):2333-2342.

120. Lynn AD, Kyriakides TR, Bryant SJ. Characterization of the in vitro macrophage response and in vivo host response to poly(ethylene glycol)-based hydrogels. Journal of biomedical materials research 2010 Jun 1;93(3):941-953.

121. Kou PM, Babensee JE. Macrophage and dendritic cell phenotypic diversity in the context of biomaterials. Journal of biomedical materials research 2010 Jan;96(1):239-260.

122. Babensee JE. Interaction of dendritic cells with biomaterials. Seminars in immunology 2008 Apr;20(2):101-108.

123. Acharya AP, Dolgova NV, Moore NM, Xia CQ, Clare-Salzler MJ, Becker ML, et al. The modulation of dendritic cell integrin binding and activation by RGD-peptide density gradient substrates. Biomaterials 2011 Oct;31(29):7444-7454.

124. Cheung CY, Anseth KS. Synthesis of immunoisolation barriers that provide localized immunosuppression for encapsulated pancreatic islets. Bioconjug Chem 2006 Jul-Aug;17(4):1036-1042.

125. Leclerc C, Brose C, Nouze C, Leonard F, Majlessi L, Becker S, et al. Immobilized cytokines as biomaterials for manufacturing immune cell based vaccines. Journal of biomedical materials research 2008 Sep 15;86(4):1033-1040.

Chapter 2

Objectives

Poly(ethylene glycol) (PEG)-based materials, including PEG hydrogels, are widely investigated within the field of regenerative medicine for cell encapsulation and delivery. One of the many benefits of encapsulating cells or tissue within PEG hydrogels prior to transplantation is the theoretical immunoisolation from the host immune system, essentially creating a physical barrier or separation between the host immune cells and those of the donor tissue. As detailed in Chapter 1, however, encapsulation alone is often inadequate in providing complete immunoprotection, as several small molecules can diffuse into and out of biomaterial capsules and lead to corresponding damage of encapsulated cells.

As a result, recent interest has emerged in creating biofunctional and/or bioactive cell delivery vehicles that can locally modulate deleterious effects of the immune response. This strategy is the focus of this thesis research, and the platform of PEG hydrogels is readily amenable to introducing bioactive moieties and tailoring their presentation. Harnessing this property of local and controlled presentation of biological signals within biomaterial cell carriers, the global aim of this thesis is to explore how modifications to PEG hydrogels, through covalent incorporation of bioactive molecules, can improve the survival of encapsulated cells and, ultimately, the immunoisolation capacity of PEG hydrogels. Rationally chosen strategies to create bioactive PEG hydrogels are evaluated quantitatively in relevant *in vitro* model systems to determine

their utility. Within this global objective in mind, four specific aims are outlined below to demonstrate efficacy of specific formulations in protecting encapsulated beta cells from various immune challenges and test corresponding hypotheses. The specific aims of this thesis are as follows:

***Specific Aim 1*: Incorporate a polymerizable superoxide dismutase mimetic into PEG hydrogels and examine its ability to reduce reactive oxygen species-mediated damage to encapsulated β-cells**

One of the significant threats posed by the host inflammatory response towards implanted tissue is damage from reactive oxygen species (ROS). ROS are secreted by inflammatory cells as an immediate response to device implantation. These ROS are small enough to diffuse rapidly through capsules and illicit damage and/or death to encapsulated cells. Superoxide, one of the main ROS produced by inflammatory cells, poses an immediate threat to delivered cells, but this highly reactive specie also rapidly breaks down to form other cytotoxic and more stable species, such as hydrogen peroxide (H_2O_2) and peroxynitrite ($ONOO^-$). Previously, Cheung *et al.* synthesized a polymerizable superoxide dismutase mimetic (SODm) to catalyze the breakdown ROS within hydrogels [1]. Building from this initial work, the primary goal of Specific Aim 1 is to demonstrate that this SODm can protect encapsulated β-cells from damage mediated by superoxide produced outside of capsules.

In accordance, several objectives are considered to evaluate the ability of SODm to protect encapsulated cells. First, the cytocompatibility of the SODm is verified in

solution, as well as when polymerized into cell-laden hydrogels. Next, an adequate *in vitro* assay system is developed to generate superoxide radicals in solution. For the experiments presented herein, a chemical reaction is used to generate superoxide. Xanthine and xanthine oxide are reacted to produce uric acid and superoxide and the rate of superoxide production in solution is characterized and verified to be reproducible. SODm is then incorporated within cell-laden hydrogels to demonstrate bioactivity. Upon functionalization with various concentrations of SODm, hydrogels are treated with superoxide and cell survival is measured via a metabolic activity assay and live/dead imaging. Because superoxide and ROS are likely to be secreted by inflammatory cells throughout the first several days following transplantation, a 10-day study is performed to assess cell survival after many days of encapsulation with multiple superoxide challenges.

Specific Aim 2: **Develop and test the ability of a functionalized, PEG-based coating to present a high surface density of bioactive ligands to signal T cell apoptosis**

Small cytotoxic molecules, including superoxide, are secreted immediately following cell-laden device implantation by cells of the innate immune system. In isolation, this inflammatory response runs its course and ceases in a matter of days. Often leading to the formation of fibrous capsules surrounding inert biomaterial implants; however, the response is much more complex for cell-laden biomaterials. Cells of the adaptive immune response can become activated by local inflammation and generate specific immunity to shed antigen from encapsulated cells, especially if cell

apotosis or necrosis occurs in response to the initial insult. Unchecked, this adaptive immune response persists until all antigen is removed (i.e., until all encapsulated cells are destroyed). The T cell response by the adaptive immune system has been shown to be a significant threat to encapsulated cells and tissues. As such, functionalized coatings to suppress the T cell response by inducing local T cell apoptosis have the potential to reduce the requirement for immunosuppression (i.e., systemic T cell suppression) following the transplantation of many tissue types, including pancreatic islets.

The focus of Specific Aim 2 is to fabricate functionalized coatings that display a high surface density of anti-fas antibody (DX2 clone) to deliver apoptotic signals to T cells. Sebra *et al.* developed a living radical polymerization strategy to incorporate antibodies within polymer chains of PEG acrylate to create an ELISA-like biodetection platform [2, 3]. Building upon this strategy of controlled, high density presentation of antibodies at polymer surfaces, this thesis modifies an anti-fas antibody to render it polymerizable via the addition of acrylate groups to free amines using acryl-PEG-NHS chemistry. Subsequently, the ability to exploit a dithiocarbamate (DTC) photoiniferter to form antibody functionalized polymer chains on hard polymer substrates is examined and graft height is studied as a function of light exposure/dose. Next, an ELISA-type assay is developed to allow quantification of detectable antibody within the resulting polymer.

To evaluate the bioactivity of functional coatings, jurkat T cells, a cell line previously known to express high levels of fas receptor (comparable to activated T cells), are cultured atop functionalized coatings to verify the induction of apoptosis.

Because PEG surfaces are resistant to protein and cellular adhesion, we hypothesized that increased fas signaling may be observed after the incorporation of adhesion ligands. To introduce adhesion with specificity towards T cells and fas-responsive leukocytes, inter-cellular adhesion molecule-1 (ICAM-1) is introduced into polymer coatings along with anti-fas. These surfaces are seeded with T cells and assayed for increased apoptosis.

Specific Aim 3: **Develop cytocompatible fabrication strategies to polymerize biofunctional coatings on the external surfaces of cell-laden PEG hydrogels as a method to create composite scaffolds to deliver immuno-active signals in a spatially regulated manner.**

Building upon the findings of Specific Aim 2, Specific Aim 3 focuses on developing and testing cytocompatible polymerization strategies to functionalize cell-laden PEG-based hydrogels with biologically functional coatings. Due to technical difficulties encountered when translating DTC-mediated photopolymerization for modifying hydrogels (e.g., aqueous and cytocompatible conditions), an alternate surface-mediated polymerization strategy is investigated. Johnson et al. recently reported on a versatile, reactive dip-coating polymerization mediated by the enzyme, glucose oxidase [4, 5]. Glucose oxidase reacts with glucose to form hydrogen peroxide (H_2O_2) which further reacts with iron (Fe^{2+}), yielding hydroxyl radical, which can initiate polymerization of vinyl-functionalized macromolecules. When pre-formed hydrogels (e.g., those laden with cells) are swollen in glucose (e.g., cell culture media) and then

dipped into glucose-free pre-polymer containing low molecular weight PEG (meth)acrylates, glucose diffuses out of the hydrogel to initiate polymerization and coating formation at the hydrogel surface.

In Specific Aim 3, biomolecules are incorporated within GOx-mediated coatings with the goal of signaling external immune cells. Further, a range of cytocompatible conditions are investigated to enable coating formation in the presence of encapsulated cells. Biomolecules incorporated within the surface coatings are detected via a modified ELISA developed in Specific Aim 2. Using confocal microscopy, the thickness of the conformal polymer coating is characterized and related to the dipping time. To demonstrate the bioactivity of molecules incorporated using this polymerization mechanism, anti-fas antibody and ICAM-1 are covalently incorporated within coatings grown from PEG hydrogels. Jurkat T cells seeded atop coatings and the induction of their apoptosis are investigated via flow cytometry after 12, 24, and 48 hrs. Finally, hydrogels containing encapsulated Min6 β-cells and 3T3 fibroblasts are modified with coatings via glucose oxidase polymerization to identify conditions which are compatible with high cell survival. Overall, this GOx-mediated coating strategy has the potential to functionalize cell-laden hydrogels with bioactive molecules that remain physically separate from the encapsulated cells. While this thesis specifically evalutes the bioactivity of coatings to influence T cell activity, one might easily envision that this coating strategy could be readily applied to fabricate coatings with SODm activity, as in Specific Aim 1, or to present immunosuppressive molecules, as will be discussed in Specific Aim 4.

Specific Aim 4: **Explore how PEG hydrogels with modified with immunosuppressive proteins can reduce dendritic cell maturation upon exposure to immune stimuli**

T cells of the adaptive immune response pose a significant threat to encapsulated tissues. While Specific Aims 2 and 3 explore functionalized polymer-based strategies to reduce local T cells via apoptosis, a biomaterial able to dampen the adaptive immune response and prevent the formation of activated T cells would have great utility within the field of cell-based therapies. Dendritic cells (DCs) are one of the body's antigen presenting cells and the only cell type capable of activating naïve T cells. When exposed to antigenic material in the presence of immune stimuli, such as an implantable biomaterial construct containing live cells, DCs take up shed antigens and mature. Upon maturation, DCs present antigen to naïve T cells and elicit an immune response. When exposed to antigen under tolerogenic conditions, however, such as in the presence of the immunosuppressive proteins TGF-β1 and / or IL-10, DC maturation is reduced and the resulting DCs have been shown to induce antigen-specific tolerance. Therefore, if a biomaterial surface were to reduce dendritic cell maturation via the presentation of bioactive signals (e.g., TGF-β1 and/or IL-10), the ensuing T cell response could be dampened. In Specific Aim 4, immunosuppressive proteins are presented on the surfaces of PEG hydrogels to signal DCs and their ability to reduce DC maturation following immune stimulation.

Unlike the biomolecules investigated in Specific Aims 1–3, the immunosuppressive proteins TGF-β1 and IL-10 are active in solution at very low (1 to 10 ng/ml) concentrations and, therefore, commercially available in low quantities (i.e., 5

to 10 μg). Further, TGF-β1 is known to be sparingly soluble in biologically relevant solutions. Thus, initial work on Specific Aim 4 focuses on developing a strategy to chemically modify TGF-β1 in such a manner that it may be polymerized into hydrogels without significant loss of bioactivity. Modification of primary amines with acrylate-PEG-NHS is initially investigated, but this modification is found to induce the maturation of DCs, an unacceptable consequence. Thiolation with Traut's reagent is employed with improved results, and the bioactivity of thiolated TGF-β1-SH and IL-10-SH are assessed in solution via their capacity to reduce DC maturation upon exposure to immune stimuli. Further, the solution-phase bioactivity of TGF-β1-SH is verified via the PE-25 TGF-β reporter cell assay.

After the bioactivity of the immunosuppressive proteins are validated in solution, they are conjugated within PEG hydrogels via a thiol-ene reaction, and the resulting detectable protein surface density is characterized via the modified ELISA from Specific Aim 2. Next, the ability to reduced DC mature following immune stimulation is investigated by seeding immature DCs from the JAWSII dendritic cell line on functionalized hydrogels. Bioactivity and reduced DC maturation are assessed by ELISA and flow cytometry to measure the secretion of IL-12 and expression of MHCII, respectively.

As further evidence of the efficacy of this approach, immunosuppressive hydrogels are evaluated with primary dendritic cells isolated from non-obese diabetic (NOD) mice, which are a relevant model for dendritic cells in the context of type I diabetes. Based on the observation from Specific Aim 2 that increasing interactions between immune cells and PEG surfaces increases signaling, general cell adhesion is

promoted on immunosuppressive hydrogels via the incorporation of poly-L-lyine (PLL) and extracellular matrix (ECM) proteins, which both facilitate cell binding by increasing the adhesion of serum proteins or by directly presenting integrin binding domains, respectively.

REFERENCES

1. Cheung CY, McCartney SJ, Anseth K. Synthesis of Polymerizable Superoxide Dismutase Mimetics to Reduce Reactive Oxygen Species Damage in Transplanted Biomedical Devices. Advanced Functional Materials 2008;18:3119-3126.

2. Sebra RP, Masters KS, Bowman CN, Anseth KS. Surface grafted antibodies: controlled architecture permits enhanced antigen detection. Langmuir 2005 Nov 22;21(24):10907-10911.

3. Sebra RP, Masters KS, Cheung CY, Bowman CN, Anseth KS. Detection of antigens in biologically complex fluids with photografted whole antibodies. Anal Chem 2006 May 1;78(9):3144-3151.

4. Johnson LM, Fairbanks BD, Anseth KS, Bowman CN. Enzyme-mediated redox initiation for hydrogel generation and cellular encapsulation. Biomacromolecules 2009 Nov 9;10(11):3114-3121.

5. Johnson LM, Deforest CA, Pendurti A, Anseth KS, Bowman CN. Formation of three-dimensional hydrogel multilayers using enzyme-mediated redox chain initiation. ACS applied materials & interfaces 2010 Jul;2(7):1963-1972.

Chapter 3

Polymerizable superoxide dismutase mimetic protects cells encapsulated in PEG hydrogels from reactive oxygen species-mediated damage

A polymerizable superoxide dismutase mimetic (SODm) was incorporated into poly(ethylene glycol) (PEG) hydrogels to protect encapsulated cells from superoxide-mediated damage. Superoxide and other small reactive oxygen species (ROS) can cause oxidative damage to donor tissue encapsulated within size exclusion barrier materials. To enzymatically breakdown ROS within biomaterial cell encapsulation systems, Mn(III) Tetrakis[1-(3-acryloxy-propyl)-4-pyridyl] porphyrin (MnTTPyP-acryl), a polymerizable manganese metalloporphyrin SOD mimetic, was photopolymerized with PEG diacrylate (PEGDA) to create functional gels. In unmodified PEG hydrogels, a significant reduction in metabolic activity was observed when encapsulated Min6 β-cells were challenged with chemically-generated superoxide. Cells encapsulated within MnTPPyP-co-PEG hydrogels demonstrated greatly improved metabolic activity following superoxide challenge. To promote encapsulated cell survival throughout a 10 day period, the effect of cell seeding density on cell survival was characterized in blank PEG hydrogels and a significant improvement in viability was observed when seeded in excess of 6.7×10^6 cells/ml. Finally, cells were encapsulated and cultured for 10 days within MnTPPyP-co-PEG hydrogels and challenged with superoxide on days 4, 6, and 8. At the conclusion of this study, cells in blank PEG hydrogels had no observable

metabolic activity but when encapsulated in MnTPPyP-functionalized hydrogels, cells retained 60±5% of the metabolic activity compared to untreated controls.

3.1 INTRODUCTION

Cell-based therapies hold the potential to cure numerous diseases resulting from the damage or destruction of native tissues. As cell delivery strategies continue to improve, clinical successes [1-5] and new trials [6] have been reported in applications ranging from the delivery of dopaminergic neurons to treat Parkinson's disease to autologous chondrocytes to regenerate cartilage to the delivery of β-cells and islets for the treatment of type I diabetes. When considering strategies that rely on allogeneic cell delivery, it is crucial to consider adequate protection of donor cells from the host immune response. Generally, systemic immunosuppression is required to facilitate transplant survival [7], but this therapy carries several serious side effects that must be measured against the benefits of a cell transplant.

In contrast, cell encapsulation creates a physical barrier between donor tissue and host immune cells and has been widely investigated as a means to increase immunoisolation [8] for the delivery of cells to treat hepatic [9, 10], central nervous [11], and endocrine disorders [12], amongst other diseases. The encapsulation of pancreatic tissue has been the most commonly investigated immunoisolation system[8], and numerous materials, natural and synthetic, have been shown to promote cell survival *in vitro* and *in vivo* [8, 13-15]. As one example, poly(ethylene glycol) (PEG) diacrylate (PEGDA) hydrogels offer a desirable cell encapsulation material because PEG itself is relatively non-fouling, hydrophilic, and allows facile chemical modification. Our laboratory and others have demonstrated that blank and functionalized PEG hydrogels readily promote encapsulated cell survival and function [15-18].

The size-exclusion membrane characteristic of an encapsulation barrier blocks the passage of immune cells and large molecules like immunoglobulins[8]. However, small molecules produced by activated neutrophils and macrophages, such as reactive oxygen species (ROS) and cytokines, including tumor necrosis factor (TNF) and interleukin 1-beta (IL-1β), can readily diffuse through passive membranes and damage donor cells [19, 20]. When reactive oxygen species like superoxide, nitric oxide ($NO^{\bullet}$), hydrogen peroxide (H_2O_2), and hydroxyl radical ($HO^{\bullet}$) come into contact with transplanted cells, they induce oxidative damage to many cellular molecules including DNA, proteins, and membrane lipids, leading to cellular dysfunction and death [21-23]. Superoxide is also known to combine with $NO^{\bullet}$ to form peroxynitrite ($ONOO^{-}$), a highly reactive nitrogen species able to rapidly induce cells damage and cell death, as well as signal additional cytokine secretion [24].

To provide greater protection from small cytotoxic molecules, researchers have previously investigated methods to functionalize passive encapsulation membranes. To highlight recent approaches, Lin *et al.* tethered anti-TNF affinity peptides within cell-laden PEG hydrogels and demonstrated improved cell survival when challenged with TNF [25]. Likewise, to influence the cytokine profile around an encapsulation device, Washburn *et al.* conjugated antibodies against IL-1β and TNF to hyaluronic acid materials for cytokine sequestration and demonstrated fewer activated macrophages responding to adjacent wound sites *in vivo* [26]. While these approaches limit cytokine diffusion in and around capsules, encapsulated cells are also susceptible to damage from reactive oxygen species, and a limited number of publications report strategies to reduce ROS-mediated cell death.

Mammalian cells express several enzymes dedicated to breaking down ROS, including superoxide dismutase (SOD), which catalyzes the dismutation of superoxide into O_2 and H_2O_2. Ordinarily, endogenous SOD activity is sufficient to maintain healthy levels of superoxide, but during a diseased state or active immune response, the concentration of superoxide can exceed that which the SOD enzyme can breakdown [27]. In fact, β-cells, such as those delivered from the treatment of type I diabetes, are known to express reduced levels of antioxidants as compared to other cell types [28] and are at an increased risk of damage from ROS. Delivering SOD directly to cells [29-32] or cell transplants [33] provides protection from ROS injury. While SOD protein offers a high level of catalytic activity, whole proteins suffer from limited *in vivo* stability and have the potential for immunogenicity. Thus, SOD mimetics (SODm), small organic molecules that recapitulate the enzymatic activity of SOD protein, have gained popularity due to their increased half-life and decreased immunogenicity [34]. The most popular classes of SODm are the metalloporphyrins, which consist of a carbon-based porphyrin ring and redox metal core. Manganese porphyrins exhibit among the highest SODm activity [35] and significantly reduce ROS damage [32, 36, 37]. Manganese porphyrins also possess catalytic activity to breakdown additional ROS, including H_2O_2, peroxynitrite, and $NO^{\bullet}$ [27, 38, 39].

While the majority of research delivering SOD focuses on injecting SOD and SODm directly into tissues, recent efforts have investigated material platforms for the delivery of SOD, including modification of SOD with PEG to improve serum half-life [40, 41], release of SOD from biomaterials to increase local availability [42, 43] and encapsulation of SOD within hydrogels [44]. Each of these approaches has shown

promise, but each is limited by the aforementioned problems of using the whole SOD protein, rather than SODm. Additionally, SOD release platforms become inactive once the entire payload of SOD is released. Recently, Cheung *et al*. introduced a modified

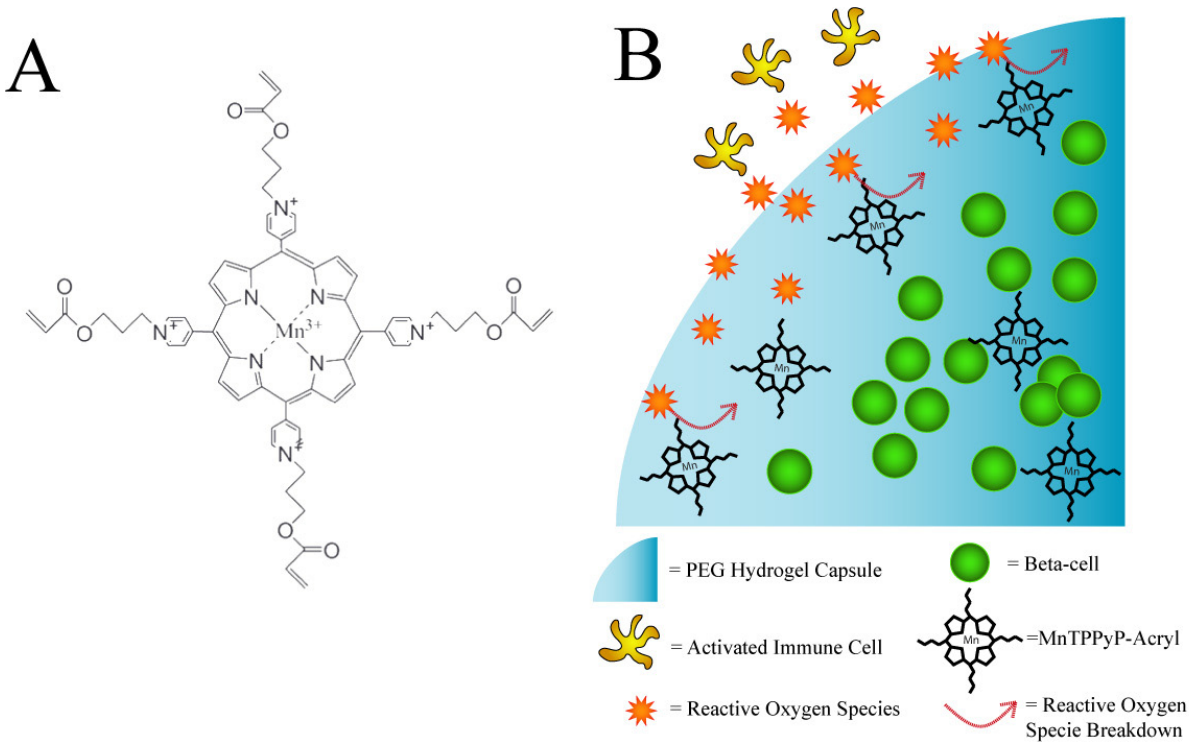

Fig. 3.1. (A) The chemical structure of the polymerizable SODm, MnTPPyP-Acryl. (B) Schematic of the MnTPPyP-co-PEG immunoisolation barrier. ROS diffuse inside the capsule but are broken down by the covalently bound SOD mimetic. ROS are indicated as being secreted by activated immune cells, as these cells are responsible for ROS secretion in response to tissue transplants. For the studies conducted herein, however, superoxide was generated chemically.

SOD mimetic, MnTPPyP-Acryl, Fig. 3.1A, with comparable enzymatic activity to commercially available SODm [45]. MnTPPyP-Acryl is unique, as it has polymerizable acrylate groups that enable covalent incorporation into polymer networks. Cheung *et al.* co-polymerized MnTPPyP-Acryl with PEG diacrylate (PEGDA) to create hydrogels functionalized with SODm, and the MnTPPyP-co-PEG hydrogels exhibited SOD enzymatic activity that was sustainable throughout several challenges with superoxide [45]. In the present study, we encapsulate Min6 β-cells within MnTPPyP-co-PEG

hydrogels to demonstrate the ability of this capsule to increase cell survival following treatment with ROS, as summarized in Fig. 3.1B.

3.2 MATERIALS & METHODS

3.2.1 Synthesis of polymerizable superoxide dismutase mimetic

The synthesis and characterization of MnTPPyP-Acrl have been previously reported in great detail[45] and is briefly summarized herein. The 4 arms of meso-Tetra(4-pyridyl)porphine (TPyP) (Frontier Scientific, Logan, UT) were quarternized with 80-fold molar excess 3-iodopropanol (Trans World Chemicals, Rockville, MD) in DMF yielding meso-Tetra[1-(3-hydroxy-propyl)-4-pyridyl] porphine (TPPyP-OH). Product was added to chloroform, extracted into water and precipitated with ammonium hexafluorophosphate (NH_4PF_6) (Sigma-Aldrich, St. Louis, MO). TPPyP-OH was acrylated in acetone via reaction with 8-fold molar excess acryloyl chloride (Sigma-Aldrich) and triethylamine (TEA, Sigma-Aldrich), yielding TPPyP-Acryl, and was precipitated via the addition of tetrabutylammonium chloride (TBAC, Sigma-Aldrich). Next, TPPyP-Acryl was reacted overnight with 20-fold molar excess $MnCl_2$ (Sigma-Aldrich) in dH_2O containing 1 M NaOH, resulting in metallation and the final product, MnTPPyP-Acryl. MnTPPyP-Acryl was precipitated with NH_4PF_6 and rinsed with 1:1 isopropanol/diethyl ether. Product was dissolved in acetone for counterion exchange to Cl^- and then precipitated by TBAC. The resulting MnTPPyP-Acryl product was desiccated overnight to yield a dry, solid product.

3.2.2 Cell culture

Murine pancreatic β-cells (Min6) were cultured in T-75 tissue culture flasks, containing 15 ml cell culture media, consisting of RPMI 1640 supplemented with 10% fetal bovine serum, 100 mg/ml Penicillin/Streptomycin, and 0.5 mg/ml Fungizone (all from Invitrogen, Carlsbad, CA). Cells were seeded at $1x10^6$ cells/ml and incubated at 37 °C in humid conditions with 5% CO_2. Fresh media was added three times per week and cells were passaged weekly, by treatment with 0.5 % trypsin EDTA, (10 ml, 5 min, Invitrogen) followed by quenching with 10 ml media. All cells used were passaged between 5 and 20 times.

3.2.3 Superoxide generation & quantification

Superoxide was generated via enzymatic breakdown of xanthine (Sigma-Aldrich) to uric acid, by xanthine oxidase (Sigma-Aldrich)[46]. In cell culture media, Xanthine (0 to 100 μM) was reacted with xanthine oxidase (10 nM). Superoxide production was quantified by measuring the oxidation of cytochrome C (Sigma-Aldrich)[47]. Xanthine/Xanthine oxidase were reacted in the presence of cytochrome C (100 μM) and the change in 550 nm absorbance was measured using UV-vis spectroscopy to calculate the superoxide production rate using Eqn. 1, adapted from Choi *et al*..

$$[O_2^-] = \frac{\Delta A \bullet v}{K \bullet l \bullet t} \quad (1)$$

Here, Δ*A* is the change in absorbance, *v* is volume, *l* is cuvette pathlength, *t* is time, and K is the extinction coefficient for the absorption difference between reduced and oxidized cytochrome C (K = 21 x 10^3 cm^{-1} M^{-1})[47, 48] at 550 nm.

3.2.4 Cyto-protection with soluble MnTPPyP-acryl

Min6 β-cells (100 000 cells/ml) were seeded in 96-well plates containing 200 µl cell culture media. After 48 hrs, fresh media was added and superoxide was generated via the addition of xanthine (100 µM) and xanthine oxidase (10 nM), with or without the addition of soluble MnTPPyP-Acryl (100 µM). 2 hrs following treatment, dead cells were visualized by trypan blue (Invitrogen) staining, whereby 180 µl media was gently removed from each well (20 µl media/well remained) and 2 µl trypan blue stain (0.4%) was added. Cells were imaged using a Nikon Eclipse TE300 microscope and blue staining indicated dead cells. Metabolic activity of Min6 cells was measured 24 hrs following superoxide treatment by adding 22 µl of AlamarBlue reagent (Invitrogen) to each condition (yielding a 10% v/v AlamarBlue solution) and incubating for 3 hrs. Fluorescence (excitation: 560 nm, emission: 590 nm) represented the metabolic activity of living cells. Percentage metabolic activity was calculated by comparing samples to untreated controls.

3.2.5 Synthesis of PEGDA

The synthesis of poly(ethylene glycol) diacrylate (PEGDA) has been previously described[49, 50]. Briefly, hydroxyl-terminated poly(ethylene glycol) (PEG, Mn = 10 000 g/mol, Sigma-Aldrich) was dissolved in 60 °C toluene and then cooled to room temperature. A 4-fold molar excess of acryloyl chloride and triethylamine (TEA) to PEG hydroxyl groups was added to the PEG and reacted overnight at room temperature. The PEGDA product was filtered through neutral alumina (Fisher Scientific, Pittsburg, PA) to remove TEA-HCl salt. Excess toluene was removed by rotovap and the resulting

product was precipitated in cold diethyl ether and desiccated overnight. The degree of acrylation was determined by ^{1}H-NMR to be in excess of 95 %.

3.2.6 Cell Encapsulation

Min6 β-cells were harvested and suspended (5 to 10 million cells/ml) in PEGDA (10 kDa, 10 wt%) macromer solution in phosphate buffered saline (PBS, pH 7.4, Invitrogen) with 1-[4-(2-hydroxyethoxy)-phenyl]-2-hydroxy-2-methyl-1-propanone (Irgacure 2959, 0.05 wt%, Ciba Specialty Chemicals, Newport, DE) as photoinitiator and 0 to 100 μM MnTPPyP-Acryl. 30 μl/gel was loaded into 1 ml syringe tips for photopolymerization under ultraviolet light (10 mW/cm^2, centered at 365 nm), for 10 min. Following encapsulation, hydrogel disks of ~ 5 mm diameter x 1 mm height were placed in individual wells of a 24-well plate containing 1 ml cell culture media and incubated overnight. Hydrogels were transferred to fresh media the day after encapsulation and media was changed every-other day thereafter. This method of encapsulation has been widely investigated and is highly cytocompatible[17, 25, 50, 51]. The intracellular ATP content of encapsulated cells was quantified via CellTiter-Glo assay (Promega, Madison, WI), where capsules were placed in 300 μl of 50 % CellTiter-Glo reagent / 50 % cell culture media. Samples were incubated at room temperature on an orbital shaker for 1 h. Next, 200 μL was transferred to white-wall 96-well plate and luminescence was detected and compared to ATP standards.

3.2.7 Challenging encapsulated β-cells with superoxide and analysis

Min6 cells were encapsulated in PEGDA with or without the addition of MnTPPyP-Acryl. These capsules were exposed to superoxide via the addition of xanthine (0 to 100 μM) and xanthine oxidase (10 nM) to 1 ml cell culture media containing one hydrogel. Cell-laden gels were incubated (37 °C, with orbital shaking) with xanthine / xanthine oxidase for 2 hrs, as this time point was considered to be sufficient for complete superoxide generation (Fig 3.2). Metabolic activity of encapsulated cells was assessed by adding 110 μl AlamarBlue reagent to each 1 ml well (yielding 10% v/v AlamarBlue). Gels were incubated overnight, then 200 μl from each well was transferred to individual wells of a 96-well plate and scanned, as described above. Percent metabolic activity was determined by comparing raw fluorescence signal to that of untreated, cell-laden, control gels containing equivalent concentrations of MnTPPyP-Acryl. Live and dead encapsulated cells were analyzed by fluorescent confocal microscopy using a membrane integrity assay. Gels were incubated 30 min (PBS, 37°C) with green fluorescent calcein AM and red fluorescent ethidium homodimer-1 (Invitrogen), to stain live and dead cells, respectively. A series of 20 projections at 10 μm intervals were captured on a Zeiss LSM 5 Pascal confocal microscope and projected onto a single plane.

3.2.8 Statistical Analysis

All results are presented as mean ± standard error of the mean. Statistical significance between datasets was determined using a two-tailed, unpaired Student's t-

test and differences were considered statistically significant when the p value was less than 0.05. All experiments were replicated at least 3 times.

3.3 RESULTS

3.3.1 Generation of superoxide

Superoxide was generated chemically via the enzymatic breakdown of xanthine by xanthine oxidase, as previously described[46]. Cytochrome C was utilized to quantify the rate of superoxide generation as a function of xanthine concentration, shown in Fig. 3.2. In the presence of 10 nM xanthine oxidase, xanthine concentrations ranging from 25 to 100 μM generated superoxide concentrations ranging from 14±4 to 27 ± 3 nmol/mL, respectively (data shown in Table 3.1).

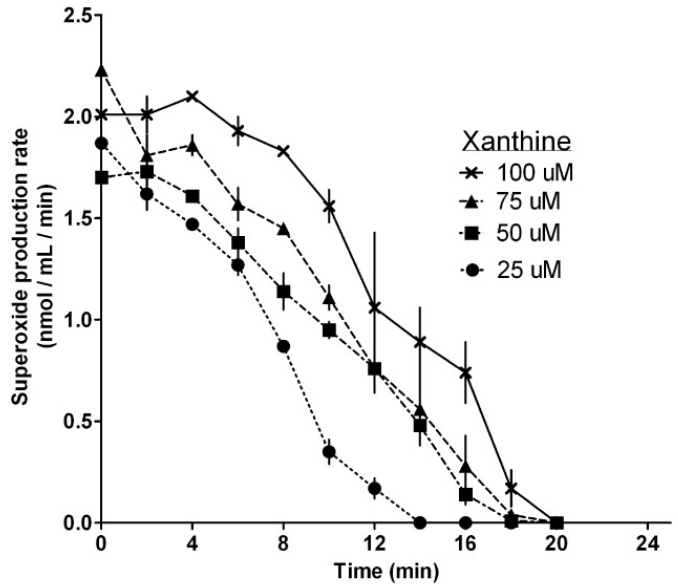

Fig. 3.2. Quantification of superoxide generated by the chemical reaction of xanthine with xanthine oxidase. Xanthine (25, 50, 75, & 100 μM) was combined with 10 nM xanthine oxidase in cell culture media and cytochrome C was used to detect the appearance of superoxide anions over time.

Xanthine (μM)	Total Superoxide (nmol / mL)
25	14 ± 4
50	19 ± 3
75	21 ± 4
100	27 ± 3

Table 3.1. Total superoxide generated throughout a chemical reaction of xanthine with xanthine oxidase. The change in absorbance of Cytochrome C enabled the detection of the total quantity of superoxide produced per reaction, per mL of media.

3.3.2 Solution-phase bioactivity of MnTPPyP-acryl

MnTPPyP-Acryl catalyzes the dismutation of superoxide anions in solution[45]. To demonstrate that this enzymatic activity is sufficient to protect living cells from superoxide damage, β-cells were seeded onto TCPS and exposed to superoxide generated by xanthine/xanthine oxidase. After two hours, dead cells were visualized, Fig. 3.3A, and cell death was observed following superoxide treatment. In the presence of soluble MnTPPyP-Acryl and superoxide, however, increased cell survival was observed. In Fig. 3.3B, 24 hrs following exposure to superoxide, β-cell metabolic activity also decreased significantly, but when MnTPPyP-Acryl and superoxide were added, the metabolic activity was rescued, such that comparable activity to non-superoxide-treated cells was observed. When added alone, xanthine, xanthine oxidase, or MnTPPyP-Acryl did not reduce cellular metabolic activity and were highly cytocompatible (data not shown).

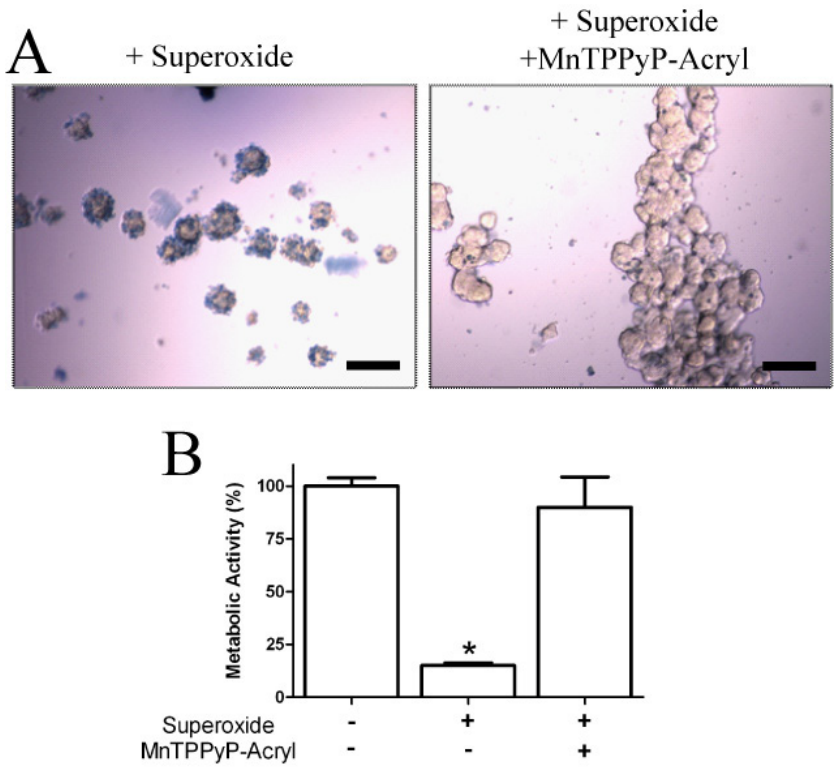

Fig. 3.3. Soluble MnTPPyP-Acryl protects β-cells plated on TCPS from damage. Superoxide was generated chemically in the presence of Min6 β-cells with or without MnTPPyP-Acryl. (A) Trypan blue staining revealed numerous dead (blue) cells in the absence of MnTPPyP-Acryl (left) but fewer dead cells with MnTPPyP-Acryl (right). Scale bar denotes 100 μm (B) Exposure to superoxide significantly reduced the metabolic activity of plated β-cells but the addition of MnTPPyP-Acryl to solution prevented this reduction. * denotes $p<0.05$ difference from other values.

3.3.3 Treating cell-laden hydrogels with superoxide

The metabolic activity of encapsulated cells was assessed following treatment with superoxide generated by xanthine/xanthine oxidase. Min6 were encapsulated at a density of $5x10^6$ cells/ml. The following day, hydrogels were treated with xanthine (0 to 100 μM) in the presence of xanthine oxidase (10 nM) and a decrease in metabolic activity related to xanthine concentration was observed, Fig. 3.4A. Live/Dead imaging of hydrogels exposed to 0, 50 and 100 μM xanthine and xanthine oxidase (10 nM), Fig. 3.4B, revealed significant cell death for samples treated with xanthine.

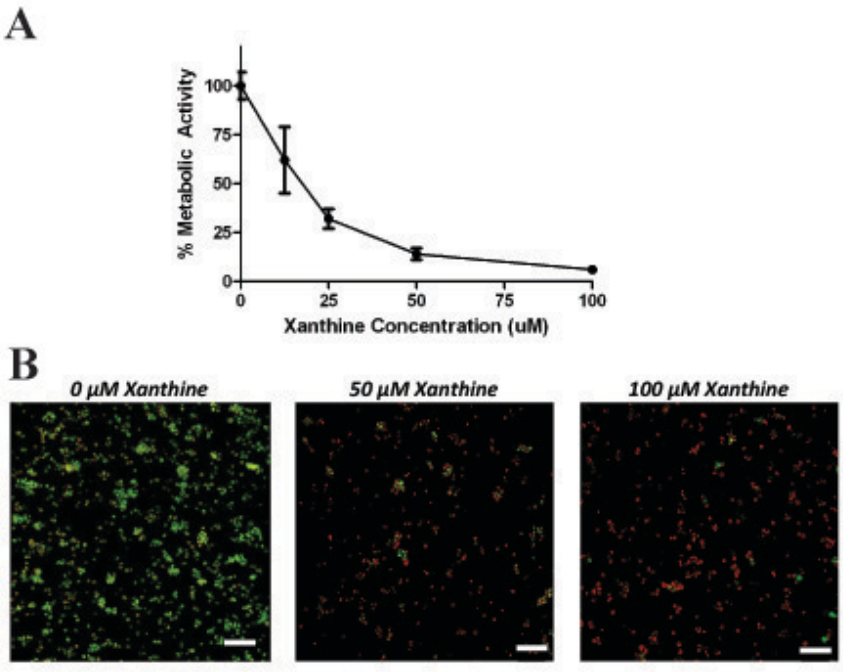

Fig. 3.4. Chemically generated superoxide damages encapsulated β-cells. (A) Metabolic activity of encapsulated cells was reduced, compared to untreated controls, as the concentration of xanthine added to solution was increased. (B) Live/dead confocal imaging enabled the visualization of live (green) and dead (red) cells. Many dead cells were visible when treated with 50 & 100 µM xanthine (and 10 nM xanthine oxidase). Scale bar denotes 100 µm.

3.3.4 Copolymerization of MnTPPyP-Acryl and PEGDA to encapsulate β-cells

MnTPPyP-Acryl (0 to 100 µM) was covalently incorporated into PEGDA hydrogels containing Min6 encapsulated at $5x10^6$ cells/ml and challenged with 25, 50 or 100 µM xanthine and xanthine oxidase (10 nM). As shown in Fig 3.5A, a decrease in metabolic activity was observed with increased xanthine, similar to the trend highlighted in Fig. 3.4A. However, as the concentration of superoxide dismutase mimetic, MnTPPyP-Acryl, polymerized into gels was increased, the metabolic activity of encapsulated cells was rescued. This rescue occurred at a low concentration of MnTPPyP-Acryl (10 µM) when challenged with the lowest concentration of xanthine

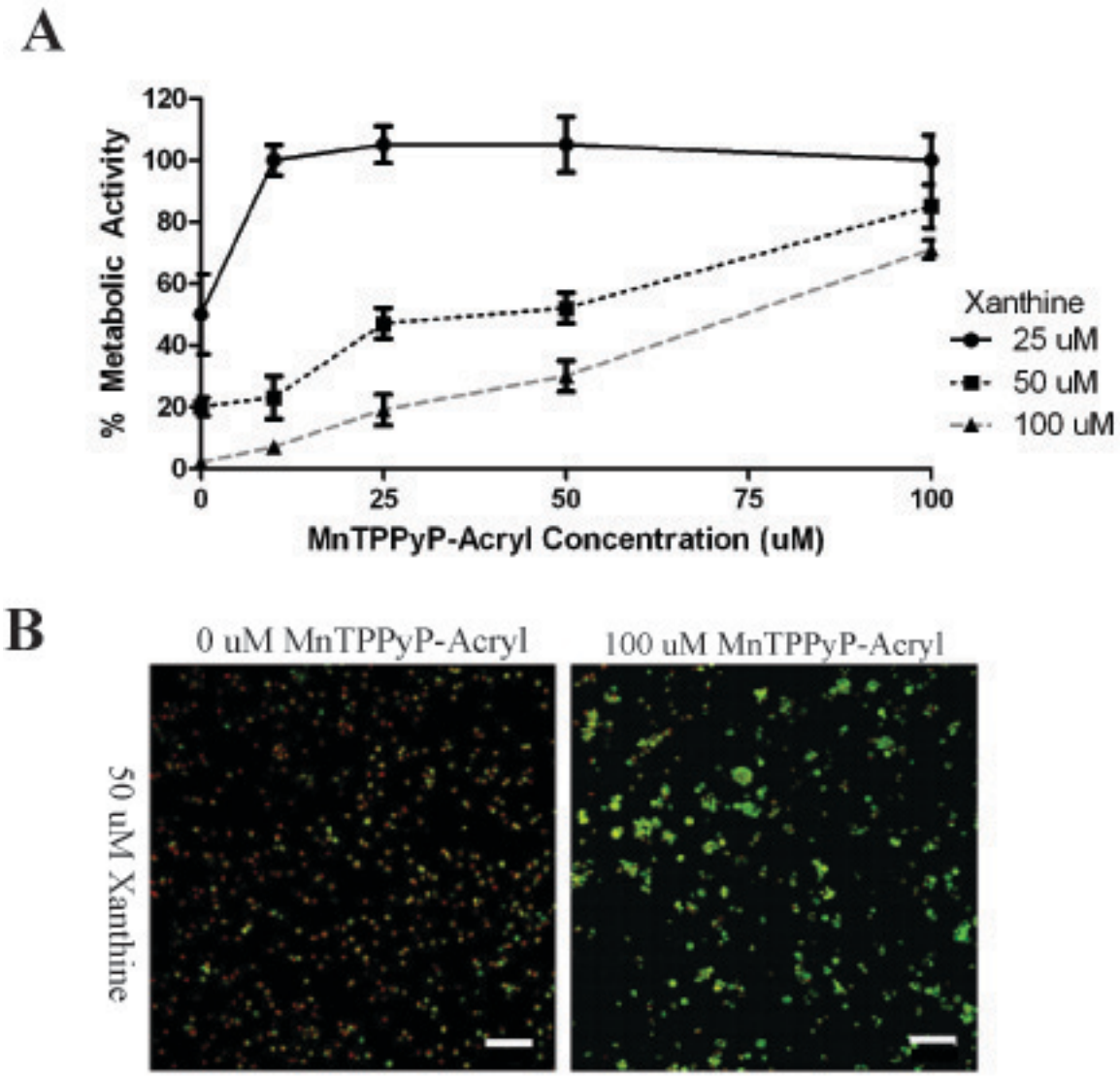

Fig. 3.5. Covalently incorporating MnTPPyP-Acryl into the hydrogel protects β-cells from ROS damage. (A) Cellular metabolic activity of encapsulated cells was monitored following treatment with xanthine (25, 50, & 100 μM) and 10 nM xanthine oxidase. As the concentration of MnTPPyP-Acryl covalently polymerized into the hydrogel was increased, the observed metabolic activity of cells was increase following exposure to superoxide. (B) Live/dead imaging verified that many more live (green) cells were visible following superoxide treatment in the presence of 100 μM MnTPPyP-Acryl (right) compared to blank gels (left). Scale bar denotes 100 μm.

(25 μM) as metabolic activity was restored to that of untreated controls. For cell-laden gels treated with 100 μM xanthine, the inclusion of MnTPPyP-Acryl (100 μM) resulted in over 70 % of the metabolic activity of controls. Live/dead imaging of encapsulated cells verified that the inclusion of polymerizable SOD mimetic, Fig. 3.5B, results in a marked increase in cell survival following superoxide treatment.

3.3.5 Cell Seeding density and β-cell survival

We were interested in studying the cytoprotective capability of polymerized MnTPPyP-Acryl in extended *in vitro* culture. Previous studies, however, have revealed that non-aggregated β-cells encapsulated at low cell seeding density in un-modified PEG-based hydrogels exhibit reduced viability after several days of *in vitro* culture [18, 51, 52]. Incorporating extracellular matrix proteins (collagen, laminin, etc,) or peptide mimetics (RGDS, IKVAV, etc.) only delay the process of cell apoptosis due to the lack of cell-cell interactions in PEG hydrogels [18, 52]. To improve the viability of β-cells in PEGDA hydrogels, we studied the effects of Min6 β-cell seeding density over the course of 10 days. As shown in Fig. 3.6A, when encapsulated at $5x10^6$ cells/ml in blank PEGDA hydrogels, Min6 viability decreased with time, in agreement with prior studies [18, 51, 52]. When encapsulated at cell densities equal to or greater than $6.7x10^6$ cells/ml, however, viability increased with encapsulation time. Live/dead imaging was performed at days 0 and 10 and confirmed an increase in viable cells when encapsulated at densities equal to or greater than $6.7x10^6$ cells/ml, Fig. 3.6B. On day 10, almost no evidence of viability existed for capsules seeded at $5x10^6$ cells/ml. For higher seeding densities, however, there was visible evidence of intact cell aggregates. This simple approach allowed for the maintenance of Min6 viability in PEG hydrogels without the addition of ECM components, enabling the protective effects of SODm in long term culture to be evaluated.

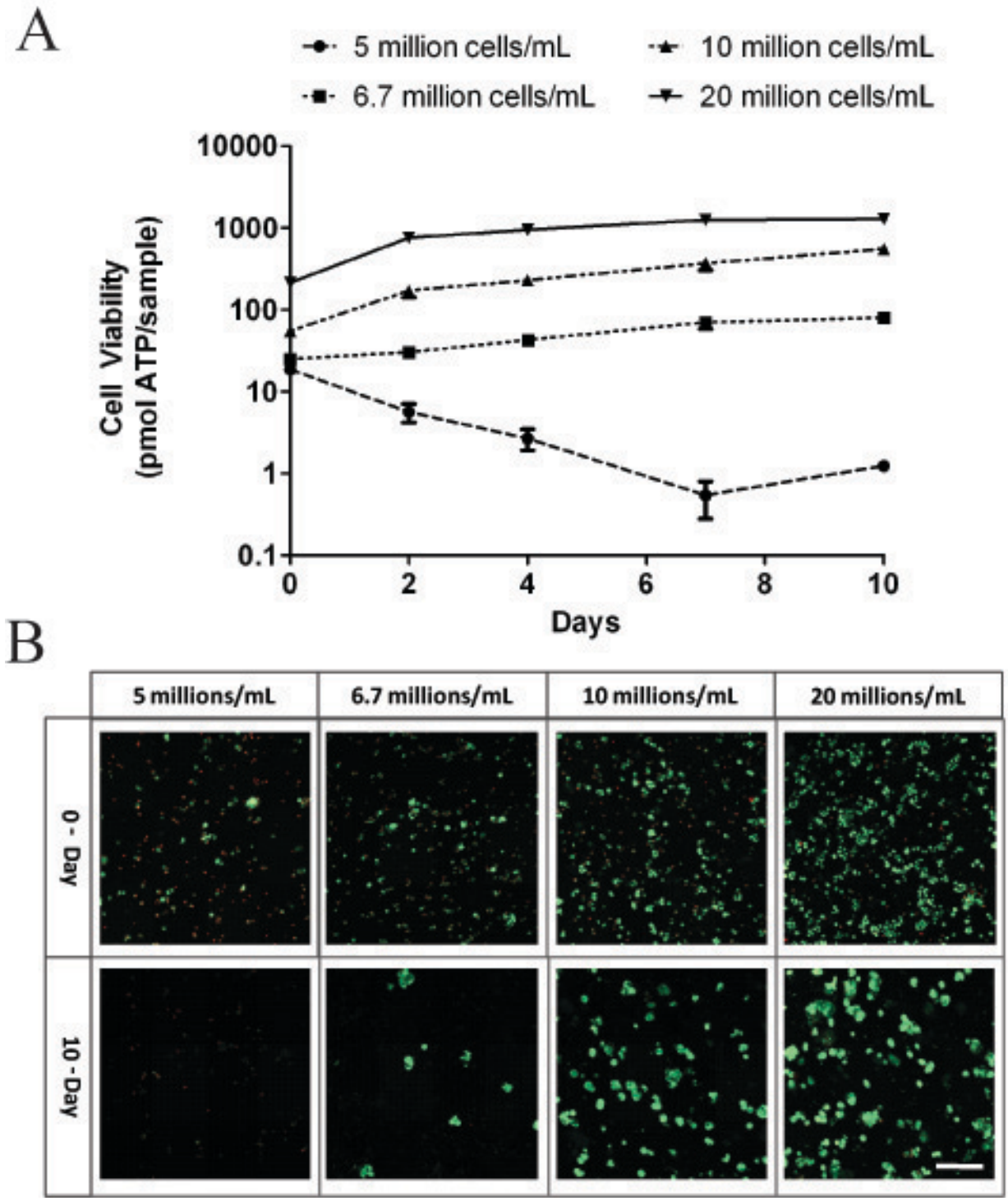

Fig. 3.6. β-cell seeding density effects long-term survival when encapsulated in PEGDA hydrogels. (A) Min6 β-cells were encapsulated at 5, 6.7, 10, & 20 million cell/mL and then assayed for viability over a 10-day period. When seeded at 5 million cells/mL, cellular viability decreased over time. Cells survived when seeded at higher densities. (B) Live/dead imaging confirmed improved viability after 10 days for higher seeding densities as larger, live (green), aggregates of β-cells were present when seeded at increased densities. Scale bar denotes 200 μm.

3.3.6 Long term study of encapsulated β-cells with superoxide

To demonstrate the potential of MnTPPyP-Acryl to protect encapsulated cells for an extended period of time, a 10 day study was completed with multiple superoxide challenges. Specifically, Min6 β-cells were encapsulated in PEGDA gels, with or without MnTPPyP-Acrl (100 μM), at a density of $10x10^6$ cells/ml. As illustrated in Fig 3.7A, cell-laden gels were treated with superoxide (100 μM xanthine, 10 nM xanthine oxidase) on days 4, 6, and 8, and metabolic activity was assayed throughout the study. The initial superoxide treatment on day 4 resulted in a 50% reduction in metabolic activity for cells within blank hydrogels, while only a 20% reduction was observed for gels containing MnTPPyP-Acryl. Following the second superoxide treatment on day 6, the metabolic activity of control gels dropped to only 8 ± 1 % of untreated control gels while the gels containing MnTPPyP-Acryl remained at 66 ± 3% of that of untreated MnTPPyP-Acryl gels. Following three superoxide treatments, on day 10, gels containing MnTPPyP-Acryl exhibited 60 ± 5% of the metabolic activity of untreated MnTPPyP-Acryl gels while no metabolic activity was observed in control gels. When analyzing gels stained for cell viability (i.e, live/dead staining) on day 10 (Fig. 3.7B), MnTPPyP-Acryl gels treated 3x with superoxide showed many healthy, cell aggregates. Imaging of control gels verified poor viability following three superoxide treatments.

3.4 DISCUSSION

This study demonstrates that MnTPPyP-Acryl protects cells from superoxide-mediated ROS damage *in vitro*. We identified concentrations of xanthine and xanthine

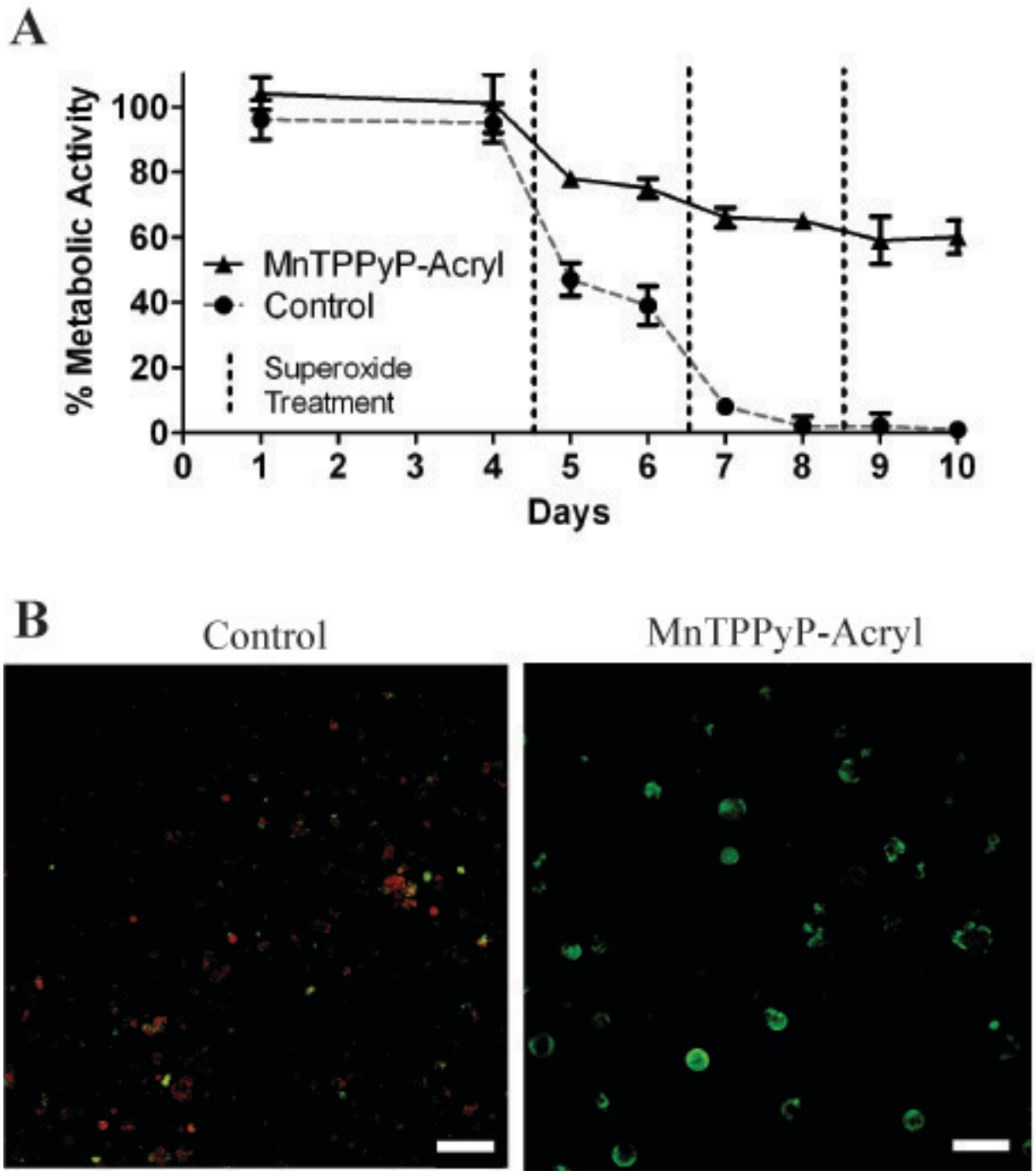

Fig. 3.7. MnTPPyP-co-PEG hydrogels retain enzymatic activity over many days and after several superoxide treatments. β-cells were encapsulated with or without MnTPPyP-Acryl and cultured for 10 days. On days 4, 6, & 8 samples were treated with superoxide (represented by the horizontal dashed line) generated by 100 μM xanthine / 10 nM xanthine oxidase. (A) Cells within hydrogels containing MnTPPyP-Acryl retained significantly more metabolic activity after repeated superoxide exposure compared to control hydrogels. (B) After 10 days in culture with superoxide treatments on days 4,6, & 8, cell-laden hydrogels were imaged via live/dead staining. Visualization confirmed the presence of many large, live (green) aggregates in gels contained MnTPPyP-Acryl (right) compared to control gels, which contained many dead (red) cells (left). Scale bar represents 100 μm.

oxidase to generate superoxide at rates comparable to those generated by activated immune cells [48, 53]. When un-encapsulated cells are exposed to the chemically generated superoxide, the concentrations of ROS were sufficient to significantly reduce overall metabolic activity, but the addition of soluble MnTPPyP-Acryl to the culture was found to preserved viability.

Min6 β-cells were then encapsulated within PEGDA hydrogels and treated with superoxide; a loss of metabolic activity was confirmed in the presence of xanthine/xanthine oxidase generated superoxide. As others have observed [42], superoxide treatment resulted in damage to encapsulated cells and, in our studies, rapidly resulted in reduced metabolic activity and cell death. Further, the extent to which cellular metabolic activity was reduced was dependent upon the concentration of superoxide generated, as controlled via the xanthine concentration. When MnTPPyP-Acryl was immobilized into the hydrogel network through copolymerization, a striking cytoprotective effect was observed; when MnTPPyP-Acryl was included at 100 μM, the highest concentration investigated, cellular metabolic activity was rescued from 0% to over 60%, when treated with 100 μM xanthine. In these studies, the highest concentration of MnTPPyP-Acryl was chosen to be 100 μM, because beyond this concentration, the polymerization rate of the hydrogel becomes inhibited, as previously reported [45], likely due to active radical scavenging by the SODm.

A major benefit of covalently incorporating MnTPPyP-Acryl into a hydrogel is the potential to extend SOD activity over time and localize the SOD activity at the site of the transplanted cells. Thus, we were interested in evaluating the capacity of MnTPPyP-Acryl to protect encapsulated cells from ROS damage over many days in culture. In

performing these studies, it became apparent that, even in the absence of any superoxide challenge, Min6 viability declined after several days in culture within unmodified PEG hydrogels [18, 51, 52]. In an effort to improve viability, we investigated the effect of initial cell seeding density on long-term Min6 survival. We chose to study the effects of cell-seeding density, as we hypothesized that increasing cell seeding/packing density increases the probability of cell-cell contact paracrine signaling that may positively influence β-cells survival when encapsulated in PEG hydrogels. Indeed, previous studies have demonstrated the importance of cell-cell contact on the proliferation, survival, and function of β-cells [54-57]. We verified this effect, Fig. 3.6, as Min6 β-cells had drastically improved viability when seeded at or in excess of 6.7 million cell/mL. These results highlight the importance of considering cell seeding density when culturing encapsulated β-cells.

To evaluate the capacity of MnTPPyP-co-PEG hydrogels to protect encapsulated cells from multiple ROS exposures over several days, Min6 were seeded at a density of 10 million cells/mL and exposed to multiple superoxide treatments. We challenged gels with a high concentration of superoxide on days 4, 6, and 8. Cheung *et al.* previously demonstrated that a single MnTPPyP-Acryl hydrogel was capable of breaking down multiple superoxide challenges with no observable loss in activity [45]. Herein, we have shown that these gels are able to protect encapsulated cells from multiple ROS challenges. A striking increase in metabolic activity was observed following three superoxide challenges within MnTPPyP-co-PEG hydrogels, compared to blank capsules. Even with the inclusion of MnTPPyP-Acryl, some loss in metabolic activity following superoxide treatment was observed, relative to untreated controls, especially

after the first treatment. Because metabolic activity was reduced to a much lesser degree following the 2nd and 3rd superoxide exposures, we initially hypothesized that cell damage during the first superoxide treatment would be those located in proximity to the exterior of the gel and that during the 2nd and 3rd superoxide treatments, ROS breakdown would occur prior to diffusing through this space. Upon analysis of live/dead cell images on day 10, however, overwhelming visual evidence of dead cells in the periphery of the gel was not observed and live cells seemed to be relatively uniformly distributed throughout the network. Thus, it is possible that the β-cell damage during the first superoxide treatment simply occurred within cells that tended to be more sensitive to ROS.

While superoxide anions were generated via the reaction of xanthine with xanthine oxidase, it was unlikely that superoxide directly elicited the destruction of encapsulated β-cells in this study. Superoxide has a short half-life and others have modeled the diffusion of superoxide into hydrogels and predicted that superoxide would penetrate only short distances within the capsule [58]. Despite the short half-life of superoxide, encapsulated cells experience oxidative damage when challenged with superoxide [42]. While superoxide is too short-lived to diffuse into the PEGDA hydrogel, the molecule rapidly reacts with $NO^{\bullet}$ to form $OONO^{-}$ and decomposes to H_2O_2 [21-23]. Both molecules have significantly longer half-lives and are predicted to diffuse deeply into the hydrogel capsule [58, 59]. It is oxidative damage from these ROS that likely mediates the reduced metabolic activity observed when cells in blank hydrogels are treated with superoxide. Fortuitously, the promiscuity of manganese porphyrin SOD mimetics has been previously demonstrated and these molecules are known to possess

enzymatic activity to breakdown H_2O_2 and $OONO^-$ [38, 39]. The breakdown of these ROS likely explains the mechanism by which MnTPPyP-Acryl preserves encapsulated cell viability in this study and further highlights the anti-oxidative benefit of MnTPPyP-functionalized PEG scaffolds.

This study showcases the capacity of polymerized MnTPPyP-Acryl to protect encapsulated cells from ROS damage, but there are still many hurdles to overcome before adequate immunoprotection will be achieved to remove the need for immunosuppression following a transplant. Towards this goal, our laboratory and others have investigated alternative approaches to reduce the concentration of cytotoxic molecules within cell-laden capsules. Peptides and antibodies have been used to sequester cytokines or inflammatory molecules within barrier materials and have been shown to increase encapsulated cell viability [25, 50]. Likewise, we have reported strategies to reduce the local population of inflammatory cells adjacent to transplants [60, 61]. We envision that MnTPPyP-Acryl might be used in tandem with these and other immunoprotection strategies to improve active immunoisolation barriers and increase cell survival. In summary, immunoisolation within MnTPPyP-co-PEG hydrogels provides localized protection of encapsulated cells from ROS damage and may provide an effective route towards improving long-term survival in future transplantation studies.

3.5 ACKNOWLEDGEMENTS

The authors wish to thank Dr. Charles Cheung for training and initial guidance in this project, Dr. Alex Aimetti for helpful discussions and Abigail Bernard for assistance with β-cell culture. We gratefully acknowledge financial support from the National

Institute of Health (RO1DK076084), the Howard Hughes Medical Institute, and the Department of Education's Graduate Assistance in Areas of National Need fellowship to P.S.H.

3.6 REFERENCES

1. Freed CR, Greene PE, Breeze RE, Tsai WY, DuMouchel W, Kao R, et al. Transplantation of embryonic dopamine neurons for severe Parkinson's disease. The New England journal of medicine 2001 Mar 8;344(10):710-719.

2. Brittberg M, Lindahl A, Nilsson A, Ohlsson C, Isaksson O, Peterson L. Treatment of deep cartilage defects in the knee with autologous chondrocyte transplantation. The New England journal of medicine 1994 Oct 6;331(14):889-895.

3. Pavlakis M, Khwaja K. Pancreas and islet cell transplantation in diabetes. Current opinion in endocrinology, diabetes, and obesity 2007 Apr;14(2):146-150.

4. Shapiro AM, Lakey JR, Ryan EA, Korbutt GS, Toth E, Warnock GL, et al. Islet transplantation in seven patients with type 1 diabetes mellitus using a glucocorticoid-free immunosuppressive regimen. The New England journal of medicine 2000 Jul 27;343(4):230-238.

5. White SA, Shaw JA, Sutherland DE. Pancreas transplantation. Lancet 2009 May 23;373(9677):1808-1817.

6. www.clinicaltrails.gov.

7. Bertuzzi F, Ricordi C. Beta-cell replacement in immunosuppressed recipients: old and new clinical indications. Acta diabetologica 2007 Dec;44(4):171-176.

8. Wilson JT, Chaikof EL. Challenges and emerging technologies in the immunoisolation of cells and tissues. Advanced drug delivery reviews 2008 Jan 14;60(2):124-145.

9. Nyberg SL, Yagi T, Matsushita T, Hardin J, Grande JP, Gibson LE, et al. Membrane barrier of a porcine hepatocyte bioartificial liver. Liver Transpl 2003 Mar;9(3):298-305.

10. Shi XL, Zhang Y, Han B, Gu JY, Chu XH, Xiao JQ, et al. Effects of Membrane Molecular Weight Cutoff on Performance of a Novel Bioartificial Liver. Artificial organs 2011 Mar 3.

11. Emerich DF, Winn SR. Immunoisolation cell therapy for CNS diseases. Crit Rev Ther Drug Carrier Syst 2001;18(3):265-298.

12. Lee MK, Bae YH. Cell transplantation for endocrine disorders. Advanced drug delivery reviews 2000 Aug 20;42(1-2):103-120.

13. de Vos P, Hamel AF, Tatarkiewicz K. Considerations for successful transplantation of encapsulated pancreatic islets. Diabetologia 2002 Feb;45(2):159-173.

14. Cui H, Tucker-Burden C, Cauffiel SM, Barry AK, Iwakoshi NN, Weber CJ, et al. Long-term metabolic control of autoimmune diabetes in spontaneously diabetic nonobese diabetic mice by nonvascularized microencapsulated adult porcine islets. Transplantation 2009 Jul 27;88(2):160-169.

15. Cruise GM, Hegre OD, Lamberti FV, Hager SR, Hill R, Scharp DS, et al. In vitro and in vivo performance of porcine islets encapsulated in interfacially photopolymerized poly(ethylene glycol) diacrylate membranes. Cell transplantation 1999 May-Jun;8(3):293-306.

16. Weber LM, Hayda KN, Anseth KS. Cell-matrix interactions improve beta-cell survival and insulin secretion in three-dimensional culture. Tissue engineering 2008 Dec;14(12):1959-1968.

17. Weber LM, Anseth KS. Hydrogel encapsulation environments functionalized with extracellular matrix interactions increase islet insulin secretion. Matrix Biol 2008 Oct;27(8):667-673.

18. Lin CC, Anseth KS. Glucagon-Like Peptide-1 Functionalized PEG Hydrogels Promote Survival and Function of Encapsulated Pancreatic beta-Cells. Biomacromolecules 2009 Sep;10(9):2460-2467.

19. Jang JY, Lee DY, Park SJ, Byun Y. Immune reactions of lymphocytes and macrophages against PEG-grafted pancreatic islets. Biomaterials 2004 Aug;25(17):3663-3669.

20. de Vos P, Marchetti P. Encapsulation of pancreatic islets for transplantation in diabetes: the untouchable islets. Trends Mol Med 2002 Aug;8(8):363-366.

21. Mohseni Salehi Monfared SS, Larijani B, Abdollahi M. Islet transplantation and antioxidant management: a comprehensive review. World J Gastroenterol 2009 Mar 14;15(10):1153-1161.

22. Hadjivassiliou V, Green MH, James RF, Swift SM, Clayton HA, Green IC. Insulin secretion, DNA damage, and apoptosis in human and rat islets of Langerhans following exposure to nitric oxide, peroxynitrite, and cytokines. Nitric Oxide 1998;2(6):429-441.

23. Di Matteo MA, Loweth AC, Thomas S, Mabley JG, Morgan NG, Thorpe JR, et al. Superoxide, nitric oxide, peroxynitrite and cytokine combinations all cause functional impairment and morphological changes in rat islets of Langerhans and insulin secreting cell lines, but dictate cell death by different mechanisms. Apoptosis 1997;2(2):164-177.

24. Delaney CA, Tyrberg B, Bouwens L, Vaghef H, Hellman B, Eizirik DL. Sensitivity of human pancreatic islets to peroxynitrite-induced cell dysfunction and death. FEBS letters 1996 Oct 7;394(3):300-306.

25. Lin CC, Metters AT, Anseth KS. Functional PEG-peptide hydrogels to modulate local inflammation induced by the pro-inflammatory cytokine TNFalpha. Biomaterials 2009 Oct;30(28):4907-4914.

26. Sun LT, Bencherif SA, Gilbert TW, Farkas AM, Lotze MT, Washburn NR. Biological activities of cytokine-neutralizing hyaluronic acid-antibody conjugates. Wound Repair Regen May-Jun;18(3):302-310.

27. Muscoli C, Cuzzocrea S, Riley DP, Zweier JL, Thiemermann C, Wang ZQ, et al. On the selectivity of superoxide dismutase mimetics and its importance in pharmacological studies. British journal of pharmacology 2003 Oct;140(3):445-460.

28. Lenzen S, Drinkgern J, Tiedge M. Low antioxidant enzyme gene expression in pancreatic islets compared with various other mouse tissues. Free radical biology & medicine 1996;20(3):463-466.

29. Grankvist K, Marklund S, Taljedal IB. Superoxide dismutase is a prophylactic against alloxan diabetes. Nature 1981 Nov 12;294(5837):158-160.

30. Piganelli JD, Flores SC, Cruz C, Koepp J, Batinic-Haberle I, Crapo J, et al. A metalloporphyrin-based superoxide dismutase mimic inhibits adoptive transfer of autoimmune diabetes by a diabetogenic T-cell clone. Diabetes 2002 Feb;51(2):347-355.

31. Thiruchelvam M, Prokopenko O, Cory-Slechta DA, Buckley B, Mirochnitchenko O. Overexpression of superoxide dismutase or glutathione peroxidase protects against the paraquat + maneb-induced Parkinson disease phenotype. The Journal of biological chemistry 2005 Jun 10;280(23):22530-22539.

32. Pedulla M, d'Aquino R, Desiderio V, de Francesco F, Puca A, Papaccio G. MnSOD mimic compounds can counteract mechanical stress and islet beta cell apoptosis, although at appropriate concentration ranges. Journal of cellular physiology 2007 Aug;212(2):432-438.

33. Nomikos IN, Wang Y, Lafferty KJ. Involvement of O2 radicals in 'autoimmune' diabetes. Immunology and cell biology 1989 Feb;67 (Pt 1):85-87.

34. Salvemini D, Riley DP, Cuzzocrea S. SOD mimetics are coming of age. Nature reviews 2002 May;1(5):367-374.

35. Pasternack RF, Banth A, Pasternack JM, Johnson CS. Catalysis of the disproportionation of superoxide by metalloporphyrins. III. Journal of inorganic biochemistry 1981 Nov;15(3):261-267.

36. Haskins K, Bradley B, Powers K, Fadok V, Flores S, Ling X, et al. Oxidative stress in type 1 diabetes. Annals of the New York Academy of Sciences 2003 Nov;1005:43-54.

37. Benov L, Batinic-Haberle I. A manganese porphyrin suppresses oxidative stress and extends the life span of streptozotocin-diabetic rats. Free radical research 2005 Jan;39(1):81-88.

38. Szabo C, Day BJ, Salzman AL. Evaluation of the relative contribution of nitric oxide and peroxynitrite to the suppression of mitochondrial respiration in immunostimulated macrophages using a manganese mesoporphyrin superoxide dismutase mimetic and peroxynitrite scavenger. FEBS letters 1996 Feb 26;381(1-2):82-86.

39. Day BJ, Fridovich I, Crapo JD. Manganic porphyrins possess catalase activity and protect endothelial cells against hydrogen peroxide-mediated injury. Archives of biochemistry and biophysics 1997 Nov 15;347(2):256-262.

40. Nakaoka R, Tabata Y, Yamaoka T, Ikada Y. Prolongation of the serum half-life period of superoxide dismutase by poly(ethylene glycol) modification. J Control Release 1997 Jun;46(3):253-261.

41. Kojima Y, Akaike T, Sato K, Maeda H, Hirano T. Polymer conjugation to Cu,Zn-SOD and suppression of hydroxyl radical generation on exposure to H2O2: Improved stability of SOD in vitro and in vivo. J Bioact Compat Polym 1996 Jul;11(3):169-190.

42. Li Z, Wang F, Roy S, Sen CK, Guan J. Injectable, highly flexible, and thermosensitive hydrogels capable of delivering superoxide dismutase. Biomacromolecules 2009 Dec 14;10(12):3306-3316.

43. Chiumiento A, Dominguez A, Lamponi S, Villalonga R, Barbucci R. Anti-inflammatory properties of superoxide dismutase modified with carboxymetil-cellulose polymer and hydrogel. Journal of materials science 2006 May;17(5):427-435.

44. Chiumiento A, Lamponi S, Barbucci R, Dominguez A, Perez Y, Villalonga R. Immobilizing Cu,Zn-superoxide dismutase in hydrogels of carboxymethylcellulose improves its stability and wound healing properties. Biochemistry (Mosc) 2006 Dec;71(12):1324-1328.

45. Cheung CY, McCartney SJ, Anseth KS. Synthesis of Polymerizable Superoxide Dismutase Mimetics to Reduce Reactive Oxygen Species Damage in Transplanted Biomedical Devices. Advanced Functional Materials 2008 Oct;18(20):3119-3126.

46. McCord JM, Fridovich I. Superoxide dismutase. An enzymic function for erythrocuprein (hemocuprein). The Journal of biological chemistry 1969 Nov 25;244(22):6049-6055.

47. Cohen HJ, Chovaniec ME. Superoxide generation by digitonin-stimulated guinea pig granulocytes. A basis for a continuous assay for monitoring superoxide production and for the study of the activation of the generating system. The Journal of clinical investigation 1978 Apr;61(4):1081-1087.

48. Choi SY, Ha H, Kim KT. Capsaicin inhibits platelet-activating factor-induced cytosolic Ca2+ rise and superoxide production. J Immunol 2000 Oct 1;165(7):3992-3998.

49. Cruise GM, Scharp DS, Hubbell JA. Characterization of permeability and network structure of interfacially photopolymerized poly(ethylene glycol) diacrylate hydrogels. Biomaterials 1998 Jul;19(14):1287-1294.

50. Lin CC, Boyer PD, Aimetti AA, Anseth KS. Regulating MCP-1 diffusion in affinity hydrogels for enhancing immuno-isolation. J Control Release 2010 Mar 19;142(3):384-391.

51. Weber LM, Hayda KN, Haskins K, Anseth KS. The effects of cell-matrix interactions on encapsulated beta-cell function within hydrogels functionalized with matrix-derived adhesive peptides. Biomaterials 2007 Jul;28(19):3004-3011.

52. Su J, Hu BH, Lowe WL, Jr., Kaufman DB, Messersmith PB. Anti-inflammatory peptide-functionalized hydrogels for insulin-secreting cell encapsulation. Biomaterials Jan;31(2):308-314.

53. Gabler WL, Creamer HR, Bullock WW. Modulation of the kinetics of induced neutrophil superoxide generation by fluoride. Journal of dental research 1986 Sep;65(9):1159-1165.

54. Luther MJ, Davies E, Muller D, Harrison M, Bone AJ, Persaud SJ, et al. Cell-to-cell contact influences proliferative marker expression and apoptosis in MIN6 cells grown in islet-like structures. American journal of physiology 2005 Mar;288(3):E502-509.

55. Hauge-Evans AC, Squires PE, Persaud SJ, Jones PM. Pancreatic beta-cell-to-beta-cell interactions are required for integrated responses to nutrient stimuli: enhanced Ca2+ and insulin secretory responses of MIN6 pseudoislets. Diabetes 1999 Jul;48(7):1402-1408.

56. Konstantinova I, Nikolova G, Ohara-Imaizumi M, Meda P, Kucera T, Zarbalis K, et al. EphA-Ephrin-A-mediated beta cell communication regulates insulin secretion from pancreatic islets. Cell 2007 Apr 20;129(2):359-370.

57. Lin CC. Cell-cell communication mimicry with PEG hydrogels for enhancing Beta-cell function. Proc Natl Acad Sci USA 2010 2011.

58. Kavdia M, Lewis RS. Free radical profiles in an encapsulated pancreatic cell matrix model. Annals of biomedical engineering 2002 May;30(5):721-730.

59. Uchiyama T, Kiritoshi Y, Watanabe J, Ishihara K. Degradation of phospholipid polymer hydrogel by hydrogen peroxide aiming at insulin release device. Biomaterials 2003 Dec;24(28):5183-5190.

60. Cheung CY, Anseth KS. Synthesis of immunoisolation barriers that provide localized immunosuppression for encapsulated pancreatic islets. Bioconjug Chem 2006 Jul-Aug;17(4):1036-1042.

61. Hume PS, Anseth KS. Inducing local T cell apoptosis with anti-Fas-functionalized polymeric coatings fabricated via surface-initiated photopolymerizations. Biomaterials 2010 Apr;31(12):3166-3174.

Chapter 4

Inducing local T cell apoptosis with anti-Fas-functionalized polymeric coatings fabricated via surface-initiated photopolymerizations

(As appears in *Biomaterials*, 31:3166-74. **2010**)

Cell encapsulation has long been investigated as a means to achieve transplant immunoprotection as it creates a physical barrier between allograft tissue and host immune cells. Encapsulation with passive barrier materials alone, however, is generally insufficient to protect donor tissue from rejection, because small cytotoxic molecules produced by activated T cells can diffuse readily into the capsule and mediate allograft death. As a means to provide bioactive protection for polymeric encapsulation devices, we investigated a functionalized polymeric coating that mimics a natural T cell regulation pathway. T cells are regulated *in vivo* via Fas, a well-known 'death receptor,' whereby effector cells express Fas ligand and elicit T cell apoptosis upon binding the Fas receptor on a T cell surface. Anti-Fas antibodies are capable of replicating this effect and induce T cell apoptosis in solution. Here, an iniferter-based living radical polymerization was utilized to fabricate surface-anchored polymer chains containing poly(ethylene glycol) with covalently-incorporated pendant anti-Fas antibody. Using this reaction mechanism, we demonstrate fabrication conditions that yield surface densities in excess of 1.5 ng/cm^2 of incorporated therapeutic, as detected by ELISA. Additionally, we show that coatings containing anti-Fas antibody induced significant T cell apoptosis,

21±2 % of cells, after 24 hours. Finally, the incorporation of a T cell adhesion ligand, intracellular adhesion molecule-1, along with anti-Fas antibody, yielded even higher levels of apoptosis, 34±1% of T cells, compared to either signal alone.

4.1 INTRODUCTION

Cell transplantation has the potential to cure numerous diseases of the endocrine, cardiovascular, and central nervous systems [1-3]. However, clinical prevalence of allogeneic cell transplantation is limited due, in part, to the side effects of immunosuppressants administered systemically for suppressing host immune rejection [4]. Encapsulating donor cells within immunoisolation barrier materials has been widely explored as a means to decrease the necessity of systemic immunosuppression, because the barrier materials can block direct contact between the transplanted grafts and the host immune cells [4]. For example, the encapsulation of pancreatic β-cells for the treatment of type I diabetes mellitus has been extensively studied over the last 30 years [5,6]. An important criterion of designing materials for immunoisolation is that the capsule should block immune cell contact, but must not restrict the diffusion of small molecules such as nutrients, glucose, and insulin, as they are necessary for maintaining β-cell survival and transplant function. While maintaining permeability of the capsule is critical, it has been shown that small cytotoxic molecules produced by activated, autoreactive T lymphocytes are capable of infiltrating the capsule and inducing donor cell apoptosis [7-9]. These cytotoxic molecules include reactive oxygen species (ROS), interleukin 1β (IL-1β), and tumor necrosis factor alpha (TNF-α), etc. While the material properties of the encapsulation systems are improving [10], systemic immunosuppression remains necessary for the long-term (>1 yr) survival of encapsulated β-cells [11,12].

Recently, efforts have been made to fabricate bioactive encapsulation barriers capable of regulating the local immune environment. For example, a polymerizable superoxide dismutase mimetic has been described which catalyzes the dismutation of superoxide into hydrogen and oxygen when co-photopolymerized with poly(ethylene glycol)-diacrylate (PEGDA) [13]. Likewise, methods to conjugate antibodies or peptides which sequester TNF-α within encapsulation materials have been developed to slow cytokine diffusion and improve encapsulated cell viability [14,15]. Unlike these approaches, which regulate the capsule's internal cytokine environment, we report an alternate strategy to functionalize the surface of polymeric encapsulation materials, such as PEGDA hydrogels, to modulate the immune reactions by inducing local T lymphocyte apoptosis.

Previously, research has investigated strategies to induce T lymphocyte apoptosis utilizing Fas signaling [16]. Fas, a cell surface receptor in the TNF-α superfamily, induces apoptosis upon Fas ligand (FasL) binding. The Fas pathway plays two important roles in normal lymphocyte regulation. First, autoreactive T cells undergo negative selection via clonal deletion mediated by Fas/FasL signaling [17]. Second, T cells strongly upregulate Fas expression upon activation, and FasL-expressing cytotoxic lymphocytes induce T cell apoptosis to clear a completed immune response [18]. To initiate the signal transduction cascade resulting in cell apoptosis, pre-associated Fas receptors on the cell membrane must bind multiple FasLs [19]. Therefore, oligomerization of FasL improves the efficacy with which apoptosis is induced [20].

DX2, an anti-Fas monoclonal antibody of the IgG1 subclone, induces apoptosis upon cross-linking the T cell Fas receptor [21]. Cheung and Anseth [16] previously

demonstrated that DX2 induces nearly 20% T cell apoptosis when covalently conjugated to the surface of gels formed from 7.5 wt% PEGDA and 2.5 wt% N-hydroxysucinimide-PEG-acrylate (NPA) hydrogel. Others have shown a local anti-inflammatory effect mediated by IgM-class anti-Fas antibodies adsorbed to polyester membranes [22,23]. While coating anti-Fas antibody directly onto biomaterial surfaces preserves some biological activity, these strategies yield a relatively low protein surface density and limited accessibility of functional groups to the surroundings. Herein, a living radical photopolymerization (LRP)-based strategy was exploited to graft PEG chains with pendant DX2 antibodies from a polymeric surface. As illustrated in Fig. 4.1, an LRP mechanism is mediated by a photoiniferter specie, containing a diethyldithiocarbamate (DTC) group able to reversibly initiate photopolymerization from a surface. DTC-mediated LRP yields uniform, highly mobile polymer chains whose length is proportional to photopolymerization time [24]. As previously reported [25,26], upon covalent modification with a polymerizable acrylate group, antibodies may be copolymerized onto these surface anchored polymer chains. This architecture provides several benefits, including improved protein accessibility to the surroundings due to high chain mobility and increased antibody surface density due to the incorporation of multiple antibodies per chain. In addition, the natural DX2 clustering that occurs as antibodies are incorporated on polymer chains may provide the added benefit of increasing the likelihood that multiple DX2 binding events occur at one T cell Fas receptor. This multimerization could improve the chance that an apoptotic signal is delivered.

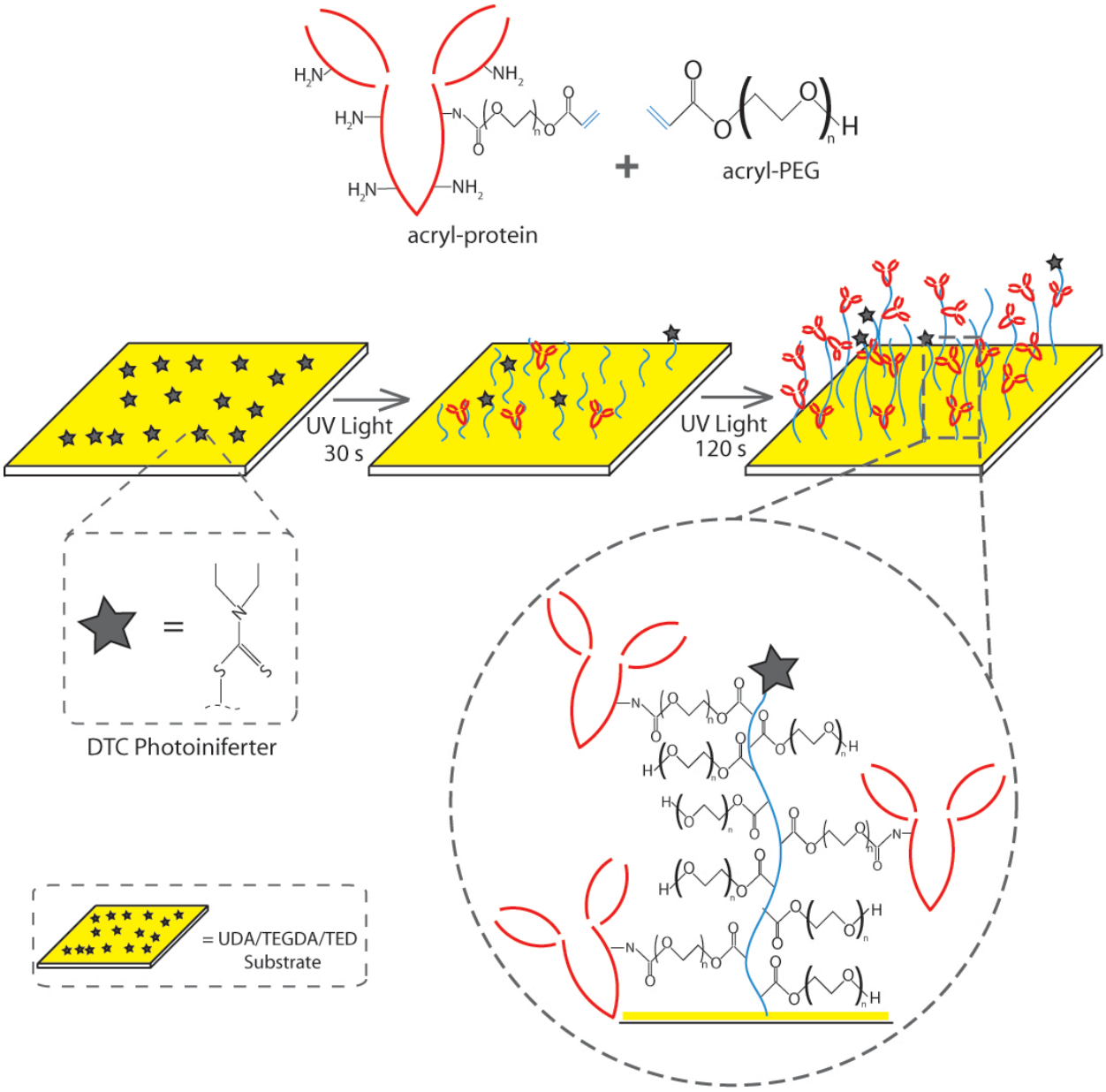

Fig. 4.1. Schematic illustrating surface-initiated polymerization of acrylated proteins. ACRYL-protein is co-photopolymerized with ACRYL-PEG atop a polymeric substrate containing a DTC photoiniferter. Polymer chains consisting of polyacrylate backbones with pendant proteins are formed on the surface, and the surface modification is proportional to UV exposure time.

Herein, the fabrication, characterization and evaluation of surface-initiated polymer chains is reported for chains consisting of PEG monoacrylate (400 Da) with a high surface density of pendant acrylated IgG. Further, cell studies were performed to evaluate the effects of DX2-conjugating polymer coatings on inducing T cell apoptosis.

Finally, a T cell adhesion ligand, Inter-Cellular Adhesion Molecule 1 (ICAM-1), was incorporated in the polymer coating to increase the interaction between T cells and the material surface. Our group has previously demonstrated that iniferter-mediated LRP allows for the fabrication of multifunctional grafts [25], and here, we report dually-functionalized polymeric coatings, containing DX2 and ICAM-1, which yield a significant increase in T cell apoptosis.

4.2 MATERIALS & METHODS

4.2.1 Materials

Mouse anti-human Fas monoclonal IgG (DX2), goat anti-Fas receptor IgG, and ICAM-1/Fc chimera fusion protein (ICAM-1) were obtained from R&D Systems. All other IgGs were obtained from Jackson Immunoresearch. Soluble Fas receptor was purchased from Peprotech. Monoacrylated poly(ethylene glycol)-N-hydroxysuccinimide (ACRYL-PEG-NHS, MW=3400) was purchased from Laysan Bio Inc. Slide-a-Lyzer dialysis cassettes (10,000 MWCO), fluoraldehyde Reagent Solution, and TMB ELISA Substrate were obtained from Thermo Fisher Scientific. Aromatic urethane diacrylate (UDA) was a generous gift donated by UCB Chemicals Corp. Triethylene glycol diacrylate (TEGDA) was purchased from Polysciences Inc. Tetraethylthiuram disulfide photoiniferter (TED) was obtained from Sigma-Aldrich. 2,2-dimethoxy-2-phenylacetophenone initiator (DMPA) was purchased from Ciba Specialty Chemicals. Monoacrylated poly(ethylene glycol) (ACRYL-PEG, MW=400) was purchased from Monomer-Polymer & Dajac Labs. Vybrant apoptosis assay kit #3, AlamarBlue reagent,

and Trypan Blue stain were obtained from Invitrogen. Vector VIP stain was obtained from Vector Labs.

4.2.2 Protein acrylation and characterization

Goat IgG (IgG), fluorescein-conjugated goat IgG (F-IgG), DX2 and ICAM-1 were acrylated by reacting proteins (2 mg/ml) with 3400 Da ACRYL-PEG-NHS at defined molar ratios in 50 mM sodium bicarbonate buffer, pH 8.4. The reactions proceeded for 3 h at room temperature under constant stirring. The percentage of protein acrylation was determined immediately following reaction using Fluoraldehyde regent to compare the concentration of free amine groups prior to and following reaction. Unreacted ACRYL-PEG-NHS was removed by dialysis against deionized water for 24 hrs using a 10 000 MWCO Slide-a-Lyzer dialysis cassette. Solutions were lyophilized to yield solid acrylated IgG (ACRYL-IgG), acrylated F-IgG (F-ACRYL-IgG), acrylated DX2 (ACRYL-DX2), or acrylated ICAM-1 (ACRYL-ICAM-1).

4.2.3 Preparation of the polymer substrate

The polymeric grafting substrate used in these studies consisted of 49.125 wt% UDA, 49.125 wt% TEGDA, 0.25 wt% TED iniferter, and 1.5 wt% DMPA initiator. This pre-polymer solution was sonicated and stirred intermittently for >1 hr and was purged with argon for 2 min prior to polymerization. The base layer was photopolymerized by exposing mixed pre-polymer solution to 35 mW/cm^2 ultraviolet, collimated light

generated by a mercury arc-lamp centered at 365 nm for 500 s. Sebra *et al.* [25] has previously demonstrated that these conditions yield a polymeric network with greater than 90% double bond conversion. Polymerized UDA-TEGDA substrates were immersed in methanol for 15 min with stirring to remove unreacted monomers and excess DMPA.

4.2.4 *Surface-initiated photopolymerization of acrylated proteins*

Acrylated proteins where covalently incorporated on polymer chains using a living radical photopolymerization-based chemistry as previously described [25]. Briefly, acrylated protein, including 250 µg/ml ACRYL-IgG, 250 µg/ml ACRYL-DX2, or 25 µg/ml ACRYL-ICAM-1, was dissolved in 50% v/v 400 Da ACRYL-PEG in phosphate buffered saline (PBS, pH=7.4). This solution was applied onto the DTC-containing substrate surface prepared as described earlier and exposed to 35 mW/cm^2 collimated ultraviolet light centered at 365 nm for 0 – 900 s. Following polymerization, devices were immersed in deionized water for 1 hr, followed by rinsing in 70% ethanol overnight. Then, the devices were washed in sterile-filtered 30% ethanol for 1 hr and finally rinsed in sterile PBS overnight. All washing steps were carried out at room temperature with mixing.

4.2.5 Detection of polymerized ACRYL-IgG

The surface density of polymerized ACRYL-IgG was assessed using a modified ELISA. ACRYL-IgG coatings were incubated at room temperature for 8 min with 8

μg/ml horse radish peroxidase (HRP)-conjugated donkey anti-goat detection antibody (HRP-DAG-IgG), and then rinsed 4 times with PBS. HRP-treated coatings were either: 1) Incubated 15 min with Vector VIP reagent to stain HRP, or 2) Dissected with a biopsy punch into 6 mm diameter disks and placed in the bottom of a 96-well plate. These HRP-treated samples were incubated with 100 μl TMB ELISA substrate for 20 min with mixing to allow color change, and the reaction was quenched with the addition of 100 μl 2N H_2SO_4. The 450 nm absorbance of each sample was measured and converted to ACRYL-IgG surface density by comparing sample absorbance to that of TMB-treated control solutions with known HRP-DAG-IgG mass.

Fluorescein-conjugated ACRYL-goat IgG (F-ACRYL-IgG) was polymerized, as described above, and incubated 30 min with 8 μg/ml rhodamine-conjugated donkey anti-goat IgG (R-DAG-IgG) prior to fluorescent imaging with confocal microscopy (Axioplan 2, Zeiss). Height of dry coatings was determined using profilometry (Stylus Profiler, Dektak 6M, force = 1 mg, radium = 12.5 mm, and range = 1 mm).

4.2.6 Characterization of ACRYL-DX2-containing coatings

ACRYL-DX2 was photografted at a concentration of 250 μg/ml, as described above. Grafted ACRYL-DX2 was detected and quantified by Vector VIP staining and the modified ELISA described above, where an HRP-conjugated goat anti-mouse IgG (HRP-GAM-IgG) was used as the detection antibody. In addition, a modified sandwich ELISA was performed where devices containing polymerized ACRYL-DX2 were incubated for 1 hr with 1 μg/ml soluble Fas receptor, followed by 1 μg/ml goat anti-Fas

receptor IgG, and incubated 8 min with 5 µg/ml HRP-DAG-IgG. Samples were rinsed and stained with Vector VIP for 15 min to verify ACRYL-DX2 maintained the capacity to bind the Fas receptor following incorporation in the surface graft.

4.2.7 Cell culture

Jurkat T cell lymphoma cells and I9.2 Fas-insensitive Jurkats (ATCC, Manassas, VA) were cultured in RPMI 1640 supplemented with 10% fetal bovine serum, 100 u/ml Penicillin/Streptomycin, and 0.5 µg/ml Fungizone. Cells were incubated at 37 °C in humid conditions with 5% CO_2. The biological activity of soluble ACRYL-DX2 was assessed by incubating Jurkat T cells (50 000 cells/ml, 200 µl media) with ACRYL-DX2 at a concentration of 5 µg/ml. After 6, 12, 24, and 48 hrs, the percentage of T cells undergoing apoptosis was analyzed using an Annexin assay, as described below. Maximum T cell apoptosis was detected after 24 hrs of culture with ACRYL-DX2, so this time point was used for all subsequent studies. The biological activity of functionalized polymer coatings containing ACRYL-DX2 was also evaluated by incubation with T cells. Disks of functionalized substrate were dissected using a 6 mm diameter biopsy punch and placed in the bottom of a 96-well plate. Jurkat and I9.2 T cells were seeded atop coatings at 50 000 cells/ml in 200 µl media and cultured for 24 hrs, prior to analysis for apoptosis.

4.2.8 T cell assays

T cells were stained for apoptosis using the Vybrant apoptosis assay kit #3. Cells were stained with fluorescein-labeled Annexin V and counterstained with

propidium iodide (PI) to differentiate apoptotic and necrotic cells, respectively. Cells were imaged using a Nikon Eclipse TE300 fluorescent microscope and counted in 4 random fields of view per sample. Each field contained approximately 100-200 cells. The fraction of apoptotic cells was calculated by dividing the number of fluorescein-positive (but PI-negative) T cells by the cell number. Bulk T cell metabolic activity was also analyzed after 24 hrs by adding 22 µl of AlamarBlue reagent to each condition (resulting in a 10% v/v AlamarBlue solution) and incubating for 3 hr. Fluorescence (excitation: 560 nm, emission: 590 nm) represented the metabolic activity of the living cells. All cell data is shown as the mean of 4 replicates and each experiment has been repeated at least twice.

4.2.9 T Cell Adhesion Studies

T cells were seeded atop coatings functionalized with ACRYL-ICAM-1, ACRYL-DX2, ACRYL-ICAM-1 / ACRYL-DX2, or control, in 96-well plates, as described above. At 6 hr, 12 hr, and 24 hr time points, media was removed from each well and gently washed three times with 200 µl PBS. 50 ul of 50% Trypan Blue Stain (0.4%), 50% media was added to denote dead cells and incubated 5 minutes. Bright field microscopy was used to count the number of live cells remaining on the polymer surface and the percentage of adherent cells was calculated by dividing the number of cells remaining on the polymer surface by the total number of cells seeded.

4.2.10 Statistical analysis

Statistical significance was determined using a two-tailed, unpaired Student's t-test. Differences between datasets were considered statistically significant when the p value was less than 0.05. All results are presented as mean ± standard error of the mean.

4.3 RESULTS

4.3.1 Acrylation of IgG

IgG was acrylated prior to surface grafting by reacting primary amine groups with ACRYL-PEG-NHS. Degree of acrylation was controlled by varying the molar ratio of ACRYL-PEG-NHS to IgG from 0:1 to 25:1. While increasing the number of acrylate groups per IgG increases the likelihood that the protein will be incorporated into graft polymer chains, over-modification can reduce the biological activity of the molecule. To verify the biological activity of ACRYL-DX2 (acrylated anti-Fas IgG) post modification, ACRYL-DX2 was added to Jurkat T cell cultures for 24 hours to induce apoptosis. As shown in Fig. 4.2, a 25-fold, but not 10-fold, molar excess of ACRYL-PEG-NHS to DX2 resulted in a significant reduction in biological activity. Thus, a reaction ratio of 10 moles ACRYL-PEG-NHS per mole IgG was used for all future studies. A Fluoraldehyde assay indicated these reaction conditions yielded 2.2±0.6 % acrylation of this 150 kDa IgG.

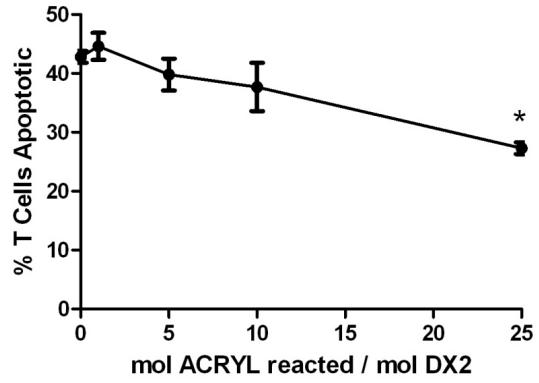

Fig. 4.2. The influence of covalent acrylation on the bioactivity of soluble ACRYL-DX2. ACRYL-PEG-NHS was reacted with DX2 in the molar ratios shown on the x-axis. As the reaction stoichiometry was increased, the efficacy with which soluble ACRYL-DX2 induced apoptosis was reduced.

4.3.2 Surface grafting of acrylated IgG

As illustrated in Fig. 4.1, ACRYL-IgG was dissolved in 50% ACRYL-PEG (400 Da) in PBS and photopolymerized from an iniferter-containing UDA-TEGDA substrate for controlled polymerization times ranging from 0 – 900 s. Because of the LRP nature of this system, one expects the polymer thickness and ACRYL-IgG incorporation to increase proportionally to light exposure time. As shown in Fig. 4.3A, profilometry of dry grafts revealed increasing dry polymer height with UV exposure time. Fig. 4.3B illustrates the relationship between detectable ACRYL-IgG surface density with photopolymerization time. Unlike dry graft height, detectable ACRYL-IgG did not consistently increase with time. Instead, a peak in detectable ACRYL-IgG existed between 120 and 180 s. ACRYL-IgG surface density was determined by a modified ELISA, so incorporated protein was only observable if bound by a detection antibody (150 kDa). We postulate that the surface-initiated chains become cross-linked for

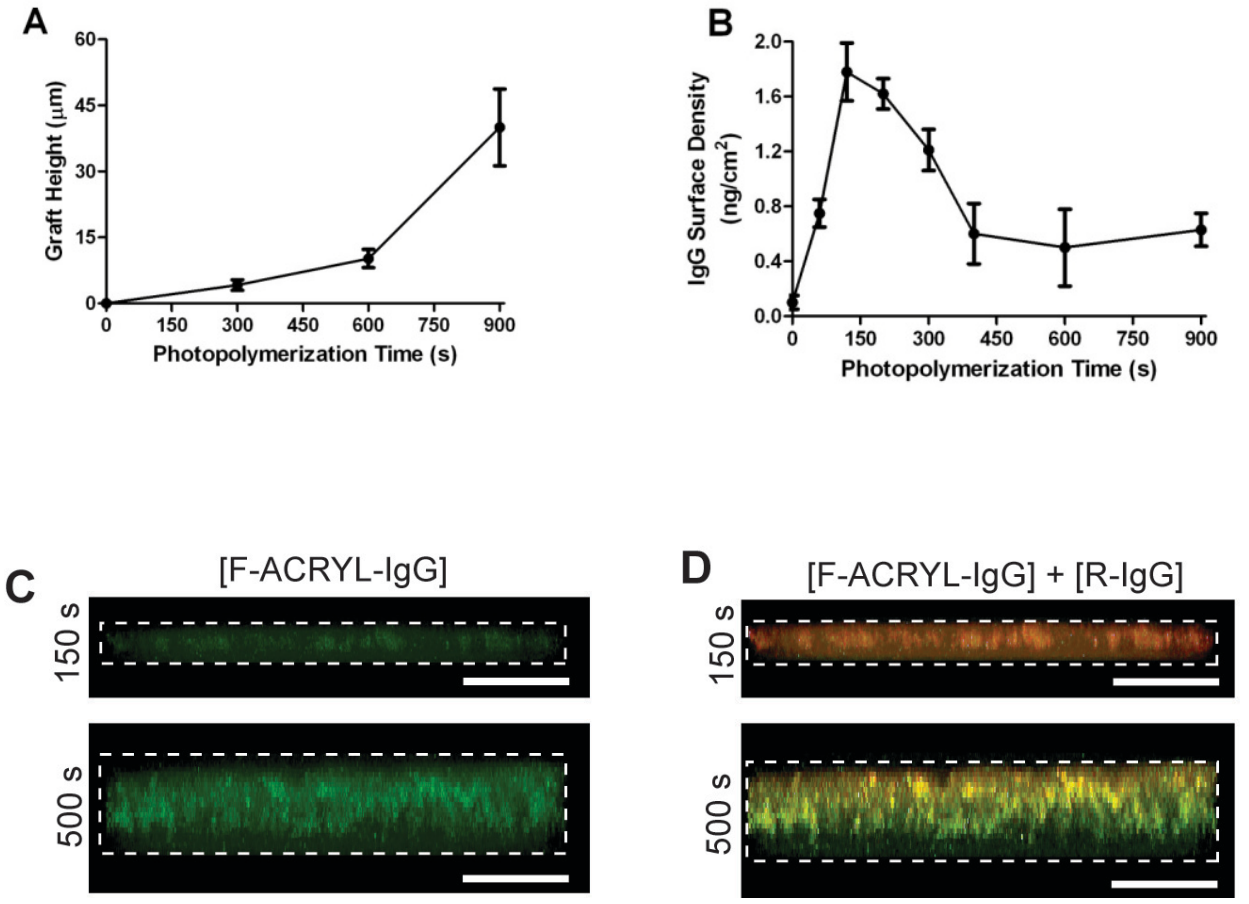

Fig. 4.3. Controlled surface-initiated photopolymerization of ACRYL-IgG. (A) Dry graft height, determined by profilometry, increases as a function of surface-initiated polymerization time. (B) Surface density of detectable ACRYL-IgG increases and then decreases as a function of polymerization time, as determined by modified ELISA. A region of high detectable ACRYL-IgG exists between 120 – 180 s fabrication times. (C) Fluorescein-tagged ACRYL-IgG from goat (F-ACRYL-IgG) was photografted for 150 and 500 s. Dashed boxes represent a cross-sectional view of the full thickness of each coating. Fluorescein is visible throughout the thickness of both samples. Scale bars = 50 μm. (D) F-ACRYL-IgG Grafts were stained with rhodamine-tagged donkey anti-goat IgG (R-IgG) to label accessible F-ACRYL-IgG. Strong full-thickness R-IgG staining is visible at 150 s but only surface staining at 500 s. Scale bars = 50 μm. (E) Surface density of detectable ACRYL-IgG decreased as a function of TED iniferter concentration in the substrate.

polymerization times greater than 180 s due to chain transfer and other non-idealities, so the detection antibody was unable to penetrate deeply into the coating. Further evidence of this phenomena is presented below.

4.3.3 Surface grafting of fluorescent ACRYL-IgG

Fluorescein-tagged ACRYL-IgG (F-ACRYL-IgG) was photografted for either 150 or 500 s. As seen in the cross-sectional images of surface-initiated coatings, shown in Fig. 4.3C, fluorescein was visible throughout the full thickness for 150 and 500 s polymerization times. Swollen coatings were approximately 10 μm and 25 μm thick, respectively. Following fabrication, surfaces were incubated with rhodamine-tagged donkey anti-goat IgG (R-IgG) to selectively label the accessible F-ACRYL-IgG. As seen in Fig. 4.3D, strong rhodamine fluorescence is visible throughout the full thickness of the 150 s graft but only observed near the top of the 500 s graft. Control coatings lacking F-ACRYL-IgG revealed no significant fluorescein or rhodamine fluorescence (data not shown), demonstrating that the presence of fluorescence is due to F-ACRYL-IgG and specific antibody binding, and not the result of physical entrapment of the antibodies. Coupled with the spike in detectable antibody observed between 120 – 180 s, we believe that the 150 and 500 s fluorescence profiles provide insight into the architecture of this surface-initiated polymer network. We postulate that non-idealities in polymer chain formation, likely due to chain transfer events, result in chain crosslinking during longer polymerization times (>300 s). This cross-linking prevents the diffusion of 150 kDa R-IgG through graft chains and indicates that ACRYL-IgG incorporated early during

the surface modification is inaccessible to the outside environment. To ensure a high surface density of accessible ACRYL-IgG, a photopolymerization time of 150 s was used for all future studies.

4.3.4 Iniferter concentration affects detectable ACRYL-IgG surface density

Surface modification and coating properties are further controlled by the density of surface grafting sites. The effect of iniferter concentration on detectable ACRYL-IgG was studied by varying the initial concentration of TED in the pre-polymer solution from 0.25 to 1.0 wt% and subsequent grafting of ACRYL-IgG for 150 s. As shown in Fig. 4.3E, maximum detectable ACRYL-IgG surface densities were observed at the lowest TED concentration, 0.25 wt%. Because TED concentration correlates with the surface bound DTC concentration, lowering the concentration of TED in the substrate reduces the total number of polymer chains initiated from the surface. By decreasing the total surface density of polymer chains, it is likely that the resulting polymer chains gain greater mobility, increasing the overall accessibility of incorporated ACRYL-IgG, and minimizes network formation via crosslinking. Minimal polymer chain initiation occurred for TED concentrations below 0.25 wt%, so lower TED concentrations were not investigated.

4.3.5 Polymerization of ACRYL-DX2 induces T cell apoptosis from a surface

ACRYL-DX2 was incorporated into surface-anchored polymer chains using the photopolymerization conditions identified to yield a high protein surface density (150 s

photopolymerization, 0.25 wt% TED). Polymers were washed > 36 hrs, as described above, to remove any unconjugated ACRYL-DX2. Incorporation of ACRYL-DX2 was verified using an ELISA-type assay and was consistently found to be between 1.4 and 1.7 ng/cm^2. Additionally, Vector VIP staining was performed prior to each ACRYL-DX2 cell experiment to verify the presence of anti-Fas IgG. The staining of circular-patterned ACRYL-DX2 grafts, shown in Fig. 4.4A, confirms the presence of ACRYL-DX2 (left) and that grafted ACRYL-DX2 remains specific binding ability to Fas receptor (right).

The biological activity of polymerized ACRYL-DX2 was assessed by its ability to induce apoptosis in T-cells. Jurkat T-cells were seeded onto surfaces with or without ACRYL-DX2 for 24 hrs. Apoptotic cells were stained with fluorescein-conjugated Annexin V. Fig. 4.4B shows representative fluorescent images of apoptotic Jurkat T-cells on a control surface, while Fig. 4.4C illustrates an increase in Jurkat apoptosis when seeded on a surface containing ACRYL-DX2. As shown in Fig. 4.4D, ACRYL-DX2 surfaces induced significant apoptosis, 21±2% of Jurkat T cells. When I9.2 T cells (Jurkats rendered insensitive to Fas-mediated apoptosis [27,28]) were exposed to ACRYL-DX2 grafts, no significant increase in apoptosis was observed. This indicates that the apoptosis induced by grafted ACRYL-DX2 is specific and mediated through DX2/Fas signaling.

4.3.6 ACRYL-ICAM-1 increases the efficacy of ACRYL-DX2

We chose to incorporate a 70 kDa ICAM-1/Fc fusion protein because its structural similarity to IgG allowed predictable acrylation using the same conditions identified for

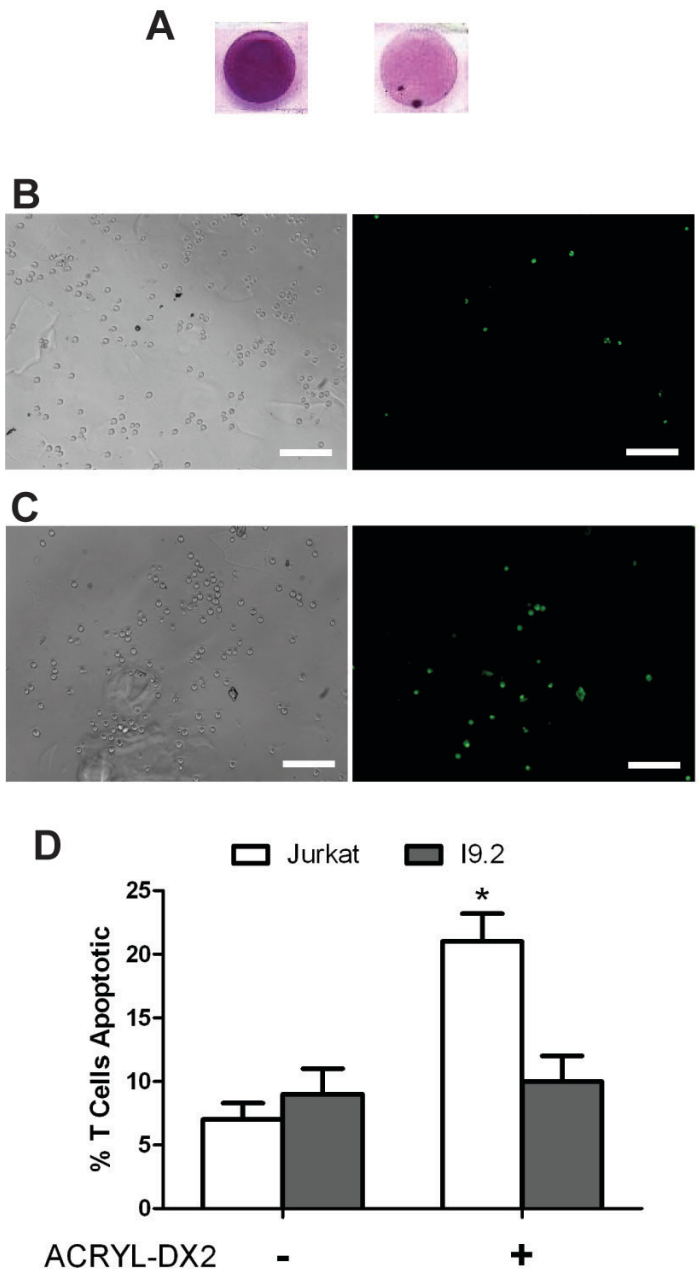

Fig. 4.4. Grafted ACRYL-DX2 induces T cell apoptosis. (A) ACRYL-DX2 was incorporated in 6 mm diameter grafts and incubated with HRP-conjugated GAM IgG (left) or soluble Fas receptor, goat anti-Fas IgG, and HRP-conguated DAG IgG (right). Both (left) and (right) were stained with Vector VIP to stain HRP. Vector VIP staining indicates (left) high ACRYL-DX2 surface density and (right) ACRYL-DX2 retains the ability to bind the Fas receptor. (B & C) Representative brightfield (right) and 480 nm fluorescent (left) images of Jurkat T cells seeded for 24 hrs on grafted (B) control and (C) ACRYL-DX2 surfaces for 24 hrs followed by staining with fluorescein-conjugated Annexin V. Apoptotic T cells are visible at 480 nm. Scale bars = 100 μm (D) Jurkat and Fas-insensitive I9.2 T cells were seeded on grafted surfaces for 24 hours and assayed for apoptosis. A statistically significant increase in apoptosis was observed for Jurkat T cells incubated on ACRYL-DX2 surfaces. Asterisks indicates a statistically significant difference ($p<0.05$) from all other values.

ACRYL-IgG. ACRYL-ICAM-1 and ACRYL-DX2 were simultaneously co-polymerized from the iniferter-containing substrates, as Sebra *et al*. [25] has previously demonstrated that multiple acrylated proteins may be simultaneously polymerized with the LRP grafting technique. As shown in Fig. 5.5A, seeding T cells on grafted polymer surfaces functionalized with ACRYL-DX2 and ACRYL-ICAM-1 resulted in ~34±1% Jurkat T cell apoptosis, an improvement of nearly 50% when compared to ACRYL-DX2 alone. Surfaces functionalized with only ACRYL-ICAM-1 did not yield a significant increase in apoptosis relative to controls, demonstrating a synergistic effect between ACRYL-ICAM-1 and ACRYL-DX2. Culturing Jurkats on ACRYL-DX2/ACRYL-ICAM-1 functionalized surfaces demonstrated more than a 50% reduction in metabolic activity when compared to control surfaces (Fig. 4.5B), likely indicating a reduction in T cell number. A statistically significant reduction in metabolic activity was not observed for T

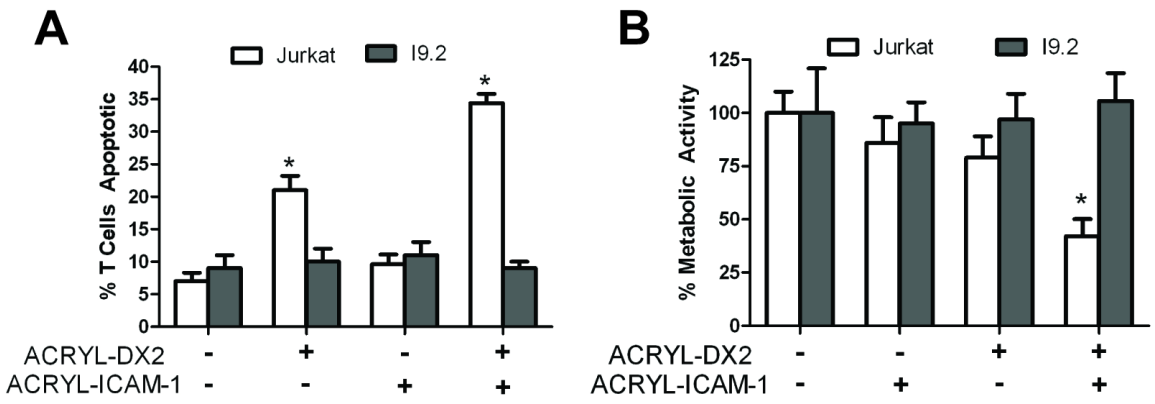

Fig. 4.5. ACRYL-ICAM-1 improves the efficacy of grafted ACRYL-DX2. (A) Grafted ACRYL-ICAM-1, when incorporated with ACRYL-DX2, increases the percentage of Jurkat T cells signaled to undergo apoptosis after 24 hrs. (B) Metabolic activity studies of Jurkat T cells seeded on control or dually-functionalized grafted surfaces for 24 hrs. Jurkat T cells show an over 50% reduction in metabolic activity when cultured on ACRYL-DX2 / ACRYL-ICAM-1 grafts. Asterisks indicates a statistically significant difference ($p<0.05$) from all other values.

cells cultured on polymeric surfaces functionalized singularly with either ACRYL-DX2 or ACRYL-ICAM-1, highlighting the importance of the synergistic effect between ACRYL-ICAM-1 and ACRYL-DX2 in reducing the population of T cells. No increase in apoptosis or decrease in metabolic activity was observed for I9.2 cells, indicating these effects were Fas-mediated.

4.3.7 Probing the T cell / material interaction

When incorporating ACRYL-ICAM-1, we considered the possibility that this ligand could enable T cells to form sustained adhesions with the functionalized surface. This behavior might be deleterious to the end goal of immunoprotection, as lymphocyte recruitment could increase the local concentration of inflammatory cytokines. T cell adherence was analyzed at 6 hr, 12 hr, and 24 hr following seeding on polymers functionalized with ACRYL-ICAM-1 and/or ACRYL-DX2. At all time points, less than 1% of cells seeded upon the polymer surface remained following a wash to remove non-adherent cells.

4.4 DISCUSSION

Towards protecting allograft tissue from rejection, cell encapsulation strategies continue to improve. Despite improvements, however, T cell-mediated rejection continues to pose a considerable hurdle to transplant acceptance. This work aimed to fabricate biomaterial coatings to reduce the local concentration of T cells. Towards that

end, we utilized an iniferter-based LRP to fabricate functionalized coatings, which mimic *in vivo* T cell signaling events.

IgG was covalently modified with acrylate groups and subsequently polymerized into surface-imitated polymer chains of poly(ethylene glycol). Using this polymer chemistry, maximum detectable IgG concentrations were identified for photopolymerization times ranging from 120-180 s, indicating that polymer networks became cross-linked for polymerization times greater than 180 s, and therefore, were less accessible to the surrounding environment. This notion was supported by the observation that fluorescently-labeled secondary antibody was able to penetrate throughout a ~20 μm coating generated by 150 s UV light exposure, but was unable to diffuse deeply within a ~50 μm coating generated by a 500 s exposure. Network cross-linking was likely the result of polymer chain transfer, and other non-idealities, which become more apparent with increased photopolymerization time. Even though polymerized fluorescent IgG was visible throughout polymer coatings grafted for 150 and 180 s, it is reasonable to assume that polymerized IgG which was not detectable by a secondary IgG would also be inaccessible to T cells. Thus, in keeping with the goal of fabricating a coating that allows bioactive molecules to be highly accessible to nearby cells, a polymerization time of 150 s was used for all future studies.

Utilizing the appropriate fabrication conditions indentified for grafting ACRL-IgG, Anti-Fas IgG (ACRYL-DX2) was incorporated into the polymer network. When T cells were seeded atop ACRYL-DX2-functionalized coatings for 24 hrs, significant apoptosis (21±2 % of cells) was observed. Prior to incubation with T cells, coatings were rinsed for 36 hrs, as described earlier, to allow for the complete removal of non-covalently

incorporated ACRYL-DX2. Therefore, the observed increase in apoptosis is due to surface-bound ACRYL-DX2, and not soluble DX2. While T cell apoptosis induced by this ACRYL-DX2-functionalized surface represents only a modest increase over the level of apoptosis induced by a previously described system, consisting of a hydrogel coated with DX2 [16], it is critical to note that our LRP grafting approach requires 80% less DX2 than the previously-investigated hydrogel coating.

While PEG is an important component of the surface-mediated polymerization, PEG is also known as a chemistry that resists non-specific protein interactions, thereby rendering it minimally adhesive for most cell types. Thus, we postulated that increased T cell apoptosis might be achieved by introducing an Inter-cellular Adhesion Molecule-1 (ICAM-1), a member of the immunoglobulin superfamily, into an ACRYL-DX2-functionalized polymeric surface. ICAM-1 is expressed by selected cell types, including endothelial cells and antigen presenting cells (APCs), and is known to bind a β2-integrin, Leukocyte Functional Antigen-1 (LFA-1), expressed on the T cell surface [29]. ICAM-1 binding is essential to initiating several T cell attachment mechanisms, including adhesion to endothelial cells for transmigration through blood vessel wall in addition to the formation of the immune synapse with an APC [29]. Furthermore, ICAM-1 binding has been shown to enhance the activity of membrane-bound FasL. Sieg *et al.* blocked ICAM-1 on the surface of FasL-expressing effector cells and observed a significant decrease in T cell apoptosis induction, suggesting that LFA-1/ICAM-1 binding stabilizes the adhesion between target and effector cells during Fas/FasL signaling [30].

Fig. 4.5 shows that the addition of acrylated ICAM-1 significantly increases (> 50%) the apoptosis induced by an ACRYL-DX2 functionalized coating and significantly

decreased (< 50 %) the overall T cell metabolic activity. Further, T cell adhesion studies indicate that this effect was possible without long-term, stable adhesion between T cells and the biomaterial surface. This is likely possible because the interaction between T cells and ICAM-1 is short lived. Others have investigated the transient nature of the interaction between T cells and ICAM-1-coated surfaces. For example, Somersalo *et al.* reported that T cells formed stable adhesions to ICAM-1 coated surfaces for approximately 15 minutes before releasing [31]. Fortuitously, the induction of Fas-mediated apoptosis occurs quickly [32], and our results indicate that the transient increase in adhesion afforded by ICAM-1 is sufficient to significantly increase ACRYL-DX2-mediated apoptosis. Further, the observed lack of sustained adhesion provides encouragement that this coating could avoid significant lymphocyte recruitment, minimizing the local concentration of inflammatory cytokines.

As with any biomaterial developed towards the eventual goal of implantation, it is important to consider the competing effects that this coating might have upon cell types not investigated herein. This is particularly important because, in addition to T cells, ICAM-1 is known to bind several classes of leukocytes. For example, ICAM-1 is implicated in neutrophil transendothelial migration [33,34] and macrophage adherence [35,36]. While the interaction that neutrophils and macrophages might have with an ICAM-1-coated biomaterial surface has not been well studied, some interaction between these cells and a coating functionalized with ACRYL-DX2/ACRYL-ICAM-1 might ultimately be beneficial toward the goal of immunoprotection. This is because, like T cells, neutrophils and macrophages have been shown to undergo apoptosis in response to Fas receptor stimulation [22,23,37-39]. Thus, the anti-inflammatory benefits of an

ACRYL-DX2/ACRYL-ICAM-1-functionlized surface could extend beyond T cells, offering greater promise that this coating may provide an active barrier against transplant rejection.

4.5 CONSLUSIONS

A surface-initiated polymerization was utilized to grow polymer chains containing anti-Fas antibody and ICAM-1 from a polymeric substrate to induce significant T cell apoptosis. Appropriate surface-mediated photopolymerization conditions were identified to polymerize a high density of detectable acrylated protein. Surfaces with polymerized ACRYL-DX2 were shown to illicit Fas-mediated T cell apoptosis, and the addition of a T cell adhesion ligand, ACRYL-ICAM-1, enhanced this pro-apoptotic affect. These findings indicate that dually functionalized (DX2 & ICAM-1) surfaces are capable of significantly reducing the local T cell population. In summary, this study introduces a new methodology to functionalize polymeric surfaces with immunosuppressive proteins and this graft architecture offers potential as a bioactive coating for future cell encapsulation devices.

4.6 ACKNOWLEDGEMENTS

The authors wish to thank Dr. Charles Cheung for training and initial guidance in this project, Dr. Chien-Chi Lin for helpful discussions regarding several aspects of this work and Dr. McKinley Lawson for training with surface-initiated polymerization.

Additionally, the authors thank Mark Tibbitt and Cole DeForest for assistance with profilometry and imaging, respectively. The authors gratefully acknowledge financial support from the National Institute of Health (R01DK076084), the Howard Hughes Medical Institute, and the Department of Education's Graduate Assistance in Areas of National Need for a fellowship to PSH.

4.7 REFERENCES

1. Wollert KC, Drexler H. Cell-based therapy for heart failure. Curr Opin Cardiol 2006;21(3):234-239.

2. Emerich DF, Winn SR. Immunoisolation cell therapy for CNS diseases. Crit Rev Ther Drug Carrier Syst 2001;18(3):265-298.

3. Lee MK, Bae YH. Cell transplantation for endocrine disorders. Adv Drug Deliv Rev 2000;42(1-2):103-120.

4. Wilson JT, Chaikof EL. Challenges and emerging technologies in the immunoisolation of cells and tissues. Adv Drug Deliv Rev 2008;60(2):124-145.

5. Lim F, Sun AM. Microencapsulated islets as bioartificial endocrine pancreas. Science 1980;210(4472):908-910.

6. Kabelitz D, Geissler EK, Soria B, Schroeder IS, Fandrich F, Chatenoud L. Toward cell-based therapy of type I diabetes. Trends Immunol 2008;29(2):68-74.

7. de Vos P, Marchetti P. Encapsulation of pancreatic islets for transplantation in diabetes: the untouchable islets. Trends Mol Med 2002;8(8):363-366.

8. Mandrup-Poulsen T, Zumsteg U, Reimers J, Pociot F, Morch L, Helqvist S, et al. Involvement of interleukin 1 and interleukin 1 antagonist in pancreatic beta-cell destruction in insulin-dependent diabetes mellitus. Cytokine 1993;5(3):185-191.

9. Jang JY, Lee DY, Park SJ, Byun Y. Immune reactions of lymphocytes and macrophages against PEG-grafted pancreatic islets. Biomaterials 2004;25(17):3663-3669.

10. Lee DY, Park SJ, Lee S, Nam JH, Byun Y. Highly poly(ethylene) glycolylated islets improve long-term islet allograft survival without immunosuppressive medication. Tissue Eng 2007;13(8):2133-2141.

11. Cui H, Tucker-Burden C, Cauffiel SM, Barry AK, Iwakoshi NN, Weber CJ, et al. Long-term metabolic control of autoimmune diabetes in spontaneously diabetic nonobese diabetic mice by nonvascularized microencapsulated adult porcine islets. Transplantation 2009;88(2):160-169.

12. Yun Lee D, Hee Nam J, Byun Y. Functional and histological evaluation of transplanted pancreatic islets immunoprotected by PEGylation and cyclosporine for 1 year. Biomaterials 2007;28(11):1957-1966.

13. Cheung CY, McCartney SJ, Anseth K. Synthesis of Polymerizable Superoxide Dismutase Mimetics to Reduce Reactive Oxygen Species Damage in Transplanted Biomedical Devices. Adv Funct Mater 2008;18:3119-3126.

14. Leung A, Lawrie G, Nielsen LK, Trau M. Synthesis and characterization of alginate/poly-L-ornithine/alginate microcapsules for local immunosuppression. J Microencapsul 2008;25(6):387-398.

15. Lin CC, Metters AT, Anseth KS. Functional PEG-peptide hydrogels to modulate local inflammation induced by the pro-inflammatory cytokine TNFalpha. Biomaterials 2009;30(28):4907-4914.

16. Cheung CY, Anseth KS. Synthesis of immunoisolation barriers that provide localized immunosuppression for encapsulated pancreatic islets. Bioconjug Chem 2006;17(4):1036-1042.

17. Palmer E. Negative selection--clearing out the bad apples from the T-cell repertoire. Nat Rev Immunol 2003;3(5):383-391.

18. Nagata S, Golstein P. The Fas death factor. Science 1995;267(5203):1449-1456.

19. Siegel RM, Frederiksen JK, Zacharias DA, Chan FK, Johnson M, Lynch D, et al. Fas preassociation required for apoptosis signaling and dominant inhibition by pathogenic mutations. Science 2000;288(5475):2354-2357.

20. Holler N, Tardivel A, Kovacsovics-Bankowski M, Hertig S, Gaide O, Martinon F, et al. Two adjacent trimeric Fas ligands are required for Fas signaling and formation of a death-inducing signaling complex. Mol Cell Biol 2003;23(4):1428-1440.

21. Cifone MG, De Maria R, Roncaioli P, Rippo MR, Azuma M, Lanier LL, et al. Apoptotic signaling through CD95 (Fas/Apo-1) activates an acidic sphingomyelinase. J Exp Med 1994;180(4):1547-1552.

22. Moreno JB, Margraf S, Schuller AM, Simon A, Moritz A, Scholz M. Inhibition of neutrophil activity in cardiac surgery with cardiopulmonary bypass: a novel strategy with the leukocyte inhibition module. Perfusion 2004;19(1):11-16.

23. Scholz M, Simon A, Berg M, Schuller AM, Hacibayramoglu M, Margraf S, et al. In vivo inhibition of neutrophil activity by a FAS (CD95) stimulating module: arterial in-line application in a porcine cardiac surgery model. J Thorac Cardiovasc Surg 2004;127(6):1735-1742.

24. Otsu T. Iniferter concept and living radical polymerization. J Polym Sci Pol Chem 2000;38(12):2121-2136.

25. Sebra RP, Masters KS, Bowman CN, Anseth KS. Surface grafted antibodies: controlled architecture permits enhanced antigen detection. Langmuir 2005;21(24):10907-10911.

26. Sebra RP, Masters KS, Cheung CY, Bowman CN, Anseth KS. Detection of antigens in biologically complex fluids with photografted whole antibodies. Anal Chem 2006;78(9):3144-3151.

27. Juo P, Kuo CJ, Yuan J, Blenis J. Essential requirement for caspase-8/FLICE in the initiation of the Fas-induced apoptotic cascade. Curr Biol 1998;8(18):1001-1008.

28. Juo P, Woo MS, Kuo CJ, Signorelli P, Biemann HP, Hannun YA, et al. FADD is required for multiple signaling events downstream of the receptor Fas. Cell Growth Differ 1999;10(12):797-804.

29. Dustin ML, Bivona TG, Philips MR. Membranes as messengers in T cell adhesion signaling. Nat Immunol 2004;5(4):363-372.

30. Sieg S, Smith D, Kaplan D. Differential activity of soluble versus cellular Fas ligand: regulation by an accessory molecule. Cell Immunol 1999;195(2):89-95.

31. Somersalo K, Anikeeva N, Sims TN, Thomas VK, Strong RK, Spies T, et al. Cytotoxic T lymphocytes form an antigen-independent ring junction. J Clin Invest 2004;113(1):49-57.

32. Weis M, Schlegel J, Kass GE, Holmstrom TH, Peters I, Eriksson J, et al. Cellular events in Fas/APO-1-mediated apoptosis in JURKAT T lymphocytes. Exp Cell Res 1995;219(2):699-708.

33. Yang L, Froio RM, Sciuto TE, Dvorak AM, Alon R, Luscinskas FW. ICAM-1 regulates neutrophil adhesion and transcellular migration of TNF-alpha-activated vascular endothelium under flow. Blood 2005;106(2):584-592.

34. Smith CW, Marlin SD, Rothlein R, Toman C, Anderson DC. Cooperative interactions of LFA-1 and Mac-1 with intercellular adhesion molecule-1 in facilitating adherence and transendothelial migration of human neutrophils in vitro. J Clin Invest 1989;83(6):2008-2017.

35. Simms MG, Walley KR. Activated macrophages decrease rat cardiac myocyte contractility: importance of ICAM-1-dependent adhesion. Am J Physiol 1999;277(1 Pt 2):H253-260.

36. Patel SS, Thiagarajan R, Willerson JT, Yeh ET. Inhibition of alpha4 integrin and ICAM-1 markedly attenuate macrophage homing to atherosclerotic plaques in ApoE-deficient mice. Circulation 1998;97(1):75-81.

37. Brown SB, Savill J. Phagocytosis triggers macrophage release of Fas ligand and induces apoptosis of bystander leukocytes. J Immunol 1999;162(1):480-485.

38. Liles WC, Kiener PA, Ledbetter JA, Aruffo A, Klebanoff SJ. Differential expression of Fas (CD95) and Fas ligand on normal human phagocytes: implications for the regulation of apoptosis in neutrophils. J Exp Med 1996;184(2):429-440.

39. Richardson BC, Lalwani ND, Johnson KJ, Marks RM. Fas ligation triggers apoptosis in macrophages but not endothelial cells. Eur J Immunol 1994;24(11):2640-2645.

Chapter 5

Functionalized PEG hydrogels through reactive dip-coating for the formation of immunoactive barriers

(As appears in *Biomaterials*, in press. **2011**)

Influencing the host immune system via implantable cell-delivery devices has the potential to reduce inflammation at the transplant site and increase the likelihood of tissue acceptance. Towards this goal, an enzymatically-initiated, dip-coating technique is adapted to fabricate conformal hydrogel layers and to create immunoactive polymer coatings on cell-laden poly(ethylene glycol) (PEG) hydrogels. Glucose oxidase (GOx)-initiated dip coatings enable the rapid formation of uniform, PEG-based coatings on the surfaces of PEG hydrogels, with thicknesses up to 500 μm where the thickness is proportional to the reaction time. Biofunctional coatings were fabricated by thiolating biomolecules that were subsequently covalently incorporated into the coating layer via thiol-acrylate copolymerization. The presence of these proteins was verified via fluorescent confocal microscopy and a modified ELISA, which indicated IgG concentrations as high as 13±1 ng / coated cm^2 were achievable. Anti-Fas antibody, known to induce T cell apoptosis, was incorporated into coatings, with or without the addition of ICAM-1 to promote T cell interaction with the functionalized coating. Jurkat T cells were seeded atop functionalized coatings and the induction of apoptosis was

measured as an indicator of coating bioactivity. After 48 hours of interaction with the functionalized coatings, 61±9% of all cells were either apoptotic or dead, compared to only 18±5% of T cells on non-functionalized coatings. Finally, the cytocompatibility of the surface-initiated GOx coating process was confirmed by modifying gels with either encapsulated β-cells or 3T3 fibroblasts within a gel that contained a PEG methacrylate coating.

5.1 INTRODUCTION

Strategies to encapsulate donor tissues within biomaterials prior to transplantation have been extensively investigated to reduce immune-mediated damage and promote cell survival. Encapsulated tissue transplants hold the potential to cure numerous diseases resulting from the loss of endocrine, cardiovascular, and neurological tissues [1]. One of the most widely studied diseases treatable with transplanted tissues is type I diabetes mellitus (TIDM). TIDM results from the autoimmune destruction of insulin-producing β-cells, located within the pancreatic islet of Langerhans cell clusters. The number of successful pancreatic tissue transplants continues to increase [2, 3] and transplant recipients experience fewer complications resulting from diabetes, compared to patients treated with daily insulin injections alone [4]. Despite continued improvements in transplantation regimens, most transplant recipients require systemic immune suppression to prevent graft rejection [2], which can lead to undesirable side effects including an increased risk of infection. Researchers have hypothesized that cell encapsulation within semi-permeable barriers prior to implantation may reduce or eliminate the requirement for systemic immunosuppression by reducing contact between donor tissue and the host immune system[1, 5]. Thus, strategies to encapsulate cells within natural and synthetic biomaterials have been extensively investigated [6]. Unfortunately, in the absence of systemic immunosuppression, encapsulated cell transplants are still likely to fail, in part because small cytokines and reactive oxygen species (ROS) are secreted by nearby immune cells, and these species remain able to diffuse into the capsule [1, 5] where they damage or destroy encapsulated cells [5, 7, 8].

To improve semi-permeable encapsulation barriers, researchers in our laboratory, as well as others, have investigated methods to functionalize biomaterials to actively modulate the local immune environment. For example, antibodies and peptides have been incorporated within capsules to bind and sequester damaging cytokines [9, 10]. Enzymes may be incorporated to breakdown ROS, like superoxide, and promote cell survival [11-14]. Further, materials have been tuned to elute anti-inflammatory molecules for localized immune suppression [14-17]. Each of these strategies has shown potential to provide protection for encapsulated cells, but no method of immune modulation has been sufficient to allow long-term transplant survival in the absence of systemic immunosuppression. Towards reducing the local concentration of activated immune cells responding to a transplant, we have recently reported a polymeric coating that induces apoptosis in T cells [18, 19], the adaptive immune cells implicated in mediating the long-term rejection of encapsulated cell transplants [20]. This coating utilized immobilized anti-fas antibody, known to induce T cell apoptosis upon engagement of the T cell fas receptor [21], and an adhesion ligand, ICAM-1 [22]. A dithiocarbamate (DTC) photoiniferter was incorporated on a hard, plastic substrate to initiate poly(ethylene glycol) (PEG) polymer chain formation with pendant anti-fas and ICAM-1 [23]. Using this chemistry, polymeric surfaces were coated with precise thicknesses and a high surface density of available biomolecules. These functionalized coatings induced T cell apoptosis and demonstrated the potential of functionalized PEG-based polymer coatings to interact with local immune cells [18]. While this previously-investigated photoiniferter-based photopolymerization enabled the formation of bioactive polymer chains, coating of cell-laden biomaterials was hindered by limited

chemical reactivity in aqueous conditions, as well as technical difficulties in forming a conformal coating on an arbitrarily shaped 3D hydrogel. Thus, an alternate strategy is investigated herein.

Many biomaterials promote encapsulated cell viability and function [6], including PEG diacrylate (PEGDA) hydrogels [24-26]. PEG hydrogels have several characteristics which make them desirable for cell encapsulation and transplantation, including a high water content which can mimic native tissue, the potential for simple chemical modifications to incorporate biomolecules, and limited immunogenicity *in vivo*. Thus, PEG hydrogels were selected as the model encapsulation material for this study. To signal apoptosis in a local population of T cells, simple approaches like the co-encapsulation of anti-fas antibody within the cell-laden hydrogel are inadequate because fas signaling is damaging to many cell types, including β-cells, and anti-fas must be physically separated from encapsulated cells [27]. Therefore, it is necessary to selectively modify the exterior of the cell-laden hydrogel with anti-fas to prevent contact with the encapsulated β-cells. Several strategies have been previously employed to functionalize the surfaces of PEG hydrogels. For example, Weber *et al.* fabricated layer-by-layer (LBL) hydrogels by immersing islet-laden PEG hydrogels into PEGDA precursor solution and photopolymerizing [28]. Likewise, Hahn *et al.* adapted traditional photolithography to pattern 3D structures and biomolecules onto the surfaces of PEG hydrogels [29, 30]. Microcontact printing, or soft lithography, has also been employed to stamp biomolecular patterns onto hydrogel surfaces [31]. While each of these modification methods provide specific advantages, it remains difficult to apply these techniques to fabricate uniform conformal coatings on 3D, cell-laden hydrogels. Though

traditional photolithography allows patterning on 2D surfaces, light attenuation prevents the simultaneous formation of uniform coatings on all facets of a 3D hydrogel. Likewise, soft lithography allows for versatile transfer of 2D patterns, but functionalizing multiple faces of a 3D object would be quite complex with this method and edges would inevitably be different in their coating as compared to the surfaces.

Recently, Johnson *et al*. introduced an innovative strategy for fabricating uniform and sequential layers of hydrogel coatings [32]. They demonstrated the formation of polymer coatings via radicals generated by the reaction of glucose with glucose oxidase (GOx) at a hydrogel surface [32]. When glucose diffuses out of a pre-swollen gel and reacts with GOx, hydrogen peroxide (H_2O_2) is generated and further reacts with Fe^{2+} to form a hydroxyl radical (HO•) capable of initiating polymerization [33]. As Johnson *et al.* demonstrated, when a PEG hydrogel was swollen in a glucose solution and then dipped into a glucose-free pre-polymer solution (PEGDA, GOx and Fe^{2+}), glucose diffuses out of all faces of the hydrogel, reacts with GOx and initiates polymerization at the surface, as summarized in Figs. 5.1A-C [32]. This reaction results in the rapid formation of polymer coatings with tunable thicknesses ranging from approx 100 to 800 μm, with the thickness proportional to the reaction time and dependent on the glucose concentration [32]. Further, this chemistry is possible in the presence of encapsulated cells [33]. Thus, the simplicity, cytocompatibility and ability to fabricate coatings of precisely controlled thicknesses on 3D hydrogels makes GOx-mediated dip-coating desirable for functionalizing β-cell-laden hydrogels for immune cell signaling.

In our present report, we modify the previously-reported GOx-initiated polymer coating strategy to coat cell-laden hydrogels with conformal coatings functionalized with

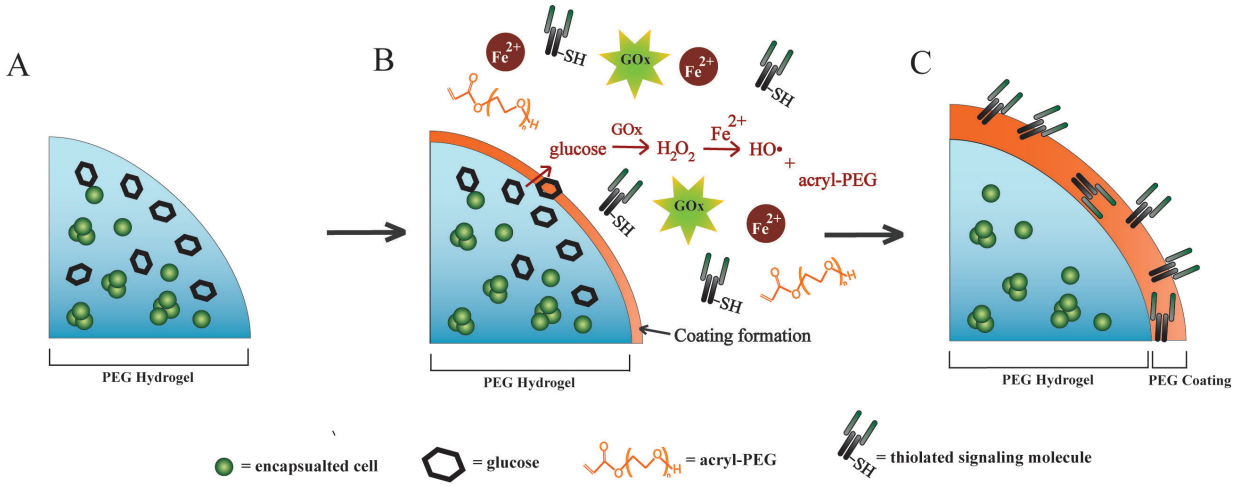

D

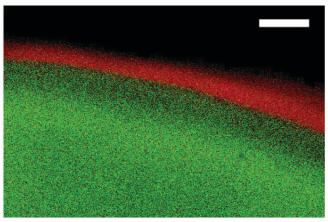

Fig. 5.1. Schematic illustrating the formation of polymer coatings initiated by glucose oxidase (GOx). (A) Cell-laden PEG hydrogels are swollen in a glucose-containing media and then (B) dipped into a pre-polymer solution containing acryl-PEG, GOx, Fe^{2+}, and thiolated signaling molecules. Glucose diffuses out of the gel, reacts with GOx and initiates polymerization at the surface of the hydrogel. (C) Reactive coating results in conformal PEG layers. Schematic not to scale. (D) Confocal micrograph of PEG hydrogel (green) with GOx-mediated polymer coating (red). Scale = 200 μm.

anti-fas antibody and ICAM-1 to induce T cell apoptosis. We demonstrate this polymerization strategy allows for the rapid formation of thin polymer coatings with a high density of available bioactive molecules. Further, we demonstrate the induction of T cell apoptosis atop bioactive coatings and verify that cell viability is maintained within GOx-coated capsules. Finally, we examine the range of cytocompatible reaction conditions. Ultimately, we highlight the capacity for GOx-mediated polymerizations to create multifunctional hydrogels with spatially defined signals to create cell-laden hydrogels with the potential to signal and regulate external cells.

5.2 MATERIALS & METHODS

5.2.1 Materials

Poly(ethylene glycol), poly(ethylene glycol) monomethacrylate, triethyl-amine, acryloyl chloride, glucose oxidase enzyme, Fe^{2+}, catalase, bovine serum albumin, EDTA, and D-glucose were obtained from Sigma-Adrich, St. Louis MO. All cell culture media, trypsin EDTA, fetal bovine serum, penicillin/streptomycin, fungizone, and live/dead staining assay were obtained from Invitrogen, Carlsbad, CA. Anti-fas antibody (DX2 clone) and ICAM-1/Fc chimera were obtained from R&D Systems, Minneapolis, MN. All other antibodies were obtained from Jackson ImmunoResearch, West Grove, PA. Traut's reagent, Zeba Spin filtration columns, Ellman's reagent, fluoraldehyde reagent solution, and TMB ELISA substrate were each obtained from Thermo Fisher Scientific, Rockford, IL. 2-hydroxy-4′-(2-hydroxyethoxy)-2-methylpropiophenone (Irgacure 2959) was obtained from Ciba Specialty Chemicals, Basel, Switzerland. Cell Titer Glo viability assay was obtained from Promega, Madison, WI. All compounds were used as received without additional purification steps.

5.2.2 Cell culture

All cells were cultured at 37°C, in 5% CO_2 and humid conditions. Min6 β-cells and Jurkat T cells were maintained in RMPI 1640 media supplemented with fetal bovine serum (FBS, 10%), penicillin/streptomycin (1%) and fungizone (0.5 μg/ml). Jurkat T cells were passaged every other day and seeded at $2.5x10^5$ cell/ml. Min6 β-cells were passaged once per week by treatment with 0.5 % trypsin EDTA (10 ml, 5 min) and

seeded at $1x10^6$ cells/ml. Fresh Min6 media was exchanged every other day. 3T3 fibroblasts were cultured in Dulbecco's Modified Eagle Medium (DMEM) supplemented with fetal bovine serum (FBS, 10%), penicillin/streptomycin (1%) and fungizone (0.5 µg/ml). 3T3s were passaged every 4 days by treatment with 0.5 % trypsin EDTA (10 ml, 5 min) and seeded at $1x10^5$ cell/ml.

5.2.3 Synthesis of poly(ethylene glycol) diacrylate (PEGDA) and formation of hydrogels

The synthesis of PEGDA has been described elsewhere [24, 34] and will be summarized herein. Briefly, hydroxyl-terminated PEG (10 kDa) was dissolved in anhydrous toluene at 60ºC and then allowed to cool to room temperature (RT). A 4-fold molar excess (per hydroxyl group) of triethylamine (TEA) and acryloyl chloride was added and the reaction was allowed to proceed overnight at RT. The following day, PEGDA was filtered through neutral alumina to remove TEA and then placed on the rotavap to remove excess toluene. Finally, PEGDA was precipitated in diethyl ether and desiccated to dryness overnight. A PEGDA (10 wt%, 10 kDa) hydrogel was used as the underlying substrate for all coating studies. Hydrogels were formed from pre-polymer solution containing PEGDA (10 kDa, 10 wt%) and 0.5 wt% 2-hydroxy-4′-(2-hydroxyethoxy)-2-methylpropiophenone (Irgacure 2959, as a photoinitiator) in phosphate buffered saline (PBS, pH = 7.4). 30 µl pre-polymer was added to the tip of a 1 ml syringe and polymerized for 9 minutes under ultraviolet light (centered at 365 nm, 6 mW/cm^2). Following polymerization, solid hydrogel disks were ejected from the syringe tips into >3 ml cell culture media (RPMI 1640 supplemented with 10 % fetal bovine

serum (FBS), 100 mg/ml penicillin/streptomycin, and 0.5 mg/ml Fungizone) and incubated overnight at 37°C, with 5% CO_2 and humid conditions.

5.2.4 Thiolation of IgG, anti-Fas, & ICAM-1

To covalently incorporate proteins within polymer coatings, proteins were modified via the addition of thiol groups. As previously demonstrated in our laboratory, proteins and peptides with free thiol groups may be photopolymerized via the radical-mediated thiol-acrylate polymerization [35]. Free thiol groups were added to IgGs, anti-Fas (IgG, DX2 clone), and ICAM-1 (1 mg/ml) by reacting with Traut's reagent (5 mol Traut's reagent / 1 mol protein), in PBS containing 5 mM EDTA for 1 hr with mixing. Unreacted Traut's reagent was removed via filtration through Zeba™ Spin Desalting Columns (7K MWCO). Protein solutions were diluted to a final concentration of 1 mg/ml in PBS containing bovine serum albumin (BSA, 2 mg/ml) and EDTA (5 mM) and frozen at -80°C. Thiolated proteins were thawed immediately prior to polymerization into polymer coatings.

5.2.5 Formation of GOx-mediated Polymer coatings

After swelling overnight in cell culture media, a polymer coating was formed on hydrogels using the reaction of glucose oxidase with glucose, in the presence of Fe^{2+}, to generate radicals capable of initiating polymerization. Hydrogels swollen overnight (>12 hrs) in cell culture media (containing 11.1 mM glucose) were dipped in pre-polymer

solutions containing either PEG acrylate (acryl-PEG, 25 wt%, M_n=400 Da) or PEG methacrylate (methacryl-PEG, 25 wt%, M_n=525 Da), with Fe^{2+} (4 mM) and GOx (0 to 50 μM) in phosphate buffered saline (PBS, pH=7.4) for subsequent coating formation. Methacrylated Rhodamine (methacryl-Rhod, 300 uM) was included in some coatings for visualization purposes, but did not significantly affect the polymerization or polymer film growth rate. Thiolated IgGs (from goat, blank and FitC-conjugated) and anti-Fas were incorporated into coatings at 250 μg/ml. Thiolated ICAM-1 was incorporated at 100 μg/ml. Gels were dipped in 50 μl pre-polymer in individual wells of a 96-well plate for 0 to 60 s to study varying times of coating formation. After dipping, coated hydrogels were removed and immersed in either cell culture media or PBS for further study.

5.2.6 Characterization of coatings

The thickness of the polymer coatings as a function of dipping time was measured via laser-scanning confocal microscopy (LSM 500 microscope, Zeiss). Methacryl-Rhod was co-polymerized into PEG coatings for visualization and a series of images were taken at 10 μm increments throughout the full thickness of coated hydrogels. Images were reconstructed into a 3D model of each coated hydrogel and coating thicknesses were measured via software analysis (MetaMorph, Molecular Devices, Sunnyvale, CA). A modified ELISA was employed to quantify the concentration of accessible IgG incorporated within the coatings, as we have previously described [18]. Briefly, IgG (from goat) was polymerized into coatings as described above and incubated overnight in PBS to ensure complete removal of unconjugated

proteins. Coated gels were incubated for 30 min with donkey-anti-goat secondary IgG (horse-radish peroxidase (HRP)-conjugated, 5 μg/ml) in PBS with 0.5% BSA. Gels were rinsed 4x with PBS and transferred to PBS with 0.5% BSA for an additional 30 min to remove unconjugated secondary IgGs. Gels were rinsed an additional 4x in PBS and transferred to individual wells of a 96-well plate in 70 μl PBS. TMB ELISA substrate was added to each well for 60s with frequent pipetting to mix and subsequently transferred to H_2SO_4 (2M) to quench the reaction. The absorbance was read at 450 nm and compared to signals of a calibration curve generated by known concentrations of HRP-conjugated secondary IgG. For dual-color imaging, samples were stained per the modified ELISA, except FitC-IgG (from goat) was incorporated into polymer coatings and samples were incubated in rhodamine-conjugated donkey-anti-goat secondary IgG. Coated gels were imaged via confocal microscopy and z-direction images were constructed to visualize FitC-IgG throughout the entire coating and Rhod-IgG secondary IgG that bound accessible, polymerized IgGs.

5.2.7 T cell Apoptosis studies and flow cytometry

The biological activity of anti-fas-functionalized coatings was assessed via Jurkat T cell apoptosis studies. Coatings functionalized with thiolated anti-fas antibody (DX2 clone) and/or ICAM-1-Fc chimera were formed as described above and incubated overnight (>12 hrs) in catalase-containing media with at least 3 media changes. After 24 hrs, coated gels were placed in individual wells of a 96-well plate and 100 000 T cells / well were seeded atop coatings in 200 μl media. T cells were incubated for 12, 24, or

48 hours and then analyzed for apoptosis and necrosis via Vybrant #3 apoptosis assay. T cells were stained with FitC-Annexin V and propidium iodide (PI) to label apoptotic and dead cells, respectively. Cells were analyzed using a CyAn flow cytometer (Beckman Coulter, Brea, CA). T cells were considered apoptotic if they stained positive for FitC-Annexin V and negative for PI. All cells staining positive for PI were considered dead.

5.2.8 Cell encapsulation, coating & analysis

Min6 β-cells (15 $x10^6$ cells/ml) or 3T3 fibroblasts (5 $x10^6$ cells/ml) were encapsulated within PEG hydrogels by suspension in pre-polymer solutions containing PEGDA (10 kDa, 10 wt%), 1-[4-(2-hydroxyethoxy)phenyl]-2-hydroxy-2-methyl-1-propan-1-one (I2959, 0.05 wt%) as a photoinitiator, and catalase (100 nM). The peptide CRGDS (1mM) was also added when 3T3 cells were encapsulated to avoid anoikis. 30 µl of cell-containing pre-polymer suspensions were transferred into 1 ml syringe tips and photopolymerized for 10 min, under 6 mW/cm^2 UV light centered at 365 nm, yielding hydrogel disks of ~2 mm thickness and ~5 mm in diameter. Cell-laden hydrogels were transferred to cell culture media and incubated overnight at 37°C. Coatings were formed via a GOx-mediated surface polymerization from the cell-laden gels as described above. Following the coating process, gels were transferred to cell culture media containing catalase (100 nM) and media was changed 3 times per hour for at least the first 2 hours following coating. Then, gels were incubated overnight at 37°C. Cell viability was assessed via a Live/Dead staining assay in which calcein AM labels live cells green and propidium iodide labels dead cells red. Cell-laden gels were

imaged via confocal microscopy whereby 20 images were taken at 10 μm intervals and projected into a single plane. The CellTiter glo assay was used to quantify cellular viability as follows: Cell-laden hydrogels were transferred to 50% cell titer glo solution in PBS (200 μl /sample) and incubated 40 min with orbital shaking. 100 μl / sample was transferred to an opaque-walled, white 96-well plate and luminescence was recorded and compared to that of ATP standards.

5.2.9 Statistical Analysis

Results presented herein are expressed as mean ± standard error of the mean. Two-tailed, unpaired Student's t-tests were used to determine statistical significance between datasets. Differences were considered statistically significant when the p value was less than 0.05. All experiments were replicated at least 3 times.

5.3 RESULTS

5.3.1 Glucose oxidase-mediated polymer coatings

The GOx enzyme was utilized to initiate polymerization on the surfaces of hydrogels as described above and illustrated in Figs. 5.1A-C. Uniform coatings, such as the one shown in Fig. 5.1D, were polymerized on the surfaces of PEG hydrogels by dipping glucose-swollen hydrogels into glucose-free pre-polymer containing GOx enzyme, Fe^{2+} and either PEG monoacrylate (acryl-PEG) or PEG monomethacrylate (methacryl-PEG). Coating thicknesses were controlled by varying the dipping time, and

a pseudo-linear relationship was observed between dipping time and the resulting coating thickness, as shown in Fig. 5.2. Coating thicknesses up to 450±50 μm were fabricated for dipping times ranging 0 to 60 s. As shown in Fig. 5.2, conformal coatings are formed using either acryl-PEG or methacryl-PEG. Further, 3D visualization via confocal microscopy confirmed that a conformal layer is formed on all faces of the hydrogel.

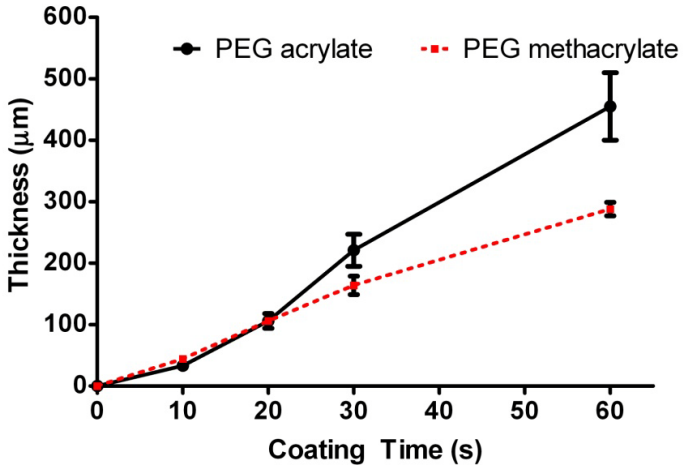

Fig. 5.2. Polymer coating thickness as a function of dipping-time. Fluorescent molecules were incorporated within polymer coatings and then visualized and measured via confocal microscopy. Coatings were formed from dipping solutions containing 25 wt% of either acryl-PEG (black line) or methacryl-PEG (dashed red line) with 50 μM GOx and 4 mM Fe^{2+}.

5.3.2 Incorporating proteins & signaling molecules into polymer coatings

IgGs, anti-Fas, and ICAM-1 were rendered polymerizable via the addition of thiol groups to free amines by reaction with Traut's reagent. The extent of protein modification was controlled by varying the molar excess of Traut's reagent relative to protein. Protein modification was confirmed in two different manners: the appearance of thiol groups on purified protein was monitored via Ellman's reagent, and the disappearance of free amines was observed using Fluoraldehyde reagent. Both measures confirmed that the extent of thiolation was proportional to the molar excess of

Traut's reagent (data not shown). Once thiolated, IgG-SH, anti-Fas-SH and ICAM-1-SH were incorporated into polymer coatings via GOx-initiated thiol-acrylate polymerization, as we have previously demonstrated that proteins and peptides containing free thiol groups may be incorporated into polymer networks via mixed mode thiol-acrylate polymerizations [35]. Briefly, the thiol acts as a chain transfer agent, having its hydrogen abstracted by the propagating radical of the growing (meth)acrylic coating. The new thiyl radical that is formed reinitiates a new (meth)acrylic polymer chain which, due to the multifunctional nature of the (meth)acrylate monomers, becomes crosslinked into the original coating, thus uniformly incorporating the peptide into the coating.

5.3.3 Characterization of proteins within polymer coatings

A previously reported modified ELISA was utilized to detect available proteins incorporated within the polymer network [18]. Thiolated IgGs from goat were incorporated at concentrations ranging from 0 to 250 μg/ml into polymer coatings and incubated with donkey anti-goat secondary antibodies with conjugated HRP or fluorophore to detect or visualize, respectively, IgGs incorporated within polymer coatings. FitC-labeled IgG-SH was polymerized into polymer coatings and then incubated with rhodamine-conjugated secondary IgG. As shown in Fig 5.3A, a green polymer coating containing FitC-IgG was visible on both faces of a coated hydrogel. Red secondary IgG (IgG-Rhod) was incubated with coatings and staining was most evident at the surface of the coating. Some staining with secondary IgG was visible within the polymer coatings (indicated by yellow). Control coatings lacking FitC-IgG-SH

were fabricated and exposed to IgG-Rhod secondary IgG and no green or red staining was visible (data not shown), indicating that the secondary IgG staining in Fig 5.3A was specific for IgGs polymerized into the coating.

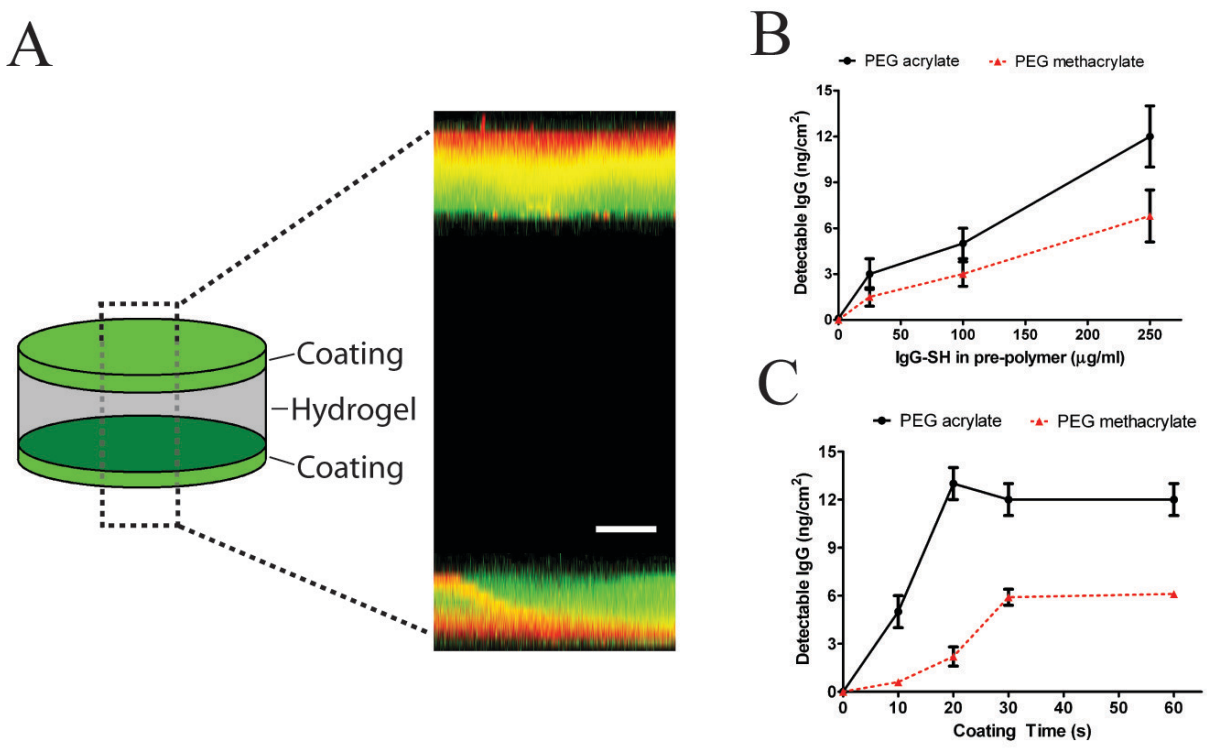

Fig. 5.3. Incorporation of biomolecules within polymer coatings. (A) z-stack confocal image of coatings on the top and bottom of a PEG hydrogel. FitC-labeled goat IgG was covalently incorporated within polymer coating (green). When incubated with rhodamine-conjugated donkey-anti-goat IgG, accessible goat IgG is fluorescently labeled (red). For simplicity, illustration shows coatings only on top and bottom of the hydrogel; actual samples were coated on all sides. (B) Concentration of accessible IgG in polymer coatings, per cm^2 of hydrogel coated, as a function of the concentration of IgG-SH loaded into the pre-polymer. (C) Concentration of accessible IgG in polymer coating as a function of dip-coating time. Coatings were formed with 25 wt% of either acryl-PEG (black line) or methacryl-PEG (dashed red line) with 50 μM GOx and 4 mM Fe^{2+}.

To quantify the amount of IgG-SH within coatings that remained accessible to the surroundings, samples were incubated with HRP-conjugated secondary IgG, reacted with TMB ELISA substrate, and the substrate absorbance change was compared to a standard curve [18]. The amount of detectable IgG was found to increase as the

concentration of IgG-SH in the coating pre-polymer solution was increased, Fig. 5.3B, and surface concentrations in excess of 10 ng IgG per coated cm^2 were achieved. The amount of detectable IgG as a function of coating formation time was also analyzed, Fig. 5.3C. For the first 20 s of coating, the amount of detectable IgG increased with time; however, the amount of detectable IgG remained constant for longer polymerization times, Fig 5.3C. This relationship suggests that IgGs were accessible to secondary IgG within approximately the outermost 100 - 150 μm of the coating (the thicknesses achieved for coating times of 20 s or 30 s for acryl-PEG or methacryl-PEG, respectively). While the overall coating thickness increases for longer reaction times, it is likely that the additional polymer formation of a thicker coating limits the accessibility of IgG near the original surface. Thus, a relatively constant amount of IgG-SH remained accessible to the surroundings for coating times in excess of ~20 to 30 s.

5.3.4 Inducing T cell apoptosis with functionalized dip coatings

Thiolated anti-Fas and ICAM-1 were incorporated into GOx-initiated polymer dip-coatings as described above. A 30 s reaction time was used for all T cell studies to allow a high concentration of accessible protein. Coated hydrogels were swollen overnight in catalase-containing cell culture media to ensure removal of unconjugated signaling proteins. The following day, Jurkat T cells were seeded atop functionalized coatings and cultured for 24 hrs. Following 24 hrs, T cells were harvested by PBS rinse and analyzed for apoptosis by FitC-Annexin V staining and flow cytometry. Samples were counter-stained with propidium iodide to label dead cells so that only live cells

were included in analysis. Flow cytometry of T cells 24 hrs following seeding atop functionalized coatings revealed significant apoptosis when cultured on coatings containing co-polymerized anti-fas, Figs. 5.4A & 5.4B. As shown in Fig. 5.4B, for T cells seeded atop blank or ICAM-1-only coatings, a low level of apoptosis was observed, 2±1% and 4±2% (for PEG acrylate-based coatings), respectively. Coatings

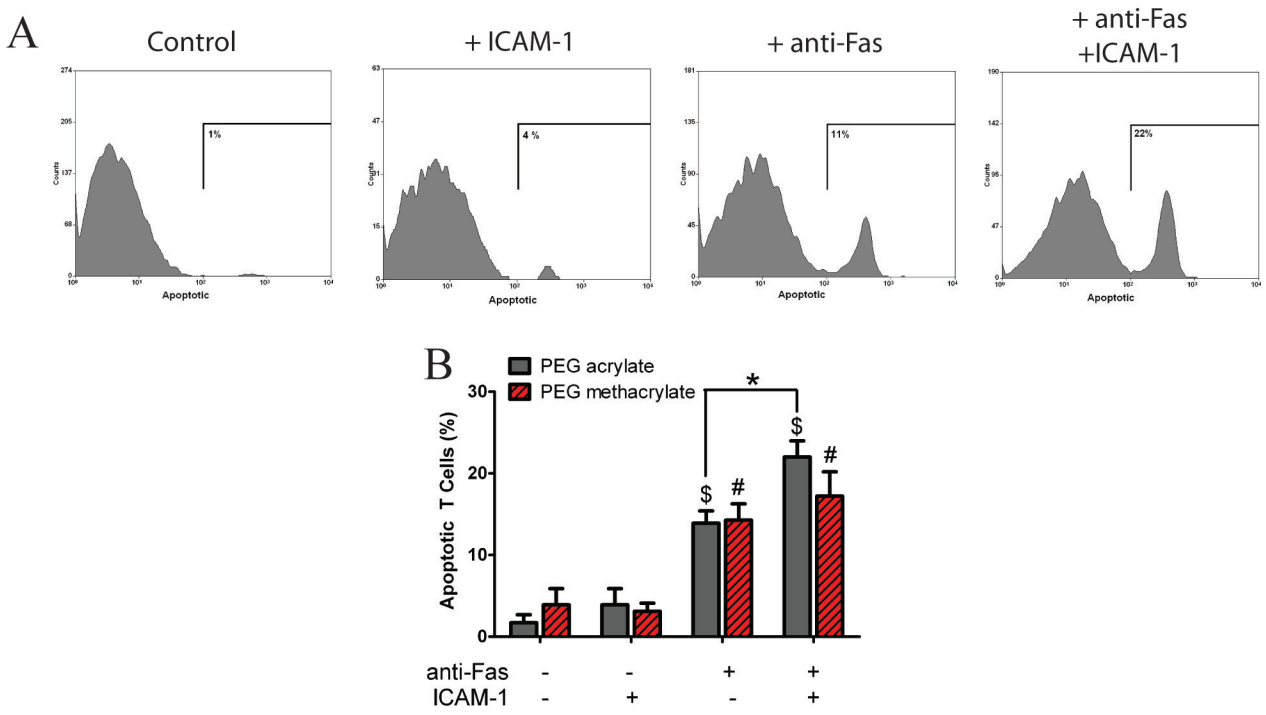

Fig. 5.4. Induction of T cell apoptosis atop functionalized PEG coatings. (A) Flow cytometry of T cells harvested from functionalized coatings fabricated with acryl-PEG. Live cells (PI neg) stained with FitC-Annexin V are shown and the percentage of cells positive for apoptosis increased with the incorporation of anti-fas and anti-fas/ICAM-1. (B) Summary of findings for functionalized coatings composed of 25 wt% of either acryl-PEG (solid bar) or methacryl-PEG (slashed red bar). * denotes $p<0.05$ difference. $ denotes $p<0.05$ difference from -/- acryl-PEG control. # denotes $p<0.05$ difference from -/- methacryl-PEG control.

functionalized with anti-fas induced significantly higher levels of apoptosis, 13±2%. Coatings fabricated with acryl-PEG that were dually-functionalized with anti-Fas and the ICAM-1 adhesion ligand induced the highest percentage of T cell apoptosis, 22±2%.

5.3.5 Apoptosis time course

To assess the impact that functionalized coatings have on the local T cell population over time, a 48 hr time course experiment was conducted. T cells seeded atop dually-functionalized (anti-Fas & ICAM-1) coatings fabricated with acryl-PEG were analyzed for apoptosis and cell death, via staining and flow cytometry, at 12, 24, and 48 hrs. For T cells seeded atop blank coatings, Fig. 5.5A, a low level of apoptosis and cell death was observed for all time points. When seeded atop dually-functionalized (anti-

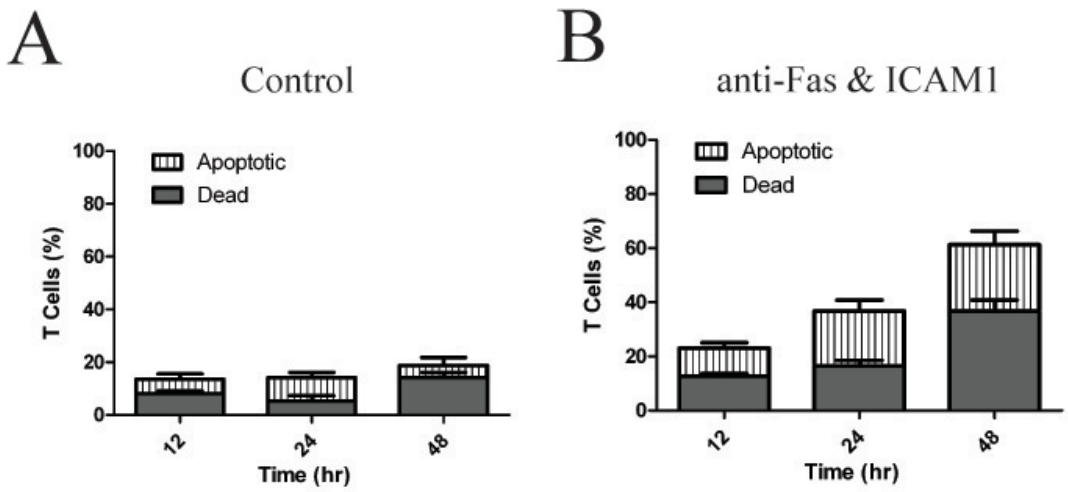

Fig. 5.5. T cells were seeded atop control (A) or dually-functionalized (anti-Fas + ICAM-1) (B) coatings composed of 25 wt% acryl-PEG for 12, 24, or 48 hrs and then analyzed via flow cytometry. The fraction of dead and apoptotic cells for each condition was measured. Functionalized coatings induced a significant increase in the number of T cells undergoing apoptosis.

Fas and ICAM-1) coatings, Fig. 5.5B, increased apoptosis was observed for all time points. The number of cells undergoing apoptosis increased from 12 to 24 hrs but remained similar from 24 hrs to 48 hrs. Interestingly, the number of dead cells increased dramatically from 24 to 48 hrs, from 17±2% to 37±4%, respectively. This observation was attributed to the likelihood that cells undergoing apoptosis eventually die, and dead cells accumulate on the gel surface over time. Following seeding atop anti-fas / ICAM-1 coatings, apoptosis was monitored over 48 hrs, and 61±9% of all cells were either

apoptotic or dead, compared to only 18±5% of T cells on non-functionalized coatings. This result indicates that anti-fas-functionalized polymer coatings formed via GOx-initiated surface-mediated polymerizations were able to significantly reduce the local T cell population in culture.

5.3.6 GOx coating of cell-laden hydrogels

A critical aspect of functionalizing cell-laden carriers is the cytocompatibility of the coating process. To assess the cytocompatibility of coatings formed via GOx-mediated polymerization on cell-laden hydrogels, Min6 β-cells and 3T3 fibroblasts were encapsulated in PEG hydrogels and then reactively dip-coated. Interestingly, low molecular weight PEG acrylates (M_n= 400 Da) were found to be highly toxic to encapsulated cells, show in Fig. 5.6, even at the shortest coating times. When immersed in low molecular weight PEG methacrylates (M_n= 525 Da), however, high cell viability was maintained. Viability was assessed 24 hrs following GOx-mediated coating via live/dead staining and confocal microscopy as well as ATP viability assay. As shown in Fig. 5.6A, high cell viability was visualized for both Min6 and 3T3-laden hydrogels dipped for 30s in methacryl-PEG-containing pre-polymer solutions containing either 0 or 50 μM GOx enzyme. Of note, immersion in the 50 μM GOx solution resulted in significant coating formation. Hydrogels containing either Min6 β-cells (Fig. 5.6B) or 3T3 fibroblasts (Fig. 5.6C) were coated via dipping in acryl-PEG or methacryl-PEG and subsequently cultured in catalase-containing cell culture media for 24 hrs before viability was quantified. As shown in Figs. 5.6B & C, high cell viability remained after 24 hrs for

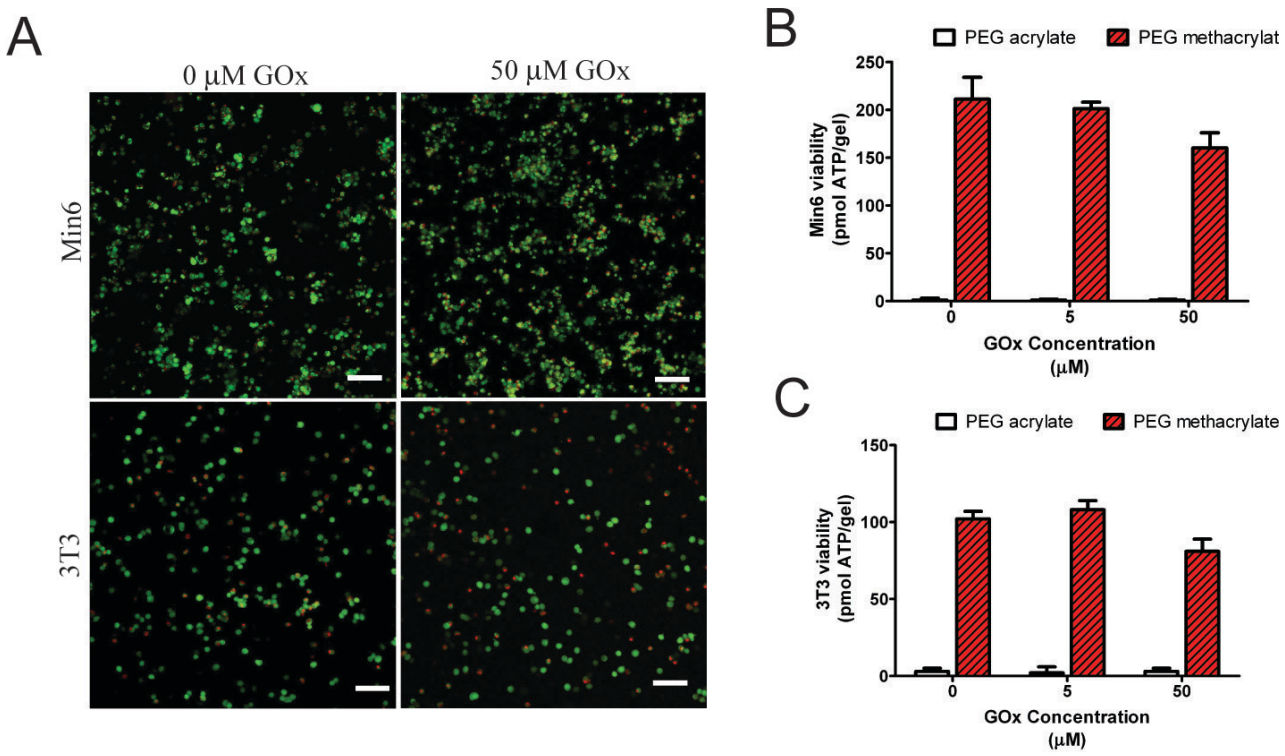

Fig. 5.6. Cytocompatibility of GOx-initiated polymer coatings toward encapsulated cells (A) Live/dead confocal microscopy of cell-laden hydrogels containing (top) Min6 β-cells or (bottom) 3T3 fibroblasts. Samples were dipped for 30 s in a pre-polymer solution containing (left) 0 μM or (right) 50 μM GOx enzyme with 25 wt% methacryl-PEG and then analyzed at 24 hrs. The 50 μM GOx condition resulted in coating formation. Green and red staining denotes live and dead cells, respectively. Scale = 100 μm. (B-C) Viability of encapsulated Min6 β-cells (B) or 3T3 fibroblasts (C) 24 hours after coating. Coatings were fabricated with 25 wt% of either acryl-PEG acrylate (solid bar) or methacryl-PEG (slashed red bar). Virtually no metabolic activity remained after 24 hrs with hydrogels dipped in acryl-PEG coating solutions.

coatings fabricated with methacryl-PEG, but essentially no viability remained after dipping in acryl-PEG.

5.4 DISCUSION

Strategies to form multi-layer hydrogel structures offer the ability to spatially regulate biological and cellular functions within biomaterials systems. Here, glucose-swollen hydrogels were dipped into pre-polymer solutions containing the glucose

oxidase enzyme to form conformal coatings on cell-laden structures and introduce biologically relevant functionalities that manipulate the local immune response. While conceptually straightforward, two critical design parameters relate to the thickness and bioactivity of the coating, combined with the cytocompatibility of the processing conditions. Many concentrations of GOx enzyme and Fe^{2+} were investigated (data not shown), but concentrations of 50 μm and 4 mM, respectively, were used for all reported studies, unless otherwise stated, as they enabled the rapid formation (0 to 60 s) of coatings (approximately 0 to 500 μm). The thicknesses of fluorescently-labeled coatings were measured via confocal microcopy and a pseudo-linear relationship was found between immersion times and coating thickness, Fig. 5.2. This relationship agreed well with that previously observed by Johnson *et al.* [32]. PEG monoacrylate (acryl-PEG, M_n=400 Da) and PEG monomethacrylate (methacryl-PEG, M_n=525 DA) were used as the base monomers for coatings in this study because we have previously demonstrated immune-cell signaling by functionalized coatings fabricated from monoacrylated PEGs [18]. While mono-(meth)acrylated PEGs were evaluated herein, di(meth)acrylated PEGs have also been shown to be suitable for GOx-mediated dip coatings [32].

Proteins were rendered reactive for copolymerization via covalent modification with free thiol groups. As previously investigated in our laboratory, thiolated peptides and proteins may be covalently conjugated into polymer networks via radical-mediated thiol-acrylate polymerizations [35, 36]. Thiolated IgGs were incorporated into coatings atop the surfaces of hydrogels via GOx-mediated dip coatings. Incorporation was verified by fluorescent confocal microscopy and ELISA-type assays, Fig. 5.3. High

concentrations of proteins were detectable within polymer coatings, exceeding 10 ng per coated cm^2 of hydrogel. These concentrations were over 7-fold greater than those that we have previously observed for functionalized, polymeric coatings fabricated via surface-initiated photopolymerizations [18]. This increase in detectable, incorporated IgG is likely due to the increased coating thickness and the higher density of initiating sites that are formed by the GOx-mediated polymerization. Previous coating thicknesses achieved by grafted photoinitiators ranged from 0 to approximately 50 μm [18].

To signal immune cells in proximity to hydrogels, thiolated anti-fas IgG was incorporated within coatings. We previously investigated the induction of T cell apoptosis by PEG-based polymer coatings and observed that significant apoptosis was induced by surfaces functionalized with anti-fas IgG [18]. Additionally, we determined that incorporating the ICAM-1 adhesion protein further improved fas signaling [18], likely by increasing the interaction between T cells and the PEG surface [37] and promoting fas signaling [38]. Because of these previous findings, we chose to incorporate anti-fas IgG and ICAM-1 into the GOx-mediated PEG coatings investigated herein. Jurkat T cell studies verified that anti-fas retained significant bioactivity when incorporated into coatings, as apoptosis was successfully induced. When analyzed for apoptosis at 12, 24 and 48 hrs, it was clear that the dually-functionalized anti-Fas / ICAM-1 coatings had a significant impact on the local T cell population. After 48 hrs atop functionalized coatings, less than 40% of cells remained healthy.

To verify the cytocompatibility of this coating process, cell-laden hydrogels were coated and subsequently cultured overnight. When dipped in pre-polymer solutions

containing acryl-PEG, interestingly, poor cell viability was observed. In fact, in the absence of any other factors, dipping in 10 wt% acryl-PEG (M_n=400 Da) for very short times (e.g., 10 s) was sufficient to result in almost complete cell death to encapsulated cells (data not shown). Coating with methacryl-PEG, however, was better-tolerated by encapsulated cells and resulted in high viability after 24 hrs. Because higher surface concentrations of detectable signaling molecules were observed on hydrogels fabricated with acryl-PEG, this coating formulation may be superior to methacryl-PEG-based coatings for the singular purpose of signaling nearby cells. If it is desirable to coat cell-laden hydrogels, however, methacryl-PEG-based coatings are clearly superior due to drastically-improved cytocompatibility of the compounds evaluated here.

Following 24 hrs, coated gels retained high viability when cultured in media containing catalase. In the absence of catalase, however, low cell viability was observed. Because the addition of catalase, a commercially available enzyme which breaks down H_2O_2, was sufficient to provide high cell viability, H_2O_2 formation likely continued after dip-coating. This observation might be attributed to the encapsulation of GOx enzyme within the polymer coatings, which may subsequently continue to react with glucose in cell culture media. Once entrapped with PEG coatings, the large (160 kDa [39]) GOx molecule is unlikely to diffuse out of the PEG network [40]. In the presence of catalase, however, high β-cell and 3T3 viability were observed. Ultimately, as previously described [33], the glucose oxidase chemistry can be highly cytocompatible.

5.5 CONCLUSIONS

We have demonstrated a cytocompatible dip-coating technique for modifying cell-laden hydrogels and for the purpose of fabricating immunoactive coatings. GOx enzyme allows for the initiation and formation of uniform, PEG-based polymer coatings with thicknesses controlled via the reaction/dipping time. Thiol-acrylate polymerization enabled thiolated biomolecules to be covalently and efficiently incorporated into the coatings, and a modified ELISA verified that a high density of incorporated protein was accessible to the surroundings. To form an immunoactive coating around PEG hydrogels, anti-fas antibody and ICAM-1 adhesion molecule were incorporated into the surface layer. Studies with T cells verified that functionalized coatings induced significant fas signaling, as over 60% of all T cells were apoptotic or dead after 48 hrs atop the coatings. Finally, the cytocompatibility of methacryl-PEG-based coatings was studied and verified in the presence of catalase. In summary, GOx-mediated dip coatings are an attractive technique for functionalizing cell-laden biomaterials with biologically active molecules to signal external cells, including immune cells.

5.6 ACKNOWLEDGEMENTS

We wish to thank Prof. Christopher Bowman for his collaboration on this project. Additionally, we thank Dr. Charles Cheung, Dr. Chien-Chi Lin, and Dr. Benjamin Fairbanks for initial guidance and helpful discussions as well as Kristina Fuerst for providing technical assistance. Thanks also to Huan (Sharon) Wang for technical assistance with flow cytometry The authors gratefully acknowledge financial support

from the National Institute of Health (R01DK076084), the Department of education's Graduate Assistance in Areas of National Need for a fellowship to PSH and the Howard Hughes Medical Institute.

5.7 REFERENCES

1. Wilson JT, Chaikof EL. Challenges and emerging technologies in the immunoisolation of cells and tissues. Advanced drug delivery reviews 2008 Jan 14;60(2):124-145.

2. White SA, Shaw JA, Sutherland DE. Pancreas transplantation. Lancet 2009 May 23;373(9677):1808-1817.

3. Pavlakis M, Khwaja K. Pancreas and islet cell transplantation in diabetes. Current opinion in endocrinology, diabetes, and obesity 2007 Apr;14(2):146-150.

4. Gremizzi C, Vergani A, Paloschi V, Secchi A. Impact of pancreas transplantation on type 1 diabetes-related complications. Current opinion in organ transplantation 2010 Feb;15(1):119-123.

5. de Vos P, Marchetti P. Encapsulation of pancreatic islets for transplantation in diabetes: the untouchable islets. Trends Mol Med 2002 Aug;8(8):363-366.

6. de Vos P, Hamel AF, Tatarkiewicz K. Considerations for successful transplantation of encapsulated pancreatic islets. Diabetologia 2002 Feb;45(2):159-173.

7. Jang JY, Lee DY, Park SJ, Byun Y. Immune reactions of lymphocytes and macrophages against PEG-grafted pancreatic islets. Biomaterials 2004 Aug;25(17):3663-3669.

8. Kulseng B, Thu B, Espevik T, Skjak-Braek G. Alginate polylysine microcapsules as immune barrier: permeability of cytokines and immunoglobulins over the capsule membrane. Cell transplantation 1997 Jul-Aug;6(4):387-394.

9. Lin CC, Metters AT, Anseth KS. Functional PEG-peptide hydrogels to modulate local inflammation induced by the pro-inflammatory cytokine TNFalpha. Biomaterials 2009 Oct;30(28):4907-4914.

10. Leung A, Lawrie G, Nielsen LK, Trau M. Synthesis and characterization of alginate/poly-L-ornithine/alginate microcapsules for local immunosuppression. J Microencapsul 2008 Sep;25(6):387-398.

11. Cheung CY, McCartney SJ, Anseth K. Synthesis of Polymerizable Superoxide Dismutase Mimetics to Reduce Reactive Oxygen Species Damage in Transplanted Biomedical Devices. Advanced Functional Materials 2008;18:3119-3126.

12. Chiumiento A, Lamponi S, Barbucci R, Dominguez A, Perez Y, Villalonga R. Immobilizing Cu,Zn-superoxide dismutase in hydrogels of carboxymethylcellulose

improves its stability and wound healing properties. Biochemistry (Mosc) 2006 Dec;71(12):1324-1328.

13. Li Z, Wang F, Roy S, Sen CK, Guan J. Injectable, highly flexible, and thermosensitive hydrogels capable of delivering superoxide dismutase. Biomacromolecules 2009 Dec 14;10(12):3306-3316.

14. Giovagnoli S, Blasi P, Luca G, Fallarino F, Calvitti M, Mancuso F, et al. Bioactive long-term release from biodegradable microspheres preserves implanted ALG-PLO-ALG microcapsules from in vivo response to purified alginate. Pharmaceutical research 2010 Feb;27(2):285-295.

15. Aimetti AA, Tibbitt MW, Anseth KS. Human neutrophil elastase responsive delivery from poly(ethylene glycol) hydrogels. Biomacromolecules 2009 Jun 8;10(6):1484-1489.

16. Ricci M, Blasi P, Giovagnoli S, Rossi C, Macchiarulo G, Luca G, et al. Ketoprofen controlled release from composite microcapsules for cell encapsulation: effect on post-transplant acute inflammation. J Control Release 2005 Oct 20;107(3):395-407.

17. Bunger CM, Tiefenbach B, Jahnke A, Gerlach C, Freier T, Schmitz KP, et al. Deletion of the tissue response against alginate-pll capsules by temporary release of co-encapsulated steroids. Biomaterials 2005 May;26(15):2353-2360.

18. Hume PS, Anseth KS. Inducing local T cell apoptosis with anti-Fas-functionalized polymeric coatings fabricated via surface-initiated photopolymerizations. Biomaterials 2010 Apr;31(12):3166-3174.

19. Cheung CY, Anseth KS. Synthesis of immunoisolation barriers that provide localized immunosuppression for encapsulated pancreatic islets. Bioconjug Chem 2006 Jul-Aug;17(4):1036-1042.

20. Kabelitz D, Geissler EK, Soria B, Schroeder IS, Fandrich F, Chatenoud L. Toward cell-based therapy of type I diabetes. Trends Immunol 2008 Feb;29(2):68-74.

21. Cifone MG, De Maria R, Roncaioli P, Rippo MR, Azuma M, Lanier LL, et al. Apoptotic signaling through CD95 (Fas/Apo-1) activates an acidic sphingomyelinase. J Exp Med 1994 Oct 1;180(4):1547-1552.

22. van de Stolpe A, van der Saag PT. Intercellular adhesion molecule-1. J Mol Med 1996 Jan;74(1):13-33.

23. Sebra RP, Masters KS, Bowman CN, Anseth KS. Surface grafted antibodies: controlled architecture permits enhanced antigen detection. Langmuir 2005 Nov 22;21(24):10907-10911.

24. Cruise GM, Hegre OD, Lamberti FV, Hager SR, Hill R, Scharp DS, et al. In vitro and in vivo performance of porcine islets encapsulated in interfacially photopolymerized poly(ethylene glycol) diacrylate membranes. Cell transplantation 1999 May-Jun;8(3):293-306.

25. Weber LM, Anseth KS. Hydrogel encapsulation environments functionalized with extracellular matrix interactions increase islet insulin secretion. Matrix Biol 2008 Oct;27(8):667-673.

26. Lin CC, Anseth KS. Glucagon-Like Peptide-1 Functionalized PEG Hydrogels Promote Survival and Function of Encapsulated Pancreatic beta-Cells. Biomacromolecules 2009 Sep;10(9):2460-2467.

27. Pearl-Yafe M, Yolcu ES, Yaniv I, Stein J, Shirwan H, Askenasy N. The dual role of Fas-ligand as an injury effector and defense strategy in diabetes and islet transplantation. Bioessays 2006 Feb;28(2):211-222.

28. Weber LM, Cheung CY, Anseth KS. Multifunctional pancreatic islet encapsulation barriers achieved via multilayer PEG hydrogels. Cell transplantation 2008;16(10):1049-1057.

29. Hahn MS, Taite LJ, Moon JJ, Rowland MC, Ruffino KA, West JL. Photolithographic patterning of polyethylene glycol hydrogels. Biomaterials 2006 Apr;27(12):2519-2524.

30. Hynd MR, Frampton JP, Burnham MR, Martin DL, Dowell-Mesfin NM, Turner JN, et al. Functionalized hydrogel surfaces for the patterning of multiple biomolecules. Journal of biomedical materials research 2007 May;81(2):347-354.

31. Zhang HB, Shepherd JNH, Nuzzo RG. Microfluidic contact printing: a versatile printing platform for patterning biomolecules on hydrogel substrates. Soft Matter;6(10):2238-2245.

32. Johnson LM, Deforest CA, Pendurti A, Anseth KS, Bowman CN. Formation of three-dimensional hydrogel multilayers using enzyme-mediated redox chain initiation. ACS applied materials & interfaces 2010 Jul;2(7):1963-1972.

33. Johnson LM, Fairbanks BD, Anseth KS, Bowman CN. Enzyme-mediated redox initiation for hydrogel generation and cellular encapsulation. Biomacromolecules 2009 Nov 9;10(11):3114-3121.

34. Hume PS. Polymerizable superoxide dismutase mimetic protects β-cells encapsulated in PEG hydrogels from reactive oxygen species-mediated damage. Tissue engineering 2011.

35. Salinas CN, Anseth KS. Mixed mode thiol-acrylate photopolymerizations for the synthesis of PEG-peptide hydrogels. Macromolecules 2008 Aug;41(16):6019-6026.

36. Lin CC. Cell-cell communication mimicry with PEG hydrogels for enhancing Beta-cell function. Proc Natl Acad Sci USA 2010 2011.

37. Dustin ML, Bivona TG, Philips MR. Membranes as messengers in T cell adhesion signaling. Nat Immunol 2004 Apr;5(4):363-372.

38. Sieg S, Smith D, Kaplan D. Differential activity of soluble versus cellular Fas ligand: regulation by an accessory molecule. Cell Immunol 1999 Aug 1;195(2):89-95.

39. Tsuge H, Natsuaki O, Ohashi K. Purification, properties, and molecular features of glucose oxidase from Aspergillus niger. Journal of biochemistry 1975 Oct;78(4):835-843.

40. Cruise GM, Scharp DS, Hubbell JA. Characterization of permeability and network structure of interfacially photopolymerized poly(ethylene glycol) diacrylate hydrogels. Biomaterials 1998 Jul;19(14):1287-1294.

Chapter 6

Strategies to reduce dendritic cell maturation and promote tolerance through functional biomaterial design

Dendritic cells play a key role in determining adaptive immunity, so the interaction between biomaterials and dendritic cells has the potential to shape whether immunity or tolerance results. Accordingly, there is growing interest in characterizing the interactions between dendritic cells and biomaterial surfaces. While contact with several common biomaterials has been shown to induce the maturation of immature dendritic cells, substrates that reduce dendritic cell maturation are particularly desirable within the field of tissue engineering, where it is often preferable to reduce the immune response to cell-laden material carrier. Towards this goal, a novel strategy was examined whereby poly(ethylene glycol) hydrogel were functionalized with immobilized immunosuppressive factors (TGF-β1 and IL-10) to reduce the maturation of immature dendritic cells. TGF-β1 and IL-10, as soluble factors, are commonly employed to program dendritic cells *in vitro*, and herein it is demonstrated these proteins retain bioactivity towards dendritic cells when immobilized on hydrogel surfaces. Following stimulation with lipopolysaccharide and/or cytokines, immature dendritic cells interacting with the surfaces of immunosuppressive hydrogels demonstrated reduced markers of maturation, including IL-12 production and MHCII, which was comparable to dendritic cells treated with soluble or immobilized TGF-β1 and IL-10. Further, the bioactivity of

these immunomodulatory hydrogels was confirmed towards immature dendritic cells isolated from non-obese diabetic (NOD) mice, a cell type relevant to type I diabetes. Finally, the addition of general adhesion to immunomodulatory hydrogels is explored and demonstrated to improve the extent to which BMDC maturation is reduced.

6.1 INTRODUCTION

Dendritic cells (DCs) bridge the innate and adaptive immune systems and are crucial to initiating and guiding the adaptive immune response. Immature dendritic cells (iDCs) survey the body's periphery in search of foreign and self antigens [1]. Upon antigen uptake, DCs present antigen to lymphocytes, but have the unique capacity to induce either immunity or tolerance to antigen [1, 2]. For example, when iDCs encounter antigen in the presence of stimulatory factors such as "danger signals" or pathogen associated molecular patterns (PAMPs), iDCs undergo maturation into mature DCs and initiate an adaptive immune response [3]. Upon maturation, DCs increase expression of MHC stimulatory molecules, B7 family co-stimulatory molecules (i.e., CD80 and CD86), and inflammatory cytokines, including IL-12, which enable the activation of naïve $CD4^+$ helper T cells to initiate an immune response [1]. Conversely, if iDCs encounter antigen under conditions which prevent full DC maturation, they may become tolerogenic DCs with decreased expression of the aforementioned maturation markers, preventing an adaptive immune response [2, 4].

Because of their critical importance in dictating the fate of the adaptive immune response, understanding interactions between iDCs and implanted biomaterial surfaces has gained considerable interest in recent years [5]. For example, several commonly-used biomaterials including poly(lactic-co-glycolic acid) (PLGA) and chitosan [6], as well as surface modifications with common extracellular matrix (ECM) proteins [7] and integrins [8], have been identified as regulators that can induce iDC maturation and initiate an adaptive immune response. The induced maturation of iDCs by biomaterials, or adjuvant effect, is desirable for biomaterial vaccines against infection and tumors

where an immune response is favorable [9]. When designing biomaterials for tissue engineering applications, such as the transplantation of tissues encapsulated within biomaterials for the treatment of diseases like type I diabetes mellitus (TIDM), however, optimal biomaterial cell carriers would minimize the adjuvant effect or even prevent the full maturation of iDCs and form tolerogenic DCs. To date, few research groups have investigated strategies to limit iDC maturation via controlled modification of biomaterial surfaces. As a result, a great potential exists for development in this area, and as one example, *Babensee and coworkers* recently demonstrated that hyaluronic acid and agarose have the capacity to limit immunogenicity compared to surfaces with known adjuvant effect [6, 10].

In previous work, tolerogenic DCs have been generated *in vitro* by culturing iDCs in the presence of one or more soluble factors [11]. A particularly well known method to generate tolerogenic DCs involves culturing iDCs in the presence media additives such as transforming growth factor β-1 (TGF-β1) and/or interleukin 10 (IL-10) [11-14]. Culturing iDCs with these immunosuppressive proteins has been shown to yield tolerogenic iDCs that undergo incomplete maturation upon immune stimulation and can promote T cell anergy or, alternatively, the formation of regulatory T cells [2]. Immature DCs primed with TGF-β1 and IL-10 in this manner have been widely investigated. For example, Torres-Aguilar *et al.* recently cultured iDCs with IL-10 and TGF-β1 in the presence of insulin to generate tolerogenic DCs, which induced antigen-specific insulin tolerance in humans [15].

In this contribution, a biomaterial surface is modified with the tethered immunosuppressive proteins TGF-β1 and / or IL-10 to create immunomodulatory

surfaces that signal iDCs and reduce maturation upon stimulation with LPS. Specifically, a poly(ethylene glycol) (PEG) hydrogel platform, which limits immunogenicity and allows facile modification to incorporate proteins, was chosen as a basis from which anti-inflammatory molecules could be tethered for iDC signaling. Numerous proteins, peptides and other molecules of interest have been previously incorporated onto biomaterial surfaces and remained bioactive for cell signaling [16, 17]. Notably, Mann *et al.* tethered TGF-β1 within PEG hydrogels to signal vascular smooth muscle cells and demonstrated that immobilized TGF-β1 maintained bioactivity and increased ECM protein synthesis [18]. In our group, we have previously investigated PEG-based surfaces for the purposes of immune signaling, and demonstrated that PEG coatings containing immobilized anti-fas are capable of interacting with T cells and inducing apoptosis [19, 20]. Further, it is known that DCs have the capacity to receive biological cues from tethered signaling proteins, as Leclerc *et al.* immobilized granulocyte-macrophage colony stimulating factor (GM-CSF) upon surfaces to promote the development of iDCs from isolated bone marrow tissue [21].

Herein, bone marrow-derived mDCs are employed to characterize the immunomodulatory capacity of PEG hydrogels modified with immunosuppressive proteins. Initial studies were conducted with the cytokine-dependent, immortalized immature dendritic cell line, JAWSII. The JAWSII dendritic cell line was originally isolated from the bone marrow of $p53^{-/-}$ C57BL/6 mice and has been previously shown to mimic the capacity of primary iDCs to undergo maturation in response to immune stimuli [22-25]. Additionally, primary bone marrow-derived DCs (BMDCs) generated from bone marrow isolated from non-obese diabetic (NOD) mice were evaluated with

immunomodulatory hydrogels. Immature DCs from NOD mice are previously known to have impaired maturation [26, 27]. Therefore, exploring the immunosuppressive capacity of functionalized PEG hydrogels towards iDCs generated from NOD mice provides greater insight into the capacity of selectively functionalized material to target cells of the adaptive immune response as related to disease models relevant to the treatment of type I diabetes mellitus.

6.2 MATERIALS & METHODS

6.2.1 Dendritic cell culture

JAWSII cells, an immortalized dendritic cell line of murine bone marrow origin (ATCC, Manassas, VA), were cultured in α-MEM media (Invitrogen, Carlsbad, CA) supplemented with 20% heat inactivated FBS (Invitrogen), 1% penicillin/streptomycin (Invitrogen, and 5 ng/ml GM-CSF (Peprotech, Rocky Hill, NJ). JAWSII were cultured in tissue culture flasks and media was changed weekly. Primary bone marrow-derived dendritic cells (BMDCs) were harvested from femurs isolated from NOD mice. The ends of femurs were cut and the marrow was rinsed with 10 ml RPMI media 1640 (Invitrogen) with a 27 gauge syringe needle. Freshly isolated samples were mixed with an 18 gauge syringe to dissociate clumps. Following isolation, samples were cultured in cell culture media consisting of RPMI 1640 medium supplemented with 1.5% mouse serum (Invitrogen), 20 ng/ml GM-CSF, and 1% penicillin/streptomycin. BMDCs were seeded onto TCPS in 6-well plates or hydrogels in 96-well plates and 50% fresh media volume was changed daily.

6.2.2 Thiolation of proteins

To incorporate TGF-β1 and IL-10 as covalent pendant functional groups within hydrogels, proteins were rendered polymerizable via modification by Traut's reagent (Thermo Scientific, Rockford, IL), which conjugates to free amines to create thiols. In brief, proteins were reconstituted in phosphate buffered saline (PBS, pH 7.4, Invitrogen) containing 2 mM EDTA (Sigma) and a 5-fold molar excess Traut's reagent per mol protein. Samples were mixed and reacted at room temperature for 1 hr. Following thiolation, unreacted Traut's reagent was removed via filtration through Zeba™ Spin Desalting Columns (7K MWCO, Thermo Scientific), yielding the final thiolated product of TGF-β1-SH or IL-10-SH. Samples were diluted to a final concentration of 25 μg/ml in PBS with 2 mM EDTA and immediately placed in a -80°C freezer. Prior to use, protein solutions were rapidly thawed and added to pre-polymer solutions in concentrations ranging from 0 to 1 μg/ml for gel formation via photopolymerization.

6.2.3 PEG hydrogel formation

The synthesis of poly(ethylene glycol) (PEG) diacrylate (PEGDA, 10 kDA) macromolecular monomers from hydroxyl-PEG (Sigma) has been described in detail elsewhere [28]. Briefly, hydroxyl PEG was dissolved in anhydrous toluene by heating to 60ºC with mixing. After the dissolved PEG was allowed to cool to room temperature (RT), triethylamine (TEA, 4-fold molar excess per hydroxyl group) and acryloyl chloride were added and reacted overnight at RT with stirring. Next, TEA was removed via filtration through neutral alumina. PEGDA was precipitated in cold diethyl ether and desiccated to dryness overnight. To ensure high levels of purity, PEGDA was dialyzed

against deionized water overnight (1 kDa MWCO membrane) with >3 dialysis volume changes.

Pre-polymer solutions were prepared consisting of 10 wt% PEGDA in PBS with 0.05 wt% of the photoinitiator 2-hydroxy-4′-(2-hydroxyethoxy)-2-methylpropiophenone (Irgacure-959, Ciba Specialty Chemicals) and thiolated proteins (0 to 1 μg/ml). For selected studies, poly-L-lysine (PLL, 10 μM, Sigma), laminin (200 μg/ml, BD Biosciences, Bedford, MA) or fibronectin (200 μg/ml, BD Biosciences) were also included in pre-polymer solutions. Pre-polymer solutions were loaded into the tips of 1 ml syringes (30 μl) and polymerized for 10 min under ultraviolet light (6 mW/cm^2, centered at 365 nm) for gel formation. Following polymerization, hydrogels were incubated overnight in either PBS or cell culture media (4°C, with orbital shaking) with at least two solution changes to ensure complete removal of residual photoinitiator and untethered proteins. The final, swollen hydrogels were disks with a diameter of ~5.5 mm and height of ~2 mm.

6.2.4 Measurement of incorporated proteins

TGF-β1 was added to pre-polymer solutions in concentrations ranging from 0 to 1 μg /ml. Following photopolymerization, functionalized hydrogels were rinsed overnight in 3 ml PBS with >2 solution changes to ensure complete removal of non-covalently bound protein. The following day, a modified ELISA was employed to quantify the concentration of protein on the gel surface. Hydrogels were incubated with anti-TGF-β1 monoclonal antibody from mouse (5 μg/ml, Peprotech) in ELISA buffer (sterile filtered PBS with 0.1% BSA and 0.05% TWEEN-20) for 1.5 hrs and then rinsed three times with

ELISA buffer. Next, samples were incubated with horseradish peroxidase-conjugated goat anti-mouse secondary antibody (100 ng/ml, Jackson ImmunoResearch, West Grove, PA) for 30 min, followed by three rinses with PBS. Samples were then incubated for 60 minutes in ELISA buffer, rinsed three times, and incubated another 15 min in ELISA buffer to ensure complete removal of unbound antibodies. Hydrogels were distributed into individual wells of a 96-well plate containing 70 µl PBS (30 µl hydrogel plus 70 µl PBS resulted in roughly 100 µl total volume / well), and the TMB ELISA substrate (100 µl/well, Thermo Scientific) was added for 20 minutes. Finally, the reaction was quenched via the addition of 100 µl H_2SO_4 100 µl combined TMB /H_2SO_4 and the absorbance was measured at 450 nm and compared to that of standards prepared from known quantities of secondary antibody, TMB, and H_2SO_4.

6.2.5 PE-25 TGF-β reporter cell assay

The presence of biologically active TGF-β1 on hydrogel surfaces was verified using a PE-25 TGF-β reporter cell line (i.e., mink lung epithelial cells (Mv1Lu or CCL-64)) containing a stably transfected luciferase reporter gene for TGF-β which were generously donated by Dr. Xuedong Liu [29]). PE-25 cells were seeded atop functionalized hydrogels at a density of $1x10^5$ cells/ml for 24 hrs in 200 µl Dulbecco's Modified Eagle Medium (Invitrogen). The following day, the media was gently removed and samples were lysed via the addition of 200 µl passive lysis buffer (Promega, Madison, WI) and incubated for 10 min at 37°C, with shaking, and finally stored at -80°C for >2 hr. Next, the samples were thawed, transferred to microcentrifuge tubes and centrifuged for 10 min (13,000 rpm, 4°C). The lysate was transferred to white, opaque-

walled 96-well plate (100 µl per well), and 50 µl luciferase substrate (Promega) was added to each well for 5 min and then luminescence was quantified.

6.2.6 JAWSII DC studies

JAWSII DCs were seeded into 96-well plates on either empty wells (TCPS) or atop hydrogels at a density of $3.0x10^5$ cell/ml in 200 µl JAWSII cell culture media. Cells were cultured atop blank and functionalized (TGF-β1-SH and/or IL-10-SH) hydrogels or on TCPS with or without the addition of soluble TGF-β1 and/or IL-10-SH for three days. On day 4, DCs were activated via the addition of lipopolysaccharide (LPS, 1 µg/ml, Sigma), with interferon gamma (IFN-γ, 10 ng/ml), tumor necrosis factor alpha (TNF-α, 10 ng/ml) and interleukin 4 (IL-4, 10 ng/ml), each obtained from Peprotech. On day 6, 100 µl of each sample was analyzed for IL-12p70 production via an ELISA kit (eBioscience, San Diego, CA) per the manufacturer's instructions. For flow cytometry analysis, JAWSII were removed from TCPS and hydrogels via incubation in cold PBS (10 min on ice). For flow cytometry analysis, samples were rinsed in PBS + 10% FBS and then incubated for 10 min at 4°C with Fc Block (anti-mouse CD16/CD32, Fcγ III/II Receptor, BD Pharmingen, San Diego, CA). FitC-rat anti-mouse I-A/I-E (clone 2G9, BD Pharmingen) and PE-rat anti-mouse CD86 (clone GL1, BD Pharmingen); antibodies were added and allowed to stain for 60 min at 4°C. Fluorescently labeled antibody isotypes were included as controls. Following staining, samples were rinsed and then analyzed using a CyAn Flow Cytometer and Summit software (Beckman Coulter) and more than 25,000 events were collected per sample.

6.2.7 BMDC studies

BMDCs were harvested and then seeded in 6 well plates at $5x10^6$ cells/ml, in 4 ml BMDC media for four days. Half of the BMDC media was exchanged after 2 days. BMDCs were harvested via cell lifter on day 5 and transferred to either blank or functionalized PEG hydrogels or onto TCPS in 96-well plates at a density of $2x10^5$ cells/ml in 200 µl BMDC media. Cells were cultured for an additional 3 days atop blank or functionalized gels or on TCPS in the presence or absence of soluble TGF-β-SH and or IL-10. Half of the media volume was exchanged with fresh media each day. On day 8, samples were activated via the addition of LPS (1 µg/ml). On day 9, 100 µl of supernatant per sample was harvested and the IL-12p70 concentration was quantified via ELISA. Cells were lifted for flow cytometry by incubation in PBS with 5 mM Na_2EDTA (Sigma) for 20 min at 37°C. Cells were rinsed with 1% BSA in PBS and stained with Fc block (anti-mouse CD16/CD32, Fcγ III/II Receptor, BD Pharmingen) for 10 min on ice. Next, samples were stained with FitC-anti-MHCII (Clone: RI1B, Ox-6, BD Pharmingen), FitC-anti-CD86 (Clone: GL1, BD Pharmingen), PE-anti-CD11b (Clone: M1/70, BD Pharmingen), PE-anti-CD80 (Clone: 16-10A1, BD Pharmingen), APC-Anti-CD11c (Clone: N418, BD Pharmingen), PerCP-anti-CD11b (Clone: M1/70, BD Pharmingen) were incubated for 30 min on ice. Finally, cells were rinsed 3 times and re-suspended for flow cytometry. Samples collected using a FACScan flow cytometer (BD Biosciences).

6.2.8 T cell activation studies

T cell cones, 6.9 TG.C6/T2, were derived from spleen cells harvested from 6.9 TCR-Tg/NOD.C6.*scid* mice as previously described [30, 31]. Cells were maintained in complete medium (CM) consisting of Dulbecco's modified Eagle's minimal essential medium (Life Technologies, Gaithersburg, MD) supplemented with IL-2 (0.5% supernatant of phytohaemagglutinin stimulated EL-4 cells), 10 % fetal bovine serum. Cells were maintained at $1x10^6$ cells/ml and every two weeks, T cells were stimulated via incubation with antigen (10 μg granule membrane protein from β-cell tumor cells) and antigen presenting cells (irradiated NOD spleen cells). At the conclusion of a two weeks cycle, T cells ($2.5x10^5$ cells/ml) were added to BMDCs ($1.88x10^5$ cells/ml) generated as described above and harvested from either TCPS, or PEG hydrogels with our without LPS stimulation and / or immunomodulation (TGF-β and IL-10) by incubating with 5 mM Na_2EDTA. T cells and BMDCs were co-cultured in CM for 72 hours. Finally, media supernatant from co-cultures was collected and analyzed by ELISA for interferon gamma (INF-γ) as a measure of T cell activation by BMDCs.

6.2.9 Statistical Analysis

Statistical significance was determined using a two-tailed, unpaired Student's t-test. Differences between datasets were considered statistically significant when the p value was less than 0.05. All results are presented as mean ± standard error of the mean. Each experiment, excepting CD80 expression of BMDCs atop immunomodulatory hydrogels, was repeated at least twice.

6.3 RESULTS

6.3.1 Bioactivity of thiolated TGF-β1

TGF-β1 was rendered polymerizable via thiolation with Traut's reagent [32], as schematically illustrated in Fig. 6.1A. To confirm that TGF-β1-SH remained bioactive, PE-25 (TGF-β reporter) cells were incubated overnight with 0, 1.0 and 10 ng/ml of soluble and unmodified TGF-β1 as compared to TGF-β1-SH. The following day, luciferase activity was quantified as a marker of TGF-β bioactivity. As shown in Fig. 6.1B, a slight reduction in TGF-β1-SH bioactivity was observed, as compared to unmodified TGF-β1, at a concentration of 1.0 ng/ml. When added at 10 ng/ml, however, both thiolated and unmodified TGF-β1 resulted in high levels of luciferase activity. Some reduction in bioactivity is to be expected following thiolation, as the nonspecific chemistry likely modifies the active site of some percentage of proteins. Despite some loss of function, though, significant bioactivity was preserved. Bioactivity was also verified via activity towards JAWSII DCs. Dendritic cells were incubated with thiolated and unmodified TGF-β1 for 24 hrs (10 ng/ml) and then activated via stimulation with LPS and IFN-γ. As presented in Fig. 6.1C, both forms of TGF-β1 were able suppress DC IL-12 production when challenged with LPS, indicating bioactivity of TGF-β1-SH was preserved. This effect was also observed for soluble IL-10-SH, shown in Fig. 6.1D. Further, the surface expression of MHCII (Fig. 6.1E) and CD86 (Fig. 6.1F) was characterized for JAWSII iDCs cultured with both soluble TGF-β1-SH and/or IL-10-SH and then stimulated. As anticipated, stimulation resulted in a large increase in MHCII expression. Pretreatment with either TGF-β or IL-10, however, resulted in DCs with decreased MHCII expression, compared to stimulated controls. Stimulation also

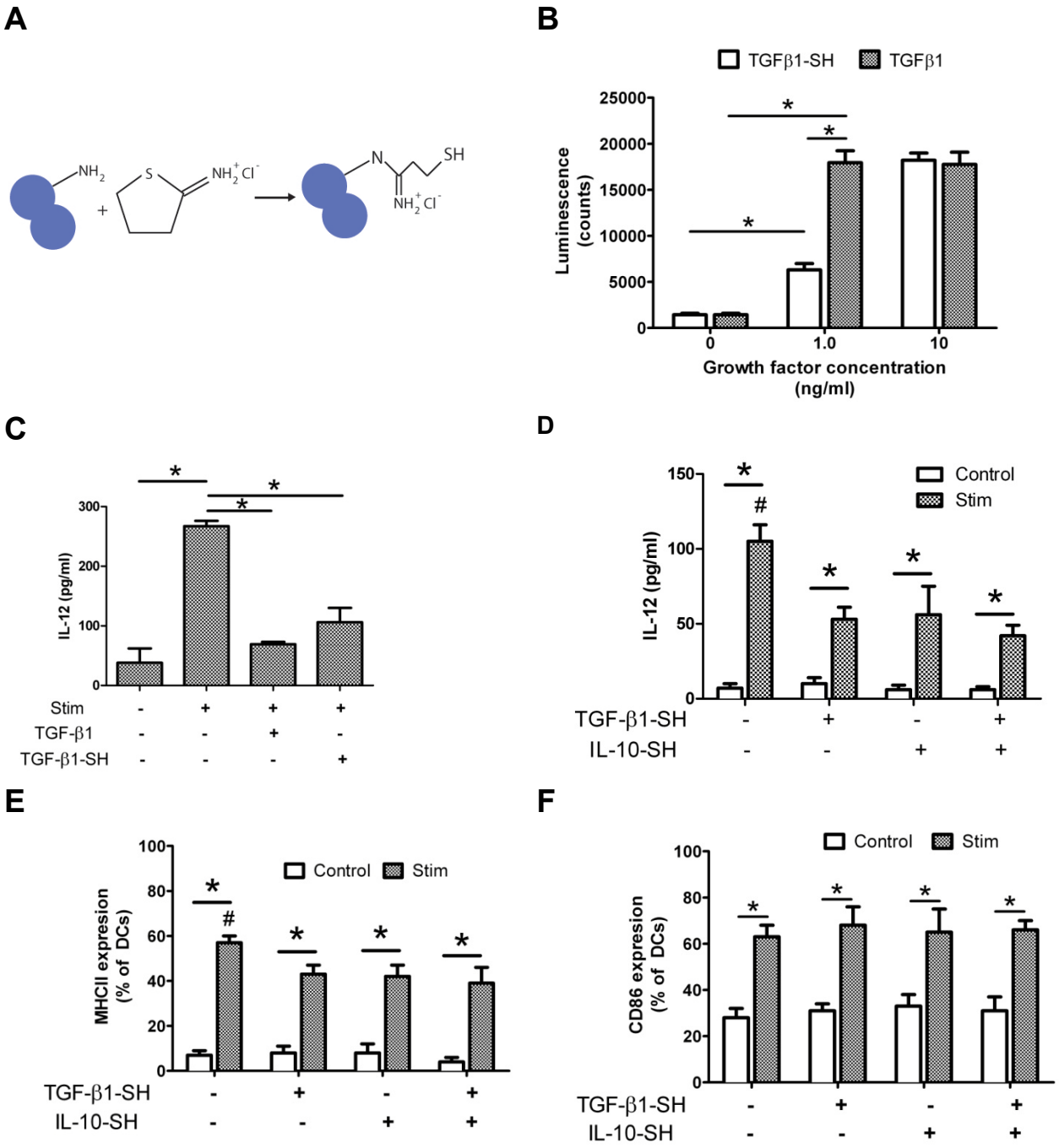

Fig. 6.1. Soluble bioactivity of modified growth factors. (A) Schematic for the thiolation of free amine groups on proteins via Traut's reagent. Circles represent one protein molecule (B) Comparison of bioactivity for thiolated and unmodified TGF-β1 via PE-25 TGF-β reporter assay. (C) IL-12 produced by JAWSII DCs cultured with soluble, thiolated and unmodified TGF-β1. (D) IL-12 produced by JAWSII cultured in the presence of TGF-β1-SH or IL-10-SH following immune stimulation with LPS and cytokines. (E) MHCII and (F) CD86 expression of JAWSII DCs cultured with or without soluble TGF-β1-SH and/or IL-10-SH. * denotes $p<0.05$ difference. # denotes $p<0.05$ difference from all other values.

increased the expression of CD86 by DCs but pre-treatment with immunosuppressants did not influence the expression of CD86 by JAWSII DCs.

6.3.2 *Formation of immunomodulatory PEG hydrogels*

To create functional material systems, PEGDA (10 kDa, 10 wt%) hydrogels were photopolymerized with or without the addition of thiolated proteins, Fig. 6.2A. Free thiols on proteins are covalently incorporated within hydrogel networks via a mixed-mode, radical-mediated, thiol-acrylate polymerization, as previously described [33]. A modified ELISA was employed to characterize the concentration of TGF-β1 available on the hydrogel surface. As illustrated in Fig. 6.2B, an increase in detectable surface TGF-β1 was observed relative to the concentration of TGF-β1-SH included in the pre-polymer solution. When 1.0 μg/ml TGF-β1-SH was included in the pre-polymer solution, 18±2 pg/cm^2 TGF-β1 was detected on the gel surface. To verify the bioactivity of functionalized TGF-β1 hydrogels, PE-25 TGF-β reporter cells were seeded atop gels

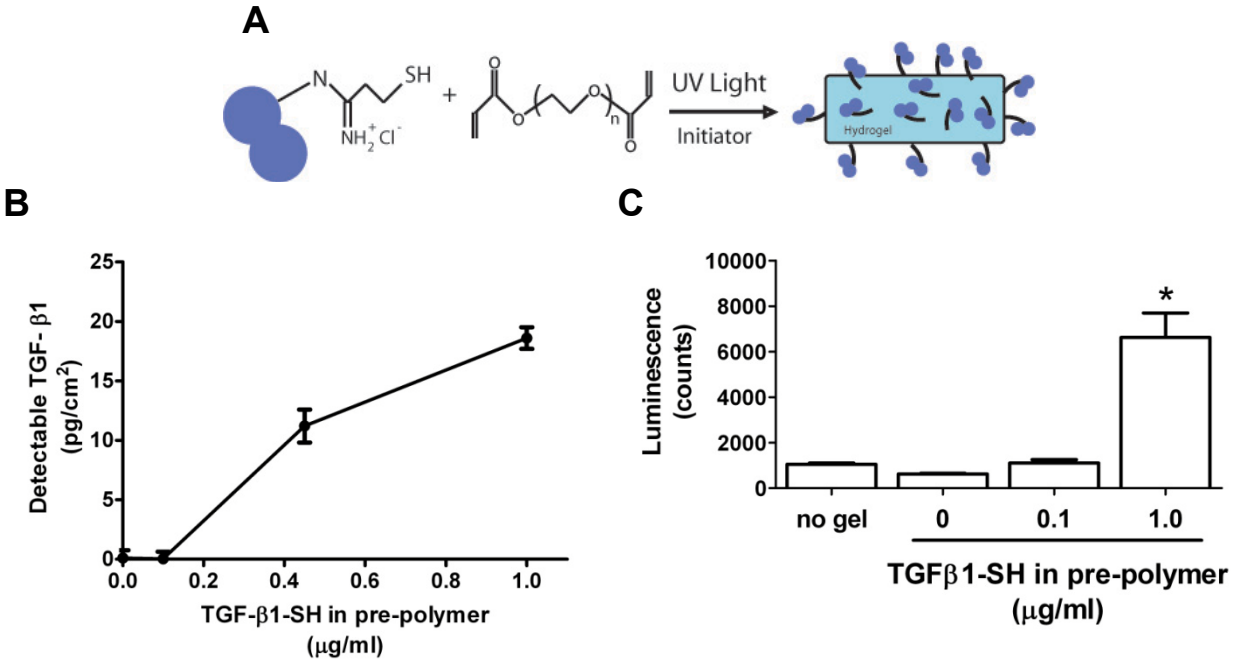

Fig. 6.2. Formation of functionalized PEG hydrogels**.** (A) Schematic of hydrogel formation in which thiolated proteins are covalently polymerize within PEG hydrogels via thiol-acrylate photopolymerization. (B) Detectable surface density of TGF-β1 on hydrogel surfaces, as detected by modified ELISA. (C) Bioactivity of TGF-β1 incorporated on functionalized hydrogels, as assessed by PE-25 TGF-β reporter cell assay. * denotes $p<0.05$ difference from all other values.

and allowed to interact for 24 hours. Luciferase activity was quantified, and significant TGF-β bioactivity was provided by the hydrogel surfaces fabricated with 1 μg/ml TGF-β-SH, shown in Fig. 6.2C.

6.3.3 JAWSII DCs on immunomodulatory hydrogels

JAWSII iDCs were seeded atop hydrogels functionalized with or without the immunosuppressive proteins TGF-β1 and or IL-10 and cultured for 3 days. As shown in

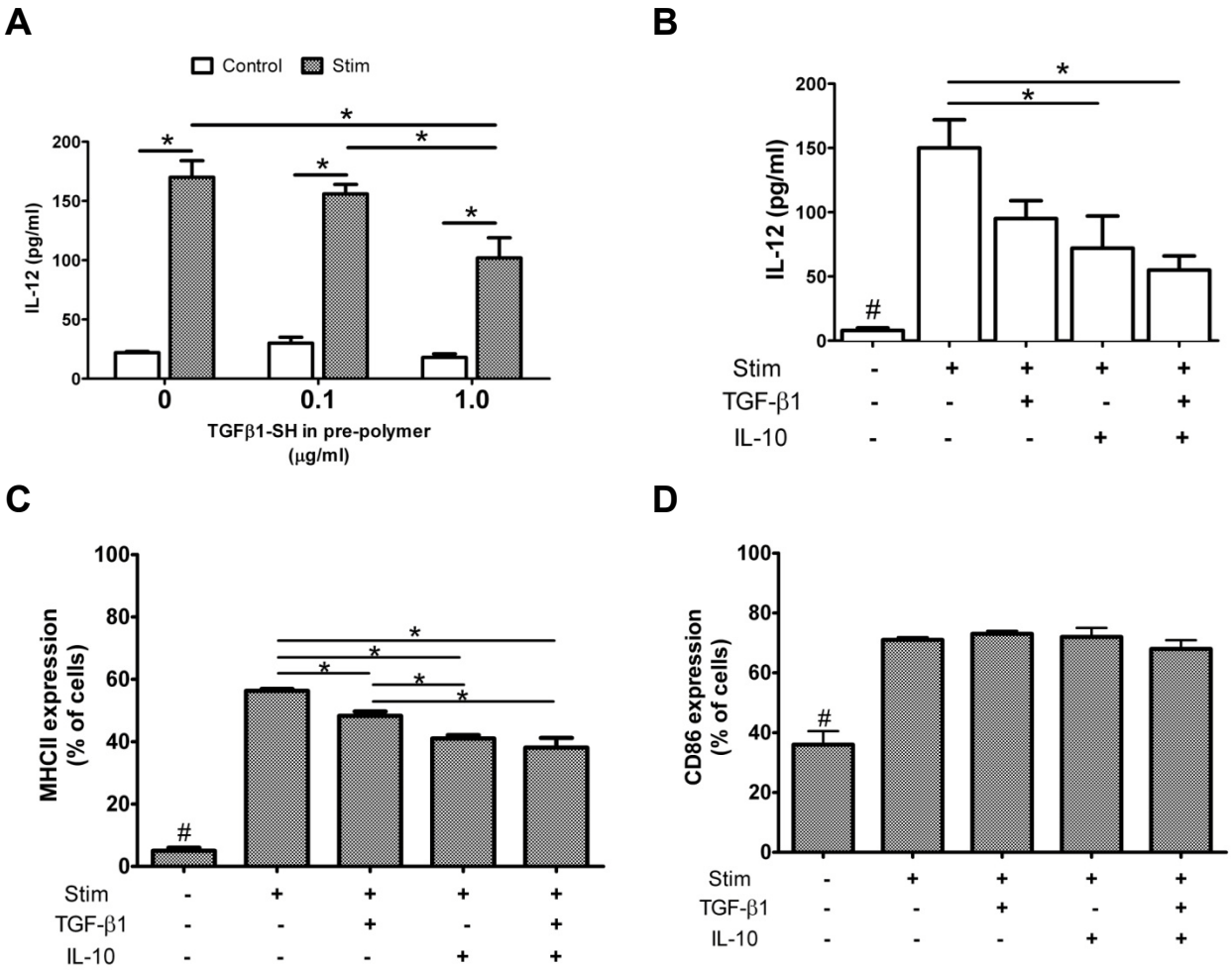

Fig. 6.3. JAWSII DCs with immunomodulatory hydrogels. (A) IL-12 production of JAWSII DCs stimulated with LPS and cytokines following cell culture atop hydrogels functionalized with various concentrations of TGF-β1. (B) IL-12 production of DCs cultured atop hydrogels polymerized with 1 μg/ml TGF-β1 and / or IL-10. (C) MCHII and (D) CD86 expression of JAWSII DCs cultured atop functionalized hydrogels. * denotes $p<0.05$ difference. # denotes $p<0.05$ difference from all other values.

Fig. 6.3A, JAWSII iDCs were seeded on hydrogels substrates fabricated with 0, 0.1, and 1.0 μg/ml TGF-β1-SH in the pre-polymer solution. Following stimulation, JAWSII cultured atop hydrogels with 1.0 μg/ml TGF-β1-SH secreted less IL-12, compared to stimulated controls. A marked reduction in IL-12 in response to stimulation was also observed for DCs seeded on hydrogel surfaces containing IL-10, as well as for surfaces dually-functionalized with TGF-β1 and IL-10, as shown in Fig. 6.3B. Stimulated JAWSII DCs atop dually-functionalized gels secreted 63% less IL-12 than DCs cultured on unmodified control hydrogels, providing evidence that the immobilized immunosuppressant biological signals remained active and signaled the DCs.

Flow cytometric analysis was performed on JAWSII DCs harvested after seeding on functionalized hydrogels. The increase in surface expression levels of the stimulatory protein MHCII and co-stimulatory protein CD86 are commonly observed markers of DC maturation, and their expression on JAWSII DCs has been previously observed to correlate with activation state [23]. In brief, JAWSII DCs upregulated MHCII (Fig. 6.3C) and CD86 (Fig. 6.3D) expression in response to stimulation. Seeding JAWSII atop TGF-β1, IL-10, or dually-functionalized gels, however, significantly decreased the percentage of $MHCII^{+}$ DCs following stimulation, Fig. 6.3C. Like the result observed when JAWSII were incubated with soluble immunosuppressants (Fig. 6.1F), CD86 expression was not affected by hydrogel functionalization (Fig. 6.3D). In all, culturing JAWSII with either soluble or immobilized immunosuppressants generated DCs with similar IL-12, MHCII, and CD86 expression, demonstrating the bioactivity of immunomodulatory hydrogels.

6.3.4 Treating BMDCs with soluble TGF-β1 and IL-10

As further evidence of localized immune modulation, we examined bone marrow-derived dendritic cells (BMDCs) harvested from NOD mice. BMDCs were first treated with soluble TGF-β1-SH and IL-10-SH, and selected samples were stimulated with LPS to induce BMDC maturation and the media supernatant was assayed for IL-12. Further, the level of surface expression of MHCII, CD80 and CD86 was assayed via flow cytometry. All samples were co-stained for the dendritic cell marker CD11b, and a high percentage of all samples were found to be $CD11b^+$. The expression of MHCII (Fig. 6.4A), CD80 (Fig. 6.4B) and CD86 (Fig. 6.4C) were each reduced amongst $CD11b^+$ DCs cells by treatment with soluble immunomodulatory factors. Upon stimulation with LPS, all samples had a higher percentage of DCs positive for stimulatory and co-stimulatory markers, but pre-treatment with the soluble immunosuppressive factors reduced the extent to which the expression of each marker was increased by stimulation, relative to stimulated controls. As shown in Fig 6.4D, control BMDC cultures treated with LPS secreted dramatically higher levels of IL-12. When pre-treated with soluble TGF-β1-SH and IL-10-SH, however, significantly lowered levels of IL-12 were detected, indicating a less mature phenotype.

6.3.5 Culturing BMDCs with immunomodulatory PEG hydrogels

BMDCs were cultured on the surfaces of functionalized and unfunctionalized gels (Fig. 6.5 A) and then stimulated via the addition of LPS. IL-12 production was quantified, as shown in Fig. 6.5B, and, as before, a significant increase in cytokine production was observed for LPS-stimulated samples. The presence of

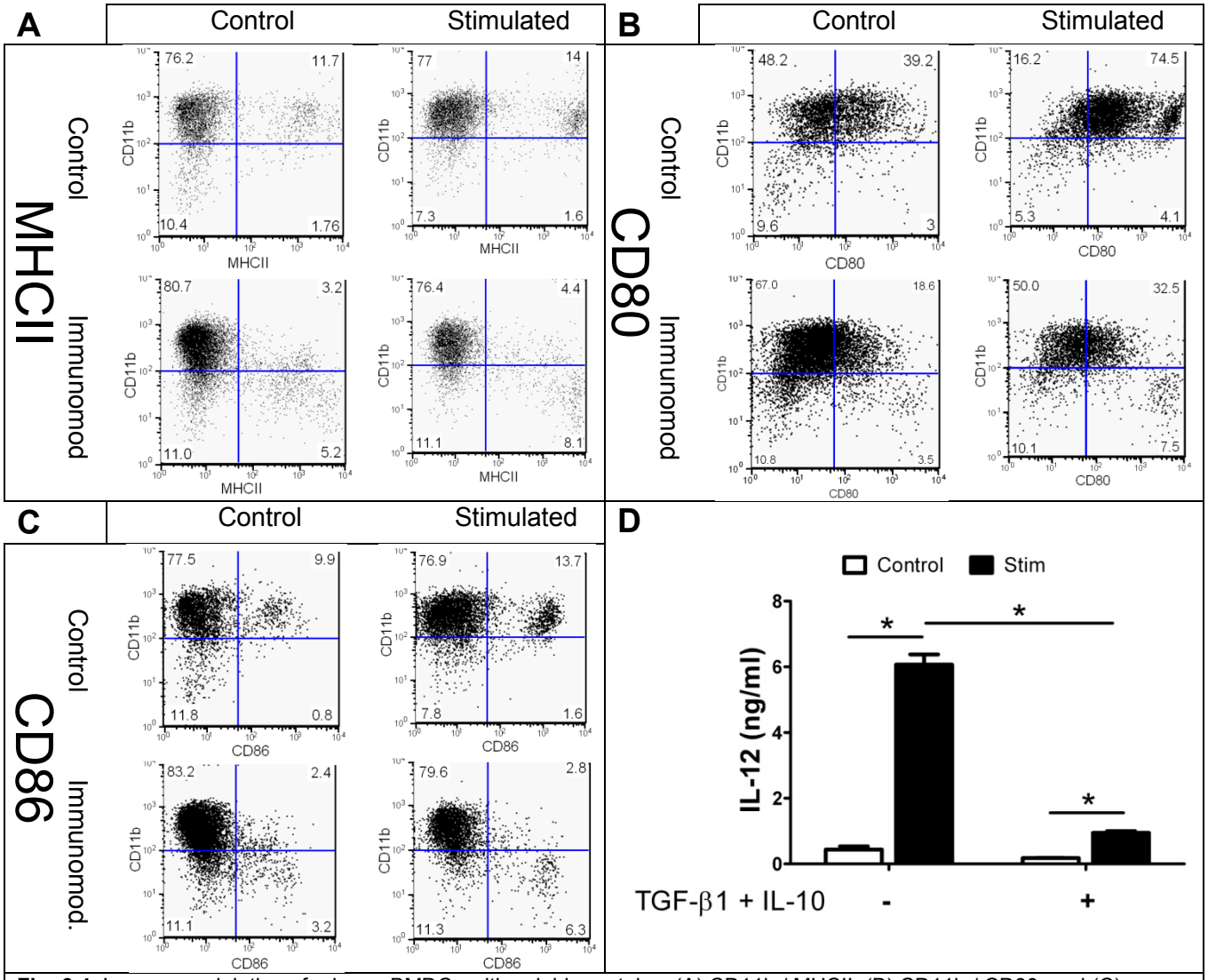

Fig. 6.4. Immunomodulation of primary BMDCs with soluble proteins. (A) CD11b / MHCII, (B) CD11b / CD80, and (C) CD11b/CD86 expression of BMDCs treated with or without soluble immunomodulation (10 ng/ml TGF-β1-SH and IL-10-SH) and with or without stimulation with LPS (1 μg/ml). Numbers are % of cells. Experiment performed by Jing He (D) IL-12 production by BMDCs treated with soluble TGF-β1-SH and IL-10-SH. * denotes $p<0.05$ difference.

immunomodulatory factors on the surfaces of otherwise blank the hydrogels, however, only slightly reduced iDC maturation, as evident by a small but significant decrease in IL-12 production with TGF-β1 and IL-10 on the hydrogel surface. We hypothesized that this effect might be due to limited interaction between the immature BMDCs and the PEG surface, as PEG is well documented to resist cell and protein adhesion.

To increase interaction between BMDCs and PEG surfaces, two strategies were explored to promote adhesion: introduction of poly-L-lysine (PLL) and the ECM proteins,

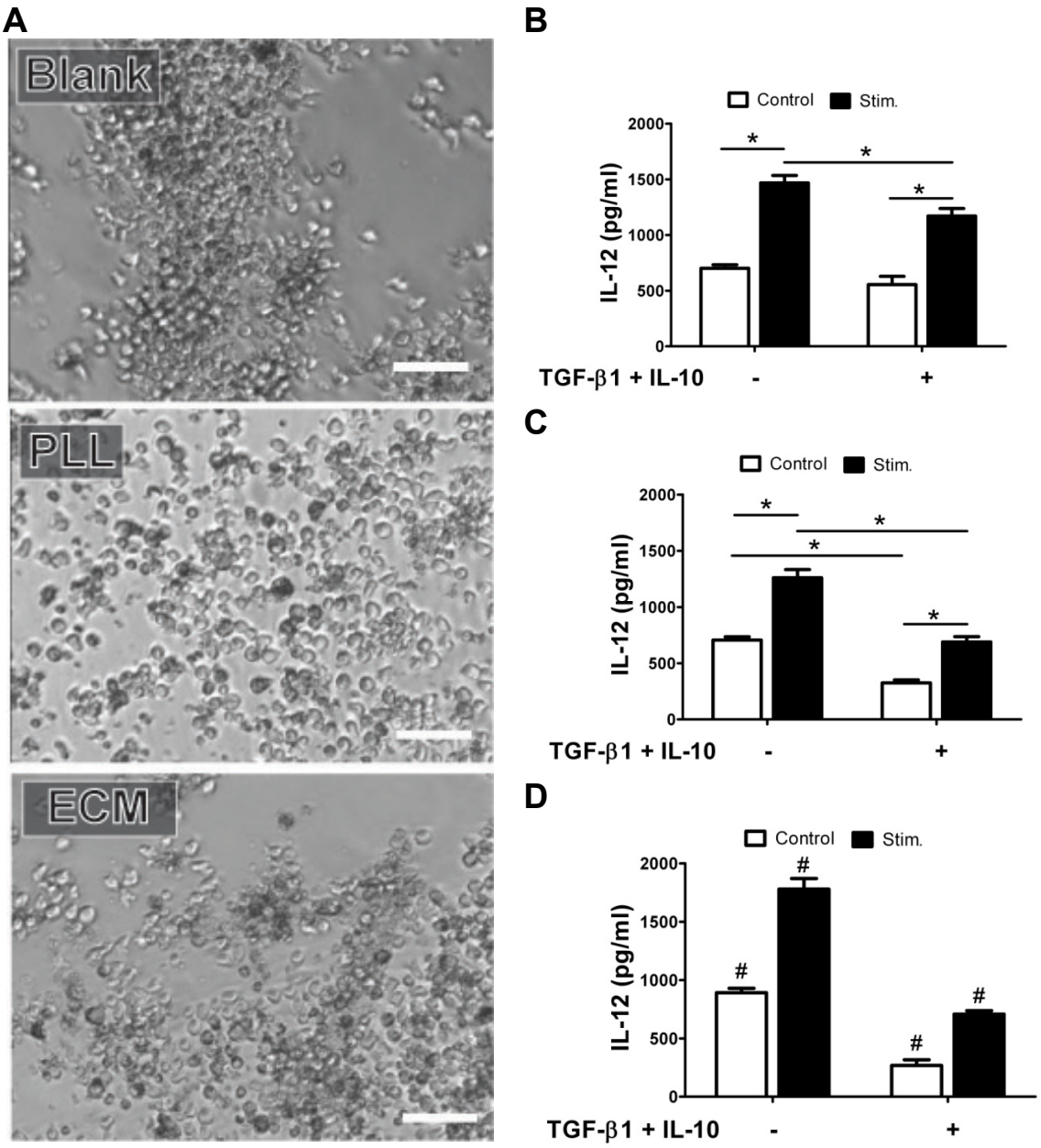

Fig. 6.5. BMDCs on immunomodulatory hydrogels. (A) Brightfield microscopy of BMDCs seeded atop PEG hydrogels that contain (top) no functionalization (middle) poly-L-lysine, and (bottom) the ECM proteins laminin and fibronectin. Scale = 60 μm (B-D) IL-12 production by BMDCS cultured on immunomodulatory hydrogels functionalized with (B) unmodified, (C) +PLL, (D) +ECM proteins. * denotes $p<0.05$ difference, # denotes $p<0.05$ difference from all values

fibronectin and laminin, on the surfaces of PEG hydrogels to promote cellular interactions. Visually, these surfaces seemed to effect iDC/surface interaction, as depicted in Fig. 6.5A. On unmodified PEG hydrogels, BMDCs had a tendency to aggregate together, while PLL hydrogels promoted single-cell attachment to the surface. Aggregation occurred for cells seeded on ECM-modified gels, but to a lesser

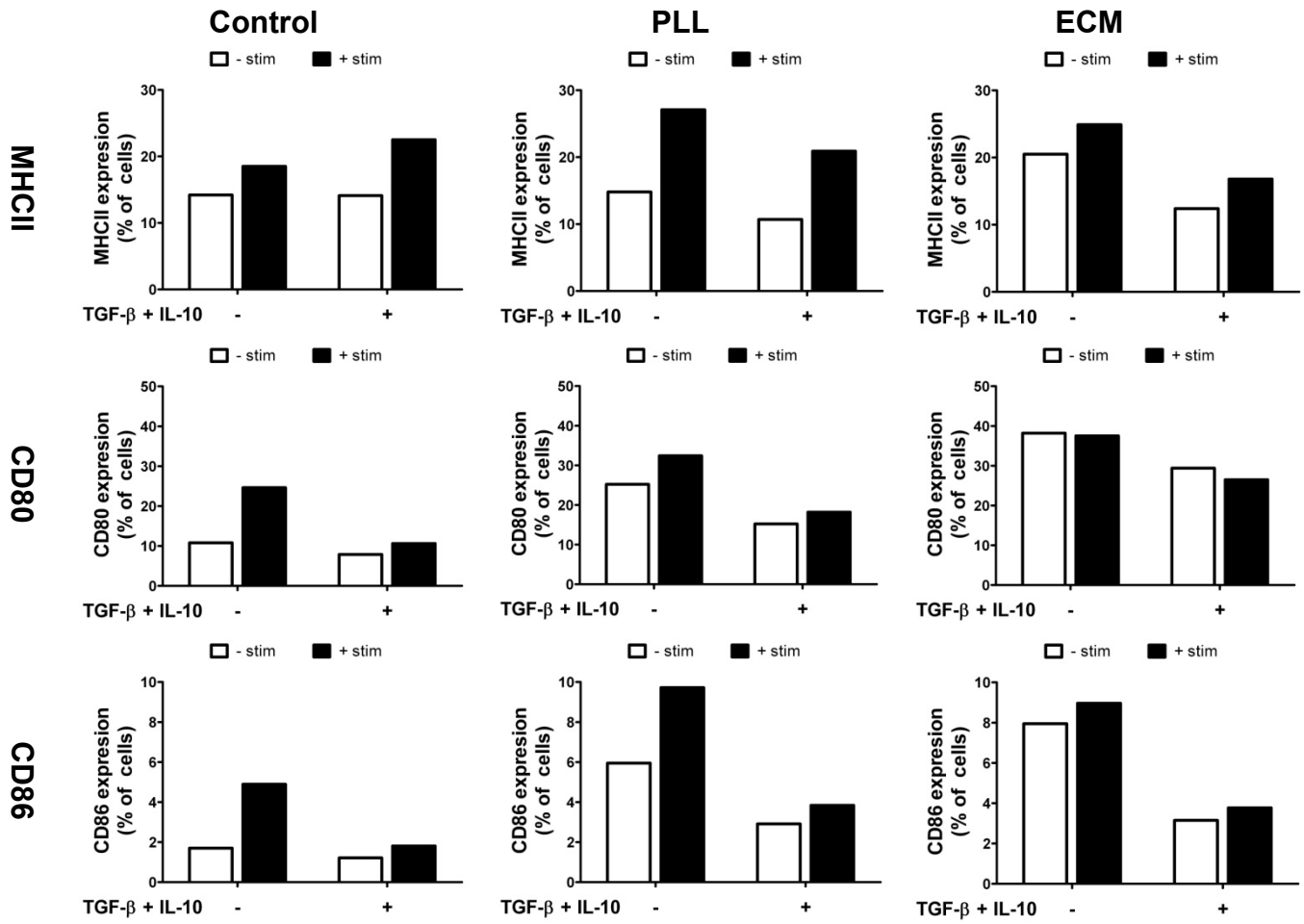

Fig. 6.6. Surface marker expression of BMDCs seeded atop control or immunomodulatory (+TGF-β1 and IL-10) hydrogels, with or without immune stimulation. Hydrogels were seeded on control hydrogels, or gels co-functionalized with either poly(L-lysine) (PLL) or hydrogels containing laminin and fibronectin (ECM). The percentage shown represents the fraction of $CD11c^{+}$ dendritic cells which stained positive for surface markers (MHCII, CD80, or CD86), as compared to isotype controls.

extent than observed on PLL hydrogels. BMDCs were cultured atop PLL and ECM hydrogels functionalized with TGF-β1 and IL-10, and then stimulated with LPS. When seeded atop hydrogels co-functionalized with PLL and immunosuppressive factors, the IL-12 measured post-stimulation was decreased by more than 50%, Fig. 6.5C. Further, the expression of the surface maturation markers MHCII, CD80 and CD86 were generally reduced prior to and following immune stimulation on immunomodulatory hydrogels, as shown in Fig. 6.6. Immunosuppressive hydrogels provided strong evidence of reduced maturation, as evident by drastic reductions in IL-12 secretion, Fig.

6.5D, as well as reduced expression of MHCII stimulatory molecules and CD80 and CD86 co-stimulatory molecules, Fig. 6.6.

6.3.6 Co-culture of BMDCs with T cells

Following culture atop immunosuppressive hydrogels, BMDCs were harvested and co-cultured with T cells to assess the functional capacity of dendritic cells to activate T cells. As illustrated in Fig. 6.7A, unstimulated dendritic cells lacked the capacity to activate T cells, characteristic of an immature dendritic cell phenotype. Upon LPS stimulation, however, BMDCs were found to have matured, as they possessed the capacity to activate T cells, shown via increased T cell IFN-γ secretion (a marker of T cell activation). When BMDCs were pre-treated with soluble TGF-β and IL-10 prior to stimulation, T cell IFN-γ production was significantly reduced, indicating reduced T cell activation by dendritic cells. This finding further highlights the

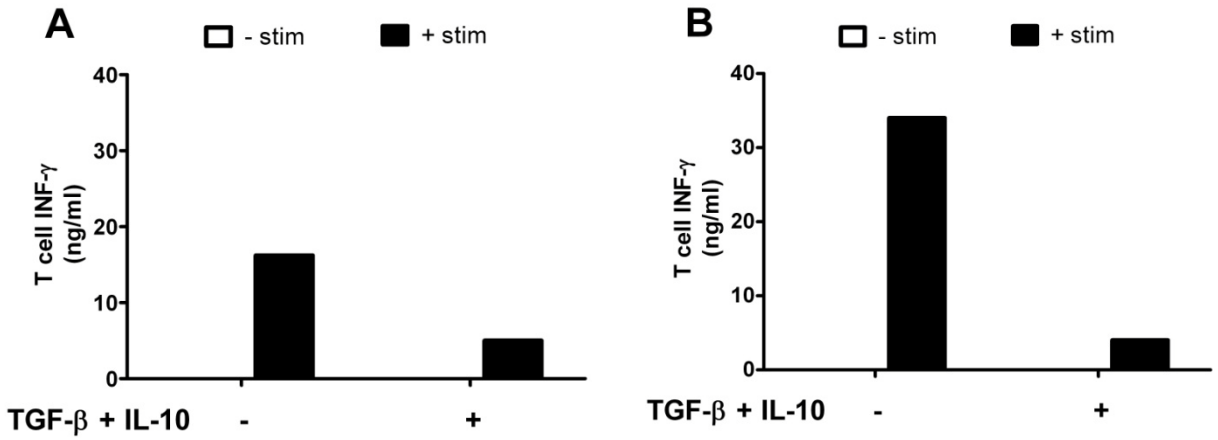

Fig. 6.7. Interferon γ (IFN-γ) production by T cells following culture with BMDCs. BMDCs were cultured on (A) TCPS or (B) PEG hydrogels functionalized with PLL. BMDCs were treated with or without (A) soluble TGF-β1 and IL-10 or (B) covalently immobilized TGF-β1 and IL-10 for two days. Then, + stim samples were treated with LPS overnight to induce DC maturation.

immunosuppressive capacity of these biomolecules towards iDCs. This effect was also observed when dendritic cells were cultured atop hydrogels functionalized with PLL to promote cell / material interactions, shown in Fig. 6.7B. In the absence of immunomodulatory factors, stimulated dendritic cells signaled T cells to secrete high levels of IFN-γ, while DCs culture atop hydrogels co-functionalized with PLL and possessed a drastically reduced capacity to activate T cells.

6.4 DISCUSSION

Covalent incorporation of the immunosuppressive proteins TGF-β1 and IL-10 on the PEG hydrogel surfaces necessitated modification to introduce functional groups compatibile with covalent conjugation during polymerization. Initially, conventional amine/NHS-succinimide chemistry was employed in which acrylate-PEG-NHS was reacted with TGF-β1 to introduce acrylate groups onto proteins for co-polymerization [20]. Upon acrylation, however, soluble acryl-TGF-β1 was found to significantly increase DC IL-12 production (data not shown). Therefore, an alternative chemistry was employed: modification of the targeted protein with Traut's reagent. Reaction with Traut's reagent introduces thiols onto proteins by modification of free amines, as evidenced by the successful detection of proteins on hydrogel surfaces. Additionally, bioactivity towards PE-25 reporter cells and JAWSII DCs was preserved.

For the hydrogel experiments reported here, thiolated proteins were added to the pre-polymer mixture for bulk polymerization into PEG hydrogels, utilizing a thiol-acrylate mixed-mode photoinitated polymerization. As a consequence, proteins were present

throughout the hydrogel as well as on the gel surface. The presence of accessible proteins on the hydrogel surfaces was verified by a modified ELISA, whereby functionalized gels were incubated with a detection antibody. As has been previously reported, antibodies (approx. 150 kDa) are unable to diffuse within PEGDA hydrogels [34], so protein was detectable only if immobilized and available for binding on the hydrogel surface. Results were verified via a visual confirmation that the color change of the cleaved TMB ELISA substrate occurred at the hydrogel surface, while the interior of the hydrogel remained clear (data not shown). Using this modified ELISA, significant protein was detectable, quantifiable, and found to be dependent upon the protein concentration added to the pre-polymer solution. Further, the bioactivity of tethered TGF-β1 was confirmed via a significant cell response upon seeding with PE-25 TGF-β reporter cells.

JAWSII iDCs were seeded on the surfaces of hydrogels functionalized with TGF-β1 and/or IL-10 to assess bioactivity towards these cells. When cultured atop these gels, IL-12 production was suppressed upon stimulation, as was MHCII expression. In fact, these markers were suppressed to a similar extent by either soluble or immobilized factors. Ultimately, this expression profile indicates decreased DC maturation and provides evidence that immobilized immunosuppressive factors remain bioactive to DCs. While the suppression of IL-12 production and MHCII expression was successfully provided by TGF-β1 and/or IL-10, CD86 co-stimulatory molecule was unaffected. This finding is in contrast to previous observations of decreased co-stimulatory marker expression on stimulated DCs that have been pre-treated with TGF-β1 and IL-10 [2]. Because this finding was consistent for pre-treatment with either soluble or immobilized

factors, it is likely that the reduced sensitivity of co-stimulatory expression to immunosuppressive signaling is an inherit property of the JAWSII cell line and not a result of signaling molecule immobilization. Therefore, JAWSII DCs serve as an imperfect model for the generation of tolerogenic DCs, but the reduction of IL-12 production and MHCII expression by functionalized hydrogels provided evidence that immobilized TGF-β1 and IL-10 retained bioactivity and that DCs were permissive to their signaling.

The bioactivity of immunomodulatory hydrogels was further assessed via experimentation with primary BMDCs isolated from NOD mice. When BMDCs were treated with soluble, thiolated immunosuppressive proteins, a reduction in stimulatory (MHCII), co-stimulatory (CD80 & CD86) and cytokine (IL-12) production was observed. In contrast to the JAWSII DCs, the observed reduction in maturation markers agrees well with previous findings [2]. BMDCs from NOD mice are known to undergo defective maturation following immune stimulation [26, 27]. Thus, the maximum levels of activation marker expression observed for non-immunomodulation controls agrees with those previously reported for mature BMDCs from NOD mice [35].

Primary BMDCs were then seeded atop functionalized hydrogels in order to assess the capacity of the immobilized proteins of interest to signal DCs. Initially, it was observed that PEG hydrogels modified with immunosuppressive factors alone delivered limited signaling to seeded BMDCs, as equivalent IL-12 was produced for either case following stimulation with LPS. We hypothesized that this effect could be due to limited interaction between cells and PEG surface, as PEG hydrogels are previously known to resist cells adhesion. Many researchers have observed that the addition of adhesion

ligands to biomaterial surfaces promotes cell attachment and increased cell signaling [36]; for example, we recently reported that the addition of ICAM-1 to PEG surfaces promoted T cell signaling [20]. Therefore, we investigated two methods of introducing adhesion molecules within the PEG hydrogels: via the addition of poly-L-lysine PLL and via the incorporation of the ECM proteins, collagen and laminin.

The ECM proteins laminin and fibronectin were incorporated into PEG hydrogels to promote DC adhesion. ECM proteins are widely employed within the field of tissue engineering to promote cell attachment to surfaces [36]. When seeded upon ECM-hydrogels, BMDCs secreted modestly elevated IL-12 in the absence of LPS stimulation, compared to cells seeded on blank hydrogels. The inherent ability of ECM-functionalized materials to induce the maturation of iDCs has been previously reported [7, 35], so it is not surprising we observed this effect. It is encouraging, however, that the introduction of TGF-β1 and IL-10 to the ECM-tethered surfaces significantly reduced the production of IL-12 and expression of MHCII, CD80 and CD86 by BMDCs. The observations that immobilized immunosuppressive proteins have the capacity to suppress ECM-mediated iDC maturation, as well as resist maturation upon LPS stimulation, provide striking evidence of the bioactivity of immunomodulatory PEG hydrogels.

Further, others have incorporated poly-L-lysine (PLL) onto surfaces to promote dendritic cell attachment [37], and it is well known that positively charged groups on PLL result in the rapid binding of serum proteins to material surfaces, enabling cell interactions [38, 39]. Additionally, serum coated surfaces (e.g., PLL-coated materials) have been used to limited the adjuvant effect [37, 40], and are therefore a suitable

platform for immunomodulation. BMDCs were seeded upon hydrogels functionalized with PLL and TGF-β1 and/or IL-10 and then stimulated. For PLL-hydrogels, an immunosuppressive effect was observed, as DC IL-12 production and surface marker expression on control and immunomodulatory hydrogels were decreased relative to controls. Further, T cell studies confirmed that PLL hydrogels functionalized with immunomodulatory factors significantly reduced dendritic cell maturation. Ultimately, these findings indicated that decreased cell-material interactions were a likely reason for limited signaling on unmodified immunomodulatory gels. Further, the immunosuppressive activity of PLL/immunomodulatory hydrogels towards BMDCs from NOD mice provides evidence that this sort of surface has the potential to interact favorably with DCs from type I diabetes.

6.5 CONCLUSIONS

In summary, we have reported a strategy for the introduction of immunosuppressive proteins, TGF-β1 and IL-10, into PEG hydrogels in a manner that preserves bioactivity towards iDCs. While future work is required to demonstrate that the DCs created by these surfaces are, in fact, tolerogenic DCs capable of inducing TREG formation, we have demonstrated that the immunomodulatory hydrogels reported herein possess bioactivity that approaches that of the soluble immunosuppressive proteins when cultured in the presence of the immortalized JAWSII DC cell line or primary BMDCs isolated from NOD mice. This immunomodulatory biomaterial platform has the potential to serve as an *in vitro* culture platform for the generation of tolerogenic

DCs. Further, this technology suggest strategies for tissue engineering applications, such as a coating of cell-laden biomaterials where it is desirable to limit the maturation of local dendritic cells and subsequently ameliorate the adaptive immune response.

6.6 ACKNOWLEDGEMENTS

The authors wish to acknowledge Kathryn Haskins for guidance and resources for the BMDC studies reported herein. Additionally, we thank Jing He for training and technical assistance with all BMDC studies as well as for performing all BMDC flow cytometry experiments. These collaborators will be co-authors on a planned manuscript that will be submitted for publication based on the results in this chapter. Thanks also to Dr. Charles Cheung and Dr. Chien-Chi Lin for initial guidance, technical assistance and helpful discussions. Additionally, we would like to thank Joshua McCall for his expertise with TGF-β and the reporter cell assay, Huan (Sharon) Wang for her assistance with JAWSII flow cytometry, and Dr. Xuedong Liu for providing PE-25 cells. Finally, we gratefully acknowledge financial support from the National Institute of Health (RO1DK076084), the Howard Hughes Medical Institute, and the Department of Education's Graduate Assistance in Areas of National Need fellowship to P.S.H.

6.7 REFERENCES

1. Banchereau J, Steinman RM. Dendritic cells and the control of immunity. Nature 1998 Mar 19;392(6673):245-252.

2. Morelli AE, Thomson AW. Tolerogenic dendritic cells and the quest for transplant tolerance. Nat Rev Immunol 2007 Aug;7(8):610-621.

3. Matzinger P. An innate sense of danger. Seminars in immunology 1998 Oct;10(5):399-415.

4. van Kooten C, Lombardi G, Gelderman KA, Sagoo P, Buckland M, Lechler R, et al. Dendritic Cells as a Tool to Induce Transplantation Tolerance: Obstacles and Opportunities. Transplantation 2011 Jan;91(1):2-7.

5. Babensee JE. Interaction of dendritic cells with biomaterials. Seminars in immunology 2008 Apr;20(2):101-108.

6. Babensee JE, Paranjpe A. Differential levels of dendritic cell maturation on different biomaterials used in combination products. Journal of biomedical materials research 2005 Sep 15;74(4):503-510.

7. Acharya AP, Dolgova NV, Clare-Salzler MJ, Keselowsky BG. Adhesive substrate-modulation of adaptive immune responses. Biomaterials 2008 Dec;29(36):4736-4750.

8. Rogers TH, Babensee JE. The role of integrins in the recognition and response of dendritic cells to biomaterials. Biomaterials 2011 Feb;32(5):1270-1279.

9. Hubbell JA, Thomas SN, Swartz MA. Materials engineering for immunomodulation. Nature 2009 Nov 26;462(7272):449-460.

10. Norton LW, Park J, Babensee JE. Biomaterial adjuvant effect is attenuated by anti-inflammatory drug delivery or material selection. J Control Release 2010 Sep 15;146(3):341-348.

11. Hackstein H, Thomson AW. Dendritic cells: emerging pharmacological targets of immunosuppressive drugs. Nat Rev Immunol 2004 Jan;4(1):24-34.

12. Kosiewicz MM, Alard P. Tolerogenic antigen-presenting cells: regulation of the immune response by TGF-beta-treated antigen-presenting cells. Immunologic research 2004;30(2):155-170.

13. Steinbrink K, Wolfl M, Jonuleit H, Knop J, Enk AH. Induction of tolerance by IL-10-treated dendritic cells. J Immunol 1997 Nov 15;159(10):4772-4780.

14. Sato K, Nagayama H, Tadokoro K, Juji T, Takahashi TA. Extracellular signal-regulated kinase, stress-activated protein kinase/c-Jun N-terminal kinase, and p38mapk are involved in IL-10-mediated selective repression of TNF-alpha-induced activation and maturation of human peripheral blood monocyte-derived dendritic cells. J Immunol 1999 Apr 1;162(7):3865-3872.

15. Torres-Aguilar H, Aguilar-Ruiz SR, Gonzalez-Perez G, Munguia R, Bajana S, Meraz-Rios MA, et al. Tolerogenic dendritic cells generated with different immunosuppressive cytokines induce antigen-specific anergy and regulatory properties in memory CD4+ T cells. J Immunol Feb 15;184(4):1765-1775.

16. Ito Y. Surface micropatterning to regulate cell functions. Biomaterials 1999 Dec;20(23-24):2333-2342.

17. Hirano Y, Mooney DJ. Peptide and protein presenting materials for tissue engineering. Adv Mater 2004 Jan;16(1):17-25.

18. Mann BK, Schmedlen RH, West JL. Tethered-TGF-beta increases extracellular matrix production of vascular smooth muscle cells. Biomaterials 2001 Mar;22(5):439-444.

19. Cheung CY, Anseth KS. Synthesis of immunoisolation barriers that provide localized immunosuppression for encapsulated pancreatic islets. Bioconjug Chem 2006 Jul-Aug;17(4):1036-1042.

20. Hume PS, Anseth KS. Inducing local T cell apoptosis with anti-Fas-functionalized polymeric coatings fabricated via surface-initiated photopolymerizations. Biomaterials 2010 Apr;31(12):3166-3174.

21. Leclerc C, Brose C, Nouze C, Leonard F, Majlessi L, Becker S, et al. Immobilized cytokines as biomaterials for manufacturing immune cell based vaccines. Journal of biomedical materials research 2008 Sep 15;86(4):1033-1040.

22. Jiang X, Shen C, Rey-Ladino J, Yu H, Brunham RC. Characterization of murine dendritic cell line JAWS II and primary bone marrow-derived dendritic cells in Chlamydia muridarum antigen presentation and induction of protective immunity. Infection and immunity 2008 Jun;76(6):2392-2401.

23. Jorgensen TN, Haase C, Michelsen BK. Treatment of an immortalized APC cell line with both cytokines and LPS ensures effective T-cell activation in vitro. Scand J Immunol 2002 Nov;56(5):492-503.

24. Otsu S, Gotoh K, Yamashiro T, Yamagata J, Shin K, Fujioka T, et al. Transfer of antigen-pulsed dendritic cells induces specific T-Cell proliferation and a therapeutic effect against long-term Helicobacter pylori infection in mice. Infection and immunity 2006 Feb;74(2):984-993.

25. Pinchuk LM, Lee SR, Filipov NM. In vitro atrazine exposure affects the phenotypic and functional maturation of dendritic cells. Toxicol Appl Pharmacol 2007 Sep 15;223(3):206-217.

26. Langmuir PB, Bridgett MM, Bothwell AL, Crispe IN. Bone marrow abnormalities in the non-obese diabetic mouse. Int Immunol 1993 Feb;5(2):169-177.

27. Peng R, Bathjat K, Li Y, Clare-Salzler MJ. Defective maturation of myeloid dendritic cell (DC) in NOD mice is controlled by IDD10/17/18. Annals of the New York Academy of Sciences 2003 Nov;1005:184-186.

28. Lin CC, Anseth KS. Controlling Affinity Binding with Peptide-Functionalized Poly(ethylene glycol) Hydrogels. Adv Funct Mater 2009 Jul 24;19(14):2325.

29. Clarke DC, Brown ML, Erickson RA, Shi Y, Liu X. Transforming growth factor beta depletion is the primary determinant of Smad signaling kinetics. Molecular and cellular biology 2009 May;29(9):2443-2455.

30. He J, Haskins K. Pathogenicity of T helper 2 T-cell clones from T-cell receptor transgenic non-obese diabetic mice is determined by tumour necrosis factor-alpha. Immunology 2008 Jan;123(1):108-117.

31. Poulin M, Haskins K. Induction of diabetes in nonobese diabetic mice by Th2 T cell clones from a TCR transgenic mouse. J Immunol 2000 Mar 15;164(6):3072-3078.

32. Traut RR, Bollen A, Sun TT, Hershey JWB, Sundberg J, Pierce LR. METHYL 4-MERCAPTOBUTYRIMIDATE AS A CLEAVABLE CROSSLINKING REAGENT AND ITS APPLICATION TO ESCHERICHIA-COLI 30S RIBOSOME. Biochemistry 1973;12(17):3266-3273.

33. Salinas CN, Anseth KS. Mixed mode thiol-acrylate photopolymerizations for the synthesis of PEG-peptide hydrogels. Macromolecules 2008 Aug;41(16):6019-6026.

34. Cruise GM, Scharp DS, Hubbell JA. Characterization of permeability and network structure of interfacially photopolymerized poly(ethylene glycol) diacrylate hydrogels. Biomaterials 1998 Jul;19(14):1287-1294.

35. Acharya AP, Dolgova NV, Xia CQ, Clare-Salzler MJ, Keselowsky BG. Adhesive substrates modulate the activation and stimulatory capacity of non-obese diabetic mouse-derived dendritic cells. Acta biomaterialia 2010 Jan;7(1):180-192.

36. Zhu J. Bioactive modification of poly(ethylene glycol) hydrogels for tissue engineering. Biomaterials 2010 Jun;31(17):4639-4656.

37. Mant A, Tourniaire G, Diaz-Mochon JJ, Elliott TJ, Williams AP, Bradley M. Polymer microarrays: identification of substrates for phagocytosis assays. Biomaterials 2006 Oct;27(30):5299-5306.

38. Jenney CR, Anderson JM. Adsorbed serum proteins responsible for surface dependent human macrophage behavior. J Biomed Mater Res 2000 Mar 15;49(4):435-447.

39. Wang GX, Deng XY, Tang CJ, Liu LS, Xiao L, Xiang LH, et al. The adhesive properties of endothelial cells on endovascular stent coated by substrates of poly-l-lysine and fibronectin. Artificial cells, blood substitutes, and immobilization biotechnology 2006;34(1):11-25.

40. Kou PM, Babensee JE. Macrophage and dendritic cell phenotypic diversity in the context of biomaterials. Journal of biomedical materials research 2010 Jan;96(1):239-260.

Chapter 7

Conclusions and Recommendations

This thesis advances the understanding of bioactive and immunoactive modifications to encapsulation barriers for the purpose of improving their immunoisolation capability. Throughout these studies, poly(ethylene glycol) (PEG) hydrogels were modified with various bioactive molecules and then investigated in relevant *in vitro* model systems. Overall, these functionalized biomaterials provided significant spatially-controllable bioactivity to ameliorate inflammatory damage within capsules, reduce the local population of T cells in proximity to cell-laden capsule, or dampen dendritic cell maturation, towards eliciting transplant tolerance.

In studies related to Specific Aim 1 (Chapter 3), a polymerizable superoxide dismutase mimetic (SODm) was incorporated into β-cell laden PEG hydrogels to prevent superoxide-mediated damage. During initial studies, the SODm was shown to be well-tolerated by encapsulated cells. To explore the molecule's potential protective benefits, superoxide was generated chemically via the reaction of xanthine with xanthine oxidase. When generated in the presence of cells, this chemically generated superoxide results in significant cell death, observed via both reduced metabolic activity and through the visualization of fewer live cells via live/dead confocal imaging. When SODm was incorporated in the cell-laden gels through copolymerization, however, a dose-response was observed whereby increased concentrations of SODm resulted in

increased cell survival as evidenced by greater metabolic activity following challenge with superoxide. Finally, a longer-term study was performed in which β-cells were encapsulated within hydrogels with or without SODm and then treated with superoxide three times over the course of ten days. This study confirmed the cytoprotective effect of SODm with multiple challenges, as cells within hydrogels functionalized with SODm demonstrated over 60% survival at the conclusion of the experiment, whereas essentially no metabolic activity remained for control gels.

Encouraged by the marked cytoprotective effect of polymerized SODm, we attempted an *in vivo* study in which murine islets were encapsulated in PEG hydrogel disks with or without SODm. These studies were conducted as part of a fruitful collaboration with Prof. Kathryn Haskins and Brenda Bradley at National Jewish,. Functionalized hydrogels were implanted in the abdominal fat and kidney capsules of mice and then explanted 7 days later to assess cell survival. Unfortunately, poor survival was observed for all implanted islets, regardless of the presence of SODm. High viability was observed, however, for control islet capsules cultured *in vitro*. As a result of the poor survival observed for all implanted islets, these studies were inadequate to improve understanding about the *in vivo* protective benefits of incorporating SODm within PEG capsules. Further investigations regarding the *in vivo* efficacy of polymerized SODm will likely yield important evidence supporting its use within cell-laden hydrogels, however, before further *in vivo* studies can be conducted, optimization of the encapsulation and transplantation systems to allow improved basal cell survival is required. Among many potential explanations for poor *in vivo* islet survival, the most likely was the unavailability of oxygen and nutrients. Thus, improved

small molecule transport could be achieved via the introduction of pores or channels within PEG hydrogel disks. Conversely, the size of capsules could be reduced (the investigated disks were ~5 mm in diameter by ~2 mm thick). Both approaches would reduce the diffusion distance between encapsulated cells and nutrients. Upon improvement to encapsulated islet survival *in vivo*, further investigations would become possible with several of the immunoisolation materials described in this thesis.

Specific Aim 2 (Chapter 4) focused on the development and testing of a surface-mediated photopolymerization for the formation of functionalized PEG chains. Anti-fas was successfully incorporated within coatings at a high surface density. When seeded with jurkat T cells, anti-fas-functionalized polymer surfaces induced significant apoptosis, which was increased by the incorporation of the ICAM-1 adhesion ligand. ICAM-1 is previously known to stabilize interactions between T cells and effector cells for the purpose of promoting cell-cell signaling, so it is likely that ICAM-1 stabilized the interaction between functionalized surfaces and T cells during fas signaling.

While the DTC-mediated functionalization strategy enabled the formation of surface-initiated coatings, it was not readily translatable to cell-laden hydrogels. In its initial form, this surface-initiated chemistry was not compatible with aqueous conditions due to the insolubility of the DTC photoiniferter. To improve solubility, a photoiniferter was tethered to either end of PEG chains to form the molecule DTC-PEG-DTC. PEG is highly water-soluble, and therefore, PEGylation is a commonly used chemical modification to improve aqueous solubility. While DTC-PEG-DTC was successfully synthesized, as confirmed by NMR, and was soluble in aqueous buffers, the reactivity of this molecule in aqueous conditions could not be demonstrated. Perhaps further

experimentation with DTC-PEG-DTC would enable photoiniferter-mediated polymerization in aqueous conditions. Alternatively, a living radical polymerization chemistry better-suited for aqueous conditions could be employed, such as reversible addition-fragmentation chain transfer (RAFT) polymerization, to form controlled anti-fas coatings.

While DTC was not adapted to fabricate coatings atop PEG hydrogels, surface-initiated coatings mediated by the glucose oxidase (GOx) enzyme were successfully formed. As explored in experiments related to Specific Aim 3 (Chapter 5), conformal, PEG-based polymer coatings were readily formed on the surfaces of hydrogels with a high incorporation of accessible signaling molecules. Similar to the results obtained in Specific Aim 2, culturing jurkat T cells with these functionalized coating resulted in significant T cells apoptosis and cell death. After 48 hrs of seeding atop coatings dually-functionalized with anti-fas and ICAM-1, over 60% of all T cells were either apoptotic or dead.

GOx-mediated coatings were adapted for cell-laden hydrogels and eventually found to maintain high encapsulated cell viability. Initially, low molecular weight PEG mono- and di-acrylates were employed for coatings. Unfortunately, low molecular weight PEG acrylates were found to be highly toxic to encapsulated cells; to the extent that dipping a PEGDA hydrogel (4,600 Da, 10 wt%) containing β-cells into a 1 wt% PEG diacrylate (M_n=550 Da) in PBS for 10 seconds, followed by transfer to cell culture media, was adequate to kill virtually all encapsulated cells. PEG methacrylates, however, were better-tolerated by encapsulated cells, as high encapsulated cell viability was maintained following 60s dippings into 25 wt% PEG methacrylate (M_n=525 Da).

Further, PEG methacrylates demonstrated comparable reactivity when employed in GOx-mediated dip-coatings. Therefore, PEG methacrylates are considered a superior choice for coating cell-laden hydrogels. While GOx-mediated coatings were utilized to provide anti-fas functionality on the surfaces of PEG hydrogels, GOx coatings should find broad appeal within the field of regenerative medicine. One could envision numerous useful applications for functionalized, conformal coatings on cell-laden biomaterials, including fabricating multilayered hydrogels for tailorable therapeutic release, signaling additional immune cell types (e.g., macrophages), or for creating spatially and functionally-defined layered hydrogels for the co-encapsulation of multiple cell types.

In its present form, the GOx-mediated reactive chemistry is versatile and should find many applications. One limitation, however, seems to be that residual glucose oxidase enzyme is entrapped within polymer layers during formation, resulting in continued GOx activity after dip-coatings. This activity was apparent due to the requirement for catalase in cell culture media following coating, but was also evident because freshly-coated hydrogels, when placed in cell culture media containing phenol-red pH indicator, rapidly reduced the media pH. This persistence necessitated that cell-laden samples be transferred to fresh media approximately every half hour for the first 2 to 3 hrs following coating. The observed pH drop likely occurred as residual glucose oxidase in the coating reacted with glucose from cell media to form H_2O_2 and D-glucono-1,5-lactone, the latter of which rapidly hydrolyzes in water to form gluconic acid. After the first 3 hrs following fabrication of the coating, the pH change was no longer observed, indicating that residual GOx likely loses activity after a relatively short amount

of time. Ultimately, the addition of catalase to media and frequent media changes shortly after coating formation overcame the deleterious effects of residual GOx in coatings, but an orthogonal coating chemistry could eliminate these problems altogether. For example, residual GOx enzyme continues to react with glucose in cell culture media, but if an alternate oxidase enzyme, one which reacts with a substrate absent from cell culture media, were employed, oxidase activity could be confined to the dipping reaction. Towards this concept, preliminary experiments were carried out with galactose oxidase (GalOx), a commercially available enzyme which has been reported to generate H_2O_2 with a similar catalytic activity to GOx. Hydrogels were swollen in solutions containing galactose, and coating of the gel was attempted in pre-polymer containing GalOx. Unfortunately, initial studies failed to identify reaction conditions that enabled coating formation. In the future, further experimentation with the GalOx enzyme, or an alternative oxidase, could result in reactive coatings with orthogonality and improved cytocompatibility.

Throughout Specific Aim 4 (Chapter 6), PEG hydrogels were functionalized with immunosuppressive proteins to explore their potential for signaling nearby dendritic cells. Towards this objective, TGF-β1 and IL-10 were rendered polymerizable via thiolation by Traut's reagent and then successfully incorporated within PEG hydrogels. The presence of protein on hydrogel surfaces was confirmed via ELISA and by a reporter cell assay. Initial dendritic cell experiments were performed with the JAWSII immature dendritic cell (iDC) line and treatment with either soluble or immobilized TGF-β1 and / or IL-10 significantly reduced IL-12 secretion and MHCII expression following stimulation with LPS and cytokines. This study offered encouraging evidence that

immunosuppressive hydrogels exhibit substantial bioactivity, and that iDCs are capable of receiving immunosuppression signals from biomaterial surfaces.

While JAWSII DCs were successfully used to confirm the bioactivity of immunoactive hydrogels, this cell line was determined to be an imperfect cell type for the study of the immunosuppressive effects of TGF-β1 and IL-10. JAWSII DCs were not entirely permissive to immunosuppressive signaling, since soluble and immobilized TGF-β1 and IL-10 were unable to reduce the expression of co-stimulatory markers (e.g., CD86), even though this effect is commonly observed with other primary DCs. As a result, it was necessary to evaluate immunomodulatory hydrogels further with primary immature bone-marrow derived dendritic cells (BMDCs). In collaboration with the Haskins' group, primary DCs were cultured on immunosuppressive hydrogels, but only slight reductions in maturation were initially observed (e.g., reduced IL-12 production) following immune stimulation. To improve signaling between immunosuppressive hydrogels and immature BMDCs, poly-L-lysine (PLL) and extracellular matrix proteins (ECM) were introduced to increase general adhesion. With the introduction of adhesion, immunosuppressive hydrogels were observed to significantly reduce the production of IL-12 following stimulation, as well as reduce the expression of the CD80 co-stimulatory molecule before and after immune stimulation. These finding provided striking evidence that hydrogels modified with TGF-β1 and IL-10 have profound effects on nearby immature dendritic cells.

The introduction of general adhesion was found to greatly improve the signaling capacity of immunomodulatory hydrogels. In practice, however, implanting hydrogels which promote general adhesion could promote the attachment of undesirable cell

types, including macrophages and fibroblasts, which would likely result in fibrous capsule formation. Thus, future efforts might focus on developing a methodology to specifically promote interactions between PEG hydrogels and DCs. This selective adhesion could be achieved by incorporating ligands specific for dendritic cell surface markers (i.e., similar to the approach investigated in Specific Aim 2, in which ICAM-1 was utilized to promote interactions with T cells). Alternatively, the controlled release of specific, bioactive factors might be employed to attract DCs to PEG surfaces. For example, granulocyte colony stimulating factor (G-CSF) has been previously demonstrated as a chemoattractant for dendritic cells able to be programmed for tolerance. Ultimately, while surface adhesion greatly improved signaling towards immature BMDCs *in vitro*, it is possible that increased interactions between dendritic cells and PEG hydrogels could occur innately in the biologically-complex *in vivo* environment, rendering the introduction of adhesion prior to transplantation unnecessary.

For the studies described in Specific Aim 4, the primary objective was to demonstrate that immunosuppressive PEG hydrogels were capable of reducing dendritic cell maturation via material-cell signaling. In these studies, the DC maturation state was assessed because numerous reports have identified partially-mature dendritic cells as having the capability to form antigen specific tolerance via the formation of regulatory T cells (T_{REG}) or through the induction of T cell anergy. Therefore, while the studies detailed in this thesis highlight the capacity of immunomodulatory biomaterials to reduce DC maturation, further investigation is necessary to demonstrate that DCs primed by these materials are able to induce T_{REG} formation. If a sufficient *in vitro*

model were developed to test T_{REG} formation, the next step would be to incubate immature DCs atop immunomodulatory hydrogels in the presence of soluble or immobilized antigen (e.g., insulin to model DCs responding to an islet transplant) and then assay to determine if antigen specific tolerance could be achieved via the formation of anti-insulin T_{REG} cells. Demonstrating antigen-specific tolerance requires the development of a complex model system, but the encouraging results presented in this thesis provide the motivation for such experiments.

Overall, this thesis investigated strategies to introduce immunoactive modifications to PEG hydrogels for the purpose of improving their immunoisolation capacity. In general, biologically-functionalized PEG surfaces are readily able to signal nearby cells of the adaptive immune response. Further, increasing the interactions between immune cells and biomaterial surfaces via general or specific adhesions significantly improves signal delivery. Specific Aim 1 highlighted the ability of polymerized superoxide dismutase enzyme to improve cellular survival in response to reactive oxygen species, one of the major inflammatory effectors of an immune response. In Specific Aim 2, functionalized PEG surfaces signaled local T cell apoptosis, reducing the concentration of the primary responder cells responsible for maintaining the adaptive immune response. In Specific Aim 3, a versatile reactive coating strategy was adapted to present immunoactive signals from the surfaces of cell-laden hydrogels. Finally, Specific Aim 4 introduced immunosuppressive hydrogels modified with TGF-β1 and IL-10 and highlighted their capacity to reduce dendritic cell maturation, towards preventing the development of deleterious adaptive immunity altogether. Ultimately, the bioactive material platforms developed within this thesis

have great potential and suggest innovative strategies for the engineering of future immunoisolation barriers to provide localized and targeted protection of cells delivered in biomaterial carriers for implantation.

Chapter 8

Bibliography

8.1 Chapter 1 references

1. Incidence and trends of childhood Type 1 diabetes worldwide 1990-1999. Diabet Med 2006 Aug;23(8):857-866.

2. Prentki M, Tornheim K, Corkey BE. Signal transduction mechanisms in nutrient-induced insulin secretion. Diabetologia 1997 Jul;40 Suppl 2:S32-41.

3. Vanelli M, Chiarelli F. Treatment of diabetic ketoacidosis in children and adolescents. Acta Biomed 2003 Aug;74(2):59-68.

4. Lawrence SE, Cummings EA, Gaboury I, Daneman D. Population-based study of incidence and risk factors for cerebral edema in pediatric diabetic ketoacidosis. The Journal of pediatrics 2005 May;146(5):688-692.

5. Siafarikas A, O'Connell S. Type 1 diabetes in children - emergency management. Australian family physician May;39(5):290-293.

6. Gremizzi C, Vergani A, Paloschi V, Secchi A. Impact of pancreas transplantation on type 1 diabetes-related complications. Current opinion in organ transplantation 2010 Feb;15(1):119-123.

7. Sheetz MJ, King GL. Molecular understanding of hyperglycemia's adverse effects for diabetic complications. Jama 2002 Nov 27;288(20):2579-2588.

8. Goh SY, Cooper ME. Clinical review: The role of advanced glycation end products in progression and complications of diabetes. The Journal of clinical endocrinology and metabolism 2008 Apr;93(4):1143-1152.

9. The effect of intensive treatment of diabetes on the development and progression of long-term complications in insulin-dependent diabetes mellitus. The Diabetes Control and Complications Trial Research Group. The New England journal of medicine 1993 Sep 30;329(14):977-986.

10. Cryer PE, Davis SN, Shamoon H. Hypoglycemia in diabetes. Diabetes care 2003 Jun;26(6):1902-1912.

11. Hypoglycemia in the Diabetes Control and Complications Trial. The Diabetes Control and Complications Trial Research Group. Diabetes 1997 Feb;46(2):271-286.

12. Boyle PJ, Kempers SF, O'Connor AM, Nagy RJ. Brain glucose uptake and unawareness of hypoglycemia in patients with insulin-dependent diabetes mellitus. The New England journal of medicine 1995 Dec 28;333(26):1726-1731.

13. Jun HS, Yoon JW. Approaches for the cure of type 1 diabetes by cellular and gene therapy. Current gene therapy 2005 Apr;5(2):249-262.

14. Yechoor V, Chan L. Gene therapy progress and prospects: gene therapy for diabetes mellitus. Gene therapy 2005 Jan;12(2):101-107.

15. Aye T, Block J, Buckingham B. Toward closing the loop: an update on insulin pumps and continuous glucose monitoring systems. Endocrinology and metabolism clinics of North America 2010 Sep;39(3):609-624.

16. Kumareswaran K, Evans ML, Hovorka R. Artificial pancreas: an emerging approach to treat Type 1 diabetes. Expert review of medical devices 2009 Jul;6(4):401-410.

17. Minkowski O. Untersuchungen über den Diabetes mellitus nach Extirpation des Pankreas. Berl Klin Wchnschr 1892;29:90.

18. Watson-Williams P. Notes on Diabetes treated with extract and by grafts of sheep's pancreas. British Medical Journal 1894;2:1303-1304.

19. Ballinger WF, Lacy PE. Transplantation of intact pancreatic islets in rats. Surgery 1972 Aug;72(2):175-186.

20. Ricordi C, Lacy PE, Finke EH, Olack BJ, Scharp DW. Automated method for isolation of human pancreatic islets. Diabetes 1988 Apr;37(4):413-420.

21. Scharp DW, Lacy PE, Santiago JV, McCullough CS, Weide LG, Falqui L, et al. Insulin independence after islet transplantation into type I diabetic patient. Diabetes 1990 Apr;39(4):515-518.

22. Alesci S, De Martino MU, Ilias I, Gold PW, Chrousos GP. Glucocorticoid-induced osteoporosis: from basic mechanisms to clinical aspects. Neuroimmunomodulation 2005;12(1):1-19.

23. Qi D, Rodrigues B. Glucocorticoids produce whole body insulin resistance with changes in cardiac metabolism. American journal of physiology 2007 Mar;292(3):E654-667.

24. Shapiro AM, Lakey JR, Ryan EA, Korbutt GS, Toth E, Warnock GL, et al. Islet transplantation in seven patients with type 1 diabetes mellitus using a glucocorticoid-free immunosuppressive regimen. The New England journal of medicine 2000 Jul 27;343(4):230-238.

25. Ryan EA, Lakey JR, Paty BW, Imes S, Korbutt GS, Kneteman NM, et al. Successful islet transplantation: continued insulin reserve provides long-term glycemic control. Diabetes 2002 Jul;51(7):2148-2157.

26. Goss JA, Schock AP, Brunicardi FC, Goodpastor SE, Garber AJ, Soltes G, et al. Achievement of insulin independence in three consecutive type-1 diabetic patients via pancreatic islet transplantation using islets isolated at a remote islet isolation center. Transplantation 2002 Dec 27;74(12):1761-1766.

27. Ricordi C. Islet transplantation: a brave new world. Diabetes 2003 Jul;52(7):1595-1603.

28. Shapiro AM, Ricordi C, Hering BJ, Auchincloss H, Lindblad R, Robertson RP, et al. International trial of the Edmonton protocol for islet transplantation. The New England journal of medicine 2006 Sep 28;355(13):1318-1330.

29. Bromberg JS, LeRoith D. Diabetes cure--is the glass half full? The New England journal of medicine 2006 Sep 28;355(13):1372-1374.

30. Poggioli R, Faradji RN, Ponte G, Betancourt A, Messinger S, Baidal DA, et al. Quality of life after islet transplantation. Am J Transplant 2006 Feb;6(2):371-378.

31. Gruessner AC, Sutherland DE. Pancreas transplant outcomes for United States (US) cases as reported to the United Network for Organ Sharing (UNOS) and the International Pancreas Transplant Registry (IPTR). Clinical transplants 2008:45-56.

32. White SA, Shaw JA, Sutherland DE. Pancreas transplantation. Lancet 2009 May 23;373(9677):1808-1817.

33. Fiorina P, Venturini M, Folli F, Losio C, Maffi P, Placidi C, et al. Natural history of kidney graft survival, hypertrophy, and vascular function in end-stage renal disease type 1 diabetic kidney-transplanted patients: beneficial impact of pancreas and successful islet cotransplantation. Diabetes care 2005 Jun;28(6):1303-1310.

34. Lee TC, Barshes NR, O'Mahony CA, Nguyen L, Brunicardi FC, Ricordi C, et al. The effect of pancreatic islet transplantation on progression of diabetic retinopathy and neuropathy. Transplantation proceedings 2005 Jun;37(5):2263-2265.

35. Fiorina P, Folli F, Zerbini G, Maffi P, Gremizzi C, Di Carlo V, et al. Islet transplantation is associated with improvement of renal function among uremic patients with type I diabetes mellitus and kidney transplants. J Am Soc Nephrol 2003 Aug;14(8):2150-2158.

36. Wiseman AC. Simultaneous pancreas kidney transplantation: a critical appraisal of the risks and benefits compared with other treatment alternatives. Advances in chronic kidney disease 2009 Jul;16(4):278-287.

37. Ryan EA, Paty BW, Senior PA, Bigam D, Alfadhli E, Kneteman NM, et al. Five-year follow-up after clinical islet transplantation. Diabetes 2005 Jul;54(7):2060-2069.
38. Leitao CB, Cure P, Tharavanij T, Baidal DA, Alejandro R. Current challenges in islet transplantation. Current diabetes reports 2008 Aug;8(4):324-331.

39. Ryan EA, Bigam D, Shapiro AM. Current indications for pancreas or islet transplant. Diabetes, obesity & metabolism 2006 Jan;8(1):1-7.

40. Babensee JE, McIntire LV, Anderson JM, Mikos AG. Host response to tissue engineered devices. Advanced drug delivery reviews 1998 Aug 3;33(1-2):111-139.

41. Robitaille R, Dusseault J, Henley N, Desbiens K, Labrecque N, Halle JP. Inflammatory response to peritoneal implantation of alginate-poly-L-lysine microcapsules. Biomaterials 2005 Jul;26(19):4119-4127.

42. Berney T, Molano RD, Cattan P, Pileggi A, Vizzardelli C, Oliver R, et al. Endotoxin-mediated delayed islet graft function is associated with increased intra-islet cytokine production and islet cell apoptosis. Transplantation 2001 Jan 15;71(1):125-132.

43. Matsuda T, Omori K, Vuong T, Pascual M, Valiente L, Ferreri K, et al. Inhibition of p38 pathway suppresses human islet production of pro-inflammatory cytokines and improves islet graft function. Am J Transplant 2005 Mar;5(3):484-493.

44. Ehrnfelt C, Kumagai-Braesch M, Uzunel M, Holgersson J. Adult porcine islets produce MCP-1 and recruit human monocytes in vitro. Xenotransplantation 2004 Mar;11(2):184-194.

45. Chen MC, Proost P, Gysemans C, Mathieu C, Eizirik DL. Monocyte chemoattractant protein-1 is expressed in pancreatic islets from prediabetic NOD mice and in interleukin-1 beta-exposed human and rat islet cells. Diabetologia 2001 Mar;44(3):325-332.

46. Thomas HE, Darwiche R, Corbett JA, Kay TW. Interleukin-1 plus gamma-interferon-induced pancreatic beta-cell dysfunction is mediated by beta-cell nitric oxide production. Diabetes 2002 Feb;51(2):311-316.

47. Johansson U, Olsson A, Gabrielsson S, Nilsson B, Korsgren O. Inflammatory mediators expressed in human islets of Langerhans: implications for islet transplantation. Biochemical and biophysical research communications 2003 Aug 29;308(3):474-479.

48. Anderson JM. Inflammatory response to implants. ASAIO transactions / American Society for Artificial Internal Organs 1988 Apr-Jun;34(2):101-107.

49. Di Matteo MA, Loweth AC, Thomas S, Mabley JG, Morgan NG, Thorpe JR, et al. Superoxide, nitric oxide, peroxynitrite and cytokine combinations all cause functional impairment and morphological changes in rat islets of Langerhans and insulin secreting cell lines, but dictate cell death by different mechanisms. Apoptosis 1997;2(2):164-177.

50. Rabinovitch A, Suarez-Pinzon WL. Cytokines and their roles in pancreatic islet beta-cell destruction and insulin-dependent diabetes mellitus. Biochemical pharmacology 1998 Apr 15;55(8):1139-1149.

51. Jang JY, Lee DY, Park SJ, Byun Y. Immune reactions of lymphocytes and macrophages against PEG-grafted pancreatic islets. Biomaterials 2004 Aug;25(17):3663-3669.

52. Yoon JW, Jun HS, Santamaria P. Cellular and molecular mechanisms for the initiation and progression of beta cell destruction resulting from the collaboration between macrophages and T cells. Autoimmunity 1998;27(2):109-122.

53. Wiegand F, Kroncke KD, Kolb-Bachofen V. Macrophage-generated nitric oxide as cytotoxic factor in destruction of alginate-encapsulated islets. Protection by arginine analogs and/or coencapsulated erythrocytes. Transplantation 1993 Nov;56(5):1206-1212.

54. Gill RG. Antigen presentation pathways for immunity to islet transplants. Relevance to immunoisolation. Annals of the New York Academy of Sciences 1999 Jun 18;875:255-260.

55. Gray DW. Encapsulated islet cells: the role of direct and indirect presentation and the relevance to xenotransplantation and autoimmune recurrence. British medical bulletin 1997;53(4):777-788.

56. Wang Y, Pontesilli O, Gill RG, La Rosa FG, Lafferty KJ. The role of CD4+ and CD8+ T cells in the destruction of islet grafts by spontaneously diabetic mice. Proceedings of the National Academy of Sciences of the United States of America 1991 Jan 15;88(2):527-531.

57. Fulton B, Markham A. Mycophenolate mofetil. A review of its pharmacodynamic and pharmacokinetic properties and clinical efficacy in renal transplantation. Drugs 1996 Feb;51(2):278-298.

58. Klintmalm GB, Goldstein R, Gonwa T, Wiesner RH, Krom RA, Shaw BW, Jr., et al. Prognostic factors for successful conversion from cyclosporine to FK 506-based immunosuppressive therapy for refractory rejection after liver transplantation. US

Multicenter FK 506 Liver Study Group. Transplantation proceedings 1993 Feb;25(1 Pt 1):641-643.

59. Faulds D, Goa KL, Benfield P. Cyclosporin. A review of its pharmacodynamic and pharmacokinetic properties, and therapeutic use in immunoregulatory disorders. Drugs 1993 Jun;45(6):953-1040.

60. Stegall MD, Simon M, Wachs ME, Chan L, Nolan C, Kam I. Mycophenolate mofetil decreases rejection in simultaneous pancreas-kidney transplantation when combined with tacrolimus or cyclosporine. Transplantation 1997 Dec 27;64(12):1695-1700.

61. Cantarovich D, Vistoli F. Minimization protocols in pancreas transplantation. Transpl Int 2009 Jan;22(1):61-68.

62. Algire GH. An adaption of the transparant chamber technique to the mouse. Journal of the National Cancer Institute 1943;4:1-11.

63. Chick WL, Like AA, Lauris V. Beta cell culture on synthetic capillaries: an artificial endocrine pancreas. Science (New York, NY 1975 Mar 7;187(4179):847-849.

64. Lim F, Sun AM. Microencapsulated islets as bioartificial endocrine pancreas. Science (New York, NY 1980 Nov 21;210(4472):908-910.

65. de Vos P, Spasojevic M, Faas MM. Treatment of diabetes with encapsulated islets. Advances in experimental medicine and biology 2010;670:38-53.

66. de Vos P, Marchetti P. Encapsulation of pancreatic islets for transplantation in diabetes: the untouchable islets. Trends Mol Med 2002 Aug;8(8):363-366.

67. Sun AM, Parisius W, Healy GM, Vacek I, Macmorine HG. The use, in diabetic rats and monkeys, of artificial capillary units containing cultured islets of Langerhans (artificial endocrine pancreas). Diabetes 1977 Dec;26(12):1136-1139.

68. Maki T, Lodge JP, Carretta M, Ohzato H, Borland KM, Sullivan SJ, et al. Treatment of severe diabetes mellitus for more than one year using a vascularized hybrid artificial pancreas. Transplantation 1993 Apr;55(4):713-717; discussion 717-718.

69. Beck J, Angus R, Madsen B, Britt D, Vernon B, Nguyen KT. Islet encapsulation: strategies to enhance islet cell functions. Tissue Eng 2007 Mar;13(3):589-599.

70. Wilson JT, Chaikof EL. Challenges and emerging technologies in the immunoisolation of cells and tissues. Advanced drug delivery reviews 2008 Jan 14;60(2):124-145.

71. de Vos P, Hamel AF, Tatarkiewicz K. Considerations for successful transplantation of encapsulated pancreatic islets. Diabetologia 2002 Feb;45(2):159-173.

72. Vandenbossche GM, Bracke ME, Cuvelier CA, Bortier HE, Mareel MM, Remon JP. Host reaction against empty alginate-polylysine microcapsules. Influence of preparation procedure. The Journal of pharmacy and pharmacology 1993 Feb;45(2):115-120.

73. Weber C, Ayres-Price J, Costanzo M, Becker A, Stall A. NOD mouse peritoneal cellular response to poly-L-lysine-alginate microencapsulated rat islets. Transplantation proceedings 1994 Jun;26(3):1116-1119.

74. Trivedi N, Keegan M, Steil GM, Hollister-Lock J, Hasenkamp WM, Colton CK, et al. Islets in alginate macrobeads reverse diabetes despite minimal acute insulin secretory responses. Transplantation 2001 Jan 27;71(2):203-211.

75. Soon-Shiong P, Feldman E, Nelson R, Heintz R, Yao Q, Yao Z, et al. Long-term reversal of diabetes by the injection of immunoprotected islets. Proceedings of the National Academy of Sciences of the United States of America 1993 Jun 15;90(12):5843-5847.

76. Sun Y, Ma X, Zhou D, Vacek I, Sun AM. Normalization of diabetes in spontaneously diabetic cynomologus monkeys by xenografts of microencapsulated porcine islets without immunosuppression. The Journal of clinical investigation 1996 Sep 15;98(6):1417-1422.

77. Leu FJ, Chen CF, Chiang WE, Chern HT, Shian LR, Chung TM, et al. Microencapsulated pancreatic islets: a pathologic study. Journal of the Formosan Medical Association = Taiwan yi zhi 1992 Sep;91(9):849-858.

78. O'Shea GM, Goosen MF, Sun AM. Prolonged survival of transplanted islets of Langerhans encapsulated in a biocompatible membrane. Biochimica et biophysica acta 1984 May 22;804(1):133-136.

79. Strand BL, Ryan TL, In't Veld P, Kulseng B, Rokstad AM, Skjak-Brek G, et al. Poly-L-Lysine induces fibrosis on alginate microcapsules via the induction of cytokines. Cell transplantation 2001;10(3):263-275.

80. Mallett AG, Korbutt GS. Alginate modification improves long-term survival and function of transplanted encapsulated islets. Tissue engineering 2009 Jun;15(6):1301-1309.

81. Langlois G, Dusseault J, Bilodeau S, Tam SK, Magassouba D, Halle JP. Direct effect of alginate purification on the survival of islets immobilized in alginate-based microcapsules. Acta biomaterialia 2009 Nov;5(9):3433-3440.

82. Hill RS, Cruise GM, Hager SR, Lamberti FV, Yu X, Garufis CL, et al. Immunoisolation of adult porcine islets for the treatment of diabetes mellitus. The use of photopolymerizable polyethylene glycol in the conformal coating of mass-isolated porcine islets. Annals of the New York Academy of Sciences 1997 Dec 31;831:332-343.

83. Cruise GM, Hegre OD, Lamberti FV, Hager SR, Hill R, Scharp DS, et al. In vitro and in vivo performance of porcine islets encapsulated in interfacially photopolymerized poly(ethylene glycol) diacrylate membranes. Cell transplantation 1999 May-Jun;8(3):293-306.

84. Cruise GM, Hegre OD, Scharp DS, Hubbell JA. A sensitivity study of the key parameters in the interfacial photopolymerization of poly(ethylene glycol) diacrylate upon porcine islets. Biotechnology and bioengineering 1998 Mar 20;57(6):655-665.

85. Cruise GM, Scharp DS, Hubbell JA. Characterization of permeability and network structure of interfacially photopolymerized poly(ethylene glycol) diacrylate hydrogels. Biomaterials 1998 Jul;19(14):1287-1294.

86. Thrash M. Modeling oxygen transport in a cylindrical bioartificial pancreas. Asaio J 2010 Jul-Aug;56(4):338-343.

87. Dufrane D, Goebbels RM, Gianello P. Alginate Macroencapsulation of Pig Islets Allows Correction of Streptozotocin-Induced Diabetes in Primates up to 6 Months Without Immunosuppression. Transplantation Oct 22.

88. Grundfest-Broniatowski SF, Tellioglu G, Rosenthal KS, Kang J, Erdodi G, Yalcin B, et al. A new bioartificial pancreas utilizing amphiphilic membranes for the immunoisolation of porcine islets: a pilot study in the canine. ASAIO J 2009 Jul-Aug;55(4):400-405.

89. Qi M, Gu Y, Sakata N, Kim D, Shirouzu Y, Yamamoto C, et al. PVA hydrogel sheet macroencapsulation for the bioartificial pancreas. Biomaterials 2004 Dec;25(27):5885-5892.

90. Weber LM, Anseth KS. Hydrogel encapsulation environments functionalized with extracellular matrix interactions increase islet insulin secretion. Matrix Biol 2008 Oct;27(8):667-673.

91. Weber LM, Hayda KN, Haskins K, Anseth KS. The effects of cell-matrix interactions on encapsulated beta-cell function within hydrogels functionalized with matrix-derived adhesive peptides. Biomaterials 2007 Jul;28(19):3004-3011.

92. Weber LM, Hayda KN, Anseth KS. Cell-matrix interactions improve beta-cell survival and insulin secretion in three-dimensional culture. Tissue engineering 2008 Dec;14(12):1959-1968.

93. Weber LM, Cheung CY, Anseth KS. Multifunctional pancreatic islet encapsulation barriers achieved via multilayer PEG hydrogels. Cell transplantation 2008;16(10):1049-1057.

94. Lin CC, Anseth KS. Glucagon-Like Peptide-1 Functionalized PEG Hydrogels Promote Survival and Function of Encapsulated Pancreatic beta-Cells. Biomacromolecules 2009 Sep;10(9):2460-2467.

95. Hume PS. Polymerizable superoxide dismutase mimetic protects β-cells encapsulated in PEG hydrogels from reactive oxygen species-mediated damage. Tissue engineering 2011.

96. Lin CC. Cell-cell communication mimicry with PEG hydrogels for enhancing Beta-cell function. Proc Natl Acad Sci USA 2010 2010.

97. Bryant SJ, Nuttelman CR, Anseth KS. Cytocompatibility of UV and visible light photoinitiating systems on cultured NIH/3T3 fibroblasts in vitro. J Biomater Sci Polym Ed 2000;11(5):439-457.

98. Lin CC, Metters AT, Anseth KS. Functional PEG-peptide hydrogels to modulate local inflammation induced by the pro-inflammatory cytokine TNFalpha. Biomaterials 2009 Oct;30(28):4907-4914.

99. Sun LT, Bencherif SA, Gilbert TW, Farkas AM, Lotze MT, Washburn NR. Biological activities of cytokine-neutralizing hyaluronic acid-antibody conjugates. Wound Repair Regen May-Jun;18(3):302-310.

100. Lin CC, Boyer PD, Aimetti AA, Anseth KS. Regulating MCP-1 diffusion in affinity hydrogels for enhancing immuno-isolation. J Control Release 2010 Mar 19;142(3):384-391.

101. Chae SY, Lee M, Kim SW, Bae YH. Protection of insulin secreting cells from nitric oxide induced cellular damage by crosslinked hemoglobin. Biomaterials 2004 Feb;25(5):843-850.

102. Cheung CY, McCartney SJ, Anseth K. Synthesis of Polymerizable Superoxide Dismutase Mimetics to Reduce Reactive Oxygen Species Damage in Transplanted Biomedical Devices. Advanced Functional Materials 2008;18:3119-3126.

103. Bunger CM, Tiefenbach B, Jahnke A, Gerlach C, Freier T, Schmitz KP, et al. Deletion of the tissue response against alginate-pll capsules by temporary release of co-encapsulated steroids. Biomaterials 2005 May;26(15):2353-2360.

104. Giovagnoli S, Blasi P, Luca G, Fallarino F, Calvitti M, Mancuso F, et al. Bioactive long-term release from biodegradable microspheres preserves implanted ALG-PLO-ALG microcapsules from in vivo response to purified alginate. Pharmaceutical research 2010 Feb;27(2):285-295.

105. Baruch L, Benny O, Gilert A, Ukobnik M, Ben Itzhak O, Machluf M. Alginate-PLL cell encapsulation system Co-entrapping PLGA-microspheres for the continuous release of anti-inflammatory drugs. Biomedical microdevices 2009 Jun 11.

106. Yu DG, Branford-White C, Shen XX, Zhang XF, Zhu LM. Solid Dispersions of Ketoprofen in Drug-Loaded Electrospun Nanofibers. J Dispersion Sci Technol 2010;31(7):902-908.

107. Yu DG, Branford-White C, White K, Li XL, Zhu LM. Dissolution Improvement of Electrospun Nanofiber-Based Solid Dispersions for Acetaminophen. AAPS PharmSciTech Jun;11(2):809-817.

108. Aimetti AA, Tibbitt MW, Anseth KS. Human neutrophil elastase responsive delivery from poly(ethylene glycol) hydrogels. Biomacromolecules 2009 Jun 8;10(6):1484-1489.

109. Takeda Y, Gotoh M, Dono K, Nishihara M, Grochowiecki T, Kimura F, et al. Protection of islet allografts transplanted together with Fas ligand expressing testicular allografts. Diabetologia 1998 Mar;41(3):315-321.

110. Korbutt GS, Elliott JF, Rajotte RV. Cotransplantation of allogeneic islets with allogeneic testicular cell aggregates allows long-term graft survival without systemic immunosuppression. Diabetes 1997 Feb;46(2):317-322.

111. Dufour JM, Rajotte RV, Kin T, Korbutt GS. Immunoprotection of rat islet xenografts by cotransplantation with sertoli cells and a single injection of antilymphocyte serum. Transplantation 2003 May 15;75(9):1594-1596.

112. Valdes-Gonzalez RA, Dorantes LM, Garibay GN, Bracho-Blanchet E, Mendez AJ, Davila-Perez R, et al. Xenotransplantation of porcine neonatal islets of Langerhans and Sertoli cells: a 4-year study. Eur J Endocrinol 2005 Sep;153(3):419-427.

113. Dufour JM, Rajotte RV, Korbutt GS, Emerich DF. Harnessing the immunomodulatory properties of Sertoli cells to enable xenotransplantation in type I diabetes. Immunol Invest 2003 Nov;32(4):275-297.

114. Suarez-Pinzon W, Korbutt GS, Power R, Hooton J, Rajotte RV, Rabinovitch A. Testicular sertoli cells protect islet beta-cells from autoimmune destruction in NOD mice by a transforming growth factor-beta1-dependent mechanism. Diabetes 2000 Nov;49(11):1810-1818.

115. Abdi R, Fiorina P, Adra CN, Atkinson M, Sayegh MH. Immunomodulation by mesenchymal stem cells: a potential therapeutic strategy for type 1 diabetes. Diabetes 2008 Jul;57(7):1759-1767.

116. Le Blanc K, Tammik L, Sundberg B, Haynesworth SE, Ringden O. Mesenchymal stem cells inhibit and stimulate mixed lymphocyte cultures and mitogenic responses independently of the major histocompatibility complex. Scand J Immunol 2003 Jan;57(1):11-20.

117. Tyndall A, Walker UA, Cope A, Dazzi F, De Bari C, Fibbe W, et al. Immunomodulatory properties of mesenchymal stem cells: a review based on an interdisciplinary meeting held at the Kennedy Institute of Rheumatology Division, London, UK, 31 October 2005. Arthritis Res Ther 2007;9(1):301.

118. Tibbitt MW, Anseth KS. Hydrogels as extracellular matrix mimics for 3D cell culture. Biotechnology and bioengineering 2009 Jul 1;103(4):655-663.

119. Ito Y. Surface micropatterning to regulate cell functions. Biomaterials 1999 Dec;20(23-24):2333-2342.

120. Lynn AD, Kyriakides TR, Bryant SJ. Characterization of the in vitro macrophage response and in vivo host response to poly(ethylene glycol)-based hydrogels. Journal of biomedical materials research 2010 Jun 1;93(3):941-953.

121. Kou PM, Babensee JE. Macrophage and dendritic cell phenotypic diversity in the context of biomaterials. Journal of biomedical materials research 2010 Jan;96(1):239-260.

122. Babensee JE. Interaction of dendritic cells with biomaterials. Seminars in immunology 2008 Apr;20(2):101-108.

123. Acharya AP, Dolgova NV, Moore NM, Xia CQ, Clare-Salzler MJ, Becker ML, et al. The modulation of dendritic cell integrin binding and activation by RGD-peptide density gradient substrates. Biomaterials 2011 Oct;31(29):7444-7454.

124. Cheung CY, Anseth KS. Synthesis of immunoisolation barriers that provide localized immunosuppression for encapsulated pancreatic islets. Bioconjug Chem 2006 Jul-Aug;17(4):1036-1042.

125. Leclerc C, Brose C, Nouze C, Leonard F, Majlessi L, Becker S, et al. Immobilized cytokines as biomaterials for manufacturing immune cell based vaccines. Journal of biomedical materials research 2008 Sep 15;86(4):1033-1040.

8.2 Chapter 2 references

1. Cheung CY, McCartney SJ, Anseth K. Synthesis of Polymerizable Superoxide Dismutase Mimetics to Reduce Reactive Oxygen Species Damage in Transplanted Biomedical Devices. Advanced Functional Materials 2008;18:3119-3126.

2. Sebra RP, Masters KS, Bowman CN, Anseth KS. Surface grafted antibodies: controlled architecture permits enhanced antigen detection. Langmuir 2005 Nov 22;21(24):10907-10911.

3. Sebra RP, Masters KS, Cheung CY, Bowman CN, Anseth KS. Detection of antigens in biologically complex fluids with photografted whole antibodies. Anal Chem 2006 May 1;78(9):3144-3151.

4. Johnson LM, Fairbanks BD, Anseth KS, Bowman CN. Enzyme-mediated redox initiation for hydrogel generation and cellular encapsulation. Biomacromolecules 2009 Nov 9;10(11):3114-3121.

5. Johnson LM, Deforest CA, Pendurti A, Anseth KS, Bowman CN. Formation of three-dimensional hydrogel multilayers using enzyme-mediated redox chain initiation. ACS applied materials & interfaces 2010 Jul;2(7):1963-1972.

8.3 Chapter 3 references

1. Kelly WD, Lillehei RC, Merkel FK, Idezuki Y, Goetz FC. Allotransplantation of the pancreas and duodenum along with the kidney in diabetic nephropathy. Surgery 1967 Jun;61(6):827-837.

2. Scharp DW, Lacy PE, Santiago JV, McCullough CS, Weide LG, Falqui L, et al. Insulin independence after islet transplantation into type I diabetic patient. Diabetes 1990 Apr;39(4):515-518.

3. Shapiro AM, Lakey JR, Ryan EA, Korbutt GS, Toth E, Warnock GL, et al. Islet transplantation in seven patients with type 1 diabetes mellitus using a glucocorticoid-free immunosuppressive regimen. The New England journal of medicine 2000 Jul 27;343(4):230-238.

4. Pavlakis M, Khwaja K. Pancreas and islet cell transplantation in diabetes. Current opinion in endocrinology, diabetes, and obesity 2007 Apr;14(2):146-150.

5. White SA, Shaw JA, Sutherland DE. Pancreas transplantation. Lancet 2009 May 23;373(9677):1808-1817.

6. Gremizzi C, Vergani A, Paloschi V, Secchi A. Impact of pancreas transplantation on type 1 diabetes-related complications. Current opinion in organ transplantation 2010 Feb;15(1):119-123.

7. Tyden G, Reinholt FP, Sundkvist G, Bolinder J. Recurrence of autoimmune diabetes mellitus in recipients of cadaveric pancreatic grafts. The New England journal of medicine 1996 Sep 19;335(12):860-863.

8. Bertuzzi F, Ricordi C. Beta-cell replacement in immunosuppressed recipients: old and new clinical indications. Acta diabetologica 2007 Dec;44(4):171-176.

9. Ryan EA, Bigam D, Shapiro AM. Current indications for pancreas or islet transplant. Diabetes, obesity & metabolism 2006 Jan;8(1):1-7.

10. Chick WL, Like AA, Lauris V. Beta cell culture on synthetic capillaries: an artificial endocrine pancreas. Science (New York, NY 1975 Mar 7;187(4179):847-849.

11. Wilson JT, Chaikof EL. Challenges and emerging technologies in the immunoisolation of cells and tissues. Advanced drug delivery reviews 2008 Jan 14;60(2):124-145.

12. de Vos P, Hamel AF, Tatarkiewicz K. Considerations for successful transplantation of encapsulated pancreatic islets. Diabetologia 2002 Feb;45(2):159-173.

13. Cui H, Tucker-Burden C, Cauffiel SM, Barry AK, Iwakoshi NN, Weber CJ, et al. Long-term metabolic control of autoimmune diabetes in spontaneously diabetic nonobese diabetic mice by nonvascularized microencapsulated adult porcine islets. Transplantation 2009 Jul 27;88(2):160-169.

14. Cruise GM, Hegre OD, Lamberti FV, Hager SR, Hill R, Scharp DS, et al. In vitro and in vivo performance of porcine islets encapsulated in interfacially photopolymerized poly(ethylene glycol) diacrylate membranes. Cell transplantation 1999 May-Jun;8(3):293-306.

15. Weber LM, Hayda KN, Anseth KS. Cell-matrix interactions improve beta-cell survival and insulin secretion in three-dimensional culture. Tissue engineering 2008 Dec;14(12):1959-1968.

16. Weber LM, Anseth KS. Hydrogel encapsulation environments functionalized with extracellular matrix interactions increase islet insulin secretion. Matrix Biol 2008 Oct;27(8):667-673.

17. Lin CC, Anseth KS. Glucagon-Like Peptide-1 Functionalized PEG Hydrogels Promote Survival and Function of Encapsulated Pancreatic beta-Cells. Biomacromolecules 2009 Sep;10(9):2460-2467.

18. Jang JY, Lee DY, Park SJ, Byun Y. Immune reactions of lymphocytes and macrophages against PEG-grafted pancreatic islets. Biomaterials 2004 Aug;25(17):3663-3669.

19. de Vos P, Marchetti P. Encapsulation of pancreatic islets for transplantation in diabetes: the untouchable islets. Trends Mol Med 2002 Aug;8(8):363-366.

20. Mohseni Salehi Monfared SS, Larijani B, Abdollahi M. Islet transplantation and antioxidant management: a comprehensive review. World J Gastroenterol 2009 Mar 14;15(10):1153-1161.

21. Hadjivassiliou V, Green MH, James RF, Swift SM, Clayton HA, Green IC. Insulin secretion, DNA damage, and apoptosis in human and rat islets of Langerhans following exposure to nitric oxide, peroxynitrite, and cytokines. Nitric Oxide 1998;2(6):429-441.

22. Di Matteo MA, Loweth AC, Thomas S, Mabley JG, Morgan NG, Thorpe JR, et al. Superoxide, nitric oxide, peroxynitrite and cytokine combinations all cause functional impairment and morphological changes in rat islets of Langerhans and insulin secreting cell lines, but dictate cell death by different mechanisms. Apoptosis 1997;2(2):164-177.

23. Delaney CA, Tyrberg B, Bouwens L, Vaghef H, Hellman B, Eizirik DL. Sensitivity of human pancreatic islets to peroxynitrite-induced cell dysfunction and death. FEBS letters 1996 Oct 7;394(3):300-306.

24. Muscoli C, Cuzzocrea S, Riley DP, Zweier JL, Thiemermann C, Wang ZQ, et al. On the selectivity of superoxide dismutase mimetics and its importance in pharmacological studies. British journal of pharmacology 2003 Oct;140(3):445-460.

25. Weringer EJ, Like AA. Diabetes mellitus in the BB/W rat. Insulitis in pancreatic islet grafts after transplantation in diabetic recipients. The American journal of pathology 1986 Oct;125(1):107-112.

26. Yoon JW, Jun HS, Santamaria P. Cellular and molecular mechanisms for the initiation and progression of beta cell destruction resulting from the collaboration between macrophages and T cells. Autoimmunity 1998;27(2):109-122.

27. Haskins K, Bradley B, Powers K, Fadok V, Flores S, Ling X, et al. Oxidative stress in type 1 diabetes. Annals of the New York Academy of Sciences 2003 Nov;1005:43-54.

28. Lenzen S, Drinkgern J, Tiedge M. Low antioxidant enzyme gene expression in pancreatic islets compared with various other mouse tissues. Free radical biology & medicine 1996;20(3):463-466.

29. Ho E, Bray TM. Antioxidants, NFkappaB activation, and diabetogenesis. Proceedings of the Society for Experimental Biology and Medicine Society for Experimental Biology and Medicine (New York, NY 1999 Dec;222(3):205-213.

30. Tyrberg B, Eizirik DL, Marklund SL, Olejnicka B, Madsen OD, Andersson A. Human islets in mixed islet grafts protect mouse pancreatic beta-cells from alloxan toxicity. Pharmacology & toxicology 1999 Dec;85(6):269-275.

31. Grankvist K, Marklund S, Taljedal IB. Superoxide dismutase is a prophylactic against alloxan diabetes. Nature 1981 Nov 12;294(5837):158-160.

32. Piganelli JD, Flores SC, Cruz C, Koepp J, Batinic-Haberle I, Crapo J, et al. A metalloporphyrin-based superoxide dismutase mimic inhibits adoptive transfer of autoimmune diabetes by a diabetogenic T-cell clone. Diabetes 2002 Feb;51(2):347-355.

33. Nomikos IN, Wang Y, Lafferty KJ. Involvement of O2 radicals in 'autoimmune' diabetes. Immunology and cell biology 1989 Feb;67 (Pt 1):85-87.

34. Salvemini D, Riley DP, Cuzzocrea S. SOD mimetics are coming of age. Nature reviews 2002 May;1(5):367-374.

35. Pasternack RF, Banth A, Pasternack JM, Johnson CS. Catalysis of the disproportionation of superoxide by metalloporphyrins. III. Journal of inorganic biochemistry 1981 Nov;15(3):261-267.

36. Benov L, Batinic-Haberle I. A manganese porphyrin suppresses oxidative stress and extends the life span of streptozotocin-diabetic rats. Free radical research 2005 Jan;39(1):81-88.

37. Szabo C, Day BJ, Salzman AL. Evaluation of the relative contribution of nitric oxide and peroxynitrite to the suppression of mitochondrial respiration in immunostimulated macrophages using a manganese mesoporphyrin superoxide dismutase mimetic and peroxynitrite scavenger. FEBS letters 1996 Feb 26;381(1-2):82-86.

38. Day BJ, Fridovich I, Crapo JD. Manganic porphyrins possess catalase activity and protect endothelial cells against hydrogen peroxide-mediated injury. Archives of biochemistry and biophysics 1997 Nov 15;347(2):256-262.

39. Nakaoka R, Tabata Y, Yamaoka T, Ikada Y. Prolongation of the serum half-life period of superoxide dismutase by poly(ethylene glycol) modification. J Control Release 1997 Jun;46(3):253-261.

40. Kojima Y, Akaike T, Sato K, Maeda H, Hirano T. Polymer conjugation to Cu,Zn-SOD and suppression of hydroxyl radical generation on exposure to H2O2: Improved stability of SOD in vitro and in vivo. J Bioact Compat Polym 1996 Jul;11(3):169-190.

41. Li Z, Wang F, Roy S, Sen CK, Guan J. Injectable, highly flexible, and thermosensitive hydrogels capable of delivering superoxide dismutase. Biomacromolecules 2009 Dec 14;10(12):3306-3316.

42. Chiumiento A, Dominguez A, Lamponi S, Villalonga R, Barbucci R. Anti-inflammatory properties of superoxide dismutase modified with carboxymetil-cellulose polymer and hydrogel. Journal of materials science 2006 May;17(5):427-435.

43. Chiumiento A, Lamponi S, Barbucci R, Dominguez A, Perez Y, Villalonga R. Immobilizing Cu,Zn-superoxide dismutase in hydrogels of carboxymethylcellulose improves its stability and wound healing properties. Biochemistry (Mosc) 2006 Dec;71(12):1324-1328.

44. Cheung CY, McCartney SJ, Anseth KS. Synthesis of Polymerizable Superoxide Dismutase Mimetics to Reduce Reactive Oxygen Species Damage in Transplanted Biomedical Devices. Advanced Functional Materials 2008 Oct;18(20):3119-3126.

45. McCord JM, Fridovich I. Superoxide dismutase. An enzymic function for erythrocuprein (hemocuprein). J Biol Chem 1969 Nov 25;244(22):6049-6055.

46. Cohen HJ, Chovaniec ME. Superoxide generation by digitonin-stimulated guinea pig granulocytes. A basis for a continuous assay for monitoring superoxide production and for the study of the activation of the generating system. The Journal of clinical investigation 1978 Apr;61(4):1081-1087.

47. Choi SY, Ha H, Kim KT. Capsaicin inhibits platelet-activating factor-induced cytosolic Ca2+ rise and superoxide production. J Immunol 2000 Oct 1;165(7):3992-3998.

48. Cruise GM, Scharp DS, Hubbell JA. Characterization of permeability and network structure of interfacially photopolymerized poly(ethylene glycol) diacrylate hydrogels. Biomaterials 1998 Jul;19(14):1287-1294.

49. Lin CC, Boyer PD, Aimetti AA, Anseth KS. Regulating MCP-1 diffusion in affinity hydrogels for enhancing immuno-isolation. J Control Release 2010 Mar 19;142(3):384-391.

50. Su J, Hu BH, Lowe WL, Jr., Kaufman DB, Messersmith PB. Anti-inflammatory peptide-functionalized hydrogels for insulin-secreting cell encapsulation. Biomaterials Jan;31(2):308-314.

51. Weber LM, Hayda KN, Haskins K, Anseth KS. The effects of cell-matrix interactions on encapsulated beta-cell function within hydrogels functionalized with matrix-derived adhesive peptides. Biomaterials 2007 Jul;28(19):3004-3011.

52. Gabler WL, Creamer HR, Bullock WW. Modulation of the kinetics of induced neutrophil superoxide generation by fluoride. Journal of dental research 1986 Sep;65(9):1159-1165.

53. Luther MJ, Davies E, Muller D, Harrison M, Bone AJ, Persaud SJ, et al. Cell-to-cell contact influences proliferative marker expression and apoptosis in MIN6 cells grown in islet-like structures. American journal of physiology 2005 Mar;288(3):E502-509.

54. Hauge-Evans AC, Squires PE, Persaud SJ, Jones PM. Pancreatic beta-cell-to-beta-cell interactions are required for integrated responses to nutrient stimuli: enhanced Ca2+ and insulin secretory responses of MIN6 pseudoislets. Diabetes 1999 Jul;48(7):1402-1408.

55. Konstantinova I, Nikolova G, Ohara-Imaizumi M, Meda P, Kucera T, Zarbalis K, et al. EphA-Ephrin-A-mediated beta cell communication regulates insulin secretion from pancreatic islets. Cell 2007 Apr 20;129(2):359-370.

56. Lin CC. Cell-cell communication mimicry with PEG hydrogels for enhancing Beta-cell function. Proc Natl Acad Sci USA 2010 2010.

57. Kavdia M, Lewis RS. Free radical profiles in an encapsulated pancreatic cell matrix model. Annals of biomedical engineering 2002 May;30(5):721-730.
58. Uchiyama T, Kiritoshi Y, Watanabe J, Ishihara K. Degradation of phospholipid polymer hydrogel by hydrogen peroxide aiming at insulin release device. Biomaterials 2003 Dec;24(28):5183-5190.

59. Lin CC, Metters AT, Anseth KS. Functional PEG-peptide hydrogels to modulate local inflammation induced by the pro-inflammatory cytokine TNFalpha. Biomaterials 2009 Oct;30(28):4907-4914.

60. Cheung CY, Anseth KS. Synthesis of immunoisolation barriers that provide localized immunosuppression for encapsulated pancreatic islets. Bioconjug Chem 2006 Jul-Aug;17(4):1036-1042.

61. Hume PS, Anseth KS. Inducing local T cell apoptosis with anti-Fas-functionalized polymeric coatings fabricated via surface-initiated photopolymerizations. Biomaterials 2010 Apr;31(12):3166-3174.

8.4 Chapter 4 references

1. Wollert KC, Drexler H. Cell-based therapy for heart failure. Curr Opin Cardiol 2006;21(3):234-239.

2. Emerich DF, Winn SR. Immunoisolation cell therapy for CNS diseases. Crit Rev Ther Drug Carrier Syst 2001;18(3):265-298.

3. Lee MK, Bae YH. Cell transplantation for endocrine disorders. Adv Drug Deliv Rev 2000;42(1-2):103-120.

4. Wilson JT, Chaikof EL. Challenges and emerging technologies in the immunoisolation of cells and tissues. Adv Drug Deliv Rev 2008;60(2):124-145.

5. Lim F, Sun AM. Microencapsulated islets as bioartificial endocrine pancreas. Science 1980;210(4472):908-910.

6. Kabelitz D, Geissler EK, Soria B, Schroeder IS, Fandrich F, Chatenoud L. Toward cell-based therapy of type I diabetes. Trends Immunol 2008;29(2):68-74.

7. de Vos P, Marchetti P. Encapsulation of pancreatic islets for transplantation in diabetes: the untouchable islets. Trends Mol Med 2002;8(8):363-366.

8. Mandrup-Poulsen T, Zumsteg U, Reimers J, Pociot F, Morch L, Helqvist S, et al. Involvement of interleukin 1 and interleukin 1 antagonist in pancreatic beta-cell destruction in insulin-dependent diabetes mellitus. Cytokine 1993;5(3):185-191.

9. Jang JY, Lee DY, Park SJ, Byun Y. Immune reactions of lymphocytes and macrophages against PEG-grafted pancreatic islets. Biomaterials 2004;25(17):3663-3669.

10. Lee DY, Park SJ, Lee S, Nam JH, Byun Y. Highly poly(ethylene) glycolylated islets improve long-term islet allograft survival without immunosuppressive medication. Tissue Eng 2007;13(8):2133-2141.

11. Cui H, Tucker-Burden C, Cauffiel SM, Barry AK, Iwakoshi NN, Weber CJ, et al. Long-term metabolic control of autoimmune diabetes in spontaneously diabetic nonobese diabetic mice by nonvascularized microencapsulated adult porcine islets. Transplantation 2009;88(2):160-169.

12. Yun Lee D, Hee Nam J, Byun Y. Functional and histological evaluation of transplanted pancreatic islets immunoprotected by PEGylation and cyclosporine for 1 year. Biomaterials 2007;28(11):1957-1966.

13. Cheung CY, McCartney SJ, Anseth K. Synthesis of Polymerizable Superoxide Dismutase Mimetics to Reduce Reactive Oxygen Species Damage in Transplanted Biomedical Devices. Adv Funct Mater 2008;18:3119-3126.

14. Leung A, Lawrie G, Nielsen LK, Trau M. Synthesis and characterization of alginate/poly-L-ornithine/alginate microcapsules for local immunosuppression. J Microencapsul 2008;25(6):387-398.

15. Lin CC, Metters AT, Anseth KS. Functional PEG-peptide hydrogels to modulate local inflammation induced by the pro-inflammatory cytokine TNFalpha. Biomaterials 2009;30(28):4907-4914.

16. Cheung CY, Anseth KS. Synthesis of immunoisolation barriers that provide localized immunosuppression for encapsulated pancreatic islets. Bioconjug Chem 2006;17(4):1036-1042.

17. Palmer E. Negative selection--clearing out the bad apples from the T-cell repertoire. Nat Rev Immunol 2003;3(5):383-391.

18. Nagata S, Golstein P. The Fas death factor. Science 1995;267(5203):1449-1456.

19. Siegel RM, Frederiksen JK, Zacharias DA, Chan FK, Johnson M, Lynch D, et al. Fas preassociation required for apoptosis signaling and dominant inhibition by pathogenic mutations. Science 2000;288(5475):2354-2357.

20. Holler N, Tardivel A, Kovacsovics-Bankowski M, Hertig S, Gaide O, Martinon F, et al. Two adjacent trimeric Fas ligands are required for Fas signaling and formation of a death-inducing signaling complex. Mol Cell Biol 2003;23(4):1428-1440.

21. Cifone MG, De Maria R, Roncaioli P, Rippo MR, Azuma M, Lanier LL, et al. Apoptotic signaling through CD95 (Fas/Apo-1) activates an acidic sphingomyelinase. J Exp Med 1994;180(4):1547-1552.

22. Moreno JB, Margraf S, Schuller AM, Simon A, Moritz A, Scholz M. Inhibition of neutrophil activity in cardiac surgery with cardiopulmonary bypass: a novel strategy with the leukocyte inhibition module. Perfusion 2004;19(1):11-16.

23. Scholz M, Simon A, Berg M, Schuller AM, Hacibayramoglu M, Margraf S, et al. In vivo inhibition of neutrophil activity by a FAS (CD95) stimulating module: arterial in-line application in a porcine cardiac surgery model. J Thorac Cardiovasc Surg 2004;127(6):1735-1742.

24. Otsu T. Iniferter concept and living radical polymerization. J Polym Sci Pol Chem 2000;38(12):2121-2136.

25. Sebra RP, Masters KS, Bowman CN, Anseth KS. Surface grafted antibodies: controlled architecture permits enhanced antigen detection. Langmuir 2005;21(24):10907-10911.

26. Sebra RP, Masters KS, Cheung CY, Bowman CN, Anseth KS. Detection of antigens in biologically complex fluids with photografted whole antibodies. Anal Chem 2006;78(9):3144-3151.

27. Juo P, Kuo CJ, Yuan J, Blenis J. Essential requirement for caspase-8/FLICE in the initiation of the Fas-induced apoptotic cascade. Curr Biol 1998;8(18):1001-1008.

28. Juo P, Woo MS, Kuo CJ, Signorelli P, Biemann HP, Hannun YA, et al. FADD is required for multiple signaling events downstream of the receptor Fas. Cell Growth Differ 1999;10(12):797-804.

29. Dustin ML, Bivona TG, Philips MR. Membranes as messengers in T cell adhesion signaling. Nat Immunol 2004;5(4):363-372.

30. Sieg S, Smith D, Kaplan D. Differential activity of soluble versus cellular Fas ligand: regulation by an accessory molecule. Cell Immunol 1999;195(2):89-95.

31. Somersalo K, Anikeeva N, Sims TN, Thomas VK, Strong RK, Spies T, et al. Cytotoxic T lymphocytes form an antigen-independent ring junction. J Clin Invest 2004;113(1):49-57.

32. Weis M, Schlegel J, Kass GE, Holmstrom TH, Peters I, Eriksson J, et al. Cellular events in Fas/APO-1-mediated apoptosis in JURKAT T lymphocytes. Exp Cell Res 1995;219(2):699-708.

33. Yang L, Froio RM, Sciuto TE, Dvorak AM, Alon R, Luscinskas FW. ICAM-1 regulates neutrophil adhesion and transcellular migration of TNF-alpha-activated vascular endothelium under flow. Blood 2005;106(2):584-592.

34. Smith CW, Marlin SD, Rothlein R, Toman C, Anderson DC. Cooperative interactions of LFA-1 and Mac-1 with intercellular adhesion molecule-1 in facilitating adherence and transendothelial migration of human neutrophils in vitro. J Clin Invest 1989;83(6):2008-2017.

35. Simms MG, Walley KR. Activated macrophages decrease rat cardiac myocyte contractility: importance of ICAM-1-dependent adhesion. Am J Physiol 1999;277(1 Pt 2):H253-260.

36. Patel SS, Thiagarajan R, Willerson JT, Yeh ET. Inhibition of alpha4 integrin and ICAM-1 markedly attenuate macrophage homing to atherosclerotic plaques in ApoE-deficient mice. Circulation 1998;97(1):75-81.

37. Brown SB, Savill J. Phagocytosis triggers macrophage release of Fas ligand and induces apoptosis of bystander leukocytes. J Immunol 1999;162(1):480-485.

38. Liles WC, Kiener PA, Ledbetter JA, Aruffo A, Klebanoff SJ. Differential expression of Fas (CD95) and Fas ligand on normal human phagocytes: implications for the regulation of apoptosis in neutrophils. J Exp Med 1996;184(2):429-440.

39. Richardson BC, Lalwani ND, Johnson KJ, Marks RM. Fas ligation triggers apoptosis in macrophages but not endothelial cells. Eur J Immunol 1994;24(11):2640-2645.

8.5 Chapter 5 references

1. Wilson JT, Chaikof EL. Challenges and emerging technologies in the immunoisolation of cells and tissues. Advanced drug delivery reviews 2008 Jan 14;60(2):124-145.

2. White SA, Shaw JA, Sutherland DE. Pancreas transplantation. Lancet 2009 May 23;373(9677):1808-1817.

3. Pavlakis M, Khwaja K. Pancreas and islet cell transplantation in diabetes. Current opinion in endocrinology, diabetes, and obesity 2007 Apr;14(2):146-150.

4. Gremizzi C, Vergani A, Paloschi V, Secchi A. Impact of pancreas transplantation on type 1 diabetes-related complications. Current opinion in organ transplantation 2010 Feb;15(1):119-123.

5. de Vos P, Marchetti P. Encapsulation of pancreatic islets for transplantation in diabetes: the untouchable islets. Trends Mol Med 2002 Aug;8(8):363-366.

6. de Vos P, Hamel AF, Tatarkiewicz K. Considerations for successful transplantation of encapsulated pancreatic islets. Diabetologia 2002 Feb;45(2):159-173.

7. Jang JY, Lee DY, Park SJ, Byun Y. Immune reactions of lymphocytes and macrophages against PEG-grafted pancreatic islets. Biomaterials 2004 Aug;25(17):3663-3669.

8. Kulseng B, Thu B, Espevik T, Skjak-Braek G. Alginate polylysine microcapsules as immune barrier: permeability of cytokines and immunoglobulins over the capsule membrane. Cell transplantation 1997 Jul-Aug;6(4):387-394.

9. Lin CC, Metters AT, Anseth KS. Functional PEG-peptide hydrogels to modulate local inflammation induced by the pro-inflammatory cytokine TNFalpha. Biomaterials 2009 Oct;30(28):4907-4914.

10. Leung A, Lawrie G, Nielsen LK, Trau M. Synthesis and characterization of alginate/poly-L-ornithine/alginate microcapsules for local immunosuppression. J Microencapsul 2008 Sep;25(6):387-398.

11. Cheung CY, McCartney SJ, Anseth K. Synthesis of Polymerizable Superoxide Dismutase Mimetics to Reduce Reactive Oxygen Species Damage in Transplanted Biomedical Devices. Advanced Functional Materials 2008;18:3119-3126.

12. Chiumiento A, Lamponi S, Barbucci R, Dominguez A, Perez Y, Villalonga R. Immobilizing Cu,Zn-superoxide dismutase in hydrogels of carboxymethylcellulose improves its stability and wound healing properties. Biochemistry (Mosc) 2006 Dec;71(12):1324-1328.

13. Li Z, Wang F, Roy S, Sen CK, Guan J. Injectable, highly flexible, and thermosensitive hydrogels capable of delivering superoxide dismutase. Biomacromolecules 2009 Dec 14;10(12):3306-3316.

14. Giovagnoli S, Blasi P, Luca G, Fallarino F, Calvitti M, Mancuso F, et al. Bioactive long-term release from biodegradable microspheres preserves implanted ALG-PLO-ALG microcapsules from in vivo response to purified alginate. Pharmaceutical research 2010 Feb;27(2):285-295.

15. Aimetti AA, Tibbitt MW, Anseth KS. Human neutrophil elastase responsive delivery from poly(ethylene glycol) hydrogels. Biomacromolecules 2009 Jun 8;10(6):1484-1489.

16. Ricci M, Blasi P, Giovagnoli S, Rossi C, Macchiarulo G, Luca G, et al. Ketoprofen controlled release from composite microcapsules for cell encapsulation: effect on post-transplant acute inflammation. J Control Release 2005 Oct 20;107(3):395-407.

17. Bunger CM, Tiefenbach B, Jahnke A, Gerlach C, Freier T, Schmitz KP, et al. Deletion of the tissue response against alginate-pll capsules by temporary release of co-encapsulated steroids. Biomaterials 2005 May;26(15):2353-2360.

18. Hume PS, Anseth KS. Inducing local T cell apoptosis with anti-Fas-functionalized polymeric coatings fabricated via surface-initiated photopolymerizations. Biomaterials 2010 Apr;31(12):3166-3174.

19. Cheung CY, Anseth KS. Synthesis of immunoisolation barriers that provide localized immunosuppression for encapsulated pancreatic islets. Bioconjug Chem 2006 Jul-Aug;17(4):1036-1042.

20. Kabelitz D, Geissler EK, Soria B, Schroeder IS, Fandrich F, Chatenoud L. Toward cell-based therapy of type I diabetes. Trends Immunol 2008 Feb;29(2):68-74.

21. Cifone MG, De Maria R, Roncaioli P, Rippo MR, Azuma M, Lanier LL, et al. Apoptotic signaling through CD95 (Fas/Apo-1) activates an acidic sphingomyelinase. J Exp Med 1994 Oct 1;180(4):1547-1552.

22. van de Stolpe A, van der Saag PT. Intercellular adhesion molecule-1. J Mol Med 1996 Jan;74(1):13-33.

23. Sebra RP, Masters KS, Bowman CN, Anseth KS. Surface grafted antibodies: controlled architecture permits enhanced antigen detection. Langmuir 2005 Nov 22;21(24):10907-10911.

24. Cruise GM, Hegre OD, Lamberti FV, Hager SR, Hill R, Scharp DS, et al. In vitro and in vivo performance of porcine islets encapsulated in interfacially photopolymerized poly(ethylene glycol) diacrylate membranes. Cell transplantation 1999 May-Jun;8(3):293-306.

25. Weber LM, Anseth KS. Hydrogel encapsulation environments functionalized with extracellular matrix interactions increase islet insulin secretion. Matrix Biol 2008 Oct;27(8):667-673.

26. Lin CC, Anseth KS. Glucagon-Like Peptide-1 Functionalized PEG Hydrogels Promote Survival and Function of Encapsulated Pancreatic beta-Cells. Biomacromolecules 2009 Sep;10(9):2460-2467.

27. Pearl-Yafe M, Yolcu ES, Yaniv I, Stein J, Shirwan H, Askenasy N. The dual role of Fas-ligand as an injury effector and defense strategy in diabetes and islet transplantation. Bioessays 2006 Feb;28(2):211-222.

28. Weber LM, Cheung CY, Anseth KS. Multifunctional pancreatic islet encapsulation barriers achieved via multilayer PEG hydrogels. Cell transplantation 2008;16(10):1049-1057.

29. Hahn MS, Taite LJ, Moon JJ, Rowland MC, Ruffino KA, West JL. Photolithographic patterning of polyethylene glycol hydrogels. Biomaterials 2006 Apr;27(12):2519-2524.

30. Hynd MR, Frampton JP, Burnham MR, Martin DL, Dowell-Mesfin NM, Turner JN, et al. Functionalized hydrogel surfaces for the patterning of multiple biomolecules. Journal of biomedical materials research 2007 May;81(2):347-354.

31. Zhang HB, Shepherd JNH, Nuzzo RG. Microfluidic contact printing: a versatile printing platform for patterning biomolecules on hydrogel substrates. Soft Matter;6(10):2238-2245.

32. Johnson LM, Deforest CA, Pendurti A, Anseth KS, Bowman CN. Formation of three-dimensional hydrogel multilayers using enzyme-mediated redox chain initiation. ACS applied materials & interfaces 2010 Jul;2(7):1963-1972.

33. Johnson LM, Fairbanks BD, Anseth KS, Bowman CN. Enzyme-mediated redox initiation for hydrogel generation and cellular encapsulation. Biomacromolecules 2009 Nov 9;10(11):3114-3121.

34. Hume PS. Polymerizable superoxide dismutase mimetic protects β-cells encapsulated in PEG hydrogels from reactive oxygen species-mediated damage. Tissue engineering 2011.

35. Salinas CN, Anseth KS. Mixed mode thiol-acrylate photopolymerizations for the synthesis of PEG-peptide hydrogels. Macromolecules 2008 Aug;41(16):6019-6026.

36. Lin CC. Cell-cell communication mimicry with PEG hydrogels for enhancing Beta-cell function. Proc Natl Acad Sci USA 2010 2011.

37. Dustin ML, Bivona TG, Philips MR. Membranes as messengers in T cell adhesion signaling. Nat Immunol 2004 Apr;5(4):363-372.

38. Sieg S, Smith D, Kaplan D. Differential activity of soluble versus cellular Fas ligand: regulation by an accessory molecule. Cell Immunol 1999 Aug 1;195(2):89-95.

39. Tsuge H, Natsuaki O, Ohashi K. Purification, properties, and molecular features of glucose oxidase from Aspergillus niger. Journal of biochemistry 1975 Oct;78(4):835-843.

40. Cruise GM, Scharp DS, Hubbell JA. Characterization of permeability and network structure of interfacially photopolymerized poly(ethylene glycol) diacrylate hydrogels. Biomaterials 1998 Jul;19(14):1287-1294.

8.6 Chapter 6 references

1. Banchereau J, Steinman RM. Dendritic cells and the control of immunity. Nature 1998 Mar 19;392(6673):245-252.

2. Morelli AE, Thomson AW. Tolerogenic dendritic cells and the quest for transplant tolerance. Nat Rev Immunol 2007 Aug;7(8):610-621.

3. Matzinger P. An innate sense of danger. Seminars in immunology 1998 Oct;10(5):399-415.

4. van Kooten C, Lombardi G, Gelderman KA, Sagoo P, Buckland M, Lechler R, et al. Dendritic Cells as a Tool to Induce Transplantation Tolerance: Obstacles and Opportunities. Transplantation 2011 Jan;91(1):2-7.

5. Babensee JE. Interaction of dendritic cells with biomaterials. Seminars in immunology 2008 Apr;20(2):101-108.

6. Babensee JE, Paranjpe A. Differential levels of dendritic cell maturation on different biomaterials used in combination products. Journal of biomedical materials research 2005 Sep 15;74(4):503-510.

7. Acharya AP, Dolgova NV, Clare-Salzler MJ, Keselowsky BG. Adhesive substrate-modulation of adaptive immune responses. Biomaterials 2008 Dec;29(36):4736-4750.

8. Rogers TH, Babensee JE. The role of integrins in the recognition and response of dendritic cells to biomaterials. Biomaterials 2011 Feb;32(5):1270-1279.

9. Hubbell JA, Thomas SN, Swartz MA. Materials engineering for immunomodulation. Nature 2009 Nov 26;462(7272):449-460.

10. Norton LW, Park J, Babensee JE. Biomaterial adjuvant effect is attenuated by anti-inflammatory drug delivery or material selection. J Control Release 2010 Sep 15;146(3):341-348.

11. Hackstein H, Thomson AW. Dendritic cells: emerging pharmacological targets of immunosuppressive drugs. Nat Rev Immunol 2004 Jan;4(1):24-34.

12. Kosiewicz MM, Alard P. Tolerogenic antigen-presenting cells: regulation of the immune response by TGF-beta-treated antigen-presenting cells. Immunologic research 2004;30(2):155-170.

13. Steinbrink K, Wolfl M, Jonuleit H, Knop J, Enk AH. Induction of tolerance by IL-10-treated dendritic cells. J Immunol 1997 Nov 15;159(10):4772-4780.

14. Sato K, Nagayama H, Tadokoro K, Juji T, Takahashi TA. Extracellular signal-regulated kinase, stress-activated protein kinase/c-Jun N-terminal kinase, and p38mapk

are involved in IL-10-mediated selective repression of TNF-alpha-induced activation and maturation of human peripheral blood monocyte-derived dendritic cells. J Immunol 1999 Apr 1;162(7):3865-3872.

15. Torres-Aguilar H, Aguilar-Ruiz SR, Gonzalez-Perez G, Munguia R, Bajana S, Meraz-Rios MA, et al. Tolerogenic dendritic cells generated with different immunosuppressive cytokines induce antigen-specific anergy and regulatory properties in memory CD4+ T cells. J Immunol Feb 15;184(4):1765-1775.

16. Ito Y. Surface micropatterning to regulate cell functions. Biomaterials 1999 Dec;20(23-24):2333-2342.

17. Hirano Y, Mooney DJ. Peptide and protein presenting materials for tissue engineering. Adv Mater 2004 Jan;16(1):17-25.

18. Mann BK, Schmedlen RH, West JL. Tethered-TGF-beta increases extracellular matrix production of vascular smooth muscle cells. Biomaterials 2001 Mar;22(5):439-444.

19. Cheung CY, Anseth KS. Synthesis of immunoisolation barriers that provide localized immunosuppression for encapsulated pancreatic islets. Bioconjug Chem 2006 Jul-Aug;17(4):1036-1042.

20. Hume PS, Anseth KS. Inducing local T cell apoptosis with anti-Fas-functionalized polymeric coatings fabricated via surface-initiated photopolymerizations. Biomaterials 2010 Apr;31(12):3166-3174.

21. Leclerc C, Brose C, Nouze C, Leonard F, Majlessi L, Becker S, et al. Immobilized cytokines as biomaterials for manufacturing immune cell based vaccines. Journal of biomedical materials research 2008 Sep 15;86(4):1033-1040.

22. Jiang X, Shen C, Rey-Ladino J, Yu H, Brunham RC. Characterization of murine dendritic cell line JAWS II and primary bone marrow-derived dendritic cells in Chlamydia muridarum antigen presentation and induction of protective immunity. Infection and immunity 2008 Jun;76(6):2392-2401.

23. Jorgensen TN, Haase C, Michelsen BK. Treatment of an immortalized APC cell line with both cytokines and LPS ensures effective T-cell activation in vitro. Scand J Immunol 2002 Nov;56(5):492-503.

24. Otsu S, Gotoh K, Yamashiro T, Yamagata J, Shin K, Fujioka T, et al. Transfer of antigen-pulsed dendritic cells induces specific T-Cell proliferation and a therapeutic effect against long-term Helicobacter pylori infection in mice. Infection and immunity 2006 Feb;74(2):984-993.

25. Pinchuk LM, Lee SR, Filipov NM. In vitro atrazine exposure affects the phenotypic and functional maturation of dendritic cells. Toxicol Appl Pharmacol 2007 Sep 15;223(3):206-217.

26. Langmuir PB, Bridgett MM, Bothwell AL, Crispe IN. Bone marrow abnormalities in the non-obese diabetic mouse. Int Immunol 1993 Feb;5(2):169-177.

27. Peng R, Bathjat K, Li Y, Clare-Salzler MJ. Defective maturation of myeloid dendritic cell (DC) in NOD mice is controlled by IDD10/17/18. Annals of the New York Academy of Sciences 2003 Nov;1005:184-186.

28. Lin CC, Anseth KS. Controlling Affinity Binding with Peptide-Functionalized Poly(ethylene glycol) Hydrogels. Adv Funct Mater 2009 Jul 24;19(14):2325.

29. Clarke DC, Brown ML, Erickson RA, Shi Y, Liu X. Transforming growth factor beta depletion is the primary determinant of Smad signaling kinetics. Molecular and cellular biology 2009 May;29(9):2443-2455.

30. He J, Haskins K. Pathogenicity of T helper 2 T-cell clones from T-cell receptor transgenic non-obese diabetic mice is determined by tumour necrosis factor-alpha. Immunology 2008 Jan;123(1):108-117.

31. Poulin M, Haskins K. Induction of diabetes in nonobese diabetic mice by Th2 T cell clones from a TCR transgenic mouse. J Immunol 2000 Mar 15;164(6):3072-3078.

32. Traut RR, Bollen A, Sun TT, Hershey JWB, Sundberg J, Pierce LR. METHYL 4-MERCAPTOBUTYRIMIDATE AS A CLEAVABLE CROSSLINKING REAGENT AND ITS APPLICATION TO ESCHERICHIA-COLI 30S RIBOSOME. Biochemistry 1973;12(17):3266-3273.

33. Salinas CN, Anseth KS. Mixed mode thiol-acrylate photopolymerizations for the synthesis of PEG-peptide hydrogels. Macromolecules 2008 Aug;41(16):6019-6026.

34. Cruise GM, Scharp DS, Hubbell JA. Characterization of permeability and network structure of interfacially photopolymerized poly(ethylene glycol) diacrylate hydrogels. Biomaterials 1998 Jul;19(14):1287-1294.

35. Acharya AP, Dolgova NV, Xia CQ, Clare-Salzler MJ, Keselowsky BG. Adhesive substrates modulate the activation and stimulatory capacity of non-obese diabetic mouse-derived dendritic cells. Acta biomaterialia 2010 Jan;7(1):180-192.

36. Zhu J. Bioactive modification of poly(ethylene glycol) hydrogels for tissue engineering. Biomaterials 2010 Jun;31(17):4639-4656.

37. Mant A, Tourniaire G, Diaz-Mochon JJ, Elliott TJ, Williams AP, Bradley M. Polymer microarrays: identification of substrates for phagocytosis assays. Biomaterials 2006 Oct;27(30):5299-5306.

38. Jenney CR, Anderson JM. Adsorbed serum proteins responsible for surface dependent human macrophage behavior. J Biomed Mater Res 2000 Mar 15;49(4):435-447.

39. Wang GX, Deng XY, Tang CJ, Liu LS, Xiao L, Xiang LH, et al. The adhesive properties of endothelial cells on endovascular stent coated by substrates of poly-l-lysine and fibronectin. Artificial cells, blood substitutes, and immobilization biotechnology 2006;34(1):11-25.

40. Kou PM, Babensee JE. Macrophage and dendritic cell phenotypic diversity in the context of biomaterials. Journal of biomedical materials research 2010 Jan;96(1):239-260.